



National Library  
of Canada

Acquisitions and  
Bibliographic Services Branch

395 Wellington Street  
Ottawa, Ontario  
K1A 0N4

Bibliothèque nationale  
du Canada

Direction des acquisitions et  
des services bibliographiques

395, rue Wellington  
Ottawa (Ontario)  
K1A 0N4

Your file Votre référence

Our file Notre référence

## NOTICE

The quality of this microform is heavily dependent upon the quality of the original thesis submitted for microfilming. Every effort has been made to ensure the highest quality of reproduction possible.

If pages are missing, contact the university which granted the degree.

Some pages may have indistinct print especially if the original pages were typed with a poor typewriter ribbon or if the university sent us an inferior photocopy.

Reproduction in full or in part of this microform is governed by the Canadian Copyright Act, R.S.C. 1970, c. C-30, and subsequent amendments.

La qualité de cette microforme dépend grandement de la qualité de la thèse soumise au microfilmage. Nous avons tout fait pour assurer une qualité supérieure de reproduction.

S'il manque des pages, veuillez communiquer avec l'université qui a conféré le grade.

La qualité d'impression de certaines pages peut laisser à désirer, surtout si les pages originales ont été dactylographiées à l'aide d'un ruban usé ou si l'université nous a fait parvenir une photocopie de qualité inférieure.

La reproduction, même partielle, de cette microforme est soumise à la Loi canadienne sur le droit d'auteur, SRC 1970, c. C-30, et ses amendements subséquents.

## AVIS

Canada

**An Accurate Treatment of Heliumlike Ions:**

**Properties and Wavefunctions**

by

Natalie Mary Cann

Submitted in partial fulfilment of the

requirements for the degree of

Doctor of Philosophy

at

Dalhousie University

Halifax, Nova Scotia

May 1993

© Copyright by Natalie M. Cann, 1993



National Library  
of Canada

Acquisitions and  
Bibliographic Services Branch  
  
395 Wellington Street  
Ottawa, Ontario  
K1A 0N4

Bibliothèque nationale  
du Canada

Direction des acquisitions et  
des services bibliographiques  
  
395, rue Wellington  
Ottawa (Ontario)  
K1A 0N4

Your file Votre référence

Our file Notre référence

**The author has granted an irrevocable non-exclusive licence allowing the National Library of Canada to reproduce, loan, distribute or sell copies of his/her thesis by any means and in any form or format, making this thesis available to interested persons.**

**L'auteur a accordé une licence irrévocable et non exclusive permettant à la Bibliothèque nationale du Canada de reproduire, prêter, distribuer ou vendre des copies de sa thèse de quelque manière et sous quelque forme que ce soit pour mettre des exemplaires de cette thèse à la disposition des personnes intéressées.**

**The author retains ownership of the copyright in his/her thesis. Neither the thesis nor substantial extracts from it may be printed or otherwise reproduced without his/her permission.**

**L'auteur conserve la propriété du droit d'auteur qui protège sa thèse. Ni la thèse ni des extraits substantiels de celle-ci ne doivent être imprimés ou autrement reproduits sans son autorisation.**

ISBN 0-315-93638-X

Canada



**To Brian**

## Table of Contents

Table of Contents . . . . .	v
List of Figures . . . . .	vii
List of Tables . . . . .	xii
Abstract . . . . .	xix
List of Symbols . . . . .	xx
Acknowledgements . . . . .	xxi
Chapter 1: Introduction . . . . .	1
Chapter 2: Wavefunctions and quality tests . . . . .	5
2.1 Two-electron wavefunctions: An overview . . . . .	5
2.2 Integral transform wavefunctions: Computational notes . . . . .	12
2.3 Energies and quality tests . . . . .	15
Chapter 3: Densities and intracules . . . . .	29
3.1 Overview . . . . .	29
3.2 $\rho(r)$ , $D(r)$ , $h(u)$ , and $P(u)$ : Structure, trends and moments . . . . .	34
3.3 Density derivatives for the ground states . . . . .	51
3.4 Singlet-triplet differences for $D(r)$ and $P(u)$ . . . . .	56
Chapter 4: Electron correlation . . . . .	73
4.1 Correlation coefficients and Coulomb holes: An overview . . . . .	73
4.2 Correlation coefficients: Computational notes . . . . .	77
4.3 Correlation coefficients: Results and discussion . . . . .	79

**Chapter 4 Continued.**

4.4 Coulomb holes: Computational notes . . . . .	99
4.5 Coulomb holes: Results and discussion . . . . .	100
<b>Chapter 5: Oscillator strengths . . . . .</b>	<b>115</b>
5.1 Overview . . . . .	115
5.2 Computational notes . . . . .	116
5.3 Results and discussion . . . . .	118
<b>Chapter 6: Electron scattering . . . . .</b>	<b>135</b>
6.1 Overview . . . . .	135
6.2 Computational notes . . . . .	139
6.3 Elastic scattering . . . . .	141
6.4 Inelastic scattering: Transitions from the $1^1S$ , $2^1S$ , and $2^3S$ states of He .	149
<b>Chapter 7: Conclusions . . . . .</b>	<b>192</b>
<b>Appendix 1 . . . . .</b>	<b>196</b>
<b>Appendix 2 . . . . .</b>	<b>200</b>
<b>Appendix 3 . . . . .</b>	<b>215</b>
<b>Appendix 4 . . . . .</b>	<b>230</b>
<b>Appendix 5 . . . . .</b>	<b>237</b>
<b>Appendix 6 . . . . .</b>	<b>253</b>
<b>Appendix 7 . . . . .</b>	<b>258</b>
<b>Appendix 8 . . . . .</b>	<b>263</b>
<b>References . . . . .</b>	<b>271</b>

## List of Figures

Figure	Page
2.3.1: Asymptotic density plots for the $Z=2$ (+), $Z=4$ ( $\circ$ ), $Z=6$ ( $\blacktriangle$ ), and $Z=10$ ( $\triangledown$ ) ions of the $3^1S$ , $3^1P$ , and $3^3D$ states. . . . .	24
3.2.1: Spherically averaged and radial charge and intracule densities for the $4^1S$ states of He (—), $Ne^{8+}$ (----) and $Z=\infty$ (---). . . . .	36
3.3.1: Density derivatives for the ground state of $H^-$ . . . . .	52
3.3.2: Density derivatives for the ground state of He. . . . .	53
3.3.3: Density derivatives for the ground state of $B^{3+}$ . . . . .	54
3.3.4: Density derivatives for the ground state of $Ne^{8+}$ . . . . .	55
3.4.1: Z-scaled one-electron Hund holes for the $3S$ (a), $4S$ (b), $5S$ (c), and $6S$ (d) states of He. . . . .	60
3.4.2: Z-scaled one-electron Hund holes for the $3P$ (a), $4P$ (b), $5P$ (c), and $6P$ (d) states of He. . . . .	61
3.4.3: Z-scaled one-electron Hund holes for the $3D$ (a), $4D$ (b), $5D$ (c), and $6D$ (d) states of He. . . . .	62
3.4.4: Z-scaled one-electron Hund holes for the $3S$ states of He (—), $Li^+$ (----), and $Ne^{8+}$ (---). . . . .	63
3.4.5: Z-scaled one-electron Hund holes for the $3P$ states of He (—), $Li^+$ (----), and $Ne^{8+}$ (---). . . . .	64

Figure	Page
3.4.6: Z-scaled one-electron Hund holes for the 3D states of He (—), Li <sup>+</sup> (----), and Ne <sup>8+</sup> (---). . . . .	65
3.4.7: Z-scaled two-electron Hund holes for the 3S (a), 4S (b), 5S (c), and 6S (d) states of He. . . . .	66
3.4.8: Z-scaled two-electron Hund holes for the 3P (a), 4P (b), 5P (c), and 6P (d) states of He. . . . .	67
3.4.9: Z-scaled two-electron Hund holes for the 3D (a), 4D (b), 5D (c), and 6D (d) states of He. . . . .	68
3.4.10: Z-scaled two-electron Hund holes for the 3S states of He (—), Li <sup>+</sup> (----), Ne <sup>8+</sup> (---) and the infinite Z limit (---). . . . .	69
3.4.11: Z-scaled two-electron Hund holes for the 3P states of He (—), Li <sup>+</sup> (----), Ne <sup>8+</sup> (---) and the infinite Z limit (---). . . . .	70
3.4.12: Z-scaled two-electron Hund holes for the 3D states of He (—), Li <sup>+</sup> (----), Ne <sup>8+</sup> (---) and the infinite Z limit (---). . . . .	71
3.4.13: $\Delta <1/u>$ for the nS, nP, and nD states for n=3 (+), n=4 (▲), n=5 (●) and n=6 (■). . . . .	72
4.3.1: $\tau_{1/x}$ and $\tau_{\bar{x}/x}$ for the 1 <sup>1</sup> S (Δ), 2 <sup>1</sup> S (○), 2 <sup>3</sup> S (●), 2 <sup>1</sup> P (□), and 2 <sup>3</sup> P (■) states. . . . .	84
4.3.2: $\tau_{1/x}$ and $\tau_{\bar{x}/x}$ for the 3 <sup>1</sup> S (Δ), 3 <sup>3</sup> S (▲), 3 <sup>1</sup> P (○), 3 <sup>3</sup> P (●), 3 <sup>1</sup> D (□), and 3 <sup>3</sup> D (■) states. . . . .	85

Figure	Page
4.3.3: $\tau_{1/x}$ and $\tau_{\tilde{x}/x}$ for the $4^1S$ ( $\Delta$ ), $4^3S$ ( $\blacktriangle$ ), $4^1P$ ( $\circ$ ), $4^3P$ ( $\bullet$ ), $4^1D$ ( $\square$ ), and $4^3D$ ( $\blacksquare$ ) states.	86
4.3.4: $\tau_x$ and $\tau_{\tilde{x}}$ for the $1^1S$ ( $\Delta$ ), $2^1S$ ( $\circ$ ), $2^3S$ ( $\bullet$ ), $2^1P$ ( $\square$ ), and $2^3P$ ( $\blacksquare$ ) states.	87
4.3.5: $\tau_x$ and $\tau_{\tilde{x}}$ for the $3^1S$ ( $\Delta$ ), $3^3S$ ( $\blacktriangle$ ), $3^1P$ ( $\circ$ ), $3^3P$ ( $\bullet$ ), $3^1D$ ( $\square$ ), and $3^3D$ ( $\blacksquare$ ) states.	88
4.3.6: $\tau_x$ and $\tau_{\tilde{x}}$ for the $4^1S$ ( $\Delta$ ), $4^3S$ ( $\blacktriangle$ ), $4^1P$ ( $\circ$ ), $4^3P$ ( $\bullet$ ), $4^1D$ ( $\square$ ), and $4^3D$ ( $\blacksquare$ ) states.	89
4.3.7: $\tau_{x^2}$ and $\tau_{\tilde{x}\tilde{x}}$ for the $1^1S$ ( $\Delta$ ), $2^1S$ ( $\circ$ ), $2^3S$ ( $\bullet$ ), $2^1P$ ( $\square$ ), and $2^3P$ ( $\blacksquare$ ) states.	90
4.3.8: $\tau_{x^2}$ and $\tau_{\tilde{x}\tilde{x}}$ for the $3^1S$ ( $\Delta$ ), $3^3S$ ( $\blacktriangle$ ), $3^1P$ ( $\circ$ ), $3^3P$ ( $\bullet$ ), $3^1D$ ( $\square$ ), and $3^3D$ ( $\blacksquare$ ) states.	91
4.3.9: $\tau_{x^2}$ and $\tau_{\tilde{x}\tilde{x}}$ for the $4^1S$ ( $\Delta$ ), $4^3S$ ( $\blacktriangle$ ), $4^1P$ ( $\circ$ ), $4^3P$ ( $\bullet$ ), $4^1D$ ( $\square$ ), and $4^3D$ ( $\blacksquare$ ) states.	92
4.5.1: Z-scaled one-electron density holes for the $3^1D$ state of He, $Li^+$ , $Be^{2+}$ , $C^{4+}$ , $O^{6+}$ and $Ne^{8+}$ .	102
4.5.2: Z-scaled one-electron density holes for the $3^3D$ state of He, $Li^+$ , $Be^{2+}$ , $C^{4+}$ , $O^{6+}$ and $Ne^{8+}$ .	103
4.5.3: Z-scaled Coulomb holes for the $3^1D$ state of He, $Li^+$ , $Be^{2+}$ , $C^{4+}$ , $O^{6+}$ and $Ne^{8+}$ .	107

Figure	Page
4.5.4: Z-scaled Coulomb holes for the $3^3D$ state of He, $\text{Li}^+$ , $\text{Be}^{2+}$ , $\text{C}^{4+}$ , $\text{O}^{5+}$ and $\text{Ne}^{8+}$ . . . . .	108
6.3.1: Differential cross sections for elastic scattering of 100 eV electrons incident on He ( $1^1S$ ). . . . .	147
6.3.2: Differential cross sections for elastic scattering of 400 and 700 eV electrons incident on He ( $1^1S$ ). . . . .	148
6.4.1: Differential cross sections for the $1^1S \rightarrow 2^1S$ transition with 100 eV incident electrons. . . . .	156
6.4.2: Differential cross sections for the $1^1S \rightarrow 2^1S$ transition with 400 and 700 eV incident electrons. . . . .	157
6.4.3: Differential cross sections for the $1^1S \rightarrow 3^1S$ transition with 100 eV incident electrons. . . . .	158
6.4.4: Differential cross sections for the $1^1S \rightarrow 4^1S$ transition with 100 and 200 eV incident electrons. . . . .	159
6.4.5: Differential cross sections for the $1^1S \rightarrow 5^1S$ transition with 100 and 200 eV incident electrons. . . . .	160
6.4.6: Differential cross sections for the $1^1S \rightarrow 2^1P$ transition with 100 eV incident electrons. . . . .	161
6.4.7: Differential cross sections for the $1^1S \rightarrow 2^1P$ transition with 400 and 700 eV incident electrons. . . . .	162

Figure		Page
6.4.8:	Differential cross sections for the $1^1S \rightarrow 3^1P$ transition with 100 eV incident electrons. . . . .	163
6.4.9:	Differential cross sections for the $1^1S \rightarrow 4^1P$ transition with 100 and 150 eV incident electrons. . . . .	164
6.4.10:	Differential cross sections for the $1^1S \rightarrow 5^1P$ transition with 100 and 150 eV incident electrons. . . . .	165
6.4.11:	Differential cross sections for the $1^1S \rightarrow 4^1D$ transition with 100 and 200 eV incident electrons. . . . .	166
6.4.12:	Differential cross sections for the $1^1S \rightarrow 5^1D$ transition with 100 and 200 eV incident electrons. . . . .	167

## List of Tables

Table	Page
2.3.1: Ground state energies of the two-electron ions. . . . .	16
2.3.2: Excited state energies for the two-electron ions. . . . .	17
2.3.3: Energy 1/Z expansion coefficients. . . . .	26
2.3.4: Energies, cusp ratios, and nonlinear parameters for 200-term optimized ground state wavefunctions. . . . .	28
3.2.1: Moments for the $^1S$ states of the two-electron ions. . . . .	41
3.2.2: Moments for the $^3S$ states of the two-electron ions. . . . .	43
3.2.3: Moments for the $^1P$ states of the two-electron ions. . . . .	45
3.2.4: Moments for the $^3P$ states of the two-electron ions. . . . .	46
3.2.5: Moments for the $^1D$ states of the two-electron ions. . . . .	47
3.2.6: Moments for the $^3D$ states of the two-electron ions. . . . .	49
4.3.1: 1/Z expansion coefficients of $\tau_{1/r}$ . . . . .	93
4.3.2: 1/Z expansion coefficients of $\tau_r$ . . . . .	94
4.3.3: 1/Z expansion coefficients of $\tau_{r^2}$ . . . . .	95
4.3.4: 1/Z expansion coefficients of $\tau_{\bar{r}/r}$ . . . . .	96
4.3.5: 1/Z expansion coefficients of $\tau_{\bar{r}}$ . . . . .	97
4.3.6: 1/Z expansion coefficients of $\tau_{r\bar{r}}$ . . . . .	98
4.5.1: "Exact" and correlation energies for the $3^1D$ and $3^3D$ states of the heliumlike ions. . . . .	100

Table	Page
4.5.2: Moments of the correlated radial density $D(r)$ and the density hole $\Delta D(r)$ for the $3^1D$ (S) and $3^3D$ (T) states of the heliumlike ions. . . . .	104
4.5.3: Moments of the correlated radial intracule $P(u)$ and the Coulomb hole $\Delta P(u)$ for the $3^1D$ (S) and $3^3D$ (T) states of the heliumlike ions. . . . .	109
4.5.4: Total and outer volumes of the density and Coulomb holes. . . . .	111
4.5.5: Statistical correlation coefficients from SCF and correlated wavefunctions for the $3^1D$ state of the heliumlike ions. . . . .	112
4.5.6: Statistical correlation coefficients from SCF and correlated wavefunctions for the $3^3D$ state of the heliumlike ions. . . . .	113
5.3.1: Dipole oscillator strengths for the $m^1S$ to $n^1P$ transitions in the two-electron ions. . . . .	120
5.3.2: Dipole oscillator strengths for the $m^3S$ to $n^3P$ transitions in the two-electron ions. . . . .	123
5.3.3: Dipole oscillator strengths for the $m^1P$ to $n^1D$ transitions in the two-electron ions. . . . .	126
5.3.4: Dipole oscillator strengths for the $m^3P$ to $n^3D$ transitions in the two-electron ions. . . . .	128
5.3.5: Second order coefficients for the $1/Z$ expansion of the transition moments for the $mS$ to $nP$ transitions. . . . .	132
5.3.6: Second order coefficients for the $1/Z$ expansion of the transition moments for the $mP$ to $nD$ transitions. . . . .	133

Table	Page
5.3.7: Quadrupole oscillator strengths for S→D transitions from the three lowest states of the two-electron ions. . . . .	134
6.3.1: Elastic form factors FF(K) for squared momentum transfers, K <sup>2</sup> , between 0.05 and 500 for the ground state of He. . . . .	143
6.3.2: Elastic form factors FF(K) for squared momentum transfers, K <sup>2</sup> , between 0.05 and 500 for the He 2 <sup>3</sup> S state. . . . .	144
6.3.3: Elastic form factors FF(K) for squared momentum transfers, K <sup>2</sup> , between 0.05 and 500 for the He 2 <sup>1</sup> S state. . . . .	145
6.3.4: First three small and large K form factor expansion coefficients for the He 1 <sup>1</sup> S, 2 <sup>1</sup> S, and 2 <sup>3</sup> S states. . . . .	146
6.4.1: Generalized oscillator strengths for the He 1 <sup>1</sup> S→n <sup>1</sup> S transitions. . . . .	168
6.4.2: Generalized oscillator strengths for the He 1 <sup>1</sup> S→n <sup>1</sup> P transitions. . . . .	170
6.4.3: Generalized oscillator strengths for the He 1 <sup>1</sup> S→n <sup>1</sup> D transitions. . . . .	172
6.4.4: Generalized oscillator strengths for the He 2 <sup>3</sup> S→n <sup>3</sup> S transitions. . . . .	174
6.4.5: Generalized oscillator strengths for the He 2 <sup>3</sup> S→n <sup>3</sup> P transitions. . . . .	176
6.4.6: Generalized oscillator strengths for the He 2 <sup>3</sup> S→n <sup>3</sup> D transitions. . . . .	178
6.4.7: Generalized oscillator strengths for the He 2 <sup>1</sup> S→n <sup>1</sup> S transitions. . . . .	180
6.4.8: Generalized oscillator strengths for the He 2 <sup>1</sup> S→n <sup>1</sup> P transitions. . . . .	182
6.4.9: Generalized oscillator strengths for the He 2 <sup>1</sup> S→n <sup>1</sup> D transitions. . . . .	184
6.4.10: First three small K expansion coefficients of the GOS(K) for the 1 <sup>1</sup> S→n <sup>1</sup> S, n <sup>1</sup> P, n <sup>1</sup> D, n=2-6 He transitions. . . . .	186

Table		Page
6.4.11:	First three small $K$ expansion coefficients of the $GOS(K)$ for the $2^1S \rightarrow n^1S, n^1P, n^1D, n=2-6$ He transitions. . . . .	187
6.4.12:	First three small $K$ expansion coefficients of the $GOS(K)$ for the $2^3S \rightarrow n^3S, n^3P, n^3D, n=2-6$ He transitions. . . . .	188
6.4.13:	First three large $K$ expansion coefficients of the $GOS(K)$ for the $1^1S \rightarrow n^1S, n^1P, n^1D, n=2-6$ He transitions. . . . .	189
6.4.14:	First three large $K$ expansion coefficients of the $GOS(K)$ for the $2^1S \rightarrow n^1S, n^1P, n^1D, n=2-6$ He transitions. . . . .	190
6.4.15:	First three large $K$ expansion coefficients of the $GOS(K)$ for the $2^3S \rightarrow n^3S, n^3P, n^3D, n=2-6$ He transitions. . . . .	191
A1.1:	Two iterations of Powell's algorithm for a 20 term wavefunction for the He $1^1S$ state. . . . .	196
A2.1:	$1^1S$ parallelotope parameters and virial scaling coefficients. . . . .	200
A2.2:	$2^1S$ parallelotope parameters and virial scaling coefficients. . . . .	200
A2.3:	$2^3S$ parallelotope parameters and virial scaling coefficients. . . . .	201
A2.4:	$3^1S$ parallelotope parameters and virial scaling coefficients. . . . .	201
A2.5:	$3^3S$ parallelotope parameters and virial scaling coefficients. . . . .	202
A2.6:	$4^1S$ parallelotope parameters and virial scaling coefficients. . . . .	202
A2.7:	$4^3S$ parallelotope parameters and virial scaling coefficients. . . . .	203
A2.8:	$5^1S$ parallelotope parameters and virial scaling coefficients. . . . .	203
A2.9:	$5^3S$ parallelotope parameters and virial scaling coefficients. . . . .	204

Table	Page
A2.10: $6^1S$ parallelotope parameters and virial scaling coefficients.	204
A2.11: $6^3S$ parallelotope parameters and virial scaling coefficients.	205
A2.12: $2^1P$ parallelotope parameters and virial scaling coefficients.	205
A2.13: $2^3P$ parallelotope parameters and virial scaling coefficients.	206
A2.14: $3^1P$ parallelotope parameters and virial scaling coefficients.	206
A2.15: $3^3P$ parallelotope parameters and virial scaling coefficients.	207
A2.16: $4^1P$ parallelotope parameters and virial scaling coefficients.	207
A2.17: $4^3P$ parallelotope parameters and virial scaling coefficients.	208
A2.18: $5^1P$ parallelotope parameters and virial scaling coefficients.	208
A2.19: $5^3P$ parallelotope parameters and virial scaling coefficients.	209
A2.20: $6^1P$ parallelotope parameters and virial scaling coefficients.	209
A2.21: $6^3P$ parallelotope parameters and virial scaling coefficients.	210
A2.22: $3^1D$ parallelotope parameters and virial scaling coefficients.	210
A2.23: $3^3D$ parallelotope parameters and virial scaling coefficients.	211
A2.24: $4^1D$ parallelotope parameters and virial scaling coefficients.	211
A2.25: $4^3D$ parallelotope parameters and virial scaling coefficients.	212
A2.26: $5^1D$ parallelotope parameters and virial scaling coefficients.	212
A2.27: $5^3D$ parallelotope parameters and virial scaling coefficients.	213
A2.28: $6^1D$ parallelotope parameters and virial scaling coefficients.	213
A2.29: $6^3D$ parallelotope parameters and virial scaling coefficients.	214
A3.1: Expectation values and quality checks for the $1^1S$ state.	215

Table		Page
A3.2:	Expectation values and quality checks for the $2^1S$ state. . . . .	215
A3.3:	Expectation values and quality checks for the $2^3S$ state. . . . .	216
A3.4:	Expectation values and quality checks for the $2^1P$ state. . . . .	216
A3.5:	Expectation values and quality checks for the $2^3P$ state. . . . .	217
A3.6:	Expectation values and quality checks for the $3^1S$ state. . . . .	217
A3.7:	Expectation values and quality checks for the $3^3S$ state. . . . .	218
A3.8:	Expectation values and quality checks for the $3^1P$ state. . . . .	218
A3.9:	Expectation values and quality checks for the $3^3P$ state. . . . .	219
A3.10:	Expectation values and quality checks for the $3^1D$ state. . . . .	219
A3.11:	Expectation values and quality checks for the $3^3D$ state. . . . .	220
A3.12:	Expectation values and quality checks for the $4^1S$ state. . . . .	220
A3.13:	Expectation values and quality checks for the $4^3S$ state. . . . .	221
A3.14:	Expectation values and quality checks for the $4^1P$ state. . . . .	221
A3.15:	Expectation values and quality checks for the $4^3P$ state. . . . .	222
A3.16:	Expectation values and quality checks for the $4^1D$ state. . . . .	222
A3.17:	Expectation values and quality checks for the $4^3D$ state. . . . .	223
A3.18:	Expectation values and quality checks for the $5^1S$ state. . . . .	223
A3.19:	Expectation values and quality checks for the $5^3S$ state. . . . .	224
A3.20:	Expectation values and quality checks for the $5^1P$ state. . . . .	224
A3.21:	Expectation values and quality checks for the $5^3P$ state. . . . .	225
A3.22:	Expectation values and quality checks for the $5^1D$ state. . . . .	225

Table	Page
A3.23: Expectation values and quality checks for the $5^3D$ state. . . . .	226
A3.24: Expectation values and quality checks for the $6^1S$ state. . . . .	226
A3.25: Expectation values and quality checks for the $6^3S$ state. . . . .	227
A3.26: Expectation values and quality checks for the $6^1P$ state. . . . .	227
A3.27: Expectation values and quality checks for the $6^3P$ state. . . . .	228
A3.28: Expectation values and quality checks for the $6^1D$ state. . . . .	228
A3.29: Expectation values and quality checks for the $6^3D$ state. . . . .	229
A5.1: Correlation coefficients for the ground state. . . . .	237
A5.2: $\tau_{l/r}$ for the excited states of heliumlike ions. . . . .	238
A5.3: $\tau_r$ for the excited states of heliumlike ions. . . . .	241
A5.4: $\tau_{r^2}$ for the excited states of heliumlike ions. . . . .	243
A5.5: $\tau_{\vec{r}/r}$ for the excited states of heliumlike ions. . . . .	246
A5.6: $\tau_{\vec{r}}$ for the excited states of heliumlike ions. . . . .	248
A5.7: $\tau_{\vec{r}r}$ for the excited states of heliumlike ions. . . . .	250
A7.1: Ground state elastic form factors for various Z-scaled momentum transfers. . . . .	258
A7.2: Generalized oscillator strengths for the $1^1S \rightarrow 2^1P$ for various Z-scaled momentum transfers. . . . .	260

## Abstract

Explicitly-correlated wavefunctions are generated for the  $n^1S$ ,  $n^3S$ ,  $n^1P$ ,  $n^3P$ ,  $n^1D$ , and  $n^3D$  states, where  $n \leq 6$ , of the helium isoelectronic series from He to  $\text{Ne}^{8+}$ . These 100 term wavefunctions are optimized variationally and the resulting energies are the best available for 180 of the 261 states considered. In addition to the energy, each wavefunction is assessed by its asymptotic behaviour and by the degree to which it satisfies the virial theorem, electron-electron cusp condition, and electron-nucleus cusp condition. These criteria assess the overall wavefunction behaviour as well as the behaviour at small and large interparticle separations.

The wavefunctions are used to systematically study the variation of the charge and intracule densities with respect to spin multiplicity, nuclear charge  $Z$ , degree of excitation  $n$ , and angular momentum  $L$ . The accuracy of a screened hydrogenic density model is determined for each state and ion. The  $Z$ -,  $L$ -, and  $n$ - dependence of six correlation coefficients is systematically studied. These coefficients emphasize radial and angular correlation in the inner, intermediate, and outer regions of the electron distribution. From the explicitly correlated wavefunctions and near Hartree-Fock quality self-consistent-field wavefunctions, Coulomb holes and radial density holes are obtained for the  $3^1D$  and  $3^3D$  states of the ions from He to  $\text{Ne}^{8+}$ .

For He, generalized oscillator strengths (GOS) are calculated for  $S \rightarrow S$ ,  $S \rightarrow P$ , and  $S \rightarrow D$  transitions originating from the  $1^1S$ ,  $2^1S$ , and  $2^3S$  states. Although, the GOS for each transition are calculated for over sixty momentum transfer ( $K$ ) values, several small- $K$  and large- $K$  GOS expansion coefficients are also provided. For each ion, dipole oscillator strengths (DOS) are calculated for 55 S-P and 40 P-D transitions. These DOS are more accurate than previous values for 739 of the 855 transitions considered. Quadrupole oscillator strengths (QOS) are also obtained for 44 S-D transitions of each ion.

For extrapolation to higher  $Z$ ,  $1/Z$  expansion coefficients are calculated for energies and correlation coefficients of each state, and each DOS transition.

## List of Symbols

$\hat{H}$	Hamiltonian operator	E	energy
$\Psi, \psi$	wavefunction	$E_H$	energy in Hartrees
Z	nuclear charge	$\nabla^2$	Laplacian operator
n	principal quantum number	$C_{cn}$	electron-nucleus cusp ratio
L	angular momentum	$C_{ee}$	electron-electron cusp ratio
$Y_L^m$	spherical harmonic	$\eta$	virial ratio
$\langle x \rangle$	expectation value of x	$\rho(r)$	charge density
$\delta_j$	Dirac delta function	D( $r$ )	radial charge density
$\delta(x)$	Kronecker delta function	h( $u$ )	intracule function
ln	natural logarithm	P( $u$ )	radial intracule density
$W_i$	weight function	$D_1(\vec{r}_1)$	one-electron density
$\hat{P}_{12}$	permutation operator	$D_2(\vec{r}_1, \vec{r}_2)$	electron pair density
$r_i$	electron-nucleus separation	$\tau_g$	correlation coefficient
$r_{ij}$	interelectronic separation	$d\sigma/d\Omega$	differential cross section
$\vec{r}_i$	position vector of electron i	$\sigma$	cross section
$k_i$	momentum of electron i	DOS	dipole oscillator strength
K	momentum transfer	QOS	quadrupole oscillator strength
HF	Hartree-Fock	GOS	generalized oscillator strength
SCF	self-consistent-field	FF	form factor

## Acknowledgements

Apparently anything goes on this page. It is ALL MINE! So I can do all the things I haven't been allowed to do in the rest of this document. First up, I would like to swear a bit (?\*!%\*!!!) then I'd like to misspell a few words (wavefuntion, tabble, generaliced, hellium) and last of all I would like to turn this sentence into a run-on sentence by cramming three sentences all into one and omitting the punctuation. Now that I have that out of my system, I would like to get to the business at hand.

I have had the privilege to study theoretical chemistry under the guidance of two outstanding chemists: Ajit Thakkar and Russ Boyd. From each I have learned much about chemistry and much about life. I thank them both.

Zheng Shi and I have shared an office for many years. We have had many a discussion and her advice has come in very handy. To Zheng Shi - A huge thank you.

I would also like to thank the other members of the "Boyd group" - Jian Wang, Jing Kong, Mimi Lam, Jaime Martell, and Leif Eriksson - for helping this document along in many small ways. One special thank you to Jing Kong for never complaining about walking me to the car every night!

On certain occasions, I have sought the advice of Profs. Jan Kwak and Mary Anne White. I thank them both for their openness and kindness.

My parents have always felt that education was key - and they never thought it strange that a girl should enjoy science and math. For their support and encouragement, I thank them and love them. My sister Carol and brother-in-law Leo-James also deserve a big thank you for letting me sleep on their couch and eat their food during my working trips to Fredericton.

My husband Brian has contributed, in his own way, to this document. He has lifted my spirits when I felt the task at hand seemed insurmountable, coerced me into working when I was feeling lazy, and convinced me to take a break when I'd been working too hard. Thank you, Brian. I love you. Four down, forty to go.

## CHAPTER 1

### INTRODUCTION

To chemists and physicists alike, helium is a unique element [1.1-1.3]. Its name originates from the greek *Helios* (meaning sun) since its presence was first detected by Lockyer and Frankland on August 18 1868 while observing a solar eclipse. The helium found on earth is the product of radioactive decay and is normally extracted from natural gas where its concentration is as much as 7%. Despite the small amount of He found on Earth, it is nonetheless the second most abundant element in the universe.

The past sixty years have seen many theoretical studies of helium since it is the simplest system for which quantum mechanics cannot provide an exact description. Therefore, theoretical studies are necessarily approximate and, as a result, helium has become a "testing ground" for new theoretical approaches. Experimentally, helium is a relatively simple system to study: it is nontoxic, nonflammable, inert, and readily obtained in high purity.

With the rapid development of computers over the past 20 years, quantum mechanical calculations have been applied to larger and larger systems. On the other hand, the same computers allow more and more accurate descriptions of small systems. This document is devoted entirely to the latter. In particular, the focus is on helium and the heliumlike ions from  $\text{Li}^+$  to  $\text{Ne}^{8+}$ . For each ion, 11 S states, 10 P states, and 8 D states are examined. The approach used is "even handed", that is, each state of each ion is described at an equal level of theory, even though it could be argued that helium is

sufficiently important to warrant special consideration. This consistent approach simplifies the analysis of results when effects of nuclear charge are being assessed. With the exception of a handful of studies, the previous treatments of heliumlike ions have dealt with specific properties of certain ions.

A fundamental postulate of quantum mechanics states that everything that can be known about a system is contained in its wavefunction  $\Psi$ . This function is the solution of the time-independent differential equation

$$\hat{H}\Psi = E\Psi \quad (1.1)$$

where  $\hat{H}$  is the Hamiltonian operator and  $E$  is the total energy for the system. With the exception of one-electron systems,  $\Psi$  is not known exactly: it must be approximated by some function  $\psi$ . Ideally,  $\psi$  will include many adjustable parameters which will be varied such that the approximate function reproduces  $\Psi$  as well as possible. This task is greatly simplified by using the variational theorem which states that an approximate energy obtained by minimizing

$$\tilde{E} = \frac{\int \psi^* \hat{H} \psi d\tau}{\int \psi^* \psi d\tau} \quad (1.2)$$

always lies above the true energy. The strategy is to adjust the parameters in  $\psi$  such that  $\tilde{E}$  is minimized. Equation (1.2) is so useful, in fact, that it has often led to the assessment of approximate wavefunctions based solely on the energies they predict.

Clearly, the selection and optimization of an approximate wavefunction is a critical element in any study of atomic properties. Chapter 2 introduces the

wavefunctions selected for study, their optimization, and the energies obtained. However, chapter 2 also includes several other quality checks.

Chapters 3 and 4 examine the effects, and the nature of, electron correlation in the two-electron ions. In particular, chapter 3 consists of an analysis of the effects of electron correlation, the investigation of correlation sensitive properties and their dependence on nuclear charge, principal quantum number, angular momentum and spin. Two different definitions of electron correlation, one based on conventional concepts, the other on statistics, are examined in chapter 4. Although some of the properties examined may also be measured experimentally, most cannot or have not. The purpose, however, is the understanding of which properties are sensitive to electron correlation, why these change, and how the changes will occur.

Chapters 5 and 6 consider collision processes in the two-electron ions: the former considers the absorption of light whereas electron scattering forms the topic of the latter. In particular, S $\rightarrow$ P and P $\rightarrow$ D dipole transitions and S $\rightarrow$ D quadrupole transitions for the ions from He to Ne $^{8+}$  are considered in chapter 5. It is hoped that these calculations will stimulate further experimental measurements of dipole and quadrupole transitions. High energy electron scattering from the three lowest He states forms the topic of chapter 6. Although electron scattering experiments have been published for many atoms and molecules, helium has been studied the most. Chapter 6 presents and discusses the theoretical results, as well, theory and experiment are compared whenever possible.

Each chapter has been written to be, as much as possible, stand-alone or complete. With this objective in mind, the chapters are subdivided as follows: An

introduction to previous work and a brief review of the required theoretical background; a computational notes section where mathematical and computational details are discussed; and one, or several, sections devoted to the presentation and discussion of the results. However, any formulae specific to this work are presented in appendices.

Most of the results presented in chapters 2, 3, 4, and 5 are in print [1.4][1.5], in press [1.6], or have been submitted [1.7] for publication. Atomic units have been used throughout this document.

**CHAPTER 2:**  
**WAVEFUNCTIONS AND QUALITY TESTS**

**2.1 Two-electron wavefunctions: An overview**

For two-electron atoms, the nonrelativistic, infinite nuclear mass, spin-independent Hamiltonian is given by

$$\hat{H} = -\frac{\nabla_1^2}{2} - \frac{\nabla_2^2}{2} - \frac{Z}{r_1} - \frac{Z}{r_2} + \frac{1}{r_{12}} \quad (2.1)$$

in which  $\vec{r}_i = (r_i, \Omega_i)$  is the position vector of electron  $i$ ,  $r_{12} = |\vec{r}_1 - \vec{r}_2|$  is the interelectronic distance, and  $Z$  is the nuclear charge. Trial wavefunctions for the resulting Schrödinger equation have the general form

$$\psi = \sum_k^N c_k (1 \pm \hat{P}_{12}) f_k(r_1, r_2, r_{12}) Y(1,2) \quad (2.2)$$

where  $\hat{P}_{12}$  is a permutation operator and the plus and minus signs refer to singlet and triplet states, respectively. "Explicitly correlated" wavefunctions are characterized by  $r_{12}$  appearing explicitly in at least one  $f_k(r_1, r_2, r_{12})$ .  $Y(1,2)$  represents the appropriate combination of spherical harmonics for the angular momentum or spatial symmetry of the state of interest:  $Y(1,2) = Y_L^0(\Omega_1) Y_0^0(\Omega_2)$  where  $L=0, 1$ , or  $2$  for S, P, or D states, respectively, and, for D states, the additional combination  $Y(1,2) = 2Y_1^0(\Omega_1) Y_1^0(\Omega_2) + Y_1^1(\Omega_1) Y_1^{-1}(\Omega_2) + Y_1^{-1}(\Omega_1) Y_1^1(\Omega_2)$ . D state expansions

which do not include both spherical harmonic factors will suffer from angular incompleteness [2.1][2.2].

Hylleraas [2.3] was the first to include the interelectronic distance into the form of a wavefunction. For the helium atom in its ground state, his simplest function has the form

$$\Psi = (1 + 0.364 r_{12}) \exp(-1.849(r_1 + r_2)) \quad (2.3)$$

Larger expansions included terms with powers of  $r_1$ ,  $r_2$ , and  $r_{12}$ . The phrase "Hylleraas-type expansion" often refers to wavefunctions with the general form

$$\Psi = \sum_{l,m,n} C_{lmn} (1 \pm \hat{P}_{12}) \exp(-\alpha r_1) \exp(-\beta r_2) r_1^l r_2^m r_{12}^n Y(l,2) \quad (2.4)$$

where  $\alpha$ ,  $\beta$  and the  $C_{lmn}$  are parameters.

For the helium isoelectronic series, the most extensive use of Hylleraas-type functions is contained in a series of papers by Pekeris and coworkers [2.4][2.5]. Expansions with as many as 2000 terms were used to compute energy values for several S and P states of the isoelectronic series from  $Z=2$  to  $Z=10$ . The problem of choosing  $l$ ,  $m$ , and  $n$ , was addressed by introducing a parameter  $\Omega$  such that

$$\Omega \geq l+m+n \quad l,m,n \geq 0 \quad (2.5)$$

and the total number of terms in the wavefunction is controlled by varying  $\Omega$ .

Kono and Hattori [2.6-2.9] modified the  $l,m,n$  selection scheme shown above by eliminating terms in which  $n \neq 0$  and  $|l-m|$  is large. The latter should have appreciable values when the two electrons are far apart and hence have a small  $r_{12}$  dependence. With this modification, equation (2.5) is

$$\Omega \geq l+m+n+|l-m|(1-\delta_{n0}) \quad (2.6)$$

With this generating technique, the S, P and D states of the helium atom and several P and D states for the ions from  $Z=3$  to  $Z=7$  were investigated. Instead of using only one expansion of the form given in equation (2.4), a second term of the type

$$\Psi = \sum_{l,m,n} C_{lmn} (1 \pm \hat{P}_{12}) \exp(-\gamma(r_1 + r_2)) r_1^l r_2^m r_{12}^n Y(1,2) \quad (2.7)$$

was included. The  $\alpha$  and  $\beta$  values in equation (2.4) were assigned to describe the correct asymptotic behaviour while  $\gamma$  was optimized variationally. For the D states, equation (2.7) includes both spherical harmonic combinations. By modifying Pekeris' approach, Kono and Hattori obtained comparable or improved energy values with expansions of 200 terms or less.

More recently, Drake [2.10-2.12] has extended Kono and Hattori's work for many S, P, and D states of helium. His wavefunctions include several terms with the form (2.5) as well as a term corresponding to the perfectly screened hydrogenic approximation. The usefulness of the hydrogenic term will be considered further in section 3.2. For S and P states the wavefunction is composed of the hydrogenic term and two sets of terms of the form given by equation (2.4). All four nonlinear parameters were variationally optimized. For the D states, two additional parameters, corresponding to the second combination of spherical harmonics, were also optimized. Wavefunctions with as many as 840 terms were optimized and the corresponding non-relativistic energies are generally the most accurate computed values.

For neutral He, Hylleraas-type expansions have been used for states well beyond  $n=6$  and  $L=2$ ; energies for the He Rydberg states up to  $n=10$  and  $L=6$  have recently been obtained using Hylleraas-type expansions [2.13-2.15].

Most studies of Hylleraas-type expansions have focused on positive  $l$ ,  $m$  and  $n$  values, but negative powers of  $r_{12}$  have also been investigated. Wavefunctions which include both negative and positive  $n$  values are often termed "Kinoshita-type" wavefunctions. Kinoshita's wavefunctions offer a larger selection range for  $n$ . This added flexibility allows for improved convergence. With an expansion length of 80 for the helium ground state, Kinoshita [2.16][2.17] obtained an energy which was only  $1\mu E_h$  higher than Pekeris' 1078 term value [2.4]. Clearly, wavefunctions of this form converge rapidly. One serious disadvantage with this form of wavefunction is that the calculation of properties could require the evaluation of divergent integrals although their total sum will still converge.

The use of half integral powers of the interelectronic separation also leads to rapidly convergent wavefunctions. For instance, Schwartz [2.18] matched the accuracy of the Pekeris 1078 term [2.4] helium ground state wavefunction by using a 164 term expansion with half integral powers. Although these functions have fast rates of convergence, the calculation of atomic properties using these wavefunctions will generally be difficult and possibly require numerical solutions to the integrals. Schwartz explained the convergence of his wavefunctions by noting that for the ground state of the helium atom a weak singularity of the form

$$(r_1^2 + r_2^2) \ln(r_1^2 + r_2^2) \quad (2.8)$$

was a controlling factor in the rate of wavefunction convergence. Since he considered the inclusion of a logarithmic term in the wavefunction too difficult, the logarithmic singularity was approximated by including half integral powers.

Perhaps not surprisingly, logarithmic terms have also been included in wavefunction expansions [2.19][2.20]. Recently, Baker *et al.* [2.21] and Kleindienst and Emrich [2.22] have investigated wavefunctions with logarithmic terms and negative powers. Using 476 term wavefunctions, Baker [2.21] obtained accurate ground state energies for the helium isoelectronic series. For example the calculated helium ground state energy is comparable to Drake's [2.10] value obtained using over 600 terms. Interestingly, Kleindienst and Emrich [2.22] noted that even with the inclusion of logarithmic terms, the presence of negative powers in the wavefunction expansion considerably reduced the expansion length required for a given accuracy. The logarithmic wavefunction expansions have the form

$$\Psi = \sum_{k,l,m,n} C_{klmn} \exp(-\alpha(r_1+r_2)) r_{12}^{-m} (r_1+r_2)^k (r_2-r_1)^{2l} \ln^n(r_1+r_2) Y_0^0(\Omega_1) Y_0^0(\Omega_2) \quad (2.9)$$

where k may be negative or positive. These wavefunctions have the same basic disadvantage as the Schwartz and Kinoshita type expansions: they do not easily lend themselves to the calculation of atomic properties.

Pritchard and Wallis [2.23] examined S and P states of helium using wavefunctions which included exponential terms of the interelectronic separation. This type of exponential term was originally proposed many years earlier by Slater [2.24] and

Hylleraas [2.3]. Wavefunctions of the following form

$$\Psi = \sum_{i,j,k} C_{ijk} (1 \pm \hat{P}_{12}) r_1^i r_2^{j+l} r_{12}^k \exp(-\alpha r_1) \exp(-\beta r_2) \exp(-\gamma r_{12}) Y_l^0(2) Y_0^0(1) \quad (2.10)$$

were used. The nonlinear parameters  $\alpha$ ,  $\beta$ , and  $\gamma$  were identical for all terms in the wavefunction with  $\alpha$  chosen as the nuclear charge and  $\beta$  and  $\gamma$  varied to minimize the energy.

Rosenthal [2.25], and Somorjai and Power [2.26], also used wavefunctions of this form in some of their discussions about integral wavefunction representations. They considered S state wavefunctions with the form

$$\Psi = \sum_k^N C_k (1 \pm \hat{P}_{12}) \exp(-\alpha_k r_1) \exp(-\beta_k r_2) \exp(-\gamma_k r_{12}) Y_0^0(\Omega_2) Y_0^0(\Omega_1) \quad (2.11)$$

The emphasis was placed on the selection of optimal values for the 3N nonlinear parameters. Acknowledging the integral transform arguments presented by Rosenthal [2.25], and Somorjai and Power [2.26], Winkler and Porter [2.27] assigned the nonlinear parameters as the quadrature points from multidimensional Gauss-Laguerre integration techniques and computed energies for the S states of helium. Although one set of nonlinear parameters was used for all singlet and triplet S states, the energy values compared favourably with those obtained by Pekeris.

Thakkar and Smith [2.28][2.29] performed a comprehensive study of several S and P states of the helium iso'electronic series using "integral transform" wavefunctions of the form

$$\Psi = \sum_k^N C_k (1 \pm \hat{P}_{12}) r_2^L \exp(-\alpha_k r_1) \exp(-\beta_k r_2) \exp(-\gamma_k r_{12}) Y_L^0(2) Y_0^0(1) \quad (2.12)$$

where L=0 and 1 for S and P states, respectively. The convergence of equivalent length ground state wavefunctions, differing only by the schemes used in the selection of the nonlinear parameters, were discussed and compared. Further studies consider only one such scheme, "scheme P", which was chosen since it leads to comparable energies and is more readily extendable to arbitrary expansion lengths. According to "scheme P", the nonlinear parameters are selected as follows

$$\alpha_k = [(A_2 - A_1) \ll \sqrt{2}k(k+1)/2 \gg + A_1] \quad (2.13)$$

$$\beta_k = [(B_2 - B_1) \ll \sqrt{3}k(k+1)/2 \gg + B_1] \quad (2.14)$$

$$\gamma_k = [(G_2 - G_1) \ll \sqrt{5}k(k+1)/2 \gg + G_1] \quad (2.15)$$

where  $\ll x \gg$  is defined as the fractional part of x. Since individually optimizing each nonlinear parameter is computationally impractical, this scheme offers an attractive alternative; the six parallelotope or parallelepiped parameters  $A_1$ ,  $A_2$ ,  $B_1$ ,  $B_2$ ,  $G_1$  and  $G_2$  are optimized, thus representing an 'average' optimization of the  $\alpha_k$ ,  $\beta_k$ , and  $\gamma_k$ . This effectively reduces the problem of optimizing 3N non-linear parameters to the much more tractable problem of optimizing 6 non-linear parameters. Integral transform wavefunctions were shown to possess two appealing properties: energies obtained from relatively short expansions compared favourably with the values obtained by Pekeris [2.4][2.5]; the calculation of atomic properties is relatively straightforward.

## 2.2 Integral transform wavefunctions: Computational notes

On the basis of the previous integral transform work, 100-term expansions were estimated to be sufficient to obtain an accuracy comparable to that achieved in previous work using conventional Hylleraas wavefunctions containing several hundred terms. Energy values were obtained for the  $n^1S$ ,  $n^3S$ ,  $n^1P$ ,  $n^3P$ ,  $n^1D$ , and  $n^3D$  states, with  $n < 7$ , of the two-electron ions from He through  $\text{Ne}^{8+}$ . For the S and P states, the wavefunctions have the form shown in equation (2.12) with  $N=100$ . The D state expansions have the form

$$\begin{aligned}\psi = & \sum_k^N C_k(1 \pm \hat{P}_{12}) r_2^2 \exp(-\alpha_k r_1) \exp(-\beta_k r_2) \exp(-\gamma_k r_{12}) Y_2^0(\Omega_2) Y_0^0(\Omega_1) \\ & + \sum_{k=N+1}^{N+M} D_k(1 \pm \hat{P}_{12}) r_1 r_2 \exp(-\alpha_k r_1) \exp(-\beta_k r_2) \exp(-\gamma_k r_{12}) Y(1,2)\end{aligned}\quad (2.16)$$

where

$$Y(1,2) = 2Y_1^0(\Omega_1)Y_1^0(\Omega_2) + Y_1^1(\Omega_1)Y_1^{-1}(\Omega_2) + Y_1^{-1}(\Omega_1)Y_1^1(\Omega_2)$$

For convenience, the two sets of terms in equation (2.16) will be referred to as *sd* and *pp* terms, respectively. Numerical experimentation on the  $3^1D$  state of He indicated that  $M/(N+M)=0.3$  is a good mix of *sd* and *pp* terms; therefore,  $N=70$  and  $M=30$  was chosen with the constraint that the non-linear parameters in the *pp* terms are the same as the non-linear parameters in the first  $M$  *sd* terms.

The six nonlinear parameters are optimized according to a conjugate direction algorithm proposed by Powell [2.30]. This method proves itself very useful in situations where the determination of derivatives is impractical or impossible. An iteration of the basic procedure involves four steps:

1) For  $r=1,\dots,6$  calculate  $\lambda_r$  so that  $E(\vec{p}_{r-1} + \lambda_r \vec{\xi}_r)$  is a minimum and define

$$\vec{p}_r = \vec{p}_{r-1} + \lambda_r \vec{\xi}_r.$$

2) Replace  $\vec{\xi}_r$  by  $\vec{\xi}_{r+1}$  for  $r=1,\dots,5$ .

3) Replace  $\vec{\xi}_6$  by  $(\vec{p}_n - \vec{p}_0)$  and find  $\lambda$  such that  $E(\vec{p}_6 + \lambda (\vec{p}_6 - \vec{p}_0))$  is a minimum.

4) Replace  $\vec{p}_0$  by  $\vec{p}_6 + \lambda (\vec{p}_6 - \vec{p}_0)$ .

Each wavefunction optimization requires an initial estimate

$\vec{p}_0 = (A_1, A_2, B_1, B_2, G_1, G_2)$  and the coordinate directions are chosen as the initial search directions  $\vec{\xi}_1, \dots, \vec{\xi}_6$ . In the above algorithm,  $\vec{\xi}_1$  is discarded in favour of  $(\vec{p}_6 - \vec{p}_0)$ . The algorithm implemented differs from the above in that any one of the directions  $\vec{\xi}_1, \dots, \vec{\xi}_6, (\vec{p}_6 - \vec{p}_0)$  may be discarded in an iteration. The algorithm is illustrated in appendix 1 by following the variation of the 6 nonlinear parameters for a 20 term wavefunction optimization for the ground state of He.

Square integrability requires that the nonlinear parameters satisfy the following constraints:

$$\alpha_k + \beta_k > 0 \quad (2.18)$$

$$\alpha_k + \gamma_k > 0 \quad (2.19)$$

$$\beta_k + \gamma_k > 0 \quad (2.20)$$

An energy calculation proceeds only if all 300 nonlinear parameters, obtained from "scheme P", satisfy these constraints. Otherwise new estimates of  $A_1, A_2, B_1, B_2, G_1$ , and  $G_2$  are obtained and the square integrability constraints verified.

Each energy calculation requires the evaluation of the integrals shown in equation (1.2). These are reduced [2.31] to the form

$$C \int \exp(-ar_1) \exp(-br_2) \exp(-cr_{12}) r_1^l r_2^m r_{12}^n Y_l^0(\Omega_1) Y_l^0(\Omega_2) d\vec{r}_1 d\vec{r}_2 \quad (2.21)$$

and evaluated using a modified recursion relation of Sack *et al* [2.32]. By decomposing the positive definite overlap matrix into the product of a lower triangular matrix and its transpose,  $S = LL^T$ , the secular equation is transformed into the eigenvalue equation  $H'D = ED$ , where  $D = L^T C$  and  $H' = L^{-1} H L^T$ , and solved. For an N term expansion of a given symmetry, the eigenvalue vector  $E$  contains the N lowest energies for the symmetry of interest. Clearly, an optimization proceeds by comparing the appropriate entry in the eigenvalue vector for different values of the 6 nonlinear parameters.

The six parallelopotope parameters were independently optimized for each of the 29 states of each ion and all the linear parameters were found variationally. Since all optimization methods are plagued by local minima, it was not surprising that different initial estimates of the parallelopotope parameters often led to substantially different 'optimized' values. Due to the large number of states considered, only one initial estimate was considered for each state except when the 'optimized' energies were higher than expected or the 'optimized' parameters were clearly inconsistent with physical arguments. In such instances, up to 70 initial parallelopotope parameter estimates were tried. After the necessarily imperfect optimization, each wavefunction was scaled to satisfy the virial theorem [2.3][2.33]. The scale factors never deviated from unity by more than  $10^{-6}$  reflecting the fact that the optimizations had been allowed to continue until the energies were stable to at least  $10^{-11} E_H$  - a threshold two orders of magnitude

lower than the absolute wavefunction accuracy. The optimized parallelotope parameters and virial scale factors are tabulated in appendix 2 for all 261 states considered.

For the highly excited states and, in particular, for the low- $Z$  ions, two of the parallelotope parameters have approximately converged to the nuclear charge  $Z$ . Several optimizations were performed with the constraint that two non-linear parameters were equal to  $Z$ . These expansions were clearly inadequate, even for  $n=6$ , since the energy errors increased by at least a tenfold factor.

All calculations were performed in quadruple precision ( $\approx 32$  decimal digits) to avoid computational linear dependence. The latter problem was most acute in the  $6^1S$  state of He; in that case, the smallest eigenvalue of the Gram matrix, for normalized basis geminals, was  $1.2 \times 10^{-30}$ .

### 2.3 Energies and quality tests

The calculated energies for each of the S, P and D states with  $n < 7$  are listed in tables 2.3.1-2.3.4 for He through  $\text{Ne}^{8+}$ . The overall comparison of energy values with published values is presented below, however individual comparisons for each state and ion are presented in appendix 3.

The ground state energy of  $\text{H}^-$  is included for the sake of completeness. The S state energies for 69 of the 100 S-states considered are the lowest reported so far; the improvements range up to  $12 \mu\text{E}_\text{H}$  for the  $5^1S$  states of the ions with  $Z > 3$ . The energies for the remaining 31 S-states are no more than  $20 n\text{E}_\text{H}$  above the best available results as outlined below. The  $1^1S$  and  $2^1S$  energies respectively lie no more than  $7.8 n\text{E}_\text{H}$  and

$16.9 nE_H$  above the values obtained by Freund, Huxtable and Morgan [2.34] and Frankowski [2.35] using wavefunctions containing logarithmic terms, and by Drake [2.10] from Hylleraas-type expansions containing several hundred terms. For neutral He, the higher  $^1S$  and  $^3S$  energies respectively lie no more than  $20 nE_H$  and  $0.9 nE_H$  above the results of Drake [2.10] and Kono and Hattori [2.8] obtained with Hylleraas-type expansions.

The energies of the 48 P-states with  $n=4,5$ , and 6 for the cations lie below the best available values. The  $^1P$  and  $^3P$  energies for He lie no more than  $10 nE_H$  and  $14 nE_H$  respectively above the values obtained by Drake and Makowski [2.11], and Kono and Hattori [2.8]. Most of the  $2^1P$ ,  $2^3P$ ,  $3^1P$  and  $3^3P$  energies for the cations lie above the values of Accad *et al.* [2.5] but never by more than  $30 nE_H$ .

The  $^1D$  and  $^3D$  energies for helium lie no more than  $15 nE_H$  and  $10 nE_H$  respectively above those of Drake [2.12]. The energies for the D-states of the cations are in all cases as good as or better than those in the literature [2.6].

Table 2.3.1: Ground state energies of the two-electron ions.

Z	-E	Z	-E
1	0.5277510118	6	32.4062465980
2	2.9037243736	7	44.7814451450
3	7.2799134096	8	59.1565951190
4	13.6555662340	9	75.5317123575
5	22.0309715742	10	93.9068065072

**Table 2.3.2:** Excited state energies for the two-electron ions. The tabulated entries are -E values.

<i>n</i>	<i>n</i> <sup>1</sup> S	<i>n</i> <sup>3</sup> S	<i>n</i> <sup>1</sup> P	<i>n</i> <sup>3</sup> P	<i>n</i> <sup>1</sup> D	<i>n</i> <sup>3</sup> D
<b>He</b>						
2	2.1459740292	2.175229378176	2.1238430802	2.1331641816		
3	2.0612719720	2.068689067283	2.0551463570	2.0580810772	2.0556207320	2.0556363088
4	2.0335866995	2.036512082933	2.0310696464	2.0323243343	2.0312798445	2.0312888462
5	2.0211768309	2.022618871382	2.0199059849	2.0205511765	2.0200158297	2.0200210228
6	2.0145630847	2.015377452422	2.0138339705	2.0142079455	2.0138982125	2.0139014058
<b>Li<sup>+</sup></b>						
2	5.0408767313	5.110727372509	4.9933510721	5.0277156770		
3	4.7337560778	4.752076455858	4.7202068728	4.7304596641	4.7223909884	4.7225269124
4	4.6297835973	4.637136594629	4.6241513904	4.6284635563	4.6250741241	4.6251507732
5	4.5824279527	4.586092669796	4.5795665136	4.5817684035	4.5800386956	4.5800824257
6	4.5569531770	4.559038618569	4.5553050672	4.5565767839	4.5555781668	4.5556048684

**Table 2.3.2:** Continued

$n$	$n^1S$	$n^3S$	$n^1P$	$n^3P$	$n^1D$	$n^3D$
<b>Be<sup>2+</sup></b>						
2	9.1848738775	9.297166589741	9.1107716142	9.1749731379		
3	8.5173125465	8.546972068861	8.4959696290	8.5146043598	8.5002158256	8.5005823430
4	8.2884946257	8.300455559448	8.2795901070	8.2873636556	8.2813398059	8.2815437460
5	8.1836933067	8.189674851615	8.1791606106	8.1831162879	8.1800459490	8.1801615797
6	8.1271314968	8.130543857315	8.1245176279	8.1267982858	8.1250265700	8.1250969820
<b>B<sup>3+</sup></b>						
2	14.5785280140	14.733897348781	14.4772832536	14.5731376855		
3	13.4119969317	13.453104279643	13.3827148799	13.4100684802	13.3891003003	13.3897715900
4	13.0097268262	13.026336958201	12.9974920527	13.0088461365	13.0000805582	13.0004510123
5	12.8249726477	12.833292190279	12.8187397926	12.8245054260	12.8200397689	12.8202490428
6	12.7250966433	12.729848532224	12.7215005159	12.7248212316	12.7222447566	12.7223719380

Table 2.3.2: Continued

$n$	$n^1S$	$n^3S$	$n^1P$	$n^3P$	$n^1D$	$n^3D$
<b>C<sup>4+</sup></b>						
2	21.2220176846	21.420755902276	21.0933323009	21.2217106899		
3	19.4178085256	19.470403018010	19.3805212872	19.4167350899	19.3890591297	19.3900835047
4	18.7934728766	18.814746155889	18.7778829584	18.7928646702	18.7813037746	18.7818659335
5	18.5062606182	18.516925265508	18.4983154158	18.5059126325	18.5000241801	18.5003410100
6	18.3508450160	18.356940714471	18.3462597407	18.3506323301	18.3472352426	18.3474274513
<b>N<sup>5+</sup></b>						
2	29.1154156939	29.357681737453	28.9591163884	29.1205017383		
3	26.5347425711	26.598842151505	26.4894160317	26.5345607879	26.5001032847	26.5015131871
4	25.6397276201	25.665670121432	25.6207701763	25.6394021159	25.6250147845	25.6257854177
5	25.2275537939	25.240566728042	25.2178904229	25.2273293146	25.2200020950	25.2204356552
6	25.0043744608	25.011815871593	24.9987967976	25.0042266641	24.9999996437	25.0002624364

**Table 2.3.2:** Continued

<i>n</i>	<i>n</i> <sup>1</sup> S	<i>n</i> <sup>3</sup> S	<i>n</i> <sup>1</sup> P	<i>n</i> <sup>3</sup> P	<i>n</i> <sup>1</sup> D	<i>n</i> <sup>3</sup> D
<b>O<sup>6+</sup></b>						
2	38.2587572858	38.544647320047	38.0747352216	38.2694227099		
3	34.7627955284	34.838409733347	34.7094102328	34.7635258578	34.7222401098	34.7240581557
4	33.5484880064	33.579102862297	33.5261562824	33.5484506942	33.5312171008	33.5322078221
5	32.9888503818	33.004213186445	32.9774656338	32.9887515913	32.9799754101	32.9805320322
6	32.6856837812	32.694471907219	32.6791119566	32.6856019862	32.6805390523	32.6808762344
<b>F<sup>7+</sup></b>						
2	48.6520616174	48.981638329481	48.4402442655	48.6684272877		
3	44.1019650589	44.189099531881	44.0405090344	44.1036200619	44.0554745177	44.0577170337
4	42.5197521738	42.555041240113	42.4940420497	42.5200063687	42.4999130671	42.5011322182
5	41.7901492430	41.807862859144	41.7770412551	41.7901774414	41.7799453295	41.7806295778
6	41.3947722847	41.404907718164	41.3872052791	41.3947571531	41.3888543015	41.3892685098

**Table 2.3.2:** Continued

$n$	$n^1S$	$n^3S$	$n^1P$	$n^3P$	$n^1D$	$n^3D$
<b>Ne<sup>8+</sup></b>						
2	60.2953400241	60.668646584034	60.0556767280	60.3174888147		
3	54.5522496178	54.650907980593	54.4827150911	54.5548375693	54.4998098479	54.5024889781
4	52.5535190410	52.593483453112	52.5244280976	52.5540668527	52.5311042674	52.5325580331
5	51.6314496325	51.651514721700	51.6166173033	51.6316056912	51.6199126928	51.6207279447
6	51.1316395090	51.143122668823	51.1230767283	51.1316914644	51.1249458082	51.1254391359

Independent checks of wavefunction accuracy can be made with the help of cusp conditions [2.36-2.40]. In particular, the electron-nuclear cusp condition [2.36-2.38] states

$$C_{en} = \left[ \frac{-\rho'(r)}{2Z\rho(r)} \right]_{r=0} = 1 \quad (2.22)$$

in which  $\rho(r)$  is the spherically averaged electron number density. The electron-electron cusp condition [2.36][2.37][2.39] reads

$$C_{ee} = [h'(u)/h(u)]_{u=0} = 1 \quad (2.23)$$

in which  $h(u)$  is the spherical average of the interelectronic density. Equation (2.22) is satisfied trivially by virtue of the Pauli principle for states of maximum spin multiplicity (i.e. triplet states in two-electron systems). In such cases, there is a higher-order cusp condition [2.40]:

$$C_{ee} = \left[ \frac{2h^{(3)}(u)}{3h''(u)} \right]_{u=0} = 1 \quad (2.24)$$

Since exact wavefunctions satisfy the cusp conditions exactly, a measure of the quality of an approximate wavefunction is the degree to which it satisfies them. The one-electron cusp condition of equation (2.22) is easier to satisfy than the two-electron cusp conditions of equations (2.23) and (2.24). For these 100-term expansions, the largest deviation of  $C_{en}$  from unity is only  $7.1 \times 10^{-5}$  for the  $2^1S$  state of  $B^{3+}$ , whereas the largest deviation of  $C_{ee}$  from unity is 0.20 for the  $6^1D$  state of  $B^{3+}$ . The average deviations from unity are  $9 \times 10^{-6}$  for  $C_{en}$  and 0.045 for  $C_{ee}$ . The average  $C_{ee}$  deviations for states of the

same symmetry are 0.037, 0.016, 0.031, 0.060, 0.067 and 0.071 for the  $^1S$ ,  $^3S$ ,  $^1P$ ,  $^3P$ ,  $^1D$  and  $^3D$  states, respectively. Similarly, the average  $C_{en}$  deviations for states of the same symmetry are  $1.4 \times 10^{-5}$ ,  $2.2 \times 10^{-6}$ ,  $1.3 \times 10^{-5}$ ,  $1.1 \times 10^{-5}$ ,  $6.7 \times 10^{-6}$ , and  $5.2 \times 10^{-6}$  for the  $^1S$ ,  $^3S$ ,  $^1P$ ,  $^3P$ ,  $^1D$  and  $^3D$  states, respectively. For each state, the deviations averaged over all the ions tend to increase as the principal quantum number increases. For each symmetry, the deviations averaged over principal quantum number tend to remain constant as the nuclear charge increases. For all 261 states, appendix 3 shows  $C_{en}$ ,  $\rho(0)$ ,  $C_{cc}$ , and, depending on the spin state,  $h(0)$  or  $h''(0)$ .

The exact long range behaviour [2.41][2.42] of  $\rho(r)$  can be used to determine the distance up to which the approximate wavefunctions are accurate. Thus, plots of  $\ln(\rho(r)/\rho(0))$  versus  $\alpha r = 2(2I)^{1/2}r$ , where  $I$  is the ionization energy, should become and stay linear as  $r$  becomes sufficiently large. Figure 2.3.1 shows asymptotic density plots for the  $3^1S$ ,  $3^1P$ , and  $3^1D$  states of He,  $\text{Be}^{2+}$ ,  $\text{C}^{4+}$ , and  $\text{Ne}^{8+}$ . An approximate density does lead to a linear plot at large  $r$  but deviates from linearity at an even larger  $\alpha r$ , say  $(\alpha r)_{max}$ . The latter gives the upper limit to the range within which the approximate wavefunction is accurate. With the exception of the  $3^1S$  state where  $(\alpha r)_{max} \approx 35$ , the upper limits are as follows:  $(\alpha r)_{max} \approx 40$  for the  $n=3$  and  $n=4$  states, and  $(\alpha r)_{max} \approx 45$  for the  $n=5$  and  $n=6$  states. These limits are quite conservative and may generally be extended for the triplet states and for the high-Z ions. Occasionally, as exemplified by the  $3^1S$  states of  $\text{C}^{4+}$  and  $\text{Ne}^{8+}$ , a deviation from linearity does not occur.

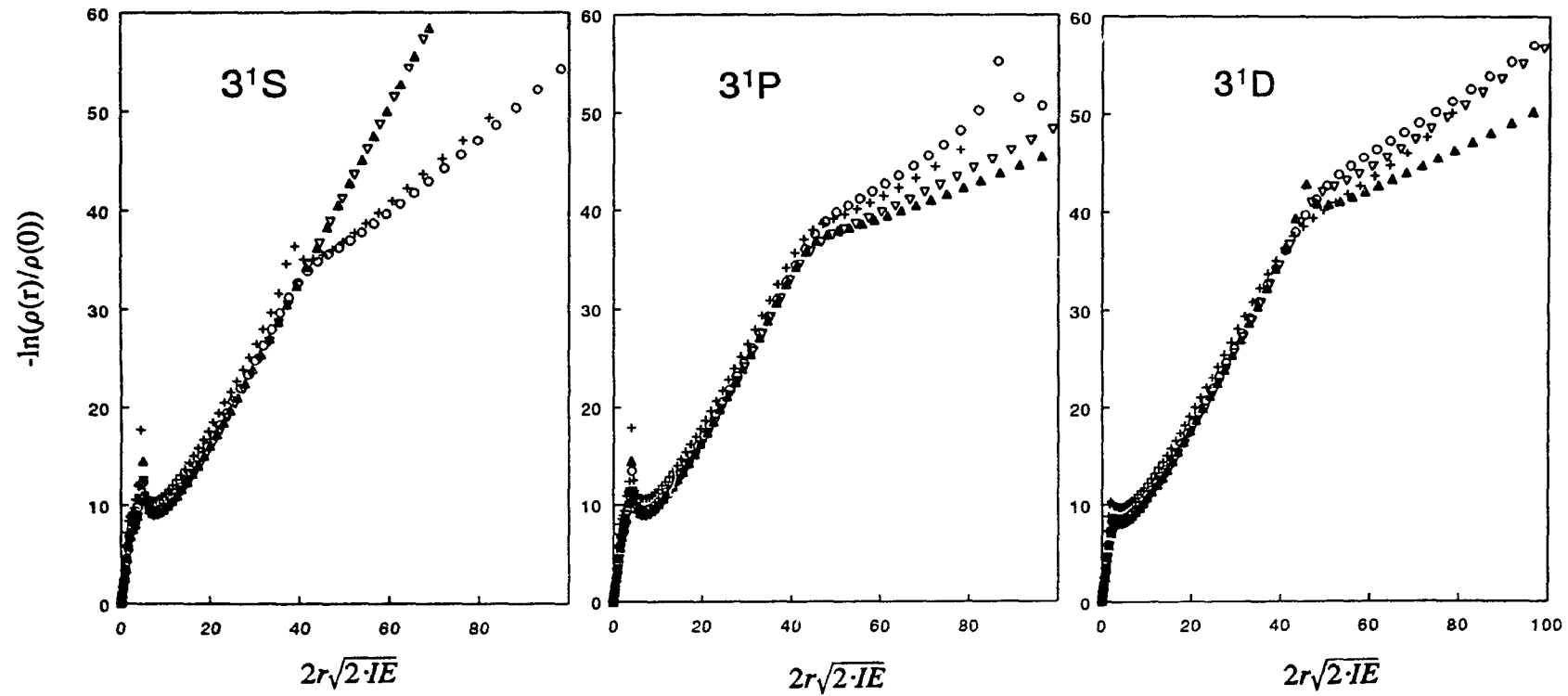


Figure 2.3.1: Asymptotic density plots for the  $Z=2$  (+),  $Z=4$  (o),  $Z=6$  (▲), and  $Z=10$  (▼) ions of the  $3^1S$ ,  $3^1P$ , and  $3^1D$  states.

Z-scaling of the coordinates and treatment of the interelectronic repulsion as a perturbation leads to so-called 1/Z perturbation theory [2.43]. Within this context, the 1/Z expansion for the energy is given by

$$E/Z^2 = \epsilon_0 + \epsilon_1/Z + \epsilon_2/Z^2 + \dots \quad (2.25)$$

The first two coefficients in this expansion are well known and have been tabulated [2.44]. Higher coefficients have been calculated for the energies of some states by variational perturbation methods [2.45-2.50][2.21] and by fitting [2.51][2.45] variationally calculated energies [2.4][2.5].

Some higher order energy coefficients were determined by fitting our calculated energies using a least squares procedure in which the first two coefficients were constrained to the known values [2.44]. Table 2.3.3 lists the estimates of  $\epsilon_i$ ,  $i=2,3,4$  for the 6S and 6P states which were not considered by Blanchard [2.51], and for all the D states calculated. The latter are included because the existing variational perturbation estimates [2.50] were based on wavefunctions that did not include  $pp$  type terms which are necessary for angular completeness [2.1][2.2]. The L state expansion coefficients should be more accurate than previous estimates.

For the 261 states considered, these variational energies are the lowest available for 180 states. The energies, the cusp conditions, and the long range behaviour of  $\rho(r)$  clearly demonstrate the accuracy of these 100-term wavefunctions. The expansions are compact enough to render the calculation of properties computationally feasible. Indeed, the following chapters explore various properties of the two-electron ions.

**Table 2.3.3:** Energy 1/Z expansion coefficients.

<b>State</b>	$\epsilon_1$	$\epsilon_2$	$\epsilon_3$	$\epsilon_4$
$6^1S$	0.02701804	-0.012902	-0.00024	-0.0006
$6^3S$	0.02566888	-0.010880	-0.00040	-0.0002
$6^1P$	0.02801529	-0.014317	-0.00026	0.0001
$6^3P$	0.02694951	-0.012256	-0.00039	-0.0003
$3^1D$	0.11127014	-0.057486	0.00609	-0.0084
$4^1D$	0.06258203	-0.032170	0.00281	-0.0038
$5^1D$	0.04004495	-0.020492	0.00149	-0.0020
$6^1D$	0.02780463	-0.014180	0.0009	-0.0012
$3^3D$	0.11077576	-0.054620	-0.00071	0.0000
$4^3D$	0.06231832	-0.030687	-0.00056	0.0001
$5^3D$	0.03989813	-0.019677	-0.00034	0.0001
$6^3D$	0.02771614	-0.013691	-0.00021	0.0001

Larger wavefunction expansions were explored for the ground states of the ions. Optimizations were performed for 200-term ground state expansions of the ions from H<sup>-</sup> to Ne<sup>8+</sup>. These wavefunctions are used only in section 3.3 where high order  $\rho(r)$  derivatives require longer expansions for improved accuracy. The energies, cusp ratios, virial scale factor and 6 nonlinear parameters are presented in table 2.3.4. Note that the energies lie no more than 0.2 nE<sub>H</sub> above the best values [2.10][2.34] and that the quality checks are generally, but not always, better than for the 100 term expansions.

Table 2.3.4: Energies, cusp ratios, and nonlinear parameters for 200-term optimized ground state wavefunctions.

Z	A <sub>1</sub>	A <sub>2</sub>	B <sub>1</sub>	B <sub>2</sub>	G <sub>1</sub>	G <sub>2</sub>	-E	1- $\eta$	1-C <sub>en</sub>	1-C <sub>ee</sub>
1	0.22277	1.58047	0.98603	1.33237	-0.16261	0.76359	0.527751016281	-1.42(-9)	5.06(-7)	1.31(-3)
2	0.93207	4.41725	1.34173	2.46510	-0.34001	4.03096	2.903724376929	-1.97(-11)	-6.78(-6)	2.42(-4)
3	2.20406	7.17283	2.63988	4.03710	-0.85676	4.82404	7.279913412524	-1.28(-12)	-1.40(-5)	6.28(-4)
4	4.35918	6.53686	3.12285	5.85291	-1.78672	7.88129	13.655566238179	-8.08(-12)	-6.37(-6)	-3.51(-5)
5	4.89692	9.36941	4.03027	6.81454	-2.46245	11.30347	22.030971580017	1.76(-11)	-1.86(-6)	-2.66(-5)
6	5.02039	13.49428	4.45850	7.72208	-1.79048	12.30529	32.406246601742	-5.83(-12)	-9.14(-7)	2.46(-4)
7	6.11702	16.25412	4.84057	8.44120	-0.11014	15.45213	44.781445148647	-3.06(-13)	-3.95(-6)	3.04(-4)
8	7.05038	19.24198	5.65154	9.63271	-0.10786	16.96292	59.156595122632	2.91(-13)	-2.86(-6)	3.19(-4)
9	8.14267	21.84701	6.26792	10.55040	-0.16743	18.98332	75.531712363809	1.01(-13)	-3.98(-7)	3.49(-4)
10	9.01270	21.68220	6.64115	12.26376	-0.15530	24.30036	93.906806514902	-6.48(-13)	-2.85(-6)	3.14(-4)

## CHAPTER 3: DENSITIES AND INTRACULES

### 3.1 Overview

The electronic charge density provides a bridge between sophisticated quantum mechanical calculations and the intuitive chemical picture of a molecule composed of atoms [3.1]. It is the fundamental quantity in density functional theory [3.2]. Generic knowledge of the intracule, or interelectronic, density [3.3] can be used to improve theories of electron correlation. Hence, charge densities, and to a much lesser extent, intracule densities, have been studied extensively by quantum chemical calculation [3.1][3.3] and by experimental techniques [3.4][3.5]. However, most such studies deal with the ground state, and those that consider excited states focus on only a few states.

The physically meaningful densities are ensemble averages over the manifold of degenerate states corresponding to the same  $n$ ,  $L$  and spin multiplicity. These ensemble averages are equivalent to a spherical average of the density of any state in this manifold. Thus the distribution functions studied are the spherically averaged charge density  $\rho(r)$ , the radial charge density  $D(r)$ , the spherically averaged intracule density  $h(u)$  and the radial intracule density  $P(u)$  where  $r$  and  $u$  are electron-nucleus and interelectronic distances, respectively. These distributions can be written as expectation values as follows:

$$D(r) = 4\pi r^2 \rho(r) = \sum_k \langle \Psi | \delta(r - r_k) | \Psi \rangle \quad (3.1)$$

and

$$P(u) = 4\pi u^2 h(u) = \sum_{i>j} \langle \Psi | \delta(u - r_{ij}) | \Psi \rangle \quad (3.2)$$

Physically,  $D(r) dx$  is the probability of finding an electron at a distance between  $r$  and  $r+dr$  from the nucleus and  $P(u) du$  is the probability of finding the two electrons separated by a distance between  $u$  and  $u+du$ . Ideally, since the state of a system is completely specified by its wavefunction, the product  $\Psi^*(\vec{x}_1, \dots, \vec{x}_n) \Psi(\vec{x}_1, \dots, \vec{x}_n) d\vec{x}_1 \cdots d\vec{x}_n$ , where  $\vec{x}_i = (\vec{r}_i, \sigma_i)$  is the combined "pace-spin coordinate, would be studied since it gives the probability of finding an electron of spin  $\sigma_1$  at  $\vec{r}_1$  with volume element  $d\vec{r}_1$ , an electron with spin  $\sigma_2$  at  $\vec{r}_2$  with volume element  $d\vec{r}_2$ , ..., and an electron with spin  $\sigma_n$  at position  $\vec{r}_n$  with volume element  $d\vec{r}_n$ . However, the latter product is a  $3n$ -dimensional function and consequently difficult to analyze and interpret. Equations (3.1) and (3.2) are two useful 1-dimensional contractions of the  $3n$ -dimensional function. Several reviews [3.6][3.3][3.7] analyze these and many other possible contractions.

An antisymmetric wavefunction must vanish when electrons of like spin occupy the same location in space; thus  $h(0) = 0$  in the triplet states. Several of the features of  $\rho(r)$  and  $h(u)$ , in particular the singlet-triplet differences, may be explained by the presence of this "Fermi" correlation in the triplet states.

Charge and intracule densities, obtained from integral transform wavefunctions, have been examined previously for the five lowest states of the two-electron ions [2.25][3.8][3.9]. Analytic  $\rho(r)$  and  $h(u)$  formulae have been published by Thakkar and Smith for the S states [3.8], and Regier and Thakkar [3.9] for the P states. The ground state functions, obtained from 20 to 66 term expansions, were examined for the two electrons ions from  $H^-$  to  $Mg^{+10}$  [3.8]. The charge and intracule densities for the  $2^1P$ ,  $2^3P$ ,  $2^1S$  and  $2^3S$  states for the ions from He to  $Mg^{+10}$  were obtained from 20 to 55 term expansions [3.9]. Several interesting features of  $\rho(r)$  and  $h(u)$  were noted in these studies. With the exception of the  $2^1S$  states of He,  $Li^+$ , and  $Be^{2+}$ , the charge densities are monotonically decreasing. For the highly charged ions in the  $2^1P$  and  $2^3P$  states,  $D(r)$  does not reveal shell structure. With the exception of the  $2^1S$  state where a local maximum appears at  $Zu \approx 2$ ,  $P(u)$  displays only one maximum.

In order to fully understand the behaviour of the charge and intracule densities for the two-electron ions, the above work was extended to the next 24 Rydberg states ( $n^1S$ ,  $n^3S$ ,  $n^1P$ ,  $n^3P$ ,  $n^1D$ , and  $n^3D$  with  $n=3-6$ ) for each of the nine heliumlike ions from He through  $Ne^{8+}$ . Charge and intracule density variations with respect to nuclear charge Z, angular momentum L, degree of excitation and spin multiplicity are examined. All calculations are performed using the-100 term integral transform wavefunctions discussed in chapter 2.

The charge and intracule densities are often compared to the distributions obtained in the limit of infinite Z. For a given n and L, hydrogenic wavefunctions of the form

$$\Psi(\vec{r}_1, \vec{r}_2) = \frac{1}{\sqrt{2}} (1 \pm \hat{P}_{12}) \psi_1^0(Z\vec{r}_1) \psi_n^L(Z\vec{r}_2), \quad (3.3)$$

where  $\psi_n^L$  are hydrogenic orbitals, are the exact infinite  $Z$  limit wavefunctions. The appropriate integrals ((3.1) and (3.2)) are evaluated using these wavefunctions. The charge and intracule densities obtained are useful references when variations with  $Z$  are under consideration.

Expectation values of the form  $\langle f(r) \rangle$  and  $\langle g(u) \rangle$ , where  $f(r)$  and  $g(u)$  are multiplicative operators, are readily obtained from the charge and intracule densities, respectively:

$$\langle f(r) \rangle = \int_0^\infty D(r) f(r) dr \quad (3.4)$$

$$\langle g(u) \rangle = \int_0^\infty P(u) g(u) du \quad (3.5)$$

The moments of  $\rho(r)$  and  $h(u)$ , obtained by choosing  $f(r)=r^k$  and  $g(u)=u^k$ , were calculated for each state of each ion and for  $k=-2, \dots, +4$ . These calculations are performed by numerically integrating the integrals in equations (3.4) and (3.5). More specifically, scaled Gauss-Laguerre quadratures are employed. This numerical integration scheme makes the approximation

$$\int_0^\infty e^{-x} f(x) dx \approx \sum_{i=1}^N w_i f(x_i) \quad (3.6)$$

where the weights  $w_i$  and quadrature points  $x_i$  are chosen to calculate  $f(x)=x^k$ , where  $k=0, \dots, 2N-1$  (ie  $\Gamma(2N), \dots, \Gamma(1)$ ) exactly. The moments are calculated using the

transformation

$$\begin{aligned} \int_0^\infty f(x) dx &= \int_0^\infty e^{-ax} e^{ax} f(x) dx = \frac{1}{a} \int_0^\infty e^{-y} e^y f(y/a) dy \\ &\approx \frac{1}{a} \sum_{i=1}^N w_i e^{y_i} f(y_i/a) \end{aligned} \quad (3.7)$$

The parameter  $a$  scales the quadrature scheme and may be varied to improve the accuracy of the moments for fixed  $N$ .

The analytic formulae for computing  $\rho(r)$  and  $h(u)$  from the D state wavefunctions are given in appendix 4. Numerical instabilities which arise for certain values of the parameters were circumvented by procedures entirely analogous to those described previously for the S [3.8] and P [3.9] states. Furthermore, all calculations were performed in quadruple precision to alleviate problems arising from near linear dependence of the basis geminals. Both  $\rho(r)$  and  $h(u)$  were tabulated on a mesh of 140 ( $Z-1$ )-scaled arguments (that is,  $a = Z-1$ ).

The moments of  $\rho(r)$  and  $h(u)$  were computed by using 64-point Gauss-Laguerre quadratures. For the  $n=3$  states, the quadratures were  $Z$ -scaled, but  $(Z-1)$ -scaling was used for the  $n=4-6$  states. The accuracy of the numerical integrations was assessed using two different techniques. The moments  $\langle r^0 \rangle$  and  $\langle u^0 \rangle$  are obtained from numerical integration and compared to their exact values:  $\langle r^0 \rangle = n$  and  $\langle u^0 \rangle = n(n-1)/2$  where  $n$  is the number of electrons. Moreover, the moments  $\langle 1/r \rangle$  and  $\langle 1/u \rangle$  were computed directly from the wavefunctions and compared with the values computed using the 64-point Gauss-Laguerre quadrature.

### 3.2 $\rho(r)$ , $D(r)$ , $h(u)$ , and $P(u)$ : Structure, trends, and moments

Representative charge densities  $\rho(r)$  and  $D(r)$  are shown in Figure 3.2.1 for the  $4^1S$  states of He,  $\text{Ne}^{8+}$ , and the infinite  $Z$  limit. It is convenient to consider the behaviour of  $\rho(r)$  in three separate regions: small  $r$  ( $0 < Zr \leq 4$ ), intermediate  $r$  ( $4 < Zr < 8$ ), and large  $r$  ( $Zr \geq 8$ ). In the small  $r$  region,  $\rho(r)$  is essentially a hydrogenic  $1s$  density. For given  $n$ ,  $L$  and spin multiplicity, the charge densities of the ions in the intermediate and large  $r$  regions can be brought into rough coincidence by  $(Z-l)$ -scaling. In the intermediate  $r$  region, the densities generally have either an inflection point or a minimum followed by a slight maximum. The inflection points are more pronounced for the low- $Z$  ions and for the singlet states. The minimum appears for all the ions in the 3D states and for the low- $Z$  ions of the higher D states. In the large  $r$  region, the charge densities of the S, P, and D states have  $n-2$ ,  $n-2$ , and  $n-3$  pseudo-nodes, respectively, that are really minima at which  $\rho(r) \approx 0$ . In the vicinity of a pseudo-node,  $\rho(r)$  changes by several orders of magnitude within a very narrow range of electron-nucleus distances; thus the pseudo-node appears at the bottom of a narrow and steep well. The depth of this well increases as the node becomes further removed from the nucleus. The triplet pseudo-nodes are more shallow than their singlet counterparts since they always appear at smaller  $r$ .

The radial probability densities for the electron-nucleus separation,  $D(r)$ , display a sharp peak at small  $r$  that corresponds to the core electron. The hydrogenic model predicts  $n-L$  peaks corresponding to the outer electron. However,  $n-2$  maxima beyond the small  $r$  peak are observed for most of the 216 states considered in this work. The

only exceptions are the  $3^1S$  and  $4^1S$  states of He which have  $n-1$  outer maxima, and the  $6^1D$  and  $6^3D$  states of the high  $Z$  ions which have  $n-3$  outer maxima.  $Z$ -scaling of  $D(r)$  for a fixed state of all the ions does bring the small  $r$  peaks into coincidence. However, as  $Z$  increases, the outer region of the  $Z$ -scaled  $D(r)$  contracts significantly, the peaks in the large  $r$  region increase in magnitude and shift to smaller  $Zr$ , and the intermediate  $r$  structure disappears.

Charge densities of the Rydberg states of the heliumlike ions can be modelled by screened hydrogenic densities of the form [2.25][3.9]

$$\hat{\rho}_{nL}(r) = (4\pi)^{-1} \left[ |R_1^0(Zr)|^2 + |R_n^L((Z-\sigma)r)|^2 \right] \quad (3.8)$$

in which  $R_n^L$  is a radial hydrogenic function. The choices  $\sigma=0$  and  $\sigma=1$  correspond to the hydrogenic and perfect screening approximations, respectively. The latter has proven useful for the analysis of charge densities for the He S states [2.25], and the 2S and 2P states of the heliumlike ions [3.9].

As discussed in chapter 2, the convergence of Hylleraas-type wavefunctions has been accelerated by including a perfectly screened hydrogenic term [2.10-2.12]. Perhaps greater acceleration could be achieved by using an optimized screening constant  $\sigma$ . There are several plausible methods for choosing  $\sigma$  including minimization of the variational energy. An obvious method is to minimize, in a least squares fashion, the difference between the model and accurate charge density. Moreover, since the screened hydrogenic term is thought to be useful because it helps get the correct nodal structure, one could also choose  $\sigma$  by forcing the model density to have a pseudo-node at the right

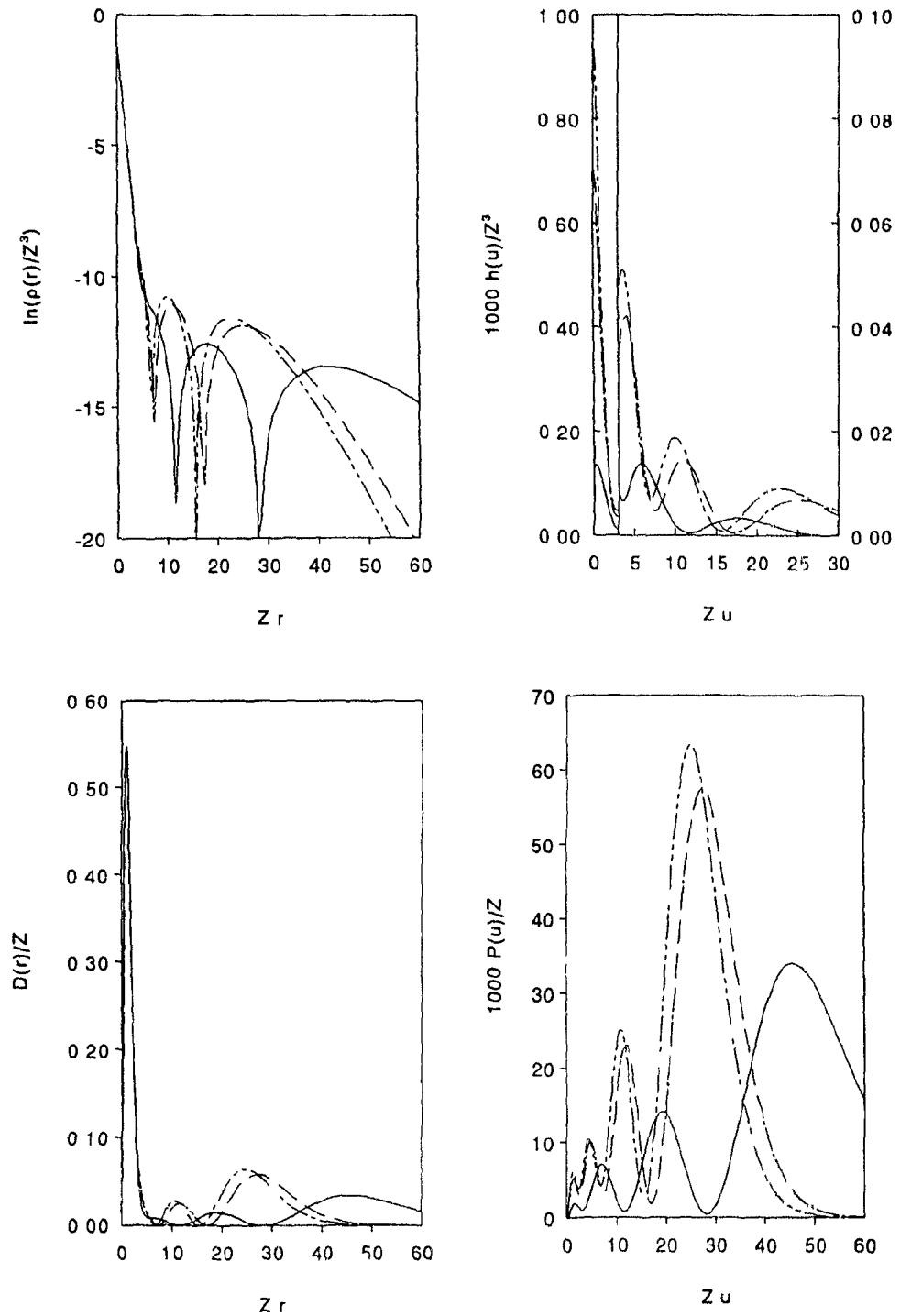


Figure 3.2.1: Spherically averaged and radial charge and intracule densities for the  $4^1S$  states of He (—),  $\text{Ne}^{8+}$  (----) and  $Z=\infty$  (---).

location. Since there are several pseudo-nodes in the states with larger  $n$ , this too leads to several estimates of  $\sigma$ .

If the screened hydrogenic model is a good one, then all the above estimates of  $\sigma$  should be similar. Consider the  $4^1S$  and  $4^3S$  states of He as test cases. The perfect screening approximation predicts pseudo-nodes at  $r=6.6$  and  $r=15.5$  whereas the observed ones occur at  $r=5.7$  and  $r=14$  for the singlet and  $r=4.9$  and  $r=12.5$  for the triplet. Exact location of the pseudo-nodes requires  $\sigma=0.84$  and  $\sigma=0.89$  for the singlet, and  $\sigma=0.65$  and  $\sigma=0.76$  for the triplet state. In both cases, larger  $\sigma$  estimates are obtained from the outer pseudo-nodes. The least squares procedure yields  $\sigma=0.88$  and  $\sigma=0.83$  for the singlet and triplet states, respectively. The sum of squares error for the triplet is twice as large as for the singlet and comparatively insensitive to changes in  $\sigma$ . The perfect screening model is clearly an inadequate representation of the  $4S$   $\rho(r)$ ; imperfectly screened models are better especially for the  $4^1S$  where  $\sigma=0.88$  leads to a qualitatively correct  $\rho(r)$ .

We obtained estimates of  $\sigma$  for all 216 states considered in this work. The least squares values of  $\sigma$  range from 0.84 to 0.89 for the  $^1S$  states, from 0.71 to 0.86 for the  $^3S$  states, and between 0.98 and 1.00 for the P and D states. The fits are invariably better for the singlet than corresponding triplet states, and improve as  $n$  and  $L$  increase. Moreover, the fits for the triplet states are relatively insensitive to  $\sigma$ . The upper and lower limits in the  $\sigma$  ranges correspond to the low- $Z$  ions in the  $n=6$  states, and the high- $Z$  ions in the  $n=3$  states, respectively. For a given state and ion, the estimates of  $\sigma$  obtained from the pseudo-nodes approach unity as the node-nucleus distance increases.

Thus, perfect screening seems reasonable for the P and D states but optimization of  $\sigma$  is preferable in the S states.

The hydrogenic model predicts that both the spherically averaged intracule density  $h(u)$  and the radial probability density for the interelectronic distance  $P(u)$  should have  $n\text{-}L$  peaks. This is the case for 180 of the 216 states considered; the exceptions are the  $^1\text{S}$  states where an additional peak appears at small  $u$ . This additional small  $u$  maximum in the  $^1\text{S}$  states could be expected for the explicitly correlated wave functions since they satisfy  $h'(0)=h(0)\geq 0$  for a singlet state [2.37] and  $h'(0)=h(0)=0$  for a triplet state [2.38]. However, the magnitude of  $h(0)$  does not determine whether an additional maximum appears for the singlet; for example,  $h(0)$  is larger for the  $3^1\text{P}$  states than for the  $6^1\text{S}$  states but the latter displays an additional small  $u$  maximum while the former does not. The first  $^3\text{S}$  maximum occurs between the first two  $^1\text{S}$  maxima, and the remaining  $n\text{-}l$  maxima occur in pairs with the triplet maximum at smaller  $u$  than the singlet one. In the  $^1\text{P}$  states, the first maximum in  $h(u)$  occurs at smaller  $u$  whereas all the others occur at larger  $u$  relative to the corresponding  $^3\text{P}$  state. The  $^3\text{D}$  maxima in  $h(u)$  occur at slightly smaller  $u$  than for the corresponding  $^1\text{D}$  state. Representative examples of  $h(u)$  and  $P(u)$  are shown in Figure 3.2.1 for the  $4^1\text{S}$  states of He,  $\text{Ne}^{8+}$ , and the infinite Z limit.

In contrast with the charge density, the basic structure of the intracule density remains the same as the nuclear charge increases. The probability density for the interelectronic separation fluctuates considerably as  $u$  increases since the maxima are separated by vanishingly small minima. Although the peaks in  $h(u)$  decrease as the

interelectronic separation increases, the maxima in  $P(u)$  increase. Consider, for instance, the extrema in  $P(u)$  for the  $5^1P$  state of He:  $P(2.9)=0.071$ ,  $P(5.5)=0.006$ ,  $P(9.2)=0.124$ ,  $P(13.4)=0.004$ ,  $P(19.5)=0.206$ ,  $P(26.5)=0.002$ , and  $P(39.1)=0.448$ .

Variations in  $Z$  and  $L$ , and to a lesser degree  $n$ , strongly affect  $h(0)$ . For the  $Z$  and  $n$  considered here,  $h(0)$  ranges from 1.7 to 0.0003, 0.5 to 0.00003, and 0.02 to 0.0000005 for the  $^1S$ ,  $^1P$  and  $^1D$  states, respectively. As  $n$  increases from 3 to 6,  $h(0)$  decreases by factors of 8, 8, and 5 for the  $^1S$ ,  $^1P$  and  $^1D$  states, respectively. As  $Z$  increases from 2 to 10,  $h(0)$  increases by factors of 700, 2000 and 7000 for the  $^1S$ ,  $^1P$  and  $^1D$  states, respectively. The values of  $h(0)$  for P states are 3 to 10 times smaller than those for the S states. In turn, the values of  $h(0)$  for D states are 19 to 110 times smaller than those for the P states. When the angular momentum increases,  $h(0)$  decreases most for the low- $Z$  ions. Individual  $h(0)$  are tabulated in appendix 3.

A comparison of the moments  $\langle r^k \rangle$  and  $\langle u^k \rangle$ , where  $k=-2,-1,+1,+2$ , with published values [2.5] reveals that, with the exception of a handful of moments, all values lie within 1 or 2 digits of the last significant figure of the reference values. This comparison of moments also indicates that the present S state densities are more compact whereas the P state densities more diffuse than the reference [2.5] densities obtained from Hylleraas-type expansions. The moments which have not been tabulated previously are given in tables 3.2.1-3.2.6. Additional, large  $r$  and large  $u$  enhancing moments, obtained from choosing  $k=+3$ ,  $+4$ , have been included in Appendix 3.

The moments are useful tools in the analysis of charge and intracule densities. For instance, consider the values of  $\langle r^{-2} \rangle$ . These moments enhance the small  $r$  region

of  $\rho(r)$  and can be used to quantify the contribution of the outer electron to the core density. Hence as  $n$  increases,  $\langle r^{-2} \rangle$  decreases. Consistent with the fact that  $\rho(0) \neq 0$  for electrons in spherically symmetric orbitals, the values are larger for the S states than for the P and D states. The effects of spin on  $\rho(r)$  are often evident from a comparison of  $\langle r^{-2} \rangle$  values for different spin states. For instance, the triplet values are generally larger than the singlet values for the S states but smaller for the P and D states. The comparison of singlet and triplet  $\rho(r)$ , discussed in section 3.4, reflect this difference in the small  $r$  region between the S states and the P and D states. Finally, the significant increase of  $\langle r^{-2} \rangle$  with  $Z$  shows the considerable contraction of  $\rho(r)$  as  $Z$  increases.

Clearly the  $\rho(r)$  and  $h(u)$  structure vary strongly with respect to  $Z$ ,  $n$ , and  $L$ . Having systematically analysed the general trends, the next two sections address more subtle effects: section 3.3 considers the monotonicity of the ground state densities; singlet-triplet differences are analysed in section 3.4.

Table 3.2.1: Moments for the  ${}^1S$  states of the two-electron ions.

	He	$\text{Li}^+$	$\text{Be}^{2+}$	$\text{B}^{3+}$	$\text{C}^{4+}$	$\text{N}^{5+}$	$\text{O}^{6+}$	$\text{F}^{7+}$	$\text{Ne}^{8+}$
$3^1\text{S}$	$\langle r^{-2} \rangle$	8.08087	18.3102	32.6874	51.2124	73.8856	100.707	131.676	166.794
	$\langle r^{-1} \rangle$	2.11703	3.22800	4.33912	5.45025	6.56137	7.67249	8.78361	9.89473
	$\langle u^{-2} \rangle$	0.04065	0.16112	0.36255	0.64432	1.00611	1.44781	1.96937	2.57075
	$\langle u^{-1} \rangle$	0.11151	0.21648	0.32185	0.42725	0.53262	0.63797	0.74330	0.84862
$4^1\text{S}$	$\langle r^{-2} \rangle$	8.03297	18.1285	32.2862	50.5064	72.7891	99.1341	129.542	164.012
	$\langle r^{-1} \rangle$	2.06497	3.12745	4.18997	5.25249	6.31500	7.37751	8.44001	9.50252
	$\langle u^{-2} \rangle$	0.01671	0.06730	0.15200	0.27043	0.42246	0.60802	0.82710	1.07969
	$\langle u^{-1} \rangle$	0.06276	0.12278	0.18290	0.24300	0.30306	0.36310	0.42312	0.48314
$5^1\text{S}$	$\langle r^{-2} \rangle$	8.01652	18.0651	32.1455	50.2577	72.4019	98.5781	128.787	163.026
	$\langle r^{-1} \rangle$	2.04125	3.08126	4.12127	5.16128	6.20129	7.24130	8.28130	9.32130
	$\langle u^{-2} \rangle$	0.00841	0.03421	0.07745	0.13793	0.21554	0.31032	0.42222	0.55120
	$\langle u^{-1} \rangle$	0.04016	0.07891	0.11771	0.15648	0.19522	0.23396	0.27268	0.31140

Table 3.2.1: Continued.

	He	$\text{Li}^+$	$\text{Be}^{2+}$	$\text{B}^{3+}$	$\text{C}^{4+}$	$\text{N}^{5+}$	$\text{O}^{6+}$	$\text{F}^{7+}$	$\text{Ne}^{8+}$	
$6'S$	$<\mathbf{r}^{-2}>$	8.00944	18.0374	32.0836	50.1484	72.2321	98.3335	128.454	162.593	200.750
	$<\mathbf{r}^{-1}>$	2.02850	3.05628	4.08407	5.11186	6.13964	7.16742	8.19520	9.22298	10.2508
	$<\mathbf{r}^{+1}>$	52.2648	26.8397	18.0734	13.6274	10.9382	9.13594	7.84383	6.87205	6.11460
	$<\mathbf{r}^{+2}>$	2965.73	775.521	350.186	198.587	127.729	88.9991	65.5460	50.2759	39.7814
	$<\mathbf{u}^{-2}>$	0.00481	0.01969	0.04466	0.07959	0.12444	0.17919	0.24383	0.31837	0.40280
	$<\mathbf{u}^{-1}>$	0.02788	0.05494	0.08203	0.10909	0.13614	0.16319	0.19022	0.21726	0.24429
	$<\mathbf{u}^{+1}>$	51.5222	26.3460	17.7036	13.3317	10.6919	8.92491	7.65923	6.70799	5.96697
	$<\mathbf{u}^{+2}>$	2965.74	775.527	350.188	198.589	127.730	88.9997	65.5464	50.2762	39.7816

Table 3.2.2: Moments for the  ${}^3S$  states of the two-electron ions.

	He	$\text{Li}^+$	$\text{Be}^{2+}$	$\text{B}^{3+}$	$\text{C}^{4+}$	$\text{N}^{5+}$	$\text{O}^{6+}$	$\text{F}^{7+}$	$\text{Ne}^{8+}$
${}^3\text{S}$	$\langle \text{r}^{-2} \rangle$	8.08588	18.3249	32.7129	51.2494	73.9343	100.767	131.749	166.878
	$\langle \text{r}^{-1} \rangle$	2.12735	3.23922	4.35053	5.46172	6.57287	7.68400	8.79513	9.90625
	$\langle \text{u}^{-2} \rangle$	0.02310	0.07445	0.15375	0.26104	0.39631	0.55958	0.75085	0.97013
	$\langle \text{u}^{-1} \rangle$	0.11732	0.21352	0.30819	0.40240	0.49642	0.59035	0.68422	0.77805
${}^4\text{S}$	$\langle \text{r}^{-2} \rangle$	8.03356	18.1311	32.2915	50.5146	72.8002	99.1484	129.559	164.032
	$\langle \text{r}^{-1} \rangle$	2.06914	3.13201	4.19461	5.25715	6.31967	7.38218	8.44469	9.50719
	$\langle \text{u}^{-2} \rangle$	0.00911	0.03052	0.06405	0.10971	0.16752	0.23746	0.31954	0.41376
	$\langle \text{u}^{-1} \rangle$	0.06526	0.12176	0.17753	0.23307	0.28852	0.34391	0.39928	0.45463
${}^5\text{S}$	$\langle \text{r}^{-2} \rangle$	8.01643	18.0654	32.1465	50.2597	72.4049	98.5822	128.791	163.033
	$\langle \text{r}^{-1} \rangle$	2.04334	3.08355	4.12360	5.16363	6.20364	7.24364	8.28365	9.32365
	$\langle \text{u}^{-2} \rangle$	0.00447	0.01532	0.03245	0.05587	0.08558	0.12158	0.16388	0.21246
	$\langle \text{u}^{-1} \rangle$	0.04145	0.07847	0.11507	0.15155	0.18798	0.22438	0.26076	0.29713

Table 3.2.2: Continued.

	He	$\text{Li}^+$	$\text{Be}^{2+}$	$\text{B}^{3+}$	$\text{C}^{4+}$	$\text{N}^{5+}$	$\text{O}^{6+}$	$\text{F}^{7+}$	$\text{Ne}^{8+}$
$6^3\text{S}$	$<\mathbf{r}^{-2}>$	8.00924	18.0372	32.0838	50.1489	72.2326	98.3347	128.455	162.595
	$<\mathbf{r}^{-1}>$	2.02969	3.05760	4.08541	5.11320	6.14098	7.16877	8.19655	9.22433
	$<\mathbf{r}^{+1}>$	49.5429	25.9163	17.6157	13.3554	10.7582	9.00817	7.74847	6.79818
	$<\mathbf{r}^{+2}>$	2661.21	722.076	332.276	190.541	123.449	86.4587	63.9167	49.1693
	$<\mathbf{u}^{-2}>$	0.00252	0.00874	0.01863	0.03218	0.04939	0.07027	0.09481	0.12301
	$<\mathbf{u}^{-1}>$	0.02863	0.05471	0.08054	0.10630	0.13202	0.15773	0.18342	0.20911
	$<\mathbf{u}^{+1}>$	48.8009	25.4230	17.2463	13.0600	10.5122	8.79741	7.56410	6.63433
	$<\mathbf{u}^{+2}>$	2661.22	722.082	332.278	190.543	123.450	86.4592	63.9171	49.1696

Table 3.2.3: Moments for the  ${}^1\text{P}$  states of the two-electron ions.

	He	$\text{Li}^+$	$\text{Be}^{2+}$	$\text{B}^{3+}$	$\text{C}^{4+}$	$\text{N}^{5+}$	$\text{O}^{6+}$	$\text{F}^{7+}$	$\text{Ne}^{8+}$	
$3^1\text{P}$	$\langle \mathbf{r}^{-2} \rangle$	8.02581	18.1038	32.2307	50.4063	72.6307	98.9043	129.227	163.600	202.021
	$\langle \mathbf{u}^{-2} \rangle$	0.02567	0.11024	0.25892	0.47244	0.75091	1.09432	1.50265	1.97591	2.51405
$4^1\text{P}$	$\langle \mathbf{r}^{-2} \rangle$	8.01095	18.0437	32.0967	50.1705	72.2645	98.3794	128.515	162.672	200.849
	$\langle \mathbf{u}^{-2} \rangle$	0.01088	0.04685	0.10988	0.20020	0.31776	0.46257	0.63459	0.83385	1.06029
$5^1\text{P}$	$\langle \mathbf{r}^{-2} \rangle$	8.00561	18.0223	32.0494	50.0871	72.1352	98.1939	128.263	162.343	200.434
	$\langle \mathbf{u}^{-2} \rangle$	0.00559	0.02407	0.05643	0.10272	0.16294	0.23706	0.32508	0.42698	0.54278
$6^1\text{P}$	$\langle \mathbf{r}^{-2} \rangle$	8.00326	18.0129	32.0287	50.0504	72.0776	98.1121	128.152	162.198	200.251
	$\langle \mathbf{r}^{-1} \rangle$	2.02763	3.05533	4.08310	5.11087	6.13865	7.16643	8.19420	9.22198	10.2498
	$\langle \mathbf{r}^{+1} \rangle$	53.9683	27.1217	18.1103	13.5930	10.8792	9.06864	7.77476	6.80401	6.04877
	$\langle \mathbf{r}^{+2} \rangle$	3176.40	795.066	352.920	198.282	126.784	87.9827	64.6051	49.4418	39.0514
	$\langle \mathbf{u}^{-2} \rangle$	0.00324	0.01396	0.03272	0.05952	0.09438	0.13727	0.18819	0.24713	0.31410
	$\langle \mathbf{u}^{-1} \rangle$	0.02759	0.05539	0.08335	0.11135	0.13937	0.16739	0.19541	0.22343	0.25145
	$\langle \mathbf{u}^{+1} \rangle$	53.2253	26.6277	17.7402	13.2971	10.6327	8.85748	7.59004	6.63985	5.90105
	$\langle \mathbf{u}^{+2} \rangle$	3176.42	795.070	352.921	198.283	126.785	87.9829	64.6052	49.4418	39.0514

Table 3.2.4: Moments for the  $^3P$  states of the two-electron ions.

	He	$\text{Li}^+$	$\text{Be}^{2+}$	$\text{B}^{3+}$	$\text{C}^{4+}$	$\text{N}^{5+}$	$\text{O}^{6+}$	$\text{F}^{7+}$	$\text{Ne}^{8+}$
$3^3\text{P}$	$\langle \text{r}^{-2} \rangle$	8.00852	18.0561	32.1537	50.3012	72.4984	98.7450	129.041	163.387
	$\langle \text{u}^{-2} \rangle$	0.02639	0.09365	0.19839	0.34069	0.52059	0.73811	0.99327	1.28606
$4^3\text{P}$	$\langle \text{r}^{-2} \rangle$	8.00358	18.0239	32.0653	50.1277	72.2112	98.3156	128.441	162.587
	$\langle \text{u}^{-2} \rangle$	0.01086	0.03857	0.08197	0.14111	0.21602	0.30672	0.41319	0.53545
$5^3\text{P}$	$\langle \text{r}^{-2} \rangle$	8.00181	18.0122	32.0335	50.0656	72.1083	98.1618	128.226	162.301
	$\langle \text{u}^{-2} \rangle$	0.00548	0.01950	0.04152	0.07158	0.10969	0.15587	0.21010	0.27240
$6^3\text{P}$	$\langle \text{r}^{-2} \rangle$	8.00105	18.0072	32.0194	50.0379	72.0627	98.0936	128.131	162.174
	$\langle \text{r}^{-1} \rangle$	2.02839	3.05631	4.08413	5.11192	6.13970	7.16749	8.19527	9.22304
$\langle \text{r}^{+1} \rangle$	52.5277	26.5119	17.7868	13.3944	10.7454	8.97254	7.70245	6.74765	6.00363
	$\langle \text{r}^{+2} \rangle$	3008.33	759.242	340.198	192.412	123.615	86.0833	63.3789	48.6051
$\langle \text{u}^{-2} \rangle$	0.00315	0.01119	0.02387	0.04119	0.06317	0.08980	0.12110	0.15705	0.19766
	$\langle \text{u}^{-1} \rangle$	0.02836	0.05578	0.08291	0.10995	0.13695	0.16394	0.19092	0.21789
$\langle \text{u}^{+1} \rangle$	51.7860	26.0192	17.4178	13.0995	10.4998	8.76210	7.51837	6.58407	5.85643
	$\langle \text{u}^{+2} \rangle$	3008.35	759.250	340.202	192.415	123.616	86.0842	63.3795	48.6055

Table 3.2.5: Moments for the  $^1D$  states of the two-electron ions.

	He	$\text{Li}^+$	$\text{Be}^{2+}$	$\text{B}^{3+}$	$\text{C}^{4+}$	$\text{N}^{5+}$	$\text{O}^{6+}$	$\text{F}^{7+}$	$\text{Ne}^{8+}$
$3^1\text{D}$									
$\langle r^{-2} \rangle$	8.01411	18.0574	32.1309	50.2345	72.3682	98.5316	128.725	162.948	201.201
$\langle r^{-1} \rangle$	2.11123	3.22230	4.33335	5.44442	6.55550	7.66659	8.77768	9.88878	10.9999
$\langle r^{+1} \rangle$	11.2315	5.74430	3.87297	2.92425	2.34975	1.96426	1.68757	1.47928	1.31680
$\langle r^{+2} \rangle$	126.336	31.7688	14.1720	7.99058	5.12212	3.56105	2.61849	2.00608	1.58586
$\langle u^{-2} \rangle$	0.01497	0.06019	0.13616	0.24319	0.38146	0.55105	0.75203	0.98444	1.24829
$\langle u^{-1} \rangle$	0.11122	0.22212	0.33298	0.44390	0.55488	0.66592	0.77700	0.88811	0.99925
$\langle u^{+1} \rangle$	10.5133	5.27216	3.52105	2.64364	2.11639	1.76450	1.51295	1.32417	1.17728
$\langle u^{+2} \rangle$	126.399	31.7938	14.1840	7.99719	5.12612	3.56366	2.62028	2.00736	1.58681
$4^1\text{D}$									
$\langle r^{-2} \rangle$	8.00591	18.0242	32.0552	50.0989	72.1553	98.2242	128.306	162.400	200.507
$\langle r^{-1} \rangle$	2.06255	3.12503	4.18750	5.24998	6.31247	7.37496	8.43745	9.49994	10.5624
$\langle r^{+1} \rangle$	21.7250	10.9925	7.37240	5.54909	4.44975	3.71431	3.18764	2.79186	2.48354
$\langle r^{+2} \rangle$	503.611	126.160	56.1471	31.6091	20.2407	14.0612	10.3334	7.91305	6.25322
$\langle u^{-2} \rangle$	0.00632	0.02543	0.05759	0.10296	0.16164	0.23365	0.31904	0.41782	0.53001
$\langle u^{-1} \rangle$	0.06255	0.12494	0.18733	0.24974	0.31219	0.37466	0.43716	0.49966	0.56218
$\langle u^{+1} \rangle$	20.9923	10.5077	7.01007	5.25977	4.20893	3.50807	3.00729	2.63161	2.33937
$\langle u^{+2} \rangle$	503.646	126.174	56.1538	31.6128	20.2429	14.0627	10.3344	7.91376	6.25375

Table 3.2.5: Continued.

	He	$\text{Li}^+$	$\text{Be}^{2+}$	$\text{B}^{3+}$	$\text{C}^{4+}$	$\text{N}^{5+}$	$\text{O}^{6+}$	$\text{F}^{7+}$	$\text{Ne}^{8+}$
$5^1\text{D}$	$\langle \text{r}^{-2} \rangle$	8.00299	18.0124	32.0282	50.0506	72.0796	98.1150	128.157	162.205
	$\langle \text{r}^{-1} \rangle$	2.04003	3.08002	4.12000	5.15999	6.19998	7.23998	8.27997	9.31997
	$\langle \text{r}^{+1} \rangle$	35.2186	17.7406	11.8718	8.92388	7.14970	5.96433	5.11626	4.47942
	$\langle \text{r}^{+2} \rangle$	1348.38	337.475	150.105	84.4731	54.0783	37.5615	27.5998	21.1330
	$\langle \text{u}^{-2} \rangle$	0.00323	0.01303	0.02952	0.05280	0.08292	0.11990	0.16376	0.21450
	$\langle \text{u}^{-1} \rangle$	0.04002	0.07997	0.11991	0.15986	0.19984	0.23982	0.27982	0.31983
	$\langle \text{u}^{+1} \rangle$	34.4795	17.2502	11.5048	8.63063	6.90551	5.75514	4.93329	4.31683
	$\langle \text{u}^{+2} \rangle$	1348.40	337.484	150.109	84.4754	54.0797	37.5624	27.6004	21.1335
$6^1\text{D}$	$\langle \text{r}^{-2} \rangle$	8.00178	18.0071	32.0163	50.0294	72.0461	98.0664	128.091	162.118
	$\langle \text{r}^{-1} \rangle$	2.02779	3.05556	4.08333	5.11110	6.13888	7.16665	8.19443	9.22220
	$\langle \text{r}^{+1} \rangle$	51.7122	25.9888	17.3712	13.0487	10.4497	8.71434	7.47345	6.54197
	$\langle \text{r}^{+2} \rangle$	2930.54	733.204	326.043	183.458	117.435	81.5620	59.9281	45.8849
	$\langle \text{u}^{-2} \rangle$	0.00187	0.00754	0.01709	0.03059	0.04804	0.06948	0.09490	0.12432
	$\langle \text{u}^{-1} \rangle$	0.02779	0.05554	0.08328	0.11103	0.13879	0.16656	0.19434	0.22212
	$\langle \text{u}^{+1} \rangle$	50.9697	25.4954	17.0016	12.7533	10.2037	8.50357	7.28908	6.37812
	$\langle \text{u}^{+2} \rangle$	2930.55	733.210	326.046	183.459	117.436	81.5626	59.9285	45.8852

Table 3.2.6: Moments for the  $^3D$  states of the two-electron ions.

	He	$\text{Li}^+$	$\text{Be}^{2+}$	$\text{B}^{3+}$	$\text{C}^{4+}$	$\text{N}^{5+}$	$\text{O}^{6+}$	$\text{F}^{7+}$	$\text{Ne}^{8+}$
$3^3\text{D}$	$\langle r^{-2} \rangle$	8.01396	18.0561	32.1274	50.2281	72.3583	98.5181	128.707	162.926
	$\langle r^{-1} \rangle$	2.11128	3.22248	4.33363	5.44475	6.55587	7.66699	8.77810	9.88922
	$\langle r^{+1} \rangle$	11.2258	5.73832	3.86827	2.92065	2.34696	1.96204	1.68578	1.47780
	$\langle r^{+2} \rangle$	126.216	31.7044	14.1380	7.97098	5.10991	3.55297	2.61287	2.00202
	$\langle u^{-2} \rangle$	0.01497	0.06004	0.13520	0.24045	0.37578	0.54120	0.73671	0.96230
	$\langle u^{-1} \rangle$	0.11130	0.22239	0.33334	0.44422	0.55506	0.66589	0.77670	0.88751
	$\langle u^{+1} \rangle$	10.5076	5.26609	3.51627	2.64000	2.11358	1.76229	1.51118	1.32273
	$\langle u^{+2} \rangle$	126.278	31.7286	14.1493	7.97712	5.11358	3.55534	2.61449	2.00317
	$4^3\text{D}$	$\langle r^{-2} \rangle$	8.00582	18.0235	32.0532	50.0954	72.1500	98.2171	128.297
	$\langle r^{-1} \rangle$	2.06258	3.12513	4.18765	5.25016	6.31267	7.37517	8.43767	9.50018
	$\langle r^{+1} \rangle$	21.7162	10.9833	7.36528	5.54366	4.44555	3.71099	3.18497	2.78966
	$\langle r^{+2} \rangle$	503.231	125.961	56.0430	31.5494	20.2037	14.0368	10.3165	7.90086
	$\langle u^{-2} \rangle$	0.00632	0.02532	0.05700	0.10133	0.15833	0.22797	0.31027	0.40521
	$\langle u^{-1} \rangle$	0.06259	0.12509	0.18752	0.24991	0.31227	0.37463	0.43697	0.49931
	$\langle u^{+1} \rangle$	20.9835	10.4985	7.00290	5.25432	4.20473	3.50475	3.00461	2.62942
	$\langle u^{+2} \rangle$	503.266	125.974	56.0493	31.5529	20.2058	14.0381	10.3174	7.90151

Table 3.2.6: Continued.

	He	$\text{Li}^+$	$\text{Be}^{2+}$	$\text{B}^{3+}$	$\text{C}^{4+}$	$\text{N}^{5+}$	$\text{O}^{6+}$	$\text{F}^{7+}$	$\text{Ne}^{8+}$	
$5^3\text{D}$	$\langle \text{r}^{-2} \rangle$	8.00297	18.0119	32.0272	50.0486	72.0764	98.1108	128.151	162.198	200.252
	$\langle \text{r}^{-1} \rangle$	2.04005	3.08007	4.12008	5.16009	6.20009	7.24010	8.28010	9.32010	10.3601
	$\langle \text{r}^{+1} \rangle$	35.2071	17.7288	11.8626	8.91690	7.14431	5.96007	5.11283	4.47659	3.98124
	$\langle \text{r}^{+2} \rangle$	1347.55	337.045	149.881	84.3451	53.9991	37.5093	27.5636	21.1070	16.6795
	$\langle \text{u}^{-2} \rangle$	0.00323	0.01296	0.02917	0.05185	0.08100	0.11662	0.15871	0.20726	0.26229
	$\langle \text{u}^{-1} \rangle$	0.04005	0.08005	0.12001	0.15995	0.19988	0.23980	0.27971	0.31962	0.35953
	$\langle \text{u}^{+1} \rangle$	34.4680	17.2383	11.4956	8.62364	6.90012	5.75088	4.92986	4.31401	3.83495
	$\langle \text{u}^{+2} \rangle$	1347.57	337.054	149.885	84.3473	54.0005	37.5101	27.5642	21.1074	16.6798
$6^3\text{D}$	$\langle \text{r}^{-2} \rangle$	8.00175	18.0068	32.0158	50.0281	72.0442	98.0642	128.088	162.115	200.146
	$\langle \text{r}^{-1} \rangle$	2.02781	3.05560	4.08338	5.11117	6.13895	7.16672	8.19450	9.22228	10.2501
	$\langle \text{r}^{+1} \rangle$	51.6984	25.9744	17.3600	13.0402	10.4431	8.70919	7.46929	6.53855	5.81413
	$\langle \text{r}^{+2} \rangle$	2929.04	732.418	325.635	183.225	117.292	81.4675	59.8626	45.8379	36.2212
	$\langle \text{u}^{-2} \rangle$	0.00187	0.00750	0.01687	0.02999	0.04685	0.06745	0.09179	0.11988	0.15170
	$\langle \text{u}^{-1} \rangle$	0.02781	0.05559	0.08334	0.11108	0.13882	0.16655	0.19427	0.22200	0.24972
	$\langle \text{u}^{+1} \rangle$	50.9559	25.4810	16.9905	12.7449	10.1971	8.49842	7.28492	6.37470	5.66670
	$\langle \text{u}^{+2} \rangle$	2929.05	732.424	325.638	183.227	117.293	81.4681	59.8630	45.8382	36.2214

### 3.3 Density derivatives for the ground states

In a series of recent papers, Angulo and Dehesa [3.10-3.14] and Gálvez and Porras [3.15][3.16] have derived bounds on moments,  $\rho(0)$  and its derivatives. In particular, Angulo and Dehesa [3.13] have investigated bounds resulting from the complete monotonicity of  $\rho(r)$ , i.e.

$$(-1)^n \rho^{(n)}(r) \geq 0 \quad \text{for } n=0, 1, 2, \dots \quad (3.9)$$

for atomic ground states from hydrogen to xenon. Since their investigation focused on densities obtained from Hartree-Fock wavefunctions, density derivatives have been obtained for the ground states of the two-electron ions from He to  $\text{Ne}^{8+}$ . The 200-term ground state expansions discussed in chapter 2 were used to generate  $\rho(r)$  derivatives up to tenth order. Figures 3.3.1-3.3.4 show  $\rho(r)$ ,  $\rho'(r)$ ,  $\rho''(r)$ , and  $\rho^{(3)}(r)$  for  $\text{H}^-$ , He,  $\text{B}^{3+}$ , and  $\text{Ne}^{8+}$ . The calculations and the figures show quite clearly that the Z-scaled derivatives lie close together and are all monotonically decreasing. These results confirm, for the ground state of two-electron ions, the complete monotonicity of  $\rho(r)$ .

Although many bounds were obtained by Angulo and Dehesa [3.13], their use will be illustrated by considering the bounds on  $\rho(0)$  for a completely monotonic density [3.13]:

$$\frac{1}{4\pi} \frac{\langle 1/r^2 \rangle^2}{\langle 1/r \rangle} \leq \rho(0) \leq \frac{Z}{2\pi} \langle 1/r^2 \rangle \quad (3.10)$$

The lower and upper limits are found to be within 10% of the true  $\rho(0)$  for the ground state of the ions. However, these bounds are roughly equidistant from the true  $\rho(0)$  and consequently, with the exception of  $\text{H}^-$ , their average is within 0.2% of  $\rho(0)$ .

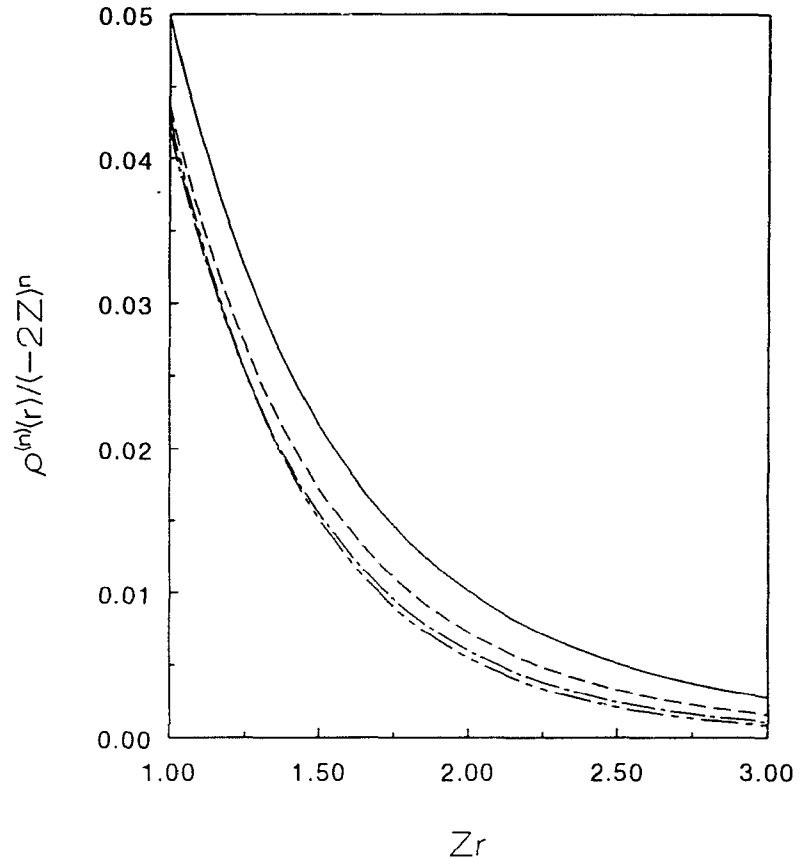
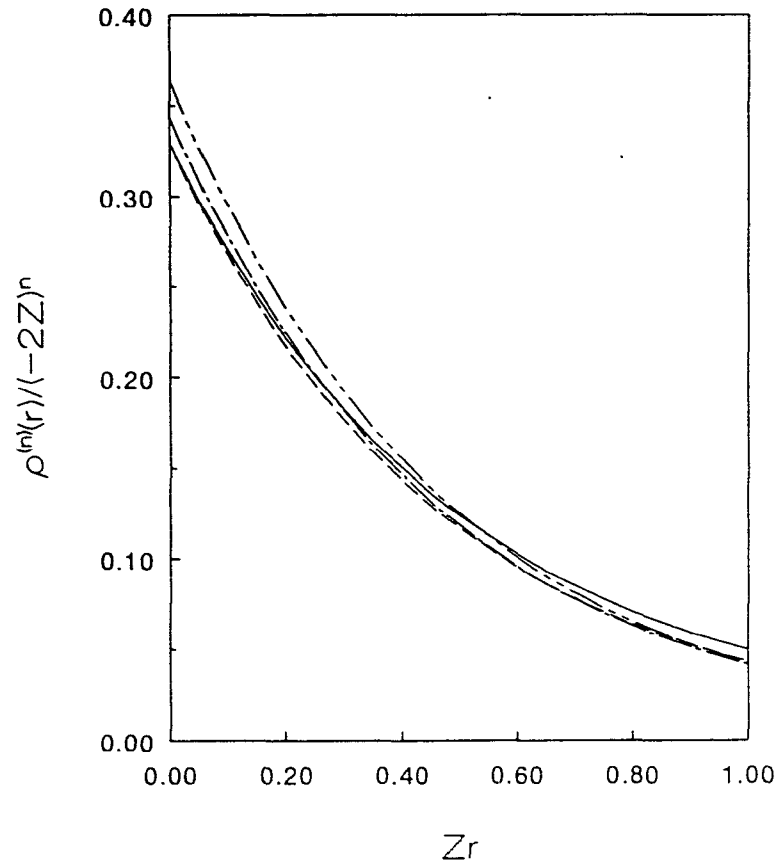


Figure 3.3.1: Density derivatives for the ground state of  $\text{H}^-$ . The solid curve is  $\rho(r)$ , the dashed curve is  $-\rho'(r)/2Z$ , the dot-dashed curve is  $\rho''(r)/4Z^2$ , and the double dot-dashed curve is  $-\rho^{(3)}(r)/8Z^3$ .

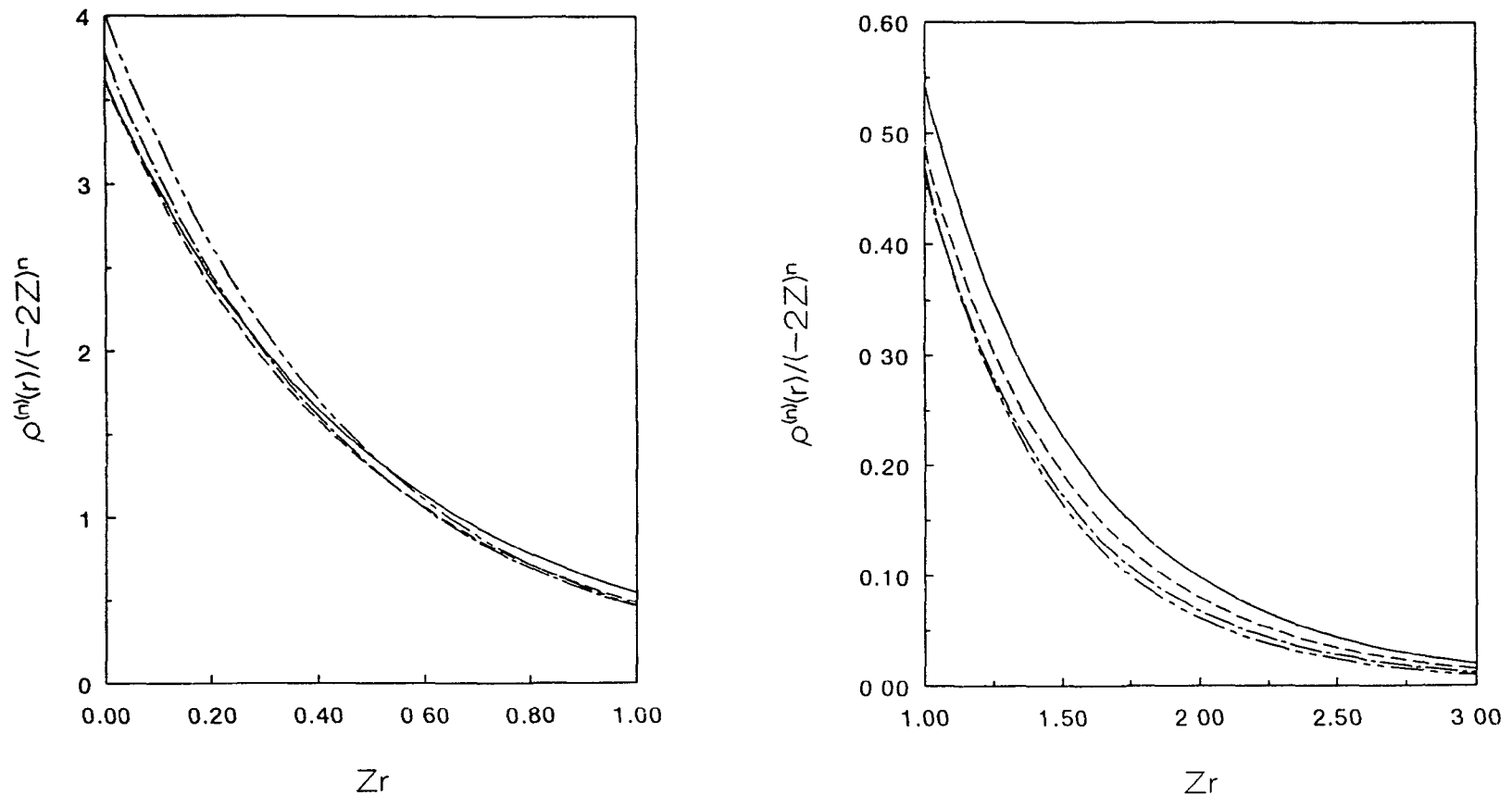


Figure 3.3.2: Density derivatives for the ground state of He. The solid curve is  $\rho(r)$ , the dashed curve is  $-\rho'(r)/2Z$ , the dot-dashed curve is  $\rho''(r)/4Z^2$ , and the double dot-dashed curve is  $-\rho^{(3)}(r)/8Z^3$ .

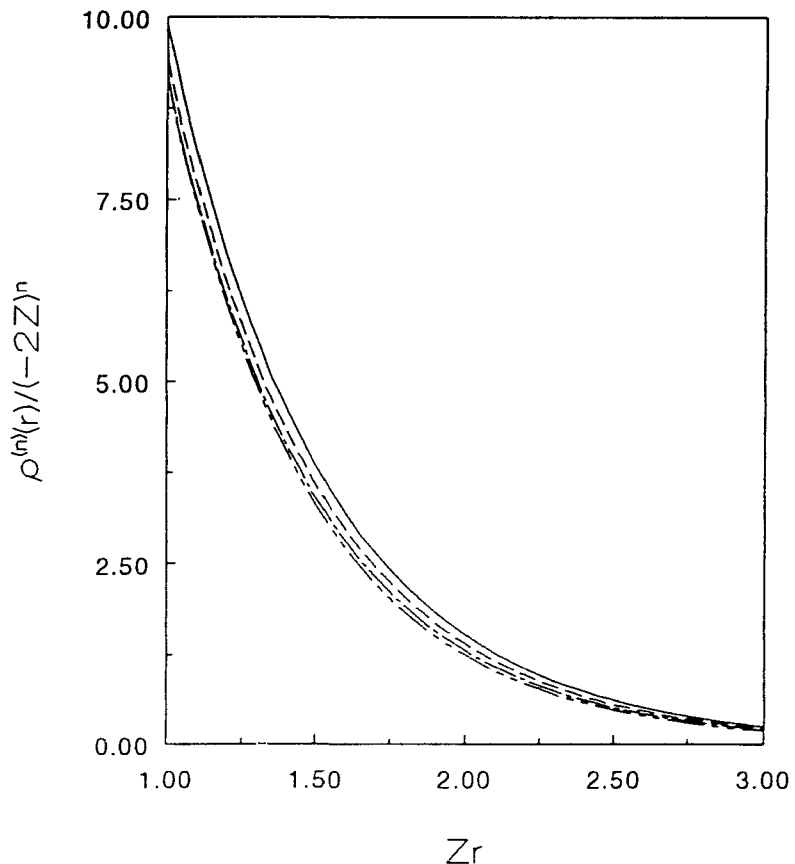
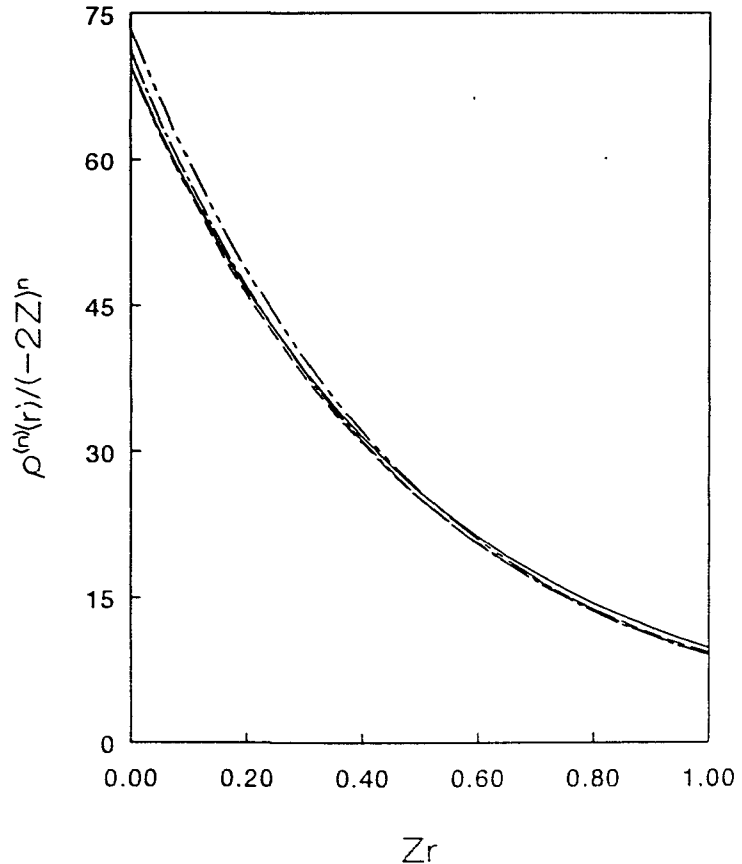


Figure 3.3.3: Density derivatives for the ground state of  $B^{3+}$ . The solid curve is  $\rho(r)$ , the dashed curve is  $-\rho'(r)/2Z$ , the dot-dashed curve is  $\rho''(r)/4Z^2$ , and the double dot-dashed curve is  $-\rho'''(r)/8Z^3$ .

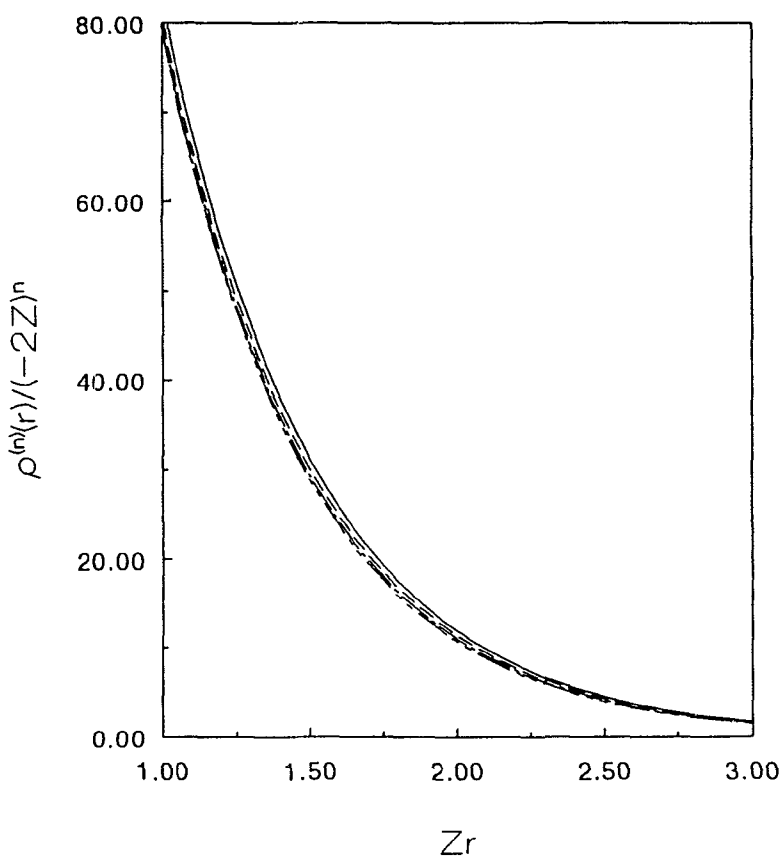
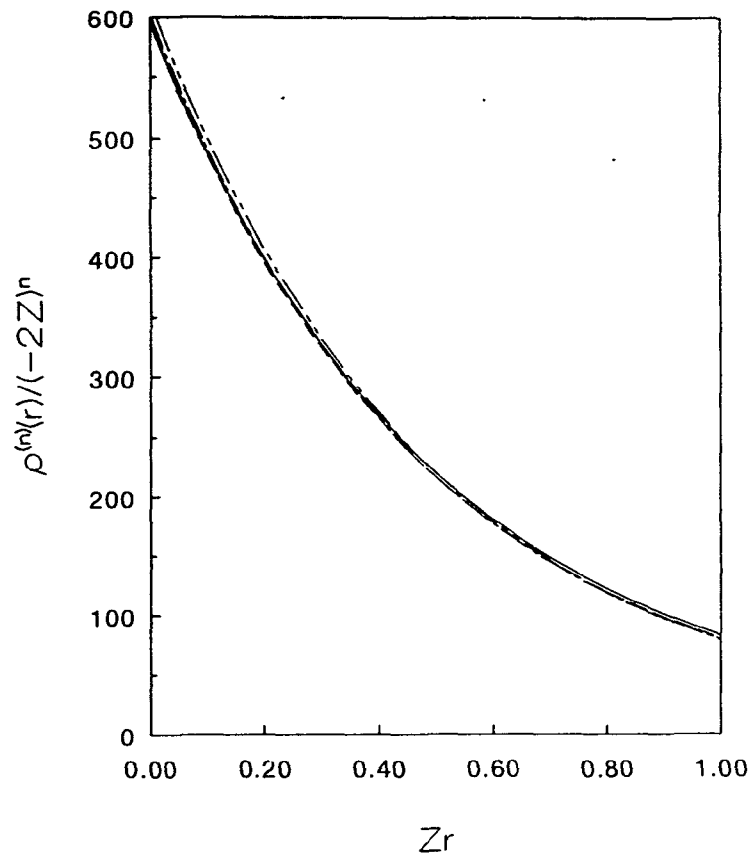


Figure 3.3.4: Density derivatives for the ground state of  $\text{Ne}^{8+}$ . The solid curve is  $\rho(r)$ , the dashed curve is  $-\rho'(r)/2Z$ , the dot-dashed curve is  $\rho''(r)/4Z^2$ , and the double dot-dashed curve is  $-\rho^{(3)}(r)/8Z^3$ .

### 3.4 Singlet-triplet differences for $D(r)$ and $P(u)$

Spin multiplicity differences between the densities of a pair of states arising from the same electron configuration of the same ion are of special interest. In two-electron ions, the hydrogenic model predicts that the charge densities  $\rho(r)$  are identical in the singlet and triplet states arising from the same electron configuration. The spin multiplicity differences can be studied by forming the differences between the radial charge and intracule densities of the singlet and triplet states corresponding to the same  $n$ ,  $L$  and  $Z$ . These holes integrate to zero. The  $\Delta D(r)$  and  $\Delta P(u)$  curves are referred to as one- and two-electron "Hund holes", respectively, because they have been found to be useful [3.9][3.17] in studies of the interpretation of Hund's first rule [3.18]. The latter says that the lowest energy state in the manifold arising from the same electron configuration is the one with the highest spin multiplicity.

One-electron Hund holes for the S, P and D states of He are shown in Figures 3.4.1, 3.4.2 and 3.4.3, respectively. First consider the core region. The S state holes have a minimum at small  $r$  that is too small to be visible in Figure 3.4.1; this implies that the electron distribution is slightly enhanced in the central core region at the expense of the inner and outer core regions of the singlet relative to the triplet. This minimum is visible in Figure 3.4.4. Figures 3.4.2 and 3.4.3 show that the core electron distribution is contracted in the P and D singlet states relative to the triplet. The charge redistribution in the core region decreases in importance as  $n$  increases. Beyond the core peak, all the holes show a series of trough-peak pairs so that the net effect of the increase in spin is to significantly contract the charge cloud. This leads to a greater electron-

nucleus attraction in the triplet which in turn leads to a lower energy for the triplet. This picture is entirely consistent with all previous energy component analyses of spin multiplicity differences [3.18-3.21]. Beyond the core peak, singlet and triplet pseudo-nodes in  $\rho(r)$  respectively lie within the  $r$  range of the troughs and peaks in the holes. The Hund holes do not have a sharp structure although the densities change by several orders of magnitude near the pseudo-nodes. However, both the pseudo-node wells and the trough-peak pairs increase in amplitude with increasing  $r$ .

As  $n$  increases from 3 to 6, the holes decrease by a factor of 4 for the S and P states and by a factor of 2 for the D states. A comparison of figures 3.4.2, 3.4.3 and 3.4.4 shows that the S state holes are approximately twice as large as the P state holes and 400 times larger than the D state holes. The  $nS$  holes have  $n$  maxima and  $n$  minima, the  $nP$  holes have  $n$  maxima and  $n-1$  minima, and the  $nD$  holes have  $n-1$  maxima and  $n-2$  minima. The first trough of the D state holes is slightly skewed whereas all the other peaks and troughs are roughly symmetrical.

The influence of increasing nuclear charge on the holes is shown in Figures 3.4.4, 3.4.5 and 3.4.6 for the 3S, 3P and 3D states, respectively. The figures show that the Z-scaled holes retain their structure but contract significantly as  $Z$  increases. In the S state holes, the core trough and peak are largest for either  $\text{Li}^+$  or  $\text{Be}^{2+}$ . Beyond the core region, the troughs and peaks are largest for He and decrease with increasing  $Z$ . The troughs and peaks of the P state holes increase from He to  $\text{Li}^+$  and decrease thereafter. The inner peak of the D state holes is generally largest for  $\text{N}^{5+}$ , whereas all other extreme points are largest for  $\text{B}^{3+}$  or  $\text{C}^{4+}$ . A similar Z-dependence of the one-electron

Hund holes has been observed previously for the 2S and 2P states [3.9].

Two-electron Hund holes for the S, P, and D states of He are shown in Figures 3.4.7, 3.4.8 and 3.4.9, respectively. In all cases, very small interelectronic distances are more probable in the singlet due to the presence of Fermi correlation for the triplet. This small  $u$  effect decreases in importance as  $n$  increases. Beyond the small  $u$  region, the two-electron holes for He qualitatively resemble the corresponding one-electron holes (see figures 3.4.1-3.4.3), and this resemblance increases with  $n$ . However, as  $Z$  increases, this similarity disappears since the one-electron holes vanish, unlike the two-electron holes that always show the effects of Fermi correlation.

Figures 3.4.10, 3.4.11 and 3.4.12 illustrate the variation of the two-electron Hund holes for the 3S, 3P and 3D states, respectively; holes for He,  $\text{Li}^+$ ,  $\text{Ne}^{8+}$ , and the infinite  $Z$  limit are shown in these figures. The holes contract as the nuclear charge increases. The outer maximum and minimum in the 3S and 3P holes disappear with increasing  $Z$ . The asymmetry of the initial minimum in the D state holes vanishes as  $Z$  increases. In the infinite  $Z$  limit, the D state holes are approximately 10 times smaller than the S and P state holes.

Hund's rule has traditionally been rationalized by arguing that Fermi correlation keeps electrons of like spin apart resulting in a decreased interelectronic repulsion and a lower energy for the high spin state. More recent studies [3.18-3.21] have shown that the lower energy in the high spin state results from increased electron-nuclear attraction. According to figure 3.4.13 and tables 3.2.1-3.2.6, the interelectronic repulsion  $\langle u^{-1} \rangle$  is greater in the singlet for all  $S$ ,  $P$  and  $D$  state ions with  $Z \geq 3, 4$ , and

7, respectively. For neutral helium and the lower members of the isoelectronic sequence, the interelectronic repulsion is actually greater in the triplet and figure 3.4.13 shows that the singlet-triplet D state differences actually decrease from  $Z=2$  to 4. These results are in clear contradiction with the naive view of Hund's rule but entirely consistent with its modern interpretation. Similar behaviour is found for the lower *S* and *P* states of the two electron ions [3.9][3.17].

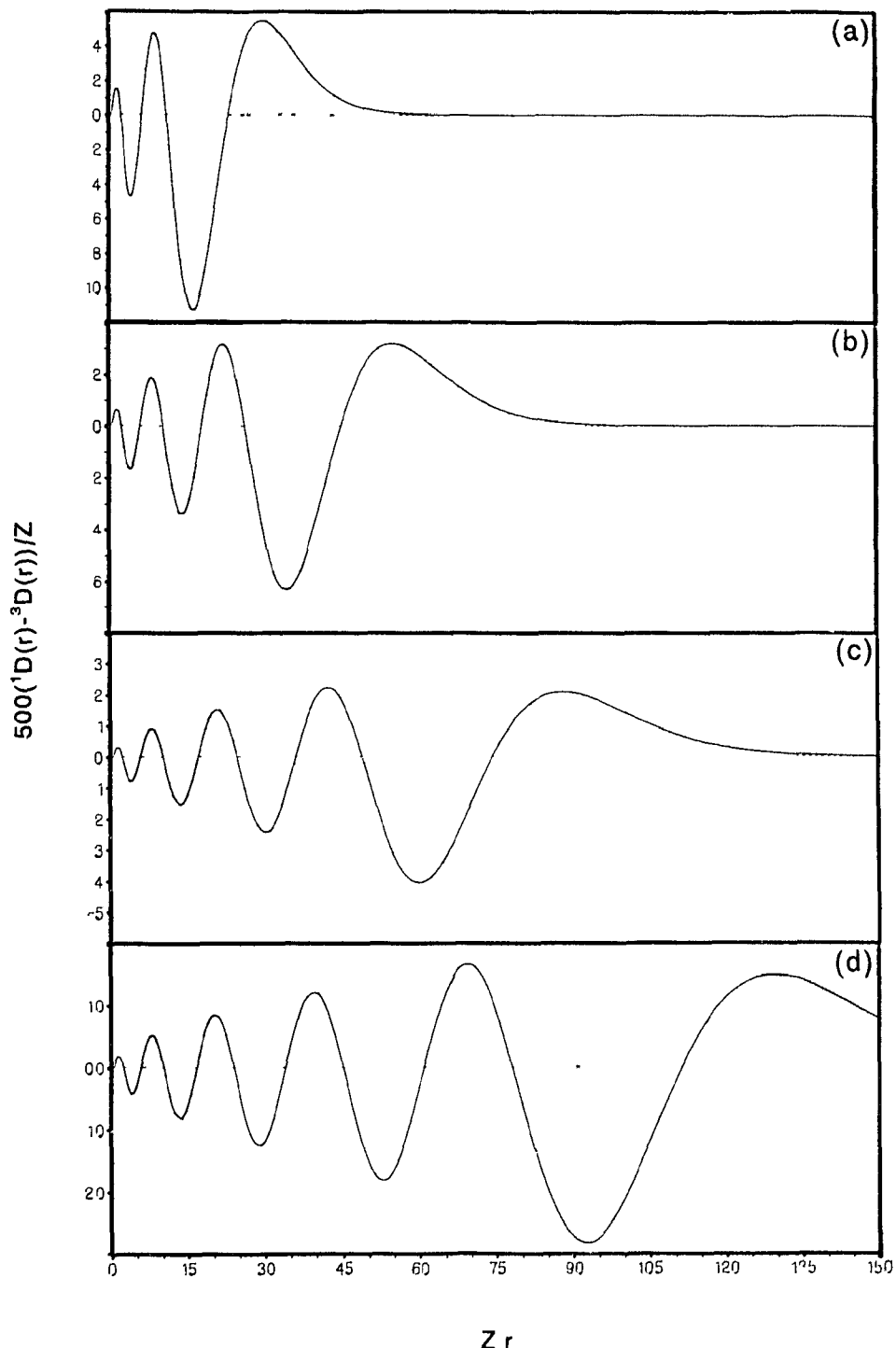


Figure 3.4 1 Z-scaled one-electron Hund holes for the 3S (a), 4S (b) 5S (c), and 6S (d) states of He.

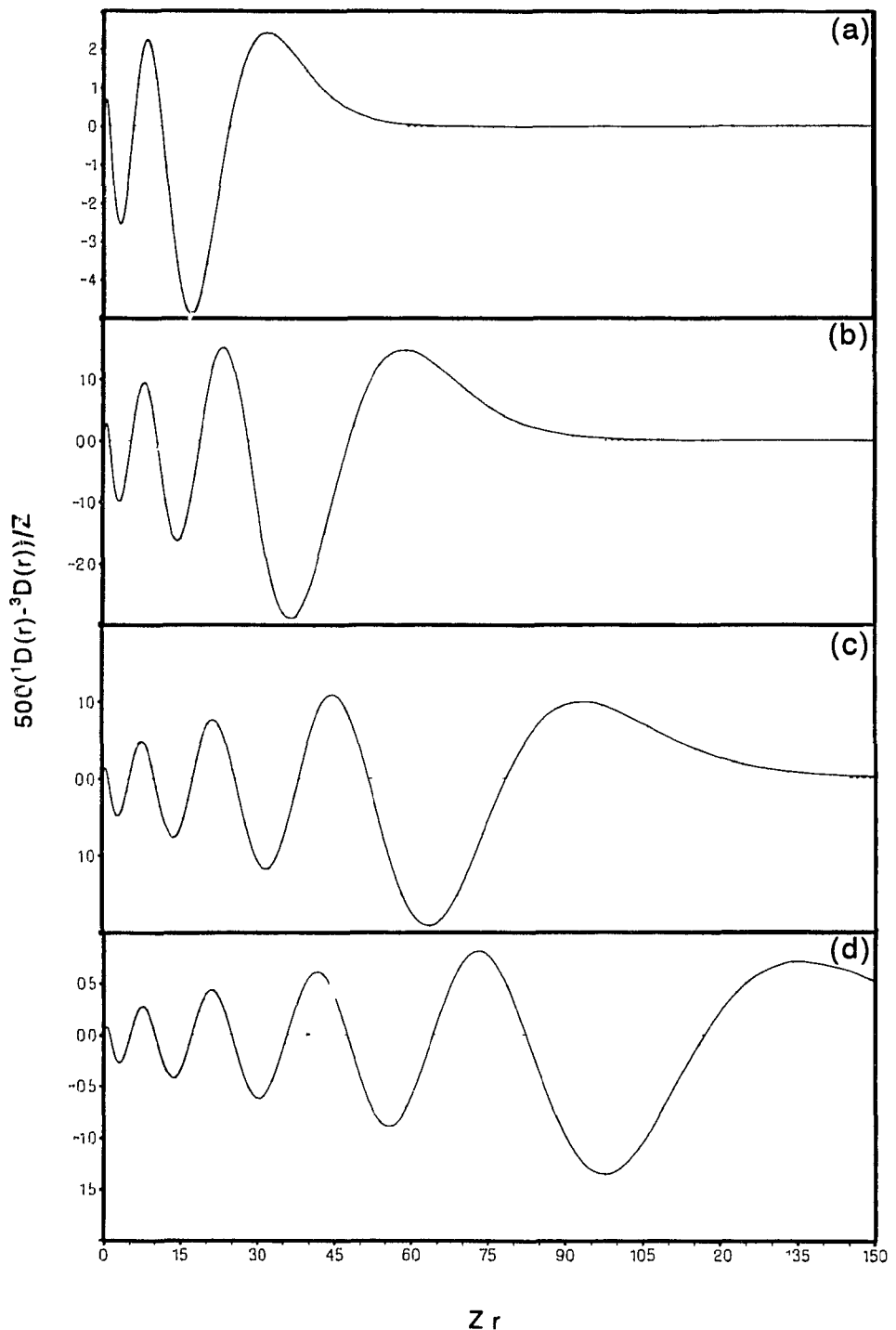


Figure 3 4 2: Z-scaled one-electron Hund holes for the 3P (a), 4P (b), 5P (c), and 6P (d) states of He.

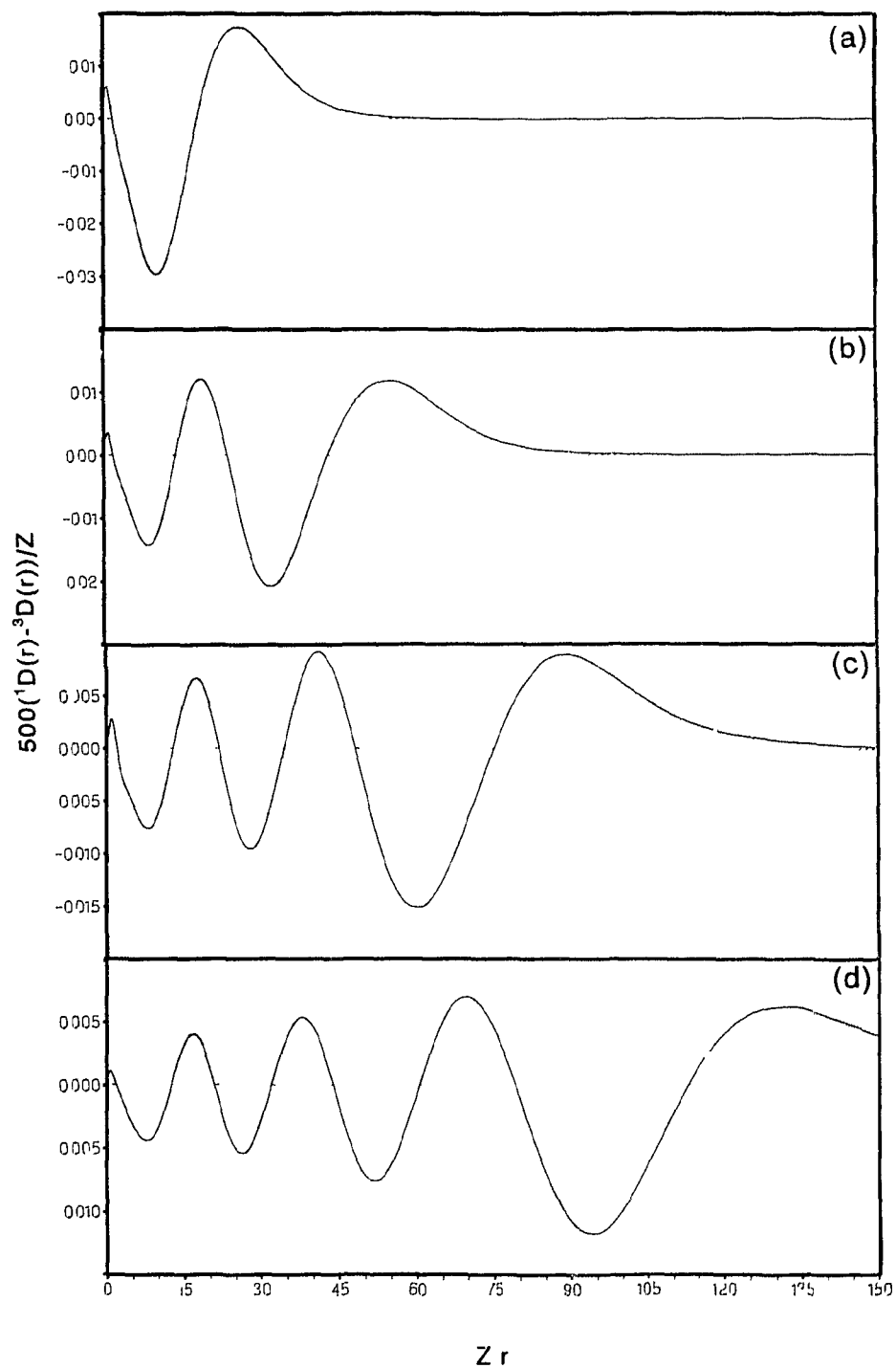


Figure 3.4.3: Z-scaled one-electron Hund holes for the 3D (a), 4D (b), 5D (c), and 6D (d) states of He.

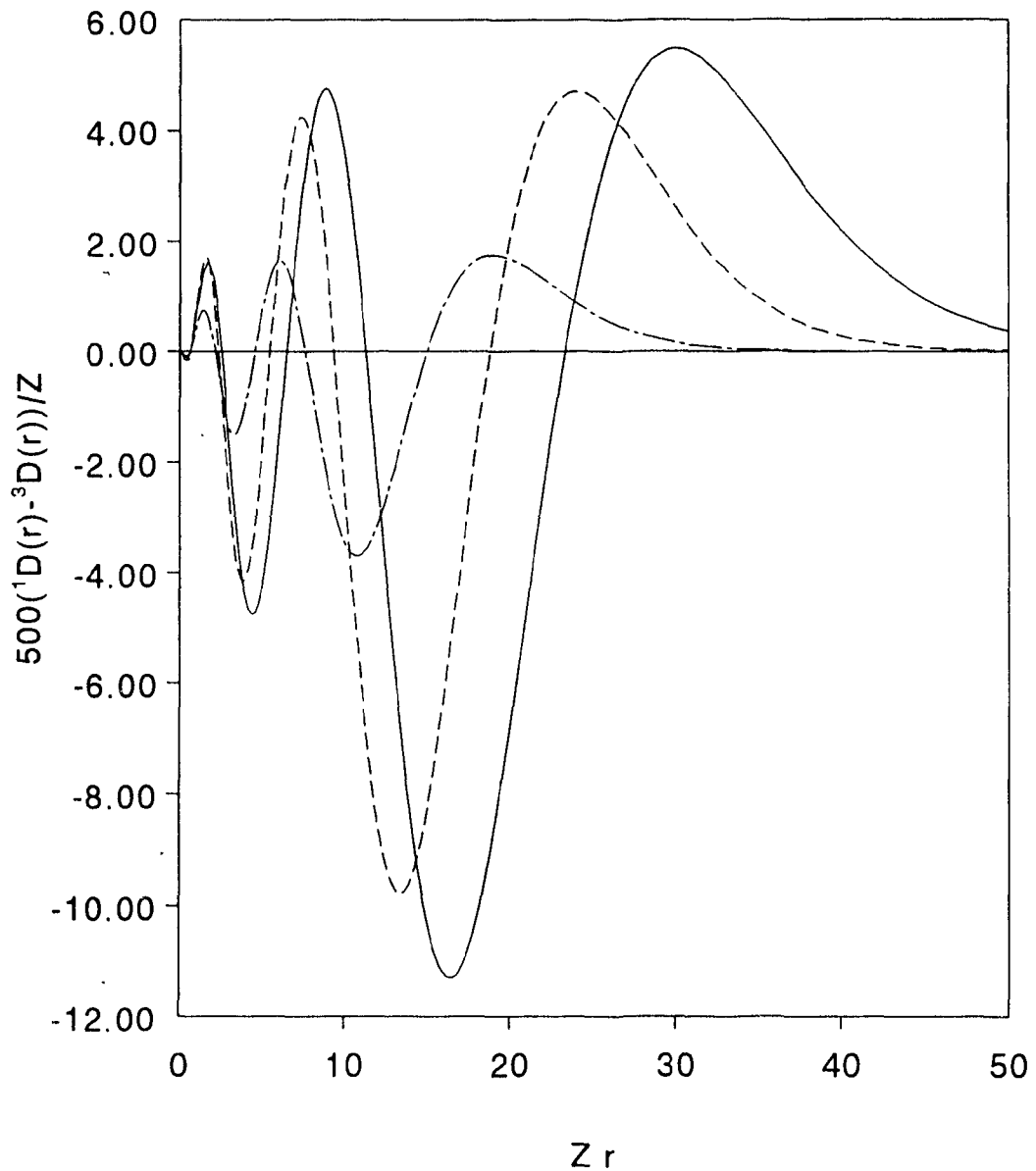


Figure 3.4.4: Z-scaled one-electron Hund holes for the 3S states of He (—), Li<sup>+</sup> (----), and Ne<sup>8+</sup> (---).

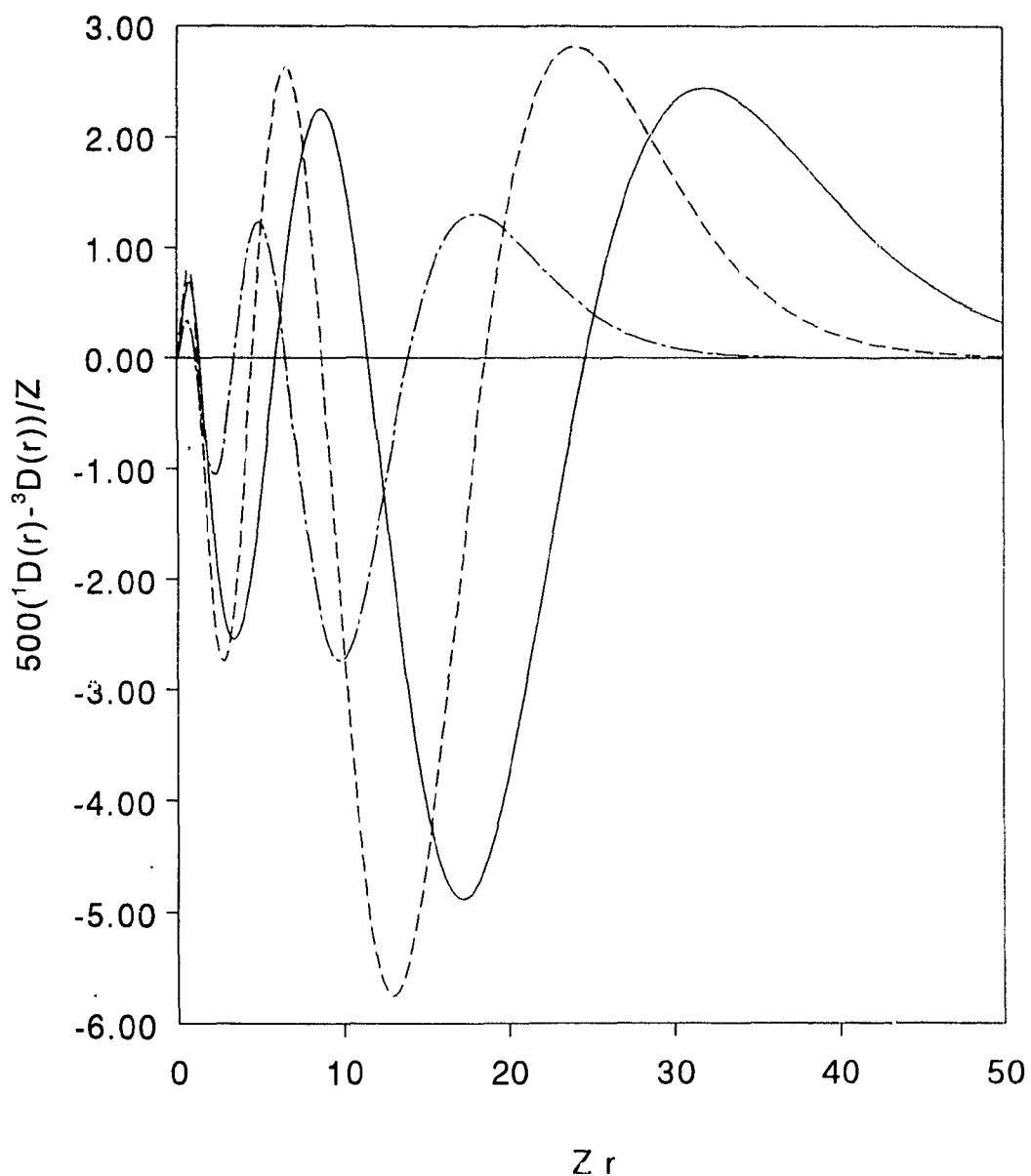


Figure 3.4.5: Z-scaled one-electron Hund holes for the 3P states of He (—), Li<sup>+</sup> (----), and Ne<sup>8+</sup> (- - -).

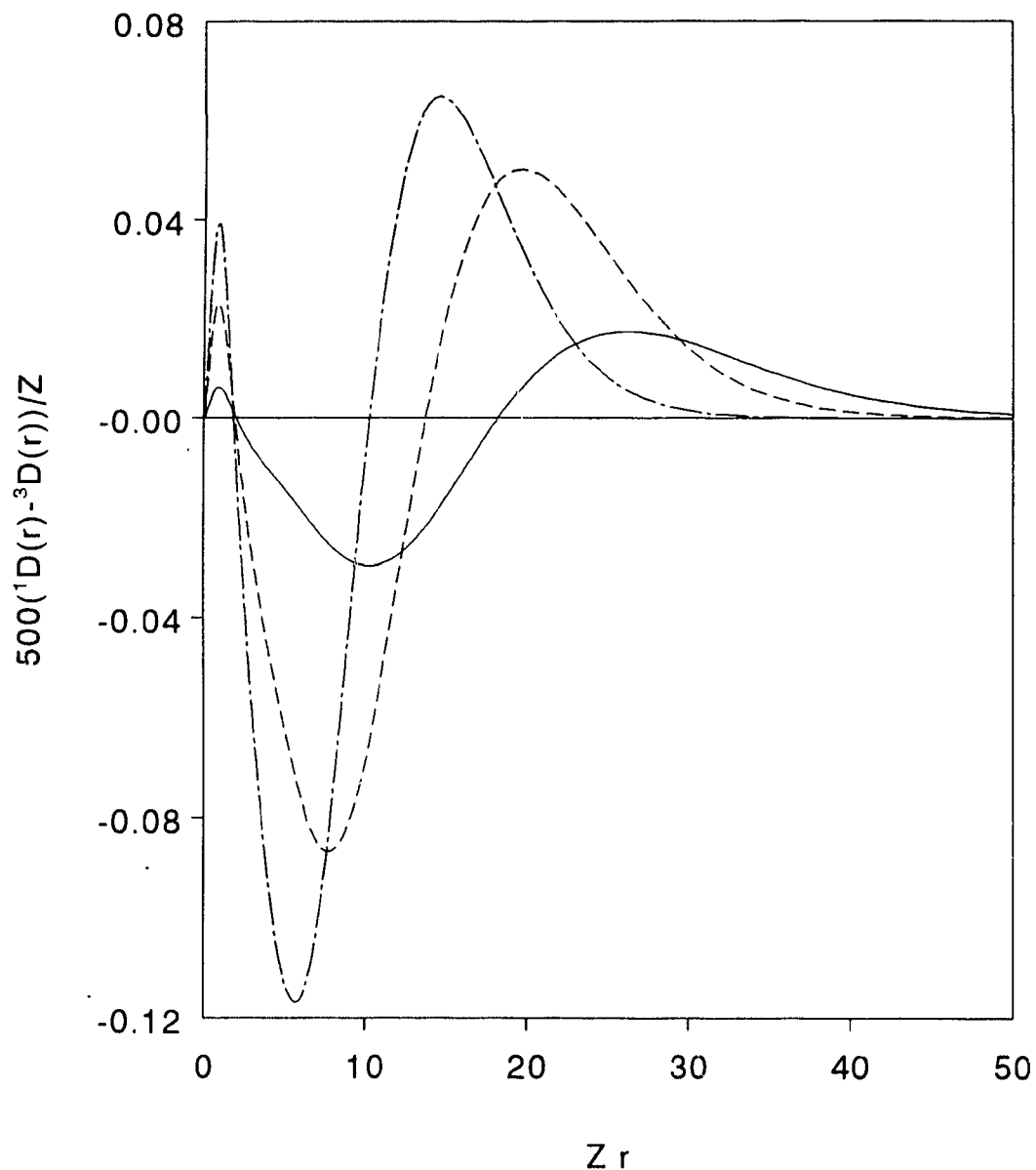


Figure 3.4.6: Z-scaled one-electron Hund holes for the 3D states of He (—), Li<sup>+</sup> (----), and Ne<sup>8+</sup> (- · - · -).

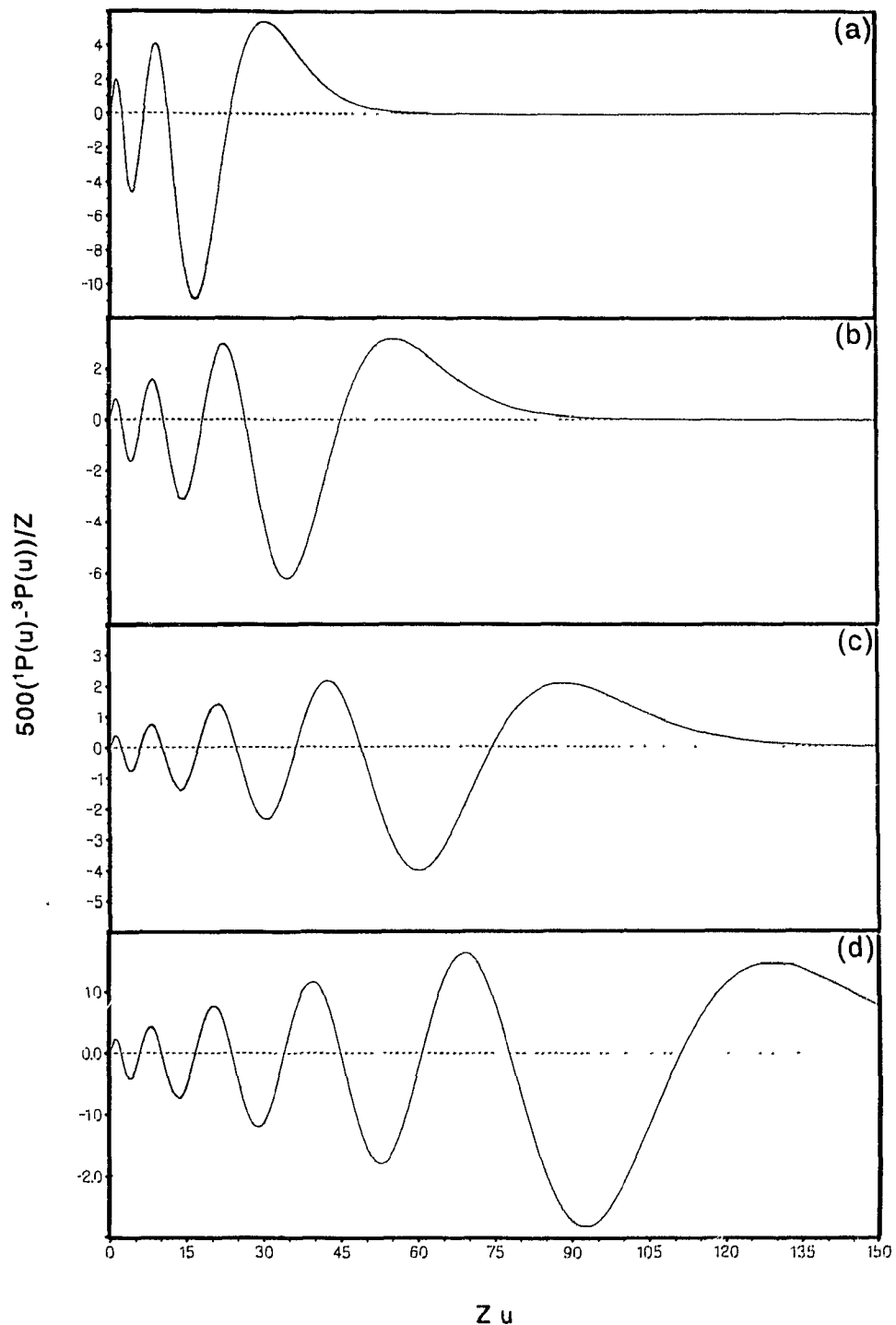


Figure 3.4.7:  $Z$ -scaled two-electron Hund holes for the 3S (a), 4S (b), 5S (c), and 6S (d) states of He.

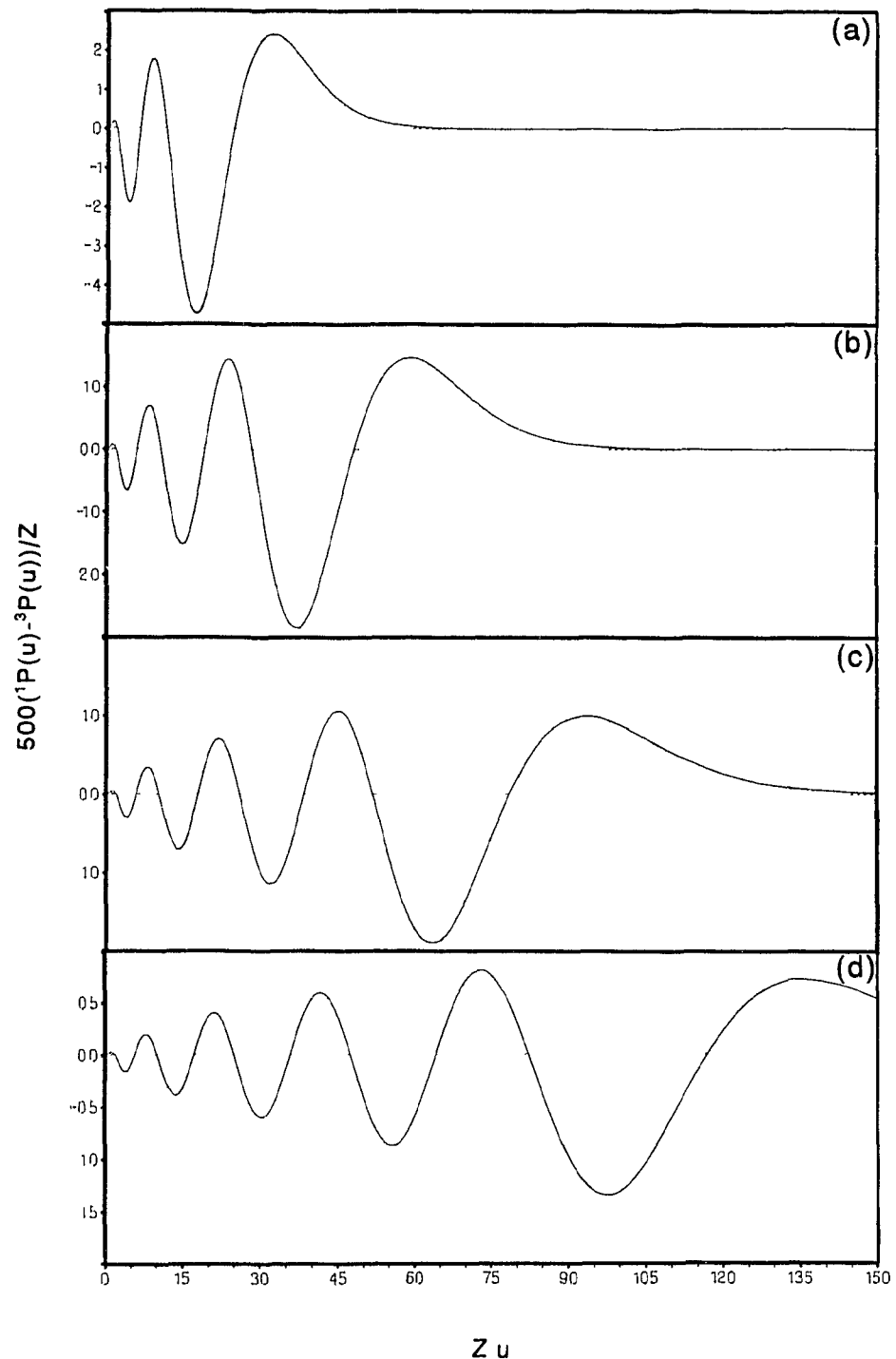


Figure 3.4.8:  $Z$ -scaled two-electron Hund holes for the 3P (a), 4P (b), 5P (c), and 6P (d) states of He.

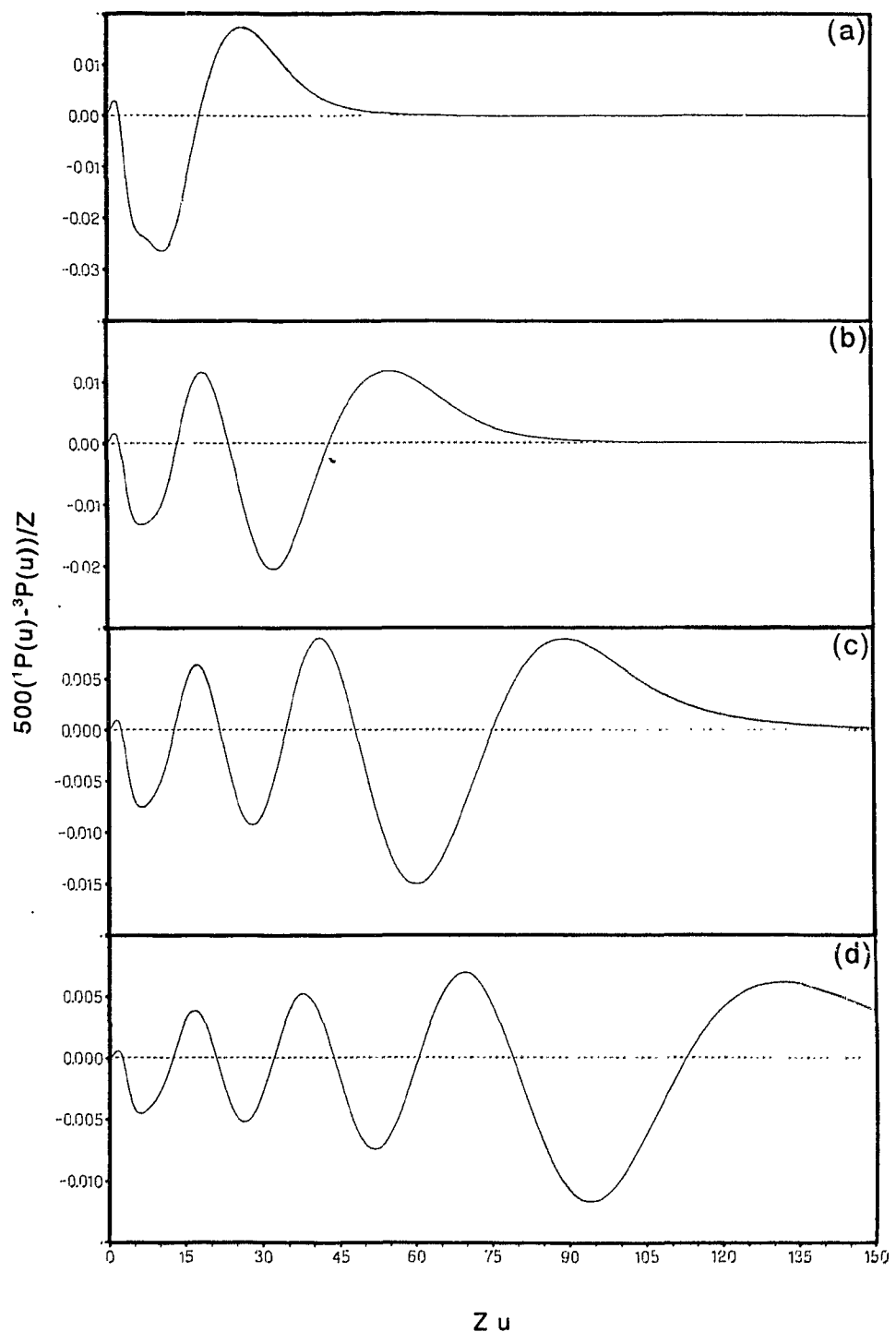


Figure 3.4.9:  $Z$ -scaled two-electron Hund holes for the 3D (a), 4D (b), 5D (c), and 6D (d) states of He.

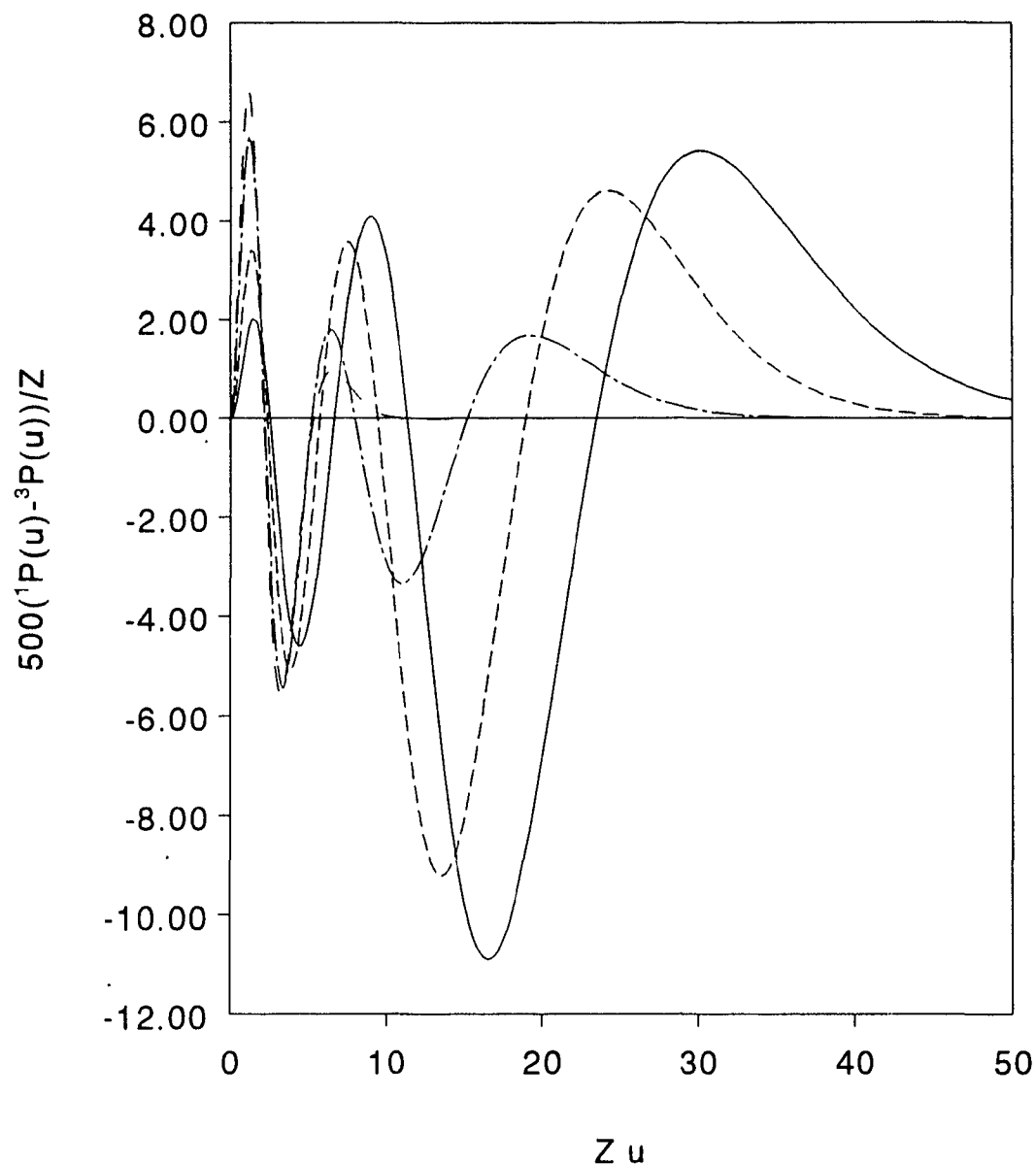


Figure 3.4.10: Z-scaled two-electron Hund holes for the 3S states of He (—), Li<sup>+</sup> (-----), Ne<sup>8+</sup> (---) and the infinite Z limit (---).

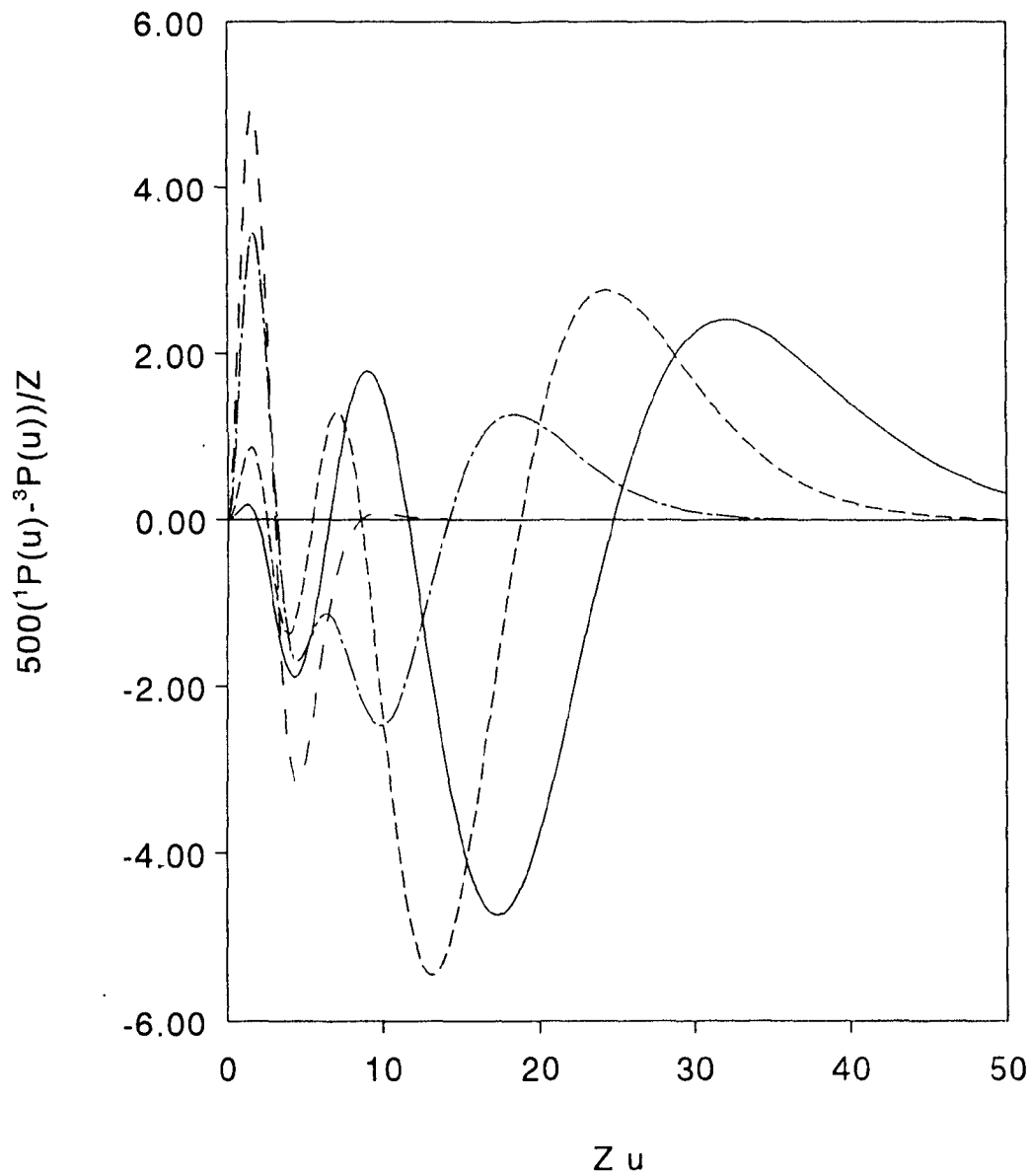


Figure 3.4.11: Z-scaled two-electron Hund holes for the 3P states of He (—),  $\text{Li}^+$  (-----),  $\text{Ne}^{8+}$  (- - -) and the infinite Z limit (- - - -).

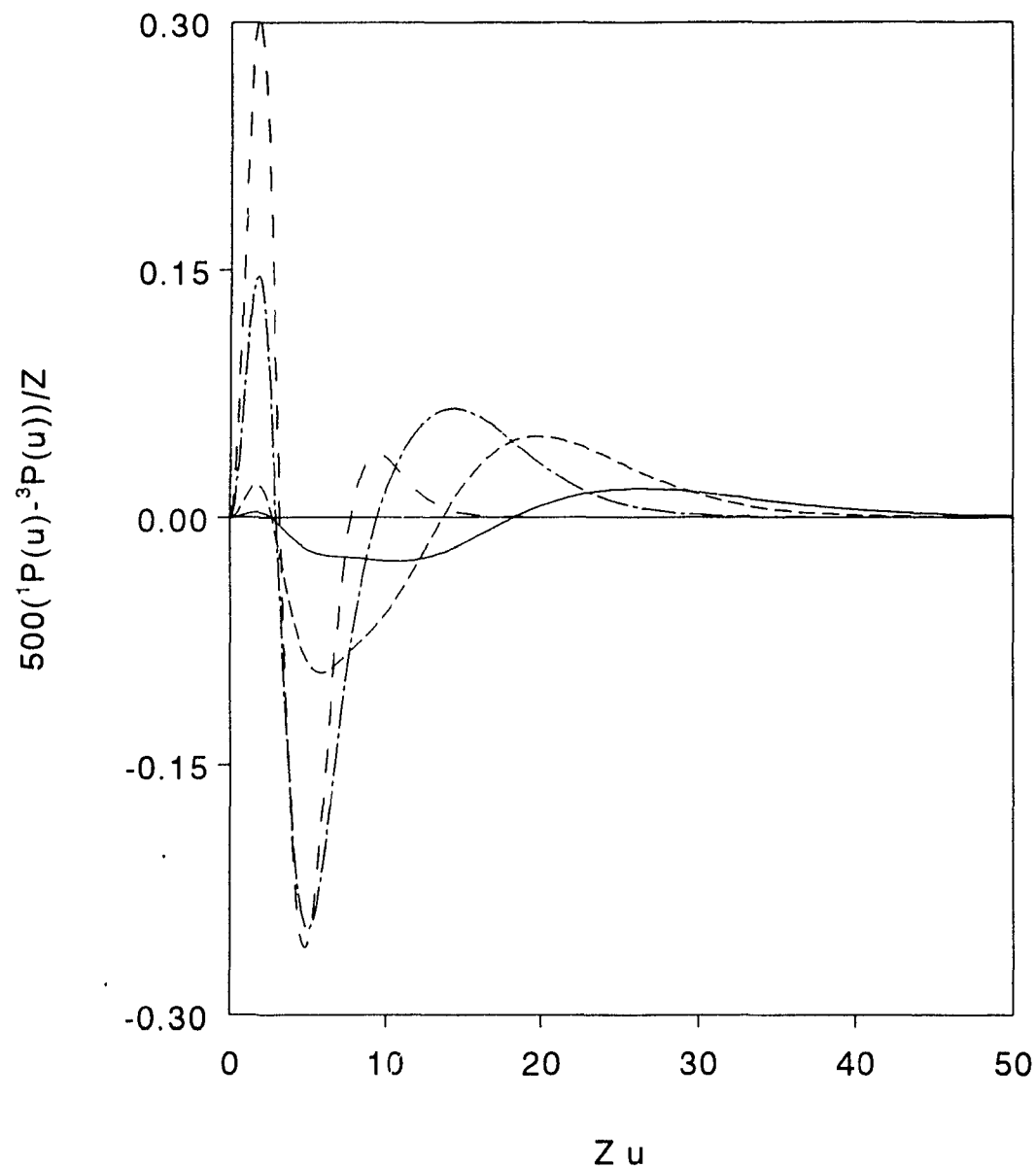


Figure 3.4.12:  $Z$ -scaled two-electron Hund holes for the 3D states of He (—),  $\text{Li}^+$  (----),  $\text{Ne}^{8+}$  (---) and the infinite  $Z$  limit (---).

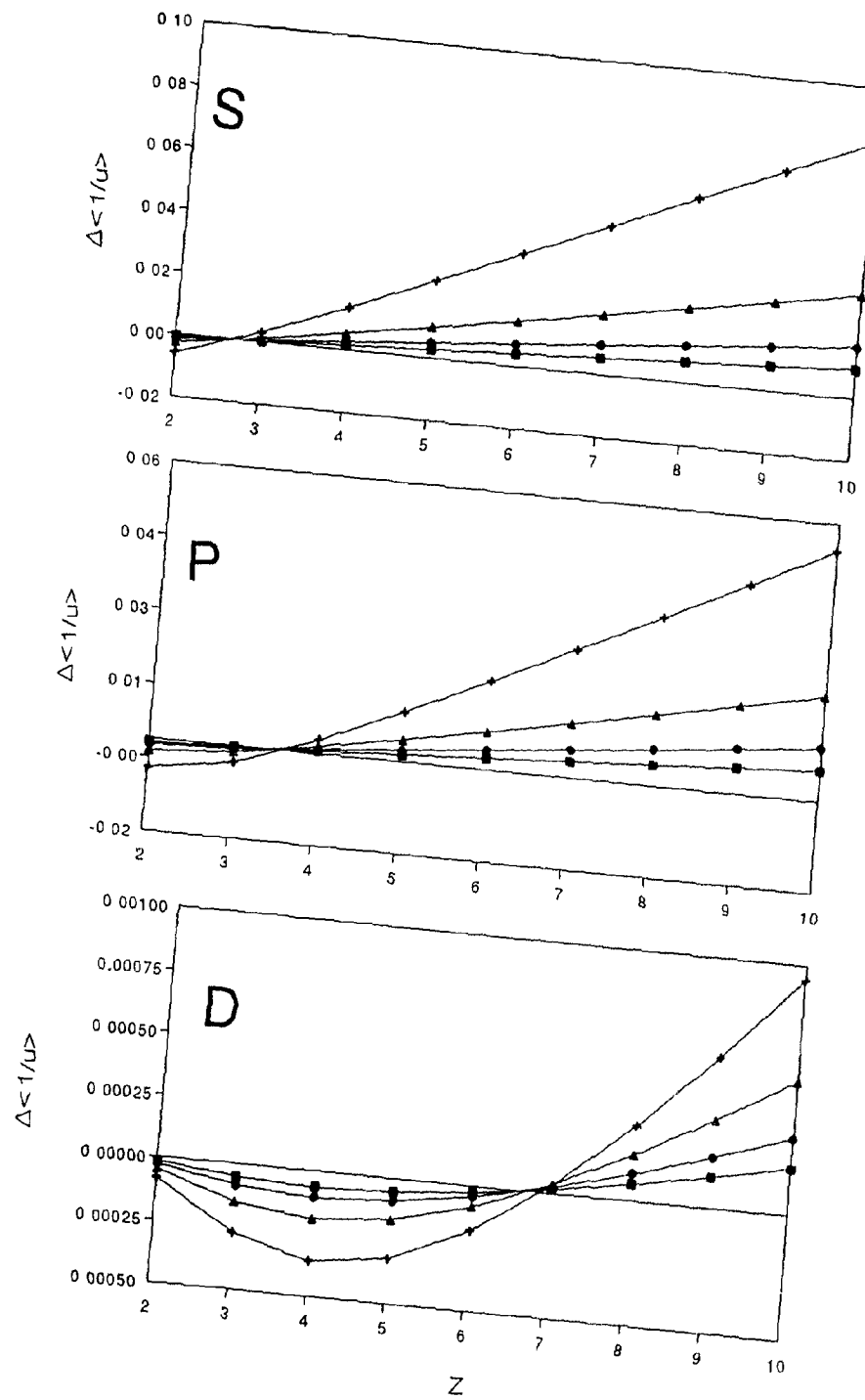


Figure 3.4.13:  $\Delta \langle 1/u \rangle$  for the  $nS$ ,  $nP$ , and  $nD$  states for  $n=3$  (+),  $n=4$  ( $\blacktriangle$ ),  $n=5$  ( $\bullet$ ) and  $n=6$  ( $\blacksquare$ ).

## CHAPTER 4:

### ELECTRON CORRELATION

#### 4.1 Correlation coefficients and Coulomb holes: An overview

In conventional quantum chemistry, electron correlation effects are those that are not taken into account by the Hartree-Fock approximation [3.3]. From a statistical perspective [3.3][3.6][4.1], electron correlation effects are those due to the difference between the true electron pair density and the product of the true one-electron densities:

$$c(\vec{r}_1, \vec{r}_2) = D_2(\vec{r}_1, \vec{r}_2) - D_1(\vec{r}_1)D_1(\vec{r}_2) \quad (4.1)$$

where

$$D_2(\vec{r}_1, \vec{r}_2) = \int \psi^*(\vec{x}_1, \vec{x}_2, \dots, \vec{x}_n) \psi(\vec{x}_1, \vec{x}_2, \dots, \vec{x}_n) d\sigma_1 d\sigma_2 d\vec{x}_3 d\vec{x}_4 \dots d\vec{x}_n \quad (4.2)$$

and

$$D_1(\vec{r}_1) = \int \psi^*(\vec{x}_1, \vec{x}_2, \dots, \vec{x}_n) \psi(\vec{x}_1, \vec{x}_2, \dots, \vec{x}_n) d\sigma_1 d\vec{x}_2 d\vec{x}_3 d\vec{x}_4 \dots d\vec{x}_n \quad (4.3)$$

The radial charge and intracule densities examined in chapter 3 can also be obtained from  $D_1(\vec{r}_1)$  and  $D_2(\vec{r}_1, \vec{r}_2)$ , respectively:

$$D(r) = n \int D_1(\vec{r}_1) \delta(r - r_1) d\vec{r}_1 \quad (4.4)$$

and

$$P(u) = \frac{n(n-1)}{2} \int D_2(\vec{r}_1, \vec{r}_2) \delta(u - r_{12}) d\vec{r}_1 d\vec{r}_2 \quad (4.5)$$

The conventional and statistical definitions of electron correlation effects are different since Hartree-Fock wavefunctions are antisymmetric and therefore account for Fermi correlation between electrons of like spin [4.2][4.3]. Thus the Hartree-Fock wavefunction leads to nonvanishing statistical correlation effects in systems with two or more electrons of like spin.

The pair correlation density,  $c(\vec{r}_1, \vec{r}_2)$ , is a rather complicated function of six variables and consequently difficult to analyze. Correlation coefficients,  $\tau_g$ , were introduced by Kutzelnigg, Del Re, and Berthier [4.4] to provide overall measures of the statistical correlation. These numerical indices are defined by

$$\tau_g = \frac{\frac{2n}{n-1} \langle \sum_{ij} g(\vec{r}_i) g(\vec{r}_j) \rangle - \langle \sum_i g(\vec{r}_i) \rangle^2}{n \langle \sum_i g^2(\vec{r}_i) \rangle - \langle \sum_i g(\vec{r}_i) \rangle^2} \quad (4.6)$$

where the product of vectors is interpreted as a scalar product. When the electrons are statistically independent  $c(\vec{r}_1, \vec{r}_2)$  vanishes and, since  $\tau_g$  may be rewritten as

$$\tau_g = \frac{\int c(\vec{r}_1, \vec{r}_2) g(\vec{r}_1) g(\vec{r}_2) d\vec{r}_1 d\vec{r}_2}{\int D_1(\vec{r}_1) D_1(\vec{r}_2) g(\vec{r}_1) [g(\vec{r}_1) - g(\vec{r}_2)] d\vec{r}_1 d\vec{r}_2} \quad (4.7)$$

$\tau_g$  vanishes also. These coefficients are origin dependent but, for atoms, the nucleus is the natural choice. When  $g(\vec{r})$  is spherically symmetric, the resulting coefficients are known as radial correlation coefficients. Otherwise, angular correlation coefficients are obtained.

The angular correlation coefficients obtained from the function  $g(\vec{r}) = \vec{r}$  has received considerable attention [4.5-4.7] since, for ground states, it can be obtained

directly from experimental measurements of diamagnetic susceptibilities and, either oscillator strengths or the small momentum-transfer behaviour of scattering (x-ray, high energy electron, high energy proton...) intensities.  $\tau_{\vec{r}}$  has also been used to test various representations of the exchange-correlation energy within the Hohenberg-Kohn-Sham theory [4.7].

Sections 4.2 and 4.3 examine several radial and angular correlation coefficients for the  $n^1S$ ,  $n^3S$ ,  $n^1P$ ,  $n^3P$ ,  $n^1D$ , and  $n^3D$  with  $n < 7$  for each of the nine heliumlike ions. The coefficients studied have been chosen to emphasize the inner or "core", intermediate, and outer regions of the electron distribution. The variations of the correlation coefficients with respect to nuclear charge  $Z$ , and angular momentum  $L$ , degree of excitation  $n$ , and spin multiplicity will be discussed. Several of the correlation coefficients considered here have been studied previously for the five lowest states of the heliumlike ions [4.5].

As noted previously, in the conventional quantum chemistry sense, electron correlation effects are those not taken into account by the Hartree-Fock approximation. Thus, the correlation energy  $E_{corr}$  was defined by Lowdin [4.8] as  $E_{corr} = E_{ex} - E_{HF}$  in which  $E_{ex}$  and  $E_{HF}$  are the exact non-relativistic energy and Hartree-Fock (HF) energy, respectively. A natural way to visualize electron correlation is to use the change in the radial intracule density  $P(u)$ . Hence, Coulson and Neilson [4.9] defined the Coulomb hole by

$$\Delta P(u) = P_{ex}(u) - P_{HF}(u) \quad (4.8)$$

in which  $P_{ex}(u)$  and  $P_{HF}(u)$  are the exact and Hartree-Fock (HF) radial intracule densities

respectively. For ground states of two-electron systems, estimates of  $\Delta P(u)$  may be obtained directly from X-ray scattering experiments [4.10]. Since  $\Delta P(u)$  does not contain information about the location of the electrons, it is useful to study the effects of correlation on the radial electron density  $D(r)$ , the radial probability density for the electron-nucleus distance  $r$ , by a density hole defined as

$$\Delta D(r) = D_{ex}(r) - D_{HF}(r) \quad (4.9)$$

Both holes integrate to zero. Hole volumes are used as measures of the charge redistribution arising from electron correlation. Thus, the total hole volume for the one-electron radial density is

$$V_{DT} = \frac{1}{2} \int_0^{\infty} |\Delta D(r)| dr = \int_{\Delta D \geq 0} |\Delta D(r)| dr = \int_{\Delta D \leq 0} |\Delta D(r)| dr \quad (4.10)$$

where the equalities hold since the hole integrates to zero. The outer hole volume is

$$V_{DO} = \int_{r_t}^{\infty} |\Delta D(r)| dr \quad (4.11)$$

where  $r_t$  is the largest finite zero. The total and outer volumes of the Coulomb hole,  $V_{PT}$  and  $V_{PO}$ , respectively, are defined by analogous integrals of  $\Delta P(u)$ .

Conventional electron correlation effects have been studied in the ground [4.11][4.12], CS [4.13][4.14], and 2P [4.15] states of the two-electron ions. Rydberg states of two-electron atoms can be expected to have relatively small electron correlation effects because the two electrons are in widely separated shells. Although these correlation effects may be small, they are rather interesting because of their subtlety.

Since, as shown in chapter 3, one- and two-electron densities of these ions change significantly with the total angular momentum  $L$ , and electron correlation effects should get more subtle as the outer electron is excited to higher levels, electron correlation effects in the D states are of some interest.

Sections 4.4 and 4.5 examine the conventional electron correlation effects in the  $3^1D$  and  $3^3D$  states of the ions from He to  $\text{Ne}^{8+}$ . Coulomb holes, density holes, and their respective hole volumes are studied. The two definitions of electron correlation are shown to be complementary for these states since the hole structures are explained by an examination of correlation coefficients.

## 4.2 Correlation coefficients: Computational notes

The radial correlation coefficients obtained from the choice  $\tau_{r^k}$  have the form

$$\tau_{r^k} = \frac{\frac{2n}{n-1} \langle \sum_{i>j} r_i^k r_j^k \rangle - \langle \sum_i r_i^k \rangle^2}{n \langle \sum_i r_i^{2k} \rangle - \langle \sum_i r_i^k \rangle^2} \quad (4.12)$$

The coefficients obtained from the choice  $k=+1$  have been studied in the five lowest states of the two-electron ions [4.5] and in the ground and first excited states of Li and Be [4.16][4.17]. In order to investigate shell effects, the  $k=-1$  coefficient was also considered in the latter studies [4.16][4.17]. Similarly, since the states considered here are relatively diffuse, we place emphasis on the outer regions by including  $k=+2$ . The  $k=-1,1,2$  coefficients are sufficient to emphasize radial correlation in the core, intermediate, and outer regions, respectively, of the charge cloud.

The angular correlation coefficients chosen to emphasize the core, intermediate, and outer regions are

$$\tau_{\vec{r}_i \vec{r}_j} = \frac{2}{n(n-1)} \left\langle \sum_{i>j} \left( \frac{\vec{r}_i}{r_i} \right) \left( \frac{\vec{r}_j}{r_j} \right) \right\rangle = \frac{2}{n(n-1)} \left\langle \sum_{i>j} \cos\theta_{ij} \right\rangle, \quad (4.13)$$

$$\tau_{\vec{r}} = \frac{2 \left\langle \sum_{i>j} \vec{r}_i \cdot \vec{r}_j \right\rangle}{(n-1) \left\langle \sum_i r_i^2 \right\rangle} = \frac{2 \left\langle \sum_{i>j} r_i r_j \cos(\theta_{ij}) \right\rangle}{(n-1) \left\langle \sum_i r_i^2 \right\rangle}, \quad (4.14)$$

and

$$\tau_{rr} = \frac{2 \left\langle \sum_{i>j} r_i r_j \vec{r}_i \cdot \vec{r}_j \right\rangle}{(n-1) \left\langle \sum_i r_i^4 \right\rangle} = \frac{2 \left\langle \sum_{i>j} r_i^2 r_j^2 \cos(\theta_{ij}) \right\rangle}{(n-1) \left\langle \sum_i r_i^4 \right\rangle}. \quad (4.15)$$

respectively, where  $\theta_{ij}$  is the angle subtended at the nucleus by the position vectors  $\vec{r}_i$  and  $\vec{r}_j$ . These angular correlation coefficients are bounded in absolute value by unity:  $\tau=1$  when the position vectors coincide, and  $\tau=-1$  when the position vectors are at diametrical positions with respect to the nucleus. The angular correlation coefficients vanish either when the electrons are independent (ie  $c(\vec{r}_1, \vec{r}_2) = 0$ ) or when their position vectors are orthogonal.

The integrals required in the evaluation of the correlation coefficients are reduced [2.29] to the form shown in equation (2.19) and evaluated using a modified recursion relation of Sack *et al* [2.30]. The calculation of  $\tau_{1/r}$  requires caution since integrals of the form  $\langle r^{-2} \rangle$  arise. These integrals, and the numerical instabilities which may arise in their evaluation, are evaluated by procedures analogous to those described previously [2.26].

Correlation coefficients for the infinite  $Z$  limit have been evaluated by substituting wavefunctions of the form shown in equation (3.3) into the correlation coefficient expressions and evaluating the appropriate integrals. With the exception of the S states, the infinite  $Z$  limit of the radial correlation coefficients are equal for the singlet and triplets (that is, at infinite  $Z$   $\tau_{r^k}(n^1L) = \tau_{r^k}(n^3L)$  for  $L \neq 0$ ). Furthermore, with the exception of the P states, the angular correlation coefficients vanish in the limit of infinite  $Z$ .

The correlation coefficients are presented graphically in this chapter. The figures for  $n=5$  and  $n=6$  are not shown since they qualitatively resemble the  $n=4$  curves. Furthermore, the trends observed as  $n$  increases from 3 to 4 persist to larger  $n$ . For  $n=5$  and 6,  $\tau_r$  and  $\tau_{rr}$  (see equations (4.14) and (4.15)) show somewhat erratic behaviour as  $Z$  increases but the overall variation with  $Z$  is consistent with the  $n=3$  and 4 results. This behaviour is considered unphysical and is due to the emphasis placed on energetically unimportant regions of the charge cloud (i.e.  $\langle r_1^2 r_2^2 \cos(\theta_{12}) \rangle$  emphasizes the situation where both electrons are distant from the nucleus).

Numerical values of the correlation coefficients are given in Appendix 5. All calculations were performed in quadruple precision using the 100-term integral transform wavefunctions discussed in chapter 2.

### 4.3 Correlation coefficients: Results and discussion

The correlation coefficients are shown in figures 4.3.1-4.3.9: Figures 4.3.1-4.3.3, 4.3.4-4.3.6, 4.3.7-4.3.9 show  $\tau_{1/r}$  and  $\tau_{z/r}$ ,  $\tau_r$  and  $\tau_z$ ,  $\tau_{r^2}$  and  $\tau_{rz}$ ,

respectively. The first figure in each sequence shows the coefficients for the  $n=1$  and  $2$  states, the second figure shows the  $n=3$  coefficients, and the last of each sequence shows the  $n=4$  results.

Radial correlation is most important in the intermediate regions of the charge cloud, followed by the outer and core regions: the ratio  $\tau_{1/r}:\tau_r:\tau_{r^2}$  is approximately 3:7:5. Angular correlation, on the other hand, decreases in importance from the core to the intermediate to the outer regions of the charge cloud. For  $n=2$ , the ratio  $\tau_{\vec{r}/r}:\tau_{\vec{r}}:\tau_{\vec{r}r}$  is 4:2:1 and angular correlation is comparatively significant in all regions of the charge cloud, but for  $n=6$  this ratio becomes 100000:500:1 and angular correlation is overwhelmingly more significant in the core region. These ratios can be understood quite simply. In the K-shell, angular correlation is more efficient than radial correlation because of the small size of the K-shell; thus, in the K-shell, correlation energy is obtained primarily through decreased shielding leading to an increase in electron-nucleus attraction. In the intermediate region, both forms of correlation can be important. In the huge Rydberg region, radial correlation is favoured because greater stabilization can be obtained by reduction of interelectronic repulsion than by increase of attraction to the distant nucleus. The probability of finding both electrons in one of these regions is greatest for the intermediate region, and so radial correlation is most significant there.

As  $n$  increases the radial correlation coefficients increase slightly in magnitude but angular correlation decreases in importance. In fact, the angular correlation coefficients change dramatically with  $n$ :  $\tau_{\vec{r}/r}$ ,  $\tau_{\vec{r}}$ , and  $\tau_{\vec{r}r}$  decrease by factors of 40, 4000, and 500000, respectively, as  $n$  increases from 2 to 6. These trends are expected since as  $n$

increases, the size of the Rydberg region increases and radial correlation increasingly overshadows angular correlation.

As shown in figures 4.3.1, 4.3.2, and 4.3.3,  $\tau_{1/r}$  decreases approximately linearly with  $1/Z$ . The maximum change in  $\tau_{1/r}$  as  $Z$  increases from 2 to  $\infty$  is 15% and 3%, for  $n=3$  and  $n=6$ , respectively. Radial correlation in the core is considerably more significant for the  $^3S$  than for the  $^1S$ , slightly more significant for the  $^1P$  than for the  $^3P$ , and virtually identical for the  $^1D$  and  $^3D$  states. The figures show that radial correlation in the core is of similar importance for the  $^3S$ ,  $^1P$ ,  $^3P$ ,  $^1D$ , and  $^3D$  states, but noticeably less important for the  $^1S$  states.

Since the  $\tau_{\vec{r}/r}$  curves for the S and D states lie close together, angular correlation in the core is of equal importance for these states. However, their  $Z$  dependence differs:  $\tau_{\vec{r}/r}$  increases with  $Z$  for the  $^3S$  states but has a slight minimum at  $Z=3$  for the  $^1S$ ,  $^1D$ , and  $^3D$  states. The  $^1P$  coefficients increase with  $Z$  becoming positive at  $Z=3$ ; angular correlation keeps the electrons on the same side of the nucleus for  $Z \geq 3$ .  $\tau_{\vec{r}/r}$  decreases steadily with  $Z$  for the  $^3P$  states, indicating that the tendency to occupy opposite sides of the nucleus increases with  $Z$ .

In the limit of  $Z=\infty$ , radial correlation for intermediate- $r$  is most important for the S states, followed by the P states, and finally the D states. As figures 4.3.4, 4.3.5, and 4.3.6 show, radial correlation is most significant for the S states for all  $Z$ . The  $^1S$  and  $^3S$  curves do cross however, with the  $^1S$  coefficients larger for small  $Z$ . On the other hand, no singlet-triplet crossings occur for the P and D states, where the triplet correlation coefficients are always slightly smaller. For  $n=3$  the D state coefficients are

larger than the P state values for  $Z \leq 10$  but, for  $n > 3$ , the D and P state curves are well separated with the order at  $Z = \infty$  persisting for all  $Z$ . Figure 4.3.6 shows that the  $Z$  dependence of  $\tau_r$  is similar for the S, P and D states, that is, the slopes are similar. As  $n$  increases, these slopes become increasingly similar and approach 0. For  $n=4$   $\tau_r$  for the P states is approximately the average of the S and D state values but, for  $n > 4$ ,  $\tau_r$  for the P states approach the S state values.

A comparison of figures 4.3.1 and 4.3.4, shows that  $\tau_{\bar{r}}$  and  $\tau_{\bar{r}/r}$  are qualitatively similar for  $n=2$ . These similarities disappear for larger  $n$ ; the intermediate- $r$  angular coefficients show stronger  $Z$  dependence, the S and D state curves are well separated, and  $\tau_{\bar{r}/r}$  becomes several orders of magnitude larger than  $\tau_{\bar{r}}$ . Also, although the  $^1P$  coefficients eventually become positive, the transition occurs at larger  $Z$  as  $n$  increases:  $\tau_{\bar{r}}$  is positive for  $Z=3, 5, 7, 10$ , and  $> 10$  for  $n=2, 3, 4, 5$ , and 6, respectively.  $\tau_{\bar{r}}$  becomes more positive along the sequence  $^3P, ^1D, ^3D, ^1S, ^3S$ , and  $^1P$ . Exceptions to this ordering occur for He where the  $^3S$  coefficient is between the  $^3P$  and  $^1D$  values, and for  $Z=3$  and  $Z=4$  ( $n > 4$ ) where the S states are interchanged. As  $n$  increases, all  $\tau_{\bar{r}}$  curves show a minimum at  $Z=3, 4$ , or 5. These are most pronounced for the  $^3P$  states where angular correlation at the minimum is twice the He value, and least pronounced for the  $^1P$  states where  $\tau_{\bar{r}}$  at the minimum is less than 20% larger than the He value.

With the exception of the  $Z \geq 6$  ions in the  $2^1S$  state, radial correlation for large- $r$  is most important for the singlet states;  $\tau_{r^2}$  decreases along the sequence  $n^1S, n^3S, n^1P, n^3P, n^1D$ , and  $n^3D$ . Similar to  $\tau_r$ , the S, P, and D state curves become well separated but the curves do not show the same  $Z$  dependence. Except for the  $2^1S$  and  $2^3P$  states,  $\tau_{r^2}$

decreases slightly for the  $n^1S$  and  $n^3P$  states. All  $n^3S$  coefficients increase with  $Z$  and all  $n^3P$ ,  $n^1D$ , and  $n^3D$  coefficients decrease with  $Z$ . However, as shown in figures 4.3.7, 4.3.8, and 4.3.9, these variations with  $Z$  are quite small (from 12% in the  $2^1P$  state to 0.04% in the  $6^3D$  state).

Angular correlation in the large- $r$  region of the charge cloud decreases along the sequence  $^1D$ ,  $^3D$ ,  $^3P$ ,  $^3S$ ,  $^1S$ , and  $^1P$ . Exceptions to this ordering do occur: for large  $Z$ , the  $^3P$  coefficient is most negative and the S states are interchanged; for small  $Z$ , the  $^3S$  coefficient becomes more negative than the  $^3P$  and even the D state values. The  $Z$  dependence of the correlation coefficients is more pronounced than for  $\tau_i$ ; angular correlation at the minimum is up to triple the He value.

Within the context of  $Z^{-1}$  perturbation theory, the correlation coefficients studied here may be expanded in the form

$$\tau_g = a_{g,0} + a_{g,1}/Z + a_{g,2}/Z^2 + \quad (4.16)$$

where the first expansion coefficient,  $a_{g,0}$ , is the infinite  $Z$  limit of the correlation coefficient. Estimates of the next coefficients in the expansion have been calculated by least squares fitting of the correlation coefficients and by differencing techniques. Tables 4.3.1-4.3.6 list the estimates of  $a_{g,1}$  obtained for the 29 states and 6 coefficients considered. Each table considers one correlation coefficient; for each state, the top entry is  $a_{g,0}$ , followed by  $a_{g,1}$ , and, when an estimate is possible,  $a_{g,2}$ . The substitution of these values into equation (4.16) will provide estimates of the correlation coefficients for  $Z$  not considered in this work.

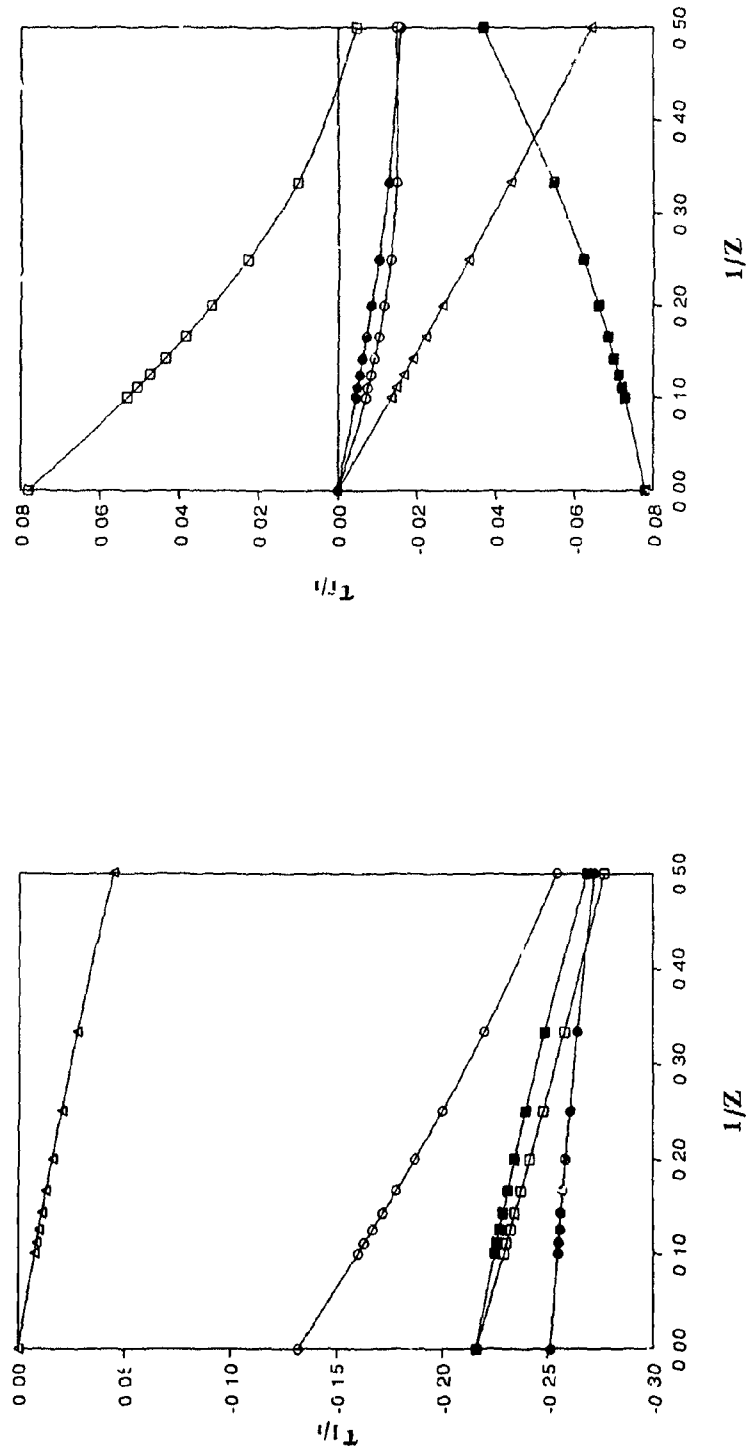


Figure 4.3.1:  $\tau_{1/r}$  and  $\tau_{r/r}$  for the  $1^1S$  ( $\Delta$ ),  $2^1S$  ( $\circ$ ),  $2^1P$  ( $\bullet$ ), and  $2^3P$  ( $\blacksquare$ ) states.

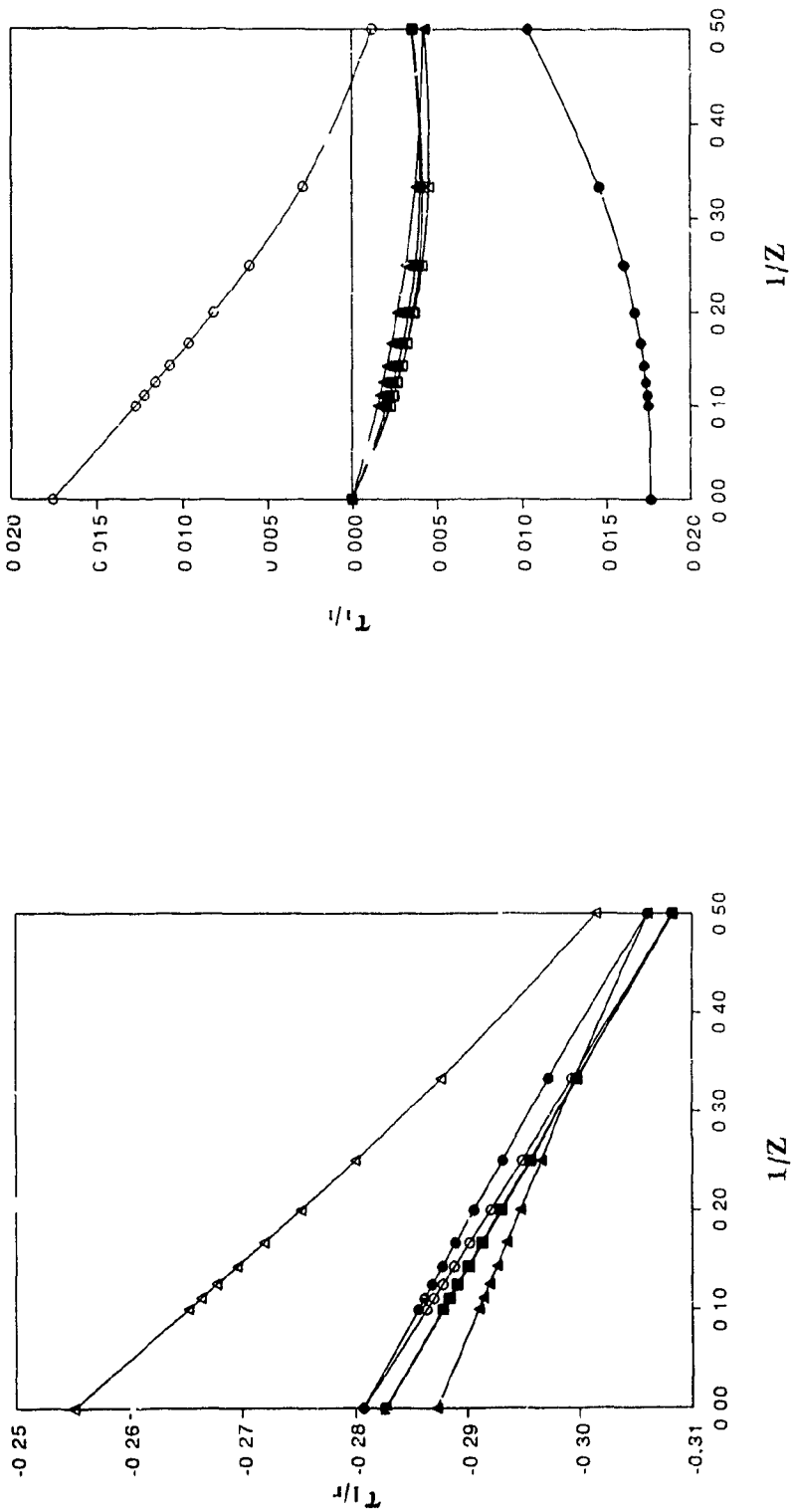


Figure 4.3.2:  $\tau_{1/r}$  and  $\tau_{z/r}$  for the  $3^1S$  ( $\Delta$ ),  $3^3S$  ( $\blacktriangle$ ),  $3^1P$  ( $\circ$ ),  $3^3P$  ( $\bullet$ ),  $3^1D$  ( $\square$ ), and  $3^3D$  ( $\blacksquare$ ) states.

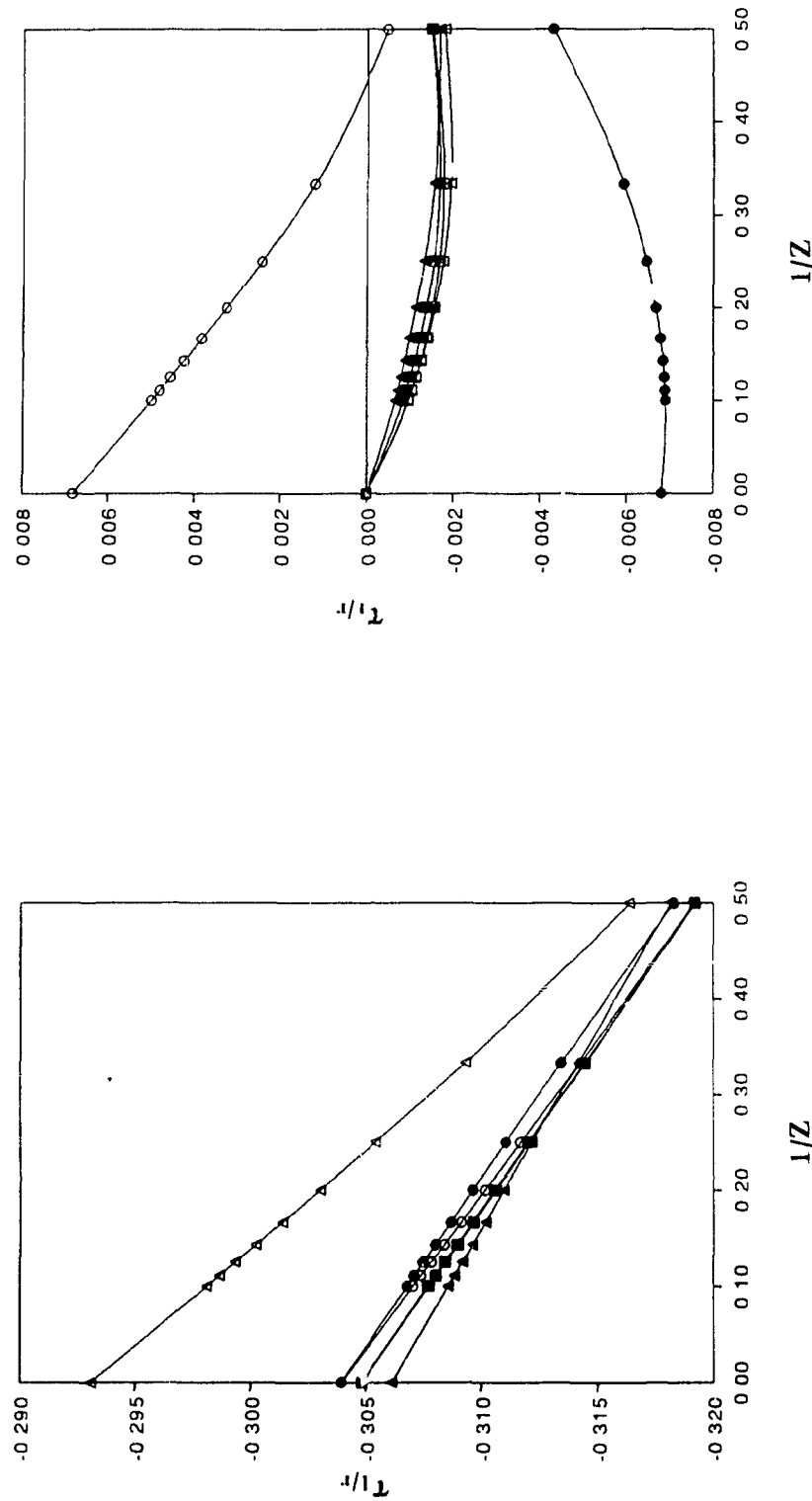


Figure 4.3.3:  $\tau_{1/r}$  and  $\tau_{r/r}$  for the  $4^1S$  ( $\Delta$ ),  $4^3S$  ( $\blacktriangle$ ),  $4^1P$  ( $\circ$ ),  $4^3P$  ( $\bullet$ ),  $4^1D$  ( $\square$ ), and  $4^3D$  ( $\blacksquare$ ) states.

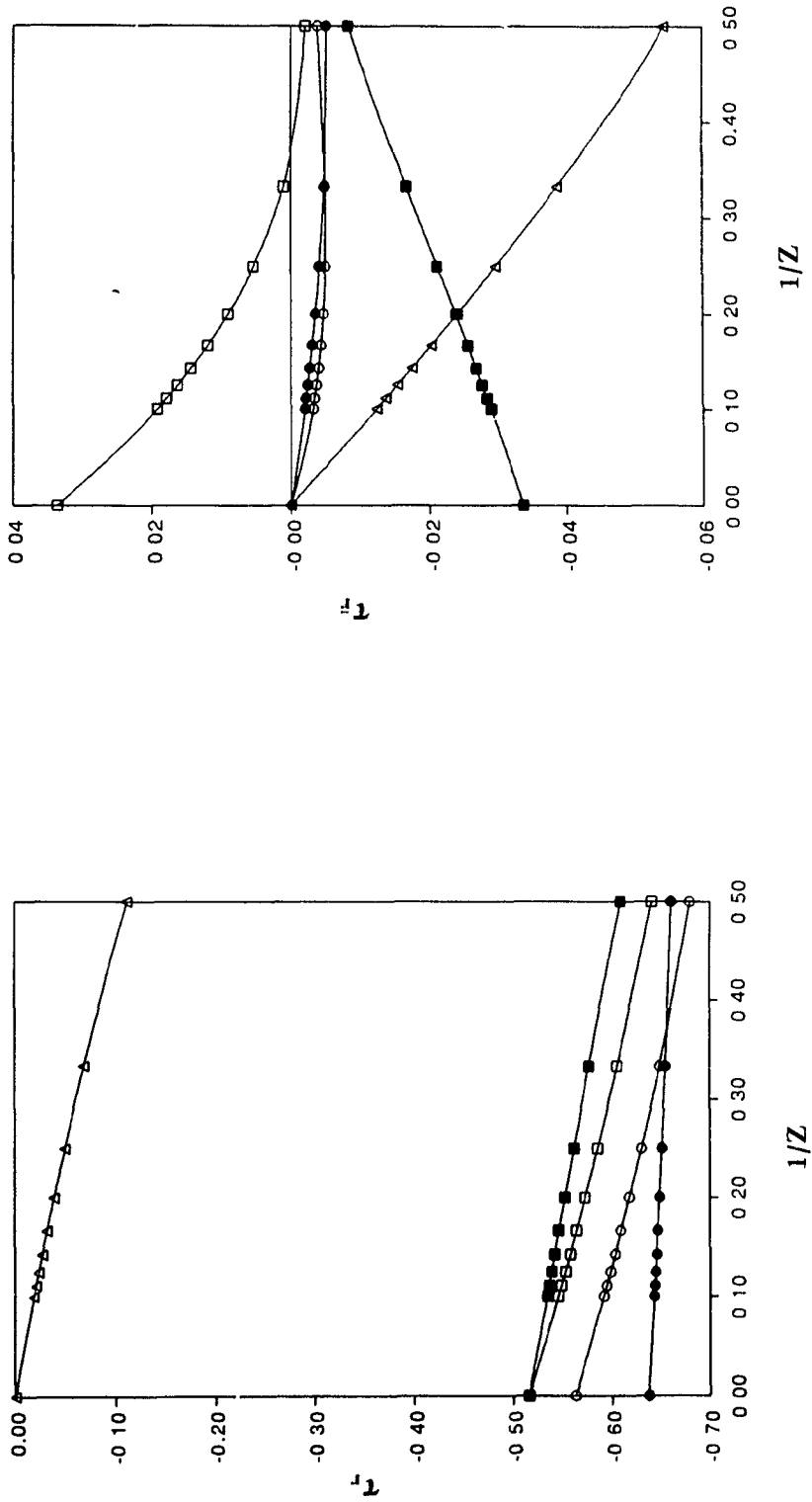


Figure 4.3.4:  $\tau_r$  and  $\tau_{r'}$  for the  $1^1S$  ( $\Delta$ ),  $2^1S$  ( $\circ$ ),  $2^3S$  ( $\bullet$ ),  $2^1P$  ( $\square$ ), and  $2^3P$  ( $\blacksquare$ ) states.

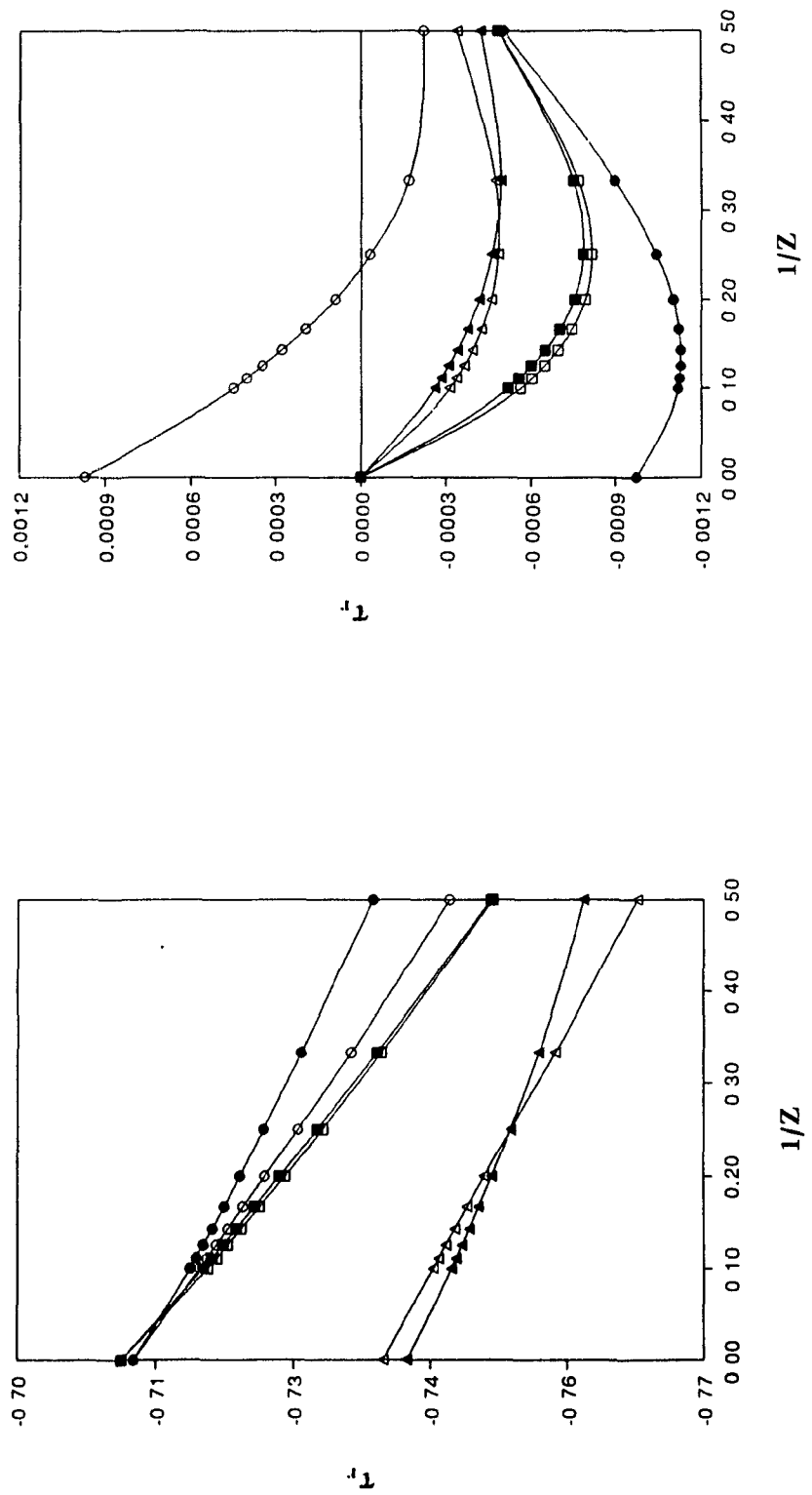


Figure 4.3.5:  $\tau_r$  and  $\tau_f$  for the  $3^1S$  ( $\Delta$ ),  $3^3S$  ( $\blacktriangle$ ),  $3^1P$  ( $\circ$ ),  $3^3P$  ( $\bullet$ ),  $3^1D$  ( $\square$ ), and  $3^3D$  ( $\blacksquare$ ) states.

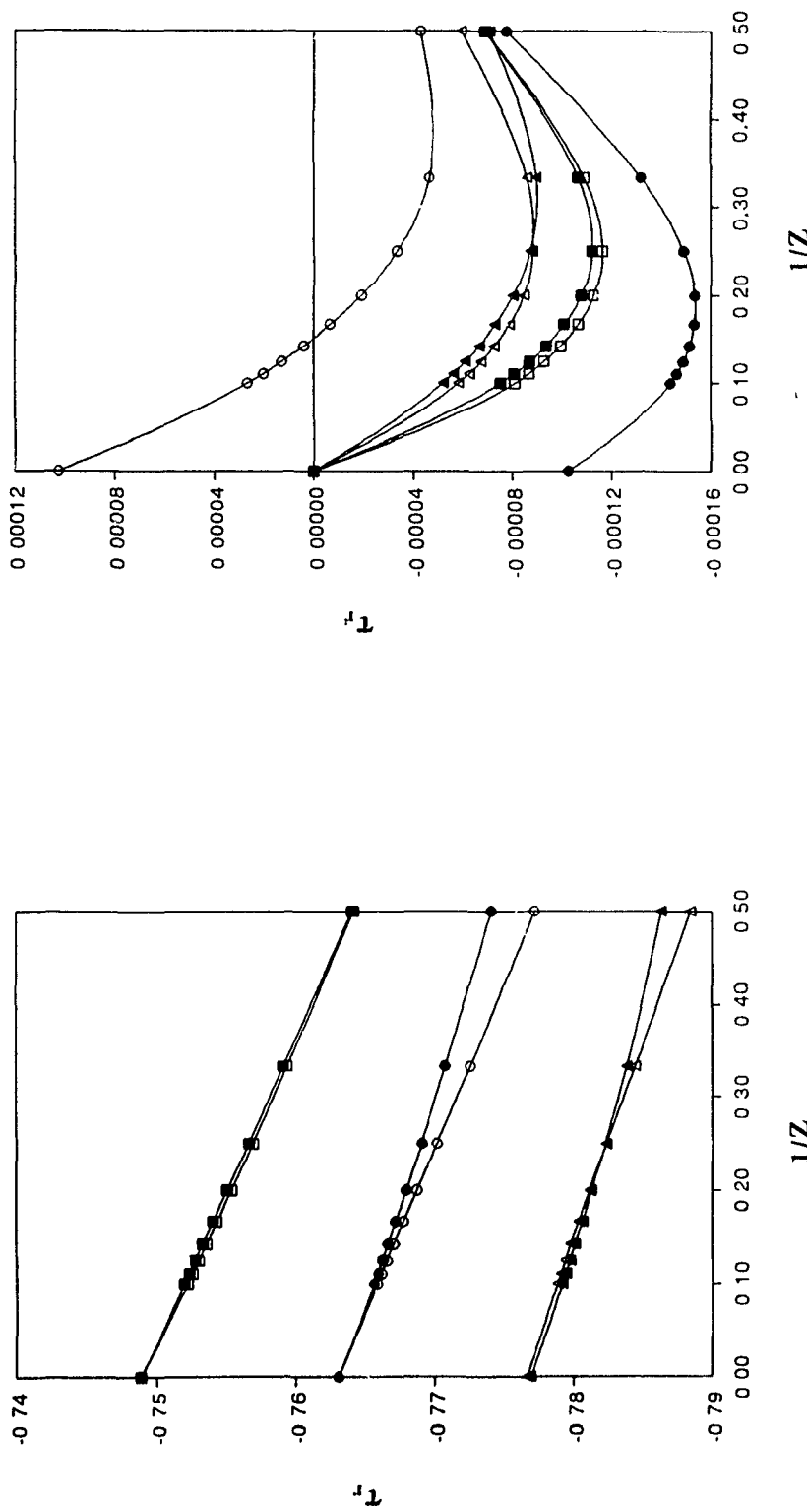


Figure 4.3.6:  $\tau_r$  and  $\tau_f$  for the  $4^1S$  ( $\Delta$ ),  $4^3S$  ( $\blacktriangle$ ),  $4^1P$  ( $\circ$ ),  $4^3P$  ( $\bullet$ ),  $4^1D$  ( $\square$ ), and  $4^3D$  ( $\blacksquare$ ) states.

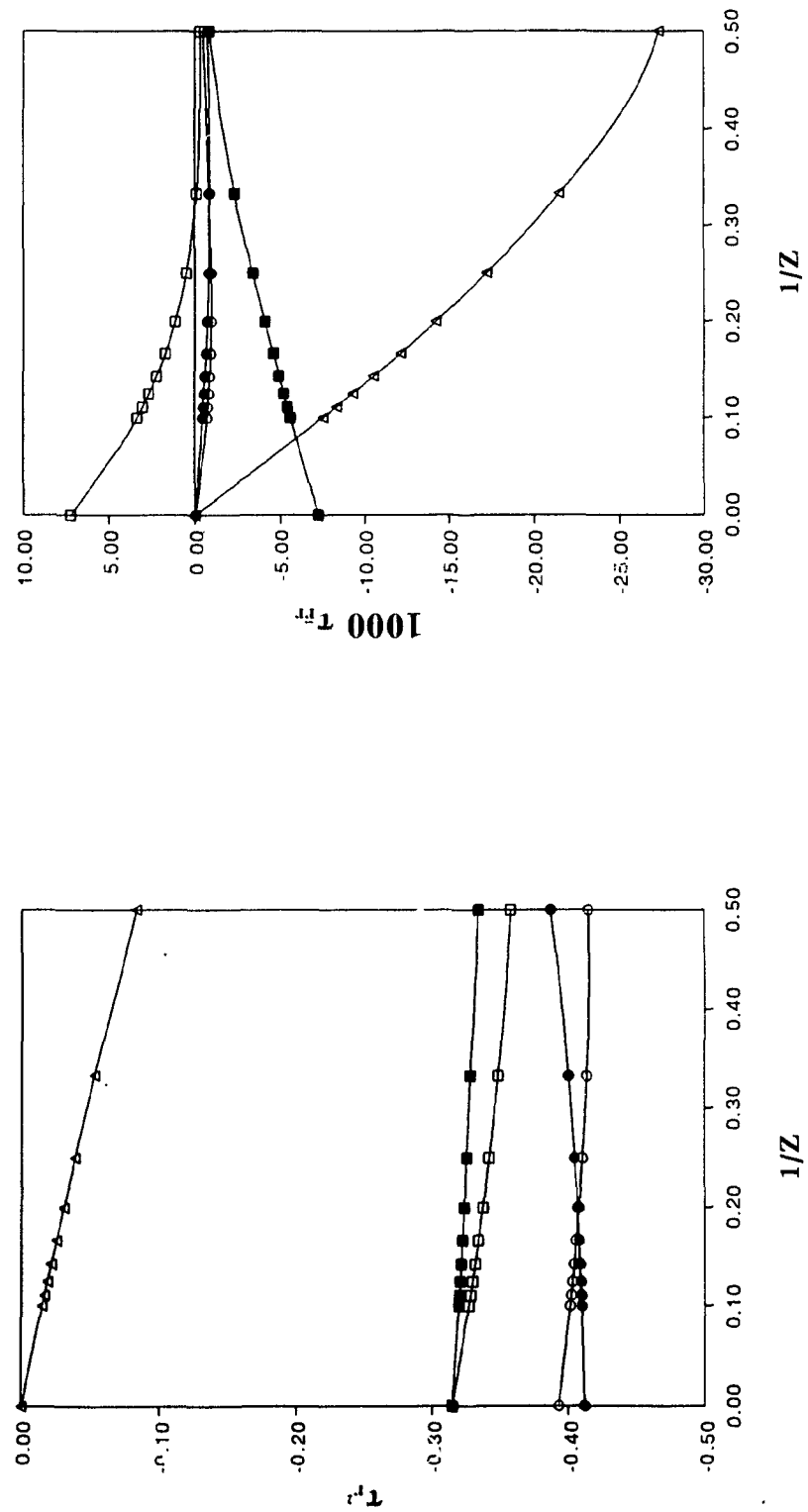


Figure 4.3.7:  $\tau_{r2}$  and  $\tau_{rr}$  for the  $1^1S$  ( $\Delta$ ),  $2^1S$  ( $\circ$ ),  $2^3S$  ( $\bullet$ ),  $2^1P$  ( $\square$ ), and  $2^3P$  ( $\blacksquare$ ) states.

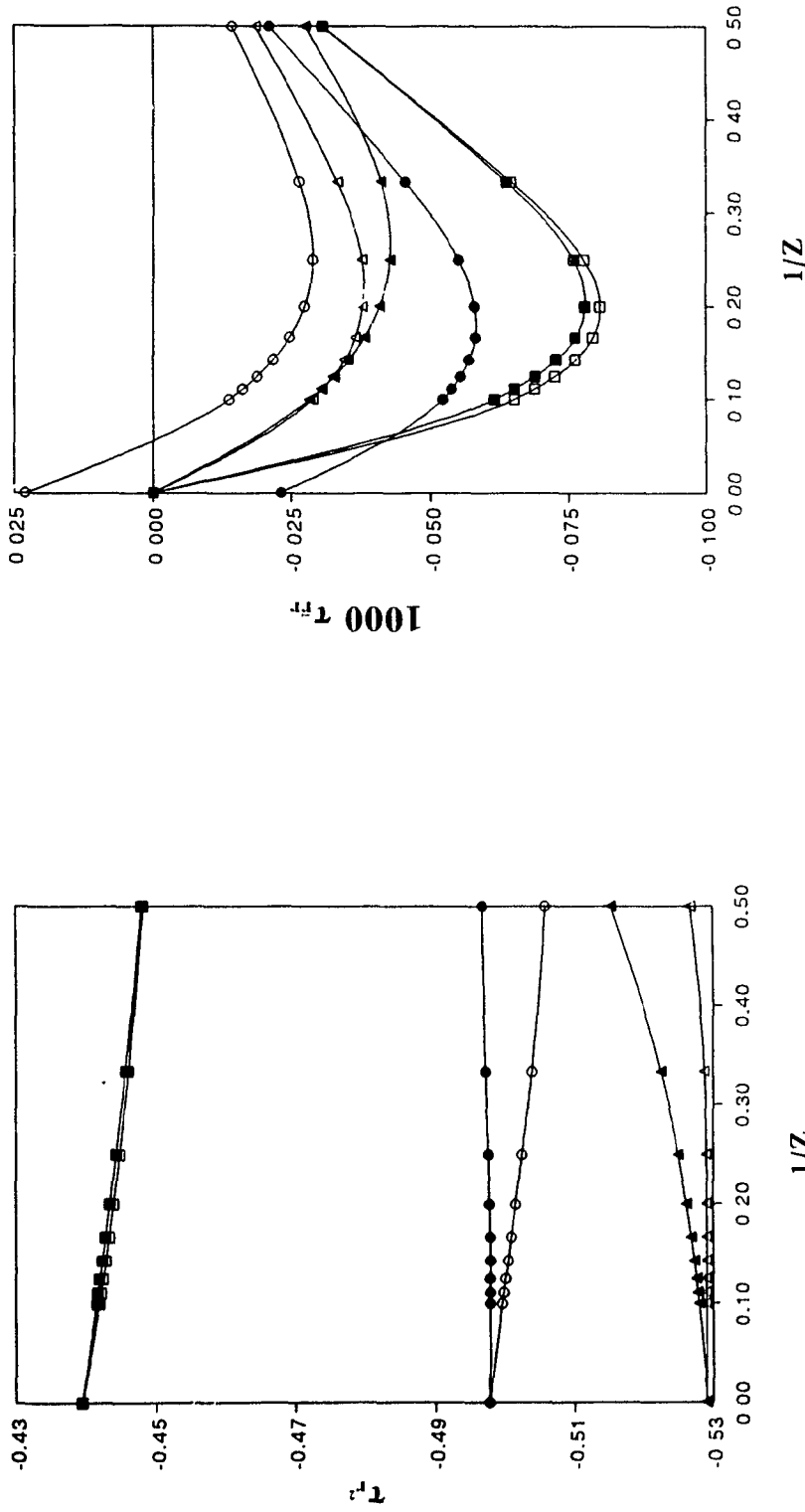


Figure 4.3.8:  $\tau_r$  and  $\tau_{r^2}$  for the  $3^1S$  ( $\Delta$ ),  $3^3S$  ( $\blacktriangle$ ),  $3^1P$  ( $\circ$ ),  $3^3P$  ( $\bullet$ ),  $3^1D$  ( $\square$ ), and  $3^3D$  ( $\blacksquare$ ) states.

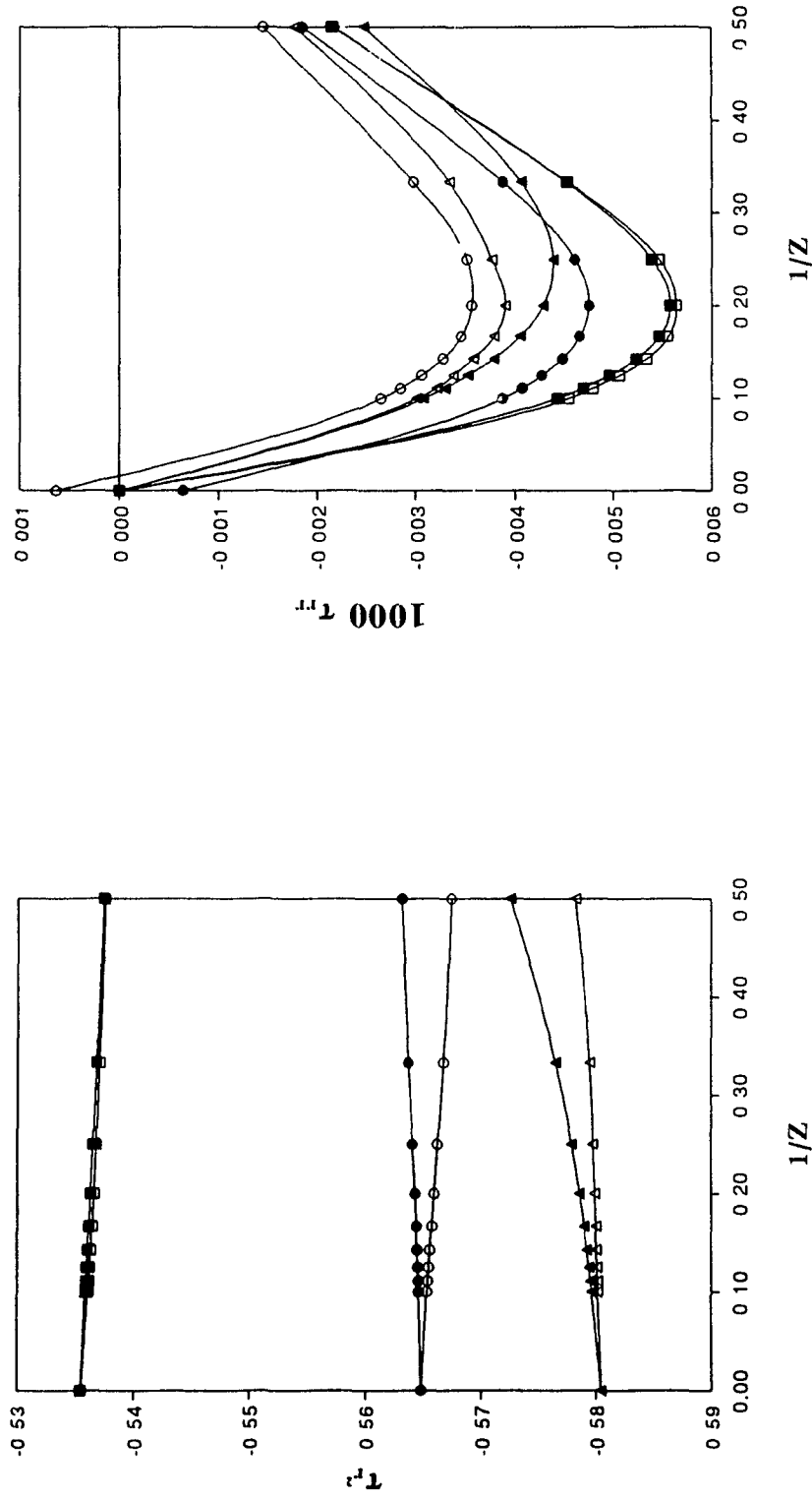


Figure 4.3.9:  $\tau_{rz}$  and  $\tau_{rr}$  for the  $4^1S$  ( $\Delta$ ),  $4^3S$  ( $\blacktriangle$ ),  $4^1P$  ( $\circ$ ),  $4^3P$  ( $\bullet$ ),  $4^1D$  ( $\square$ ), and  $4^3D$  ( $\blacksquare$ ) states.

Table 4.3.1:  $1/Z$  expansion coefficients of  $\tau_{1/r}$ .

$n^1S$	$n^3S$	$n^1P$	$n^3P$	$n^1D$	$n^3D$
<hr/>					
$n=1$					
0					
-0.0734					
-0.022					
$n=2$					
-0.131716	-0.251262	-0.216000	-0.216000		
-0.2885	-0.03303	-0.1322	-0.0843		
0.04	-0.012	0.017	-0.03		
$n=3$					
-0.255098	-0.287275	-0.280702	-0.280702	-0.282686	-0.282686
-0.1011	-0.03707	-0.0566	-0.04925	-0.0525	-0.05095
	0.002	-0.002	0.002	0.007	-0.0007
$n=4$					
-0.293086	-0.306115	-0.303917	-0.303917	-0.304795	-0.304795
-0.0502	-0.0246	-0.0313	-0.0288	-0.0296	-0.02889
	0.002		0.003	0.003	-0.0001
$n=5$					
-0.309099	-0.315630	-0.314639	-0.314639	-0.315098	-0.315098
-0.0294	-0.01672	-0.0197	-0.0186	-0.0188	-0.0185
	0.002		0.002	0.001	
$n=6$					
-0.317227	-0.320960	-0.320429	-0.320429	-0.320697	-0.320697
-0.0192	-0.0119	-0.0135	-0.0129	-0.0131	-0.0128
	0.001		0.001	0.001	

---

**Table 4.3.2:**  $1/Z$  expansion coefficients of  $\tau_x$ .

$n^1S$	$n^3S$	$n^1P$	$n^3P$	$n^1D$	$n^3D$
<hr/>					
$n=1$					
0					
-0.1794					
-0.07					
$n=2$					
-0.563005	-0.636995	-0.515789	-0.515789		
-0.2998	-0.06007	-0.3101	-0.1822		
0.116	0.012	0.118	-0.01		
$n=3$					
-0.737245	-0.739678	-0.711765	-0.711765	-0.710526	-0.710526
-0.0499	-0.04708	-0.0655	-0.0588	-0.0907	-0.0838
-0.006	0.0173	-0.005	0.025	0.05	0.017
$n=4$					
-0.776621	-0.776888	-0.763104	-0.763104	-0.748892	-0.748892
-0.0215	-0.02365	-0.0266	-0.0262	-0.0345	-0.0313
-0.004	0.0073	-0.01	0.01	0.011	0.001
$n=5$					
-0.792635	-0.792686	-0.784251	-0.784251	-0.772340	-0.772340
-0.0123	-0.01399	-0.0146	-0.01479	-0.018	-0.0165
	0.0036	-0.003	0.005		
$n=6$					
-0.800821	-0.800835	-0.795099	-0.795099	-0.785903	-0.785903
-0.0081	-0.00925	-0.0093	-0.0095	-0.0112	-0.0103
	0.00200	-0.003	0.002		

---

Table 4.3.3: 1/Z expansion coefficients of  $\tau_{x^2}$ .

	$n^1S$	$n^3S$	$n^1P$	$n^3P$	$n^1D$	$n^3D$
$n=1$						
	0					
	-0.145					
	-0.04					
$n=2$						
	-0.392985	-0.411777	-0.314767	-0.314767		
	-0.089	0.0157	-0.1284	-0.050		
	0.08	0.043	0.08	0.03		
$n=3$						
	-0.529001	-0.529123	-0.497712	-0.497712	-0.439362	-0.439362
		0.0087	-0.0176	-0.0032	-0.0274	-0.0217
		0.028	-0.01	0.017	0.03	0.009
$n=4$						
	-0.580451	-0.580456	-0.564836	-0.564836	-0.535462	-0.535462
	0.003	0.0067	-0.005	0.0013	-0.0069	-0.0041
		0.013		0.006	0.009	
$n=5$						
	-0.606524	-0.606525	-0.597238	-0.597238	-0.579556	-0.579556
	0.003	0.00438	-0.0015	0.0014	-0.0026	-0.0011
		0.0072	-0.004			
$n=6$						
	-0.621464	-0.621464	-0.615312	-0.615312	-0.603474	-0.603474
	0.0016	0.00289	-0.0005	0.0011	-0.001	-0.0003
		0.004	-0.004			

Table 4.3.4:  $1/Z$  expansion coefficients of  $\tau_{\vec{r}/r}$ .

$n^1S$	$n^3S$	$n^1P$	$n^3P$	$n^1D$	$n^3D$
<b><math>n=1</math></b>					
0					
-0.1332					
0.002					
<b><math>n=2</math></b>					
0	0	7.8037(-2)	-7.8037(-2)		
-0.0827	-0.04736	-0.2652	0.0454		
0.134	0.0237	0.144	0.068		
<b><math>n=3</math></b>					
0	0	1.7578(-2)	-1.7578(-2)	0	0
-0.0264	-0.016643	-0.04882	-0.0022	-0.0285	-0.0244
0.041	0.01596	0.002	0.032	0.059	0.039
<b><math>n=4</math></b>					
0	0	6.7948(-3)	-6.7948(-3)	0	0
-0.0114	-0.007382	-0.0180	-0.0023	-0.0122	-0.0100
0.018	0.00837		0.015	0.026	0.015
<b><math>n=5</math></b>					
0	0	3.3452(-3)	-3.3452(-3)	0	0
-0.0059	-0.003862	-0.00876	-0.0014	-0.006	-0.0051
0.009	0.0047	0.0006	0.007	0.01	0.008
<b><math>n=6</math></b>					
0	0	1.8957(-3)	-1.8957(-3)	0	0
-0.00345	-0.002261	-0.00493	-0.00091	-0.0036	-0.0029
0.006	0.00291	0.0004	0.004	0.008	0.004

Table 4.3.5:  $1/Z$  expansion coefficients of  $\tau_{\vec{r}}$ .

	$n^1S$	$n^3S$	$n^1P$	$n^3P$	$n^1D$	$n^3D$
$n=1$						
	0					
	-0.1261					
	0.02					
$n=2$						
	0	0	3.3632(-2)	-3.3632(-2)		
	-0.0421	-0.02229	-0.1647	0.0426		
	0.110	0.0217	0.213	0.033		
$n=3$						
	0	0	9.7256(-4)	-9.7256(-4)	0	0
	-0.00413	-0.003174	-0.00614	-0.00239	-0.0078	-0.0069
	0.011	0.00596	0.009	0.010	0.024	0.018
$n=4$						
	0	0	1.0257(-4)	-1.0257(-4)	0	0
	-0.00077	-0.000654	-0.00093	-0.000599	-0.00111	-0.00100
	0.002	0.00143	0.0019	0.00200	0.003	0.0027
$n=5$						
	0	0	1.9320(-4)	-1.9320(-4)	0	0
	-0.00021	-0.000183	-0.00023	-0.000174	-0.00026	-0.000245
	0.0006	0.0004	0.0005	0.00054		0.0007
$n=6$						
	0	0	5.0887(-6)	-5.0887(-6)	0	0
	-0.00007	-0.000064	-0.00008	-0.00006	-0.00008	-0.00008
	0.0002	0.00015	0.0002	0.0002	0.0002	0.0002

Table 4.3.6:  $1/Z$  expansion coefficients of  $\tau_{\bar{r}\bar{r}}$ .

$n^1S$	$n^3S$	$n^1P$	$n^3P$	$n^1D$	$n^3D$
$n=1$					
0					
-0.07957					
0.039					
$n=2$					
0	0	7.2433(-3)	-7.2433(-3)		
-0.0108	-0.00536	-0.0488	0.0162		
0.040	0.0087	0.111	0.001		
$n=3$					
0	0	2.3070(-5)	-2.3070(-5)	0	0
-0.00042	-0.000377	-0.00053	-0.00044	-0.00100	-0.000919
0.0015	0.0010	0.0019	0.0017	0.004	0.00347
$n=4$					
0	0	6.3896(-7)	-6.3896(-7)	0	0
-0.000043	-0.0000425	-0.00005	-0.000048	-0.000069	-0.00007
0.00014	0.000130	0.0002	0.00018	0.0003	0.0002
$n=5$					
0	0	4.5354(-8)	-4.5354(-8)	0	0
-0.000007	-0.0000075	-0.000008	-0.000008	-0.000010	-0.000010
0.00002	0.00002	0.00003	0.00003	0.00003	0.00003
$n=6$					
0	0	5.5094(-9)	-5.5094(-9)	0	0
-0.000002	-0.0000017	-0.000002	-0.000002	-0.000002	-0.000002
	0.000005	0.000001		0.000008	0.000007

#### 4.4 Coulomb holes: Computational notes

The evaluation of Coulomb and density holes for the 3D states requires intracule and charge densities for the exact and Hartree-Fock 3D state wavefunctions. Clearly, the exact wavefunctions and corresponding densities are approximated by those discussed in chapters 2 and 3, respectively. The Hartree-Fock (HF) wavefunctions are approximated by single-configuration, spin-free, self-consistent-field (SCF) wavefunctions of the form

$$\Psi_{SCF} = \frac{1}{\sqrt{2}}(1 \pm \hat{P}_{12})R_{1s}(r_1)Y_{0,0}(\Omega_1)R_{3d}(r_2)Y_{2,0}(\Omega_2) \quad (4.17)$$

where the upper and lower signs correspond to the  $^1D$  and  $^3D$  states, respectively. The radial orbitals are expanded in Slater-type functions (STF).  $R_{1s}$  is a linear combination of two  $1s$ -type STF of which one has an exponent equal to the nuclear charge  $Z$ .  $\Psi_{1s}$  is a linear combination of three (or two for the  $^1D$  states of  $\text{Be}^{2+}$  through  $\text{Ne}^{8+}$ )  $3d$ -type STF one of which has its exponent equal to  $\sqrt{-2\epsilon_{3d}}$  where  $\epsilon_{3d}$  is the  $3d$  orbital energy; this ensures the correct asymptotic behaviour of the one-electron density at large electron-nucleus distances. The remaining parameters were variationally determined by the Roothaan-Bagus SCF procedure [4.18] as implemented by Pitzer [4.19]. Numerical calculations were performed with a modified version of MCHF72 [4.20] to verify that the SCF wavefunctions are adequate approximations to the Hartree-Fock limits; the SCF energies lie no more than 0.11 microhartrees above the numerical ones.

#### 4.5 Coulomb holes: Results and discussion

Table 4.5.1 shows that the 3D state correlation energies are less than one millihartree which is much smaller than the 41 millihartree correlation energy for the

Table 4.5.1: "Exact" and correlation energies(in  $mE_H$ ) for the  $3^1D$  and  $3^3D$  states of the heliumlike ions.

$Z$		$E_{ex}$	$E_{corr}$	$Z$		$E_{ex}$	$E_{corr}$
2	S	-2.05562073	0.075	7	S	-26.50010328	0.650
	T	-2.05563631	0.064		T	-26.50151319	0.416
3	S	-4.72239099	0.236	8	S	-34.72224011	0.707
	T	-4.72252691	0.179		T	-34.72405816	0.445
4	S	-8.50021583	0.378	9	S	-44.05547452	0.754
	T	-8.50058234	0.268		T	-44.05771703	0.468
5	S	-13.38910030	0.491	10	S	-54.49980985	0.793
	T	-13.38977159	0.332		T	-54.50248898	0.487
6	S	-19.38905913	0.580				
	T	-19.39008350	0.380				

ground state of these ions. The correlation energies increase with  $Z$  rather than stay constant as in the ground state because the first-order terms in the  $1/Z$  perturbation expansions of the HF and exact energies do not cancel as they do in the ground state. The magnitude of the correlation energy for the  $3^1D$  state is consistently larger than its

$3^3\text{D}$  counterpart because some of the Fermi correlation in the triplet is included in the HF model.

Figures 4.5.1 and 4.5.2 show Z-scaled one-electron radial density holes for the  $3^1\text{D}$  and  $3^3\text{D}$  states. Electron correlation increases the probability of finding an electron at intermediate distances from the nucleus. Since  $\Delta D(r)$  integrates to zero, smaller and larger  $r$  have a decreased probability. For the high-Z triplets, there is an additional shift of charge from small to very small  $r$ .

The depth of the small- $r$  minimum decreases as the nuclear charge increases from  $\text{Li}^+$  to  $\text{Ne}^{8+}$ . The minimum for He lies between the values for  $\text{C}^{4+}$  and  $\text{N}^{5+}$ , and  $\text{Li}^+$  and  $\text{Be}^{2+}$  for the singlet and triplet, respectively. The small- $r$  minima in the singlet are two to three times deeper than the corresponding triplet minima. In the singlet, these minima occur near  $Zr \approx 0.78$ . For the triplet, as  $Z$  increases the minimum shifts from  $Zr \approx 0.88$  to  $Zr \approx 1.68$ . Note the presence of a maximum at very small  $r$  for  $Z \geq 5$  in the triplet. A shoulder at  $Zr \approx 4$  is present for all the ions in the singlet state and for the  $Z \leq 4$  ions in the triplet state. A shoulder at  $Zr \approx 2$  also appears in the one-electron radial density hole for the  $2^3\text{S}$  state of He [4.21].

Some correlated moments  $\langle r^k \rangle$  of  $D(r)$  and the correlation differences are listed in table 4.5.2. The SCF and correlated moments differ by less than 0.7% for the  $3^1\text{D}$  state and 0.6% for the  $3^3\text{D}$  states. For comparison, the moments were also calculated from screened hydrogenic wavefunctions in which the 1s and 3d orbitals have effective nuclear charges of  $Z$  and  $Z-1$ , respectively. For the  $3^3\text{D}$  state, the SCF values are significantly closer to the correlated values than the corresponding hydrogenic moments. However, with the exception of the high- $Z$   $\langle 1/r \rangle$  moments, the hydrogenic moments for the  $3^1\text{D}$  state lie closer than the SCF values to the correlated values. In fact, the hydrogenic

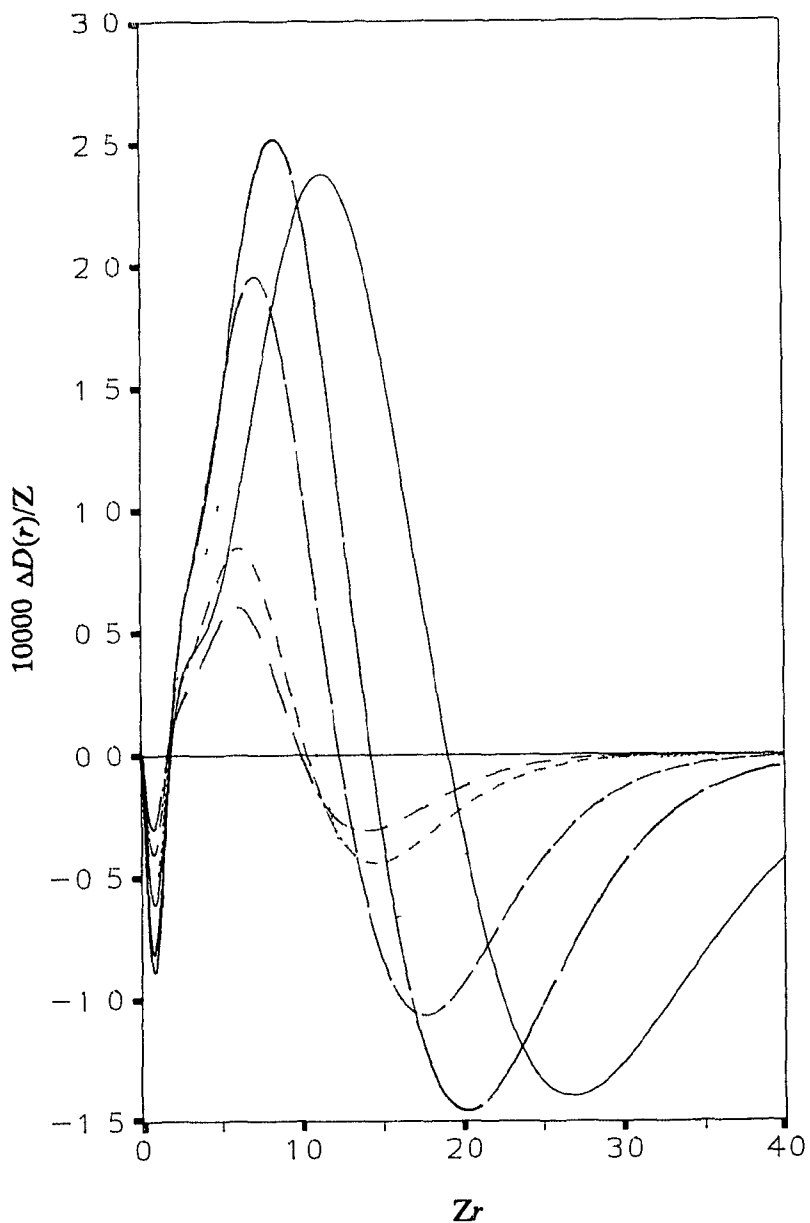


Figure 4.5.1: Z-scaled one-electron density holes for the  $3^1D$  state of He,  $\text{Li}^+$ ,  $\text{Be}^{2+}$ ,  $\text{C}^{4+}$ ,  $\text{O}^{6+}$  and  $\text{Ne}^{8+}$ . The solid line is for He, and the curves for the other ions can be identified by noting that the maximum of the hole decreases with increasing  $Z$ .

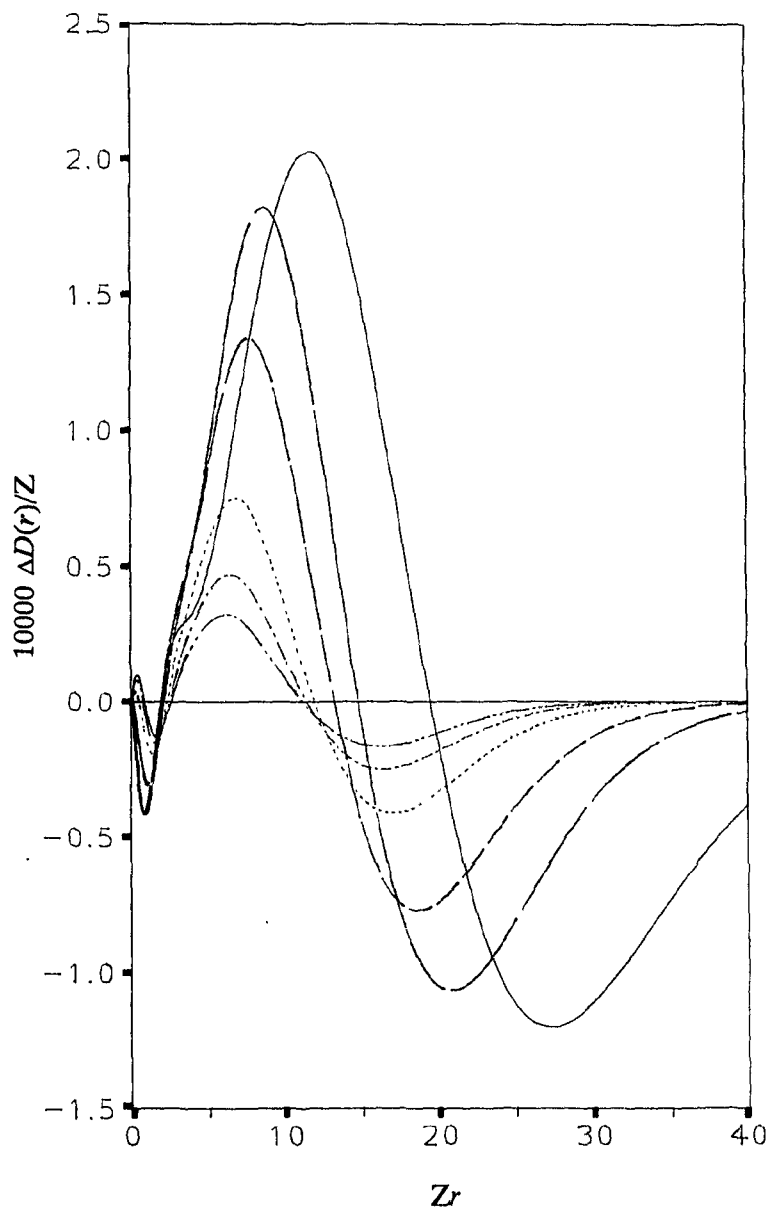


Figure 4.5.2: Z-scaled one-electron density holes for the  $3^3D$  state of He,  $\text{Li}^+$ ,  $\text{Be}^{2+}$ ,  $\text{C}^{4+}$ ,  $\text{O}^{6+}$  and  $\text{Ne}^{8+}$ . The solid line is for He, and the curves for the other ions can be identified by noting that the maximum of the hole decreases with increasing  $Z$ .

Table 4.5.2: Moments of the correlated radial density  $D(r)$  and the density hole  $\Delta D(r)$  for the  $3^1D$  (S) and  $3^3D$  (T) states of the heliumlike ions. A(-n) means  $A \times 10^{-n}$

Z	Correlated				Correlated - SCF			
	$\langle 1/r^2 \rangle$	$\langle 1/r \rangle$	$\langle r \rangle$	$\langle r^4 \rangle$	$\langle 1/r^2 \rangle$	$\langle 1/r \rangle$	$\langle r \rangle$	$\langle r^4 \rangle$
2	S 8.0141	2.11123	11.2315	25367	-8.75(-4)	1.40(-4)	-2.19(-2)	-1.74( 2)
	T 8.0140	2.11128	11.2258	25327	-5.27(-4)	1.39(-4)	-1.89(-2)	-1.55( 2)
3	S 18.057	3.22230	5.74430	1589.1	-2.90(-3)	1.28(-4)	-8.63(-3)	-8.67( 0)
	T 18.056	3.22248	5.73832	1583.6	-9.20(-4)	1.75(-4)	-6.41(-3)	-6.83( 0)
4	S 32.131	4.33335	3.87297	314.45	-4.86(-3)	5.18(-5)	-3.68(-3)	-1.05( 0)
	T 32.127	4.33363	3.86827	313.15	-6.44(-4)	1.90(-4)	-2.80(-3)	-9.06(-1)
5	S 50.235	5.44442	2.92425	99.599	-6.56(-3)	1.38(-5)	-2.00(-3)	-2.38(-1)
	T 50.228	5.44475	2.92065	99.175	5.08(-5)	2.00(-4)	-1.44(-3)	-2.00(-1)
6	S 72.368	6.55550	2.34975	40.822	-7.94(-3)	-1.21(-5)	-1.20(-3)	-7.22(-2)
	T 72.358	6.55587	2.34696	40.653	1.01(-3)	2.11(-4)	-8.37(-4)	-6.02(-2)
7	S 98.532	7.66659	1.96426	19.694	-9.19(-3)	-3.24(-5)	-7.70(-4)	-2.66(-2)
	T 98.518	7.66699	1.96204	19.616	2.20(-3)	2.23(-4)	-5.30(-4)	-2.24(-2)
8	S 128.72	8.77768	1.68757	10.633	-1.03(-2)	-4.69(-5)	-5.23(-4)	-1.13(-2)
	T 128.71	8.77810	1.68578	10.593	3.42(-3)	2.32(-4)	-3.56(-4)	-9.56(-3)
9	S 162.95	9.88878	1.47928	6.2341	-1.14(-2)	-5.61(-5)	-3.70(-4)	-5.28(-3)
	T 162.93	9.88922	1.47780	6.2121	4.73(-3)	2.40(-4)	-2.51(-4)	-4.57(-3)
10	S 201.20	10.9999	1.31680	3.8924	-1.21(-2)	-6.41(-5)	-2.71(-4)	-2.69(-3)
	T 201.18	11.0003	1.31556	3.8794	6.17(-3)	2.46(-4)	-1.84(-4)	-2.37(-3)

moments generally lie between the SCF and correlated values for the singlet. This is an interesting example of how the variational procedure can lead to wavefunctions with good energies but unexpectedly poor values for other properties.

The qualitative structure of the density holes can be deduced from their moments which are just differences between correlated and HF moments. The small- $r$  structure of  $\Delta D(r)$  is reflected by the  $\langle 1/r^2 \rangle$  moments; for the triplet, as  $Z$  increases correlated values become larger than the corresponding SCF ones and a cross over occurs at  $B^{3+}$ . For the singlets and low- $Z$  triplets, the presence of the small- $r$  minimum follows directly from the  $\langle 1/r^2 \rangle$  moments but, for the high- $Z$  triplets, must be deduced from a comparison of  $\langle 1/r^2 \rangle$  and  $\langle 1/r \rangle$ . These moments are larger for the correlated wavefunctions but the relative errors are smaller for  $\langle 1/r \rangle$ ; if the minimum was absent, this error would be significantly larger than the  $\langle 1/r^2 \rangle$  error. Since the SCF  $\langle r^4 \rangle$  values are always larger than the correlated ones, the SCF density is too diffuse and the large- $r$  region of the holes is negative. Since the holes integrate to zero, they must be positive at intermediate  $r$ . For the singlets and low- $Z$  triplets, a comparison of relative errors for the SCF moments of each ion reveals the  $Z$  dependence of the holes. In particular, the  $\langle r^4 \rangle$  errors decrease with increasing  $Z$  and, for the  $3^1D$  state, the He  $\langle 1/r^2 \rangle$  error lies between the errors for  $C^{4+}$  and  $N^{5+}$ . Two features of the density holes are not exposed by the moments: the shoulder at  $Zr \approx 4$ , and the depth of the small- $r$  minimum for the He triplet.

Since correlation brings the outermost electron closer to the nucleus, as seen in figures 4.5.1 and 4.5.2, the mean interelectronic distance should be reduced by

correlation. Thus, the Z-scaled Coulomb holes in figures 4.5.3 and 4.5.4 show that electron correlation has reduced the probability of large interelectronic distances and increased the probability of intermediate ones. As  $Z$  increases, the small- $u$  trough increases in depth whereas the large- $u$  trough disappears. A comparison of the small- $u$  behaviour in figures 4.5.3 and 4.5.4 clearly shows the effects of Fermi correlation for the triplet. The holes resemble the 2P holes published by Thakkar [4.15], but the depth of the large- $u$  trough relative to the small- $u$  trough is larger in the 3D states. The overall magnitude of the holes has decreased by a factor of 10 relative to the 2S [4.13][4.14] and 2P [4.15] states.

Several moments of  $P(u)$ ,  $\langle u^k \rangle$ , are given in table 4.5.3. The SCF and correlated moments differ by less than 1.0% for the singlet and 0.6% for the triplet. Due to Fermi correlation, the  $\langle 1/u^2 \rangle$  moments for the triplet are smaller than the corresponding moments in the singlet. Contrary to naive intuition,  $\langle u \rangle_{SCF} > \langle u \rangle_{ex}$  and  $\langle 1/u \rangle_{ex} > \langle 1/u \rangle_{SCF}$  at low  $Z$ , as in the 2P states [4.15]. The moments of  $P(u)$  were also calculated from hydrogenic wavefunctions. Interestingly, the  $\langle u^4 \rangle$  hydrogenic moments are more accurate than the SCF values for the 3<sup>1</sup>D states of the low- $Z$  ions. Similarly, in the triplet, the hydrogenic moments are closer to the correlated values for the  $\langle 1/u^2 \rangle$  and  $\langle 1/u \rangle$  moments for  $Z \leq 3$  and  $Z \geq 6$ , respectively.

With the exception of the He 3<sup>3</sup>D state, the qualitative structure of the Coulomb holes can be deduced from the moments in table 4.5.3. The  $\langle 1/u^2 \rangle$  and  $\langle u^4 \rangle$  moments show that the holes are negative at large and small  $u$ . Furthermore, the relative correlation corrections show that the outer trough decreases with increasing  $Z$  and the

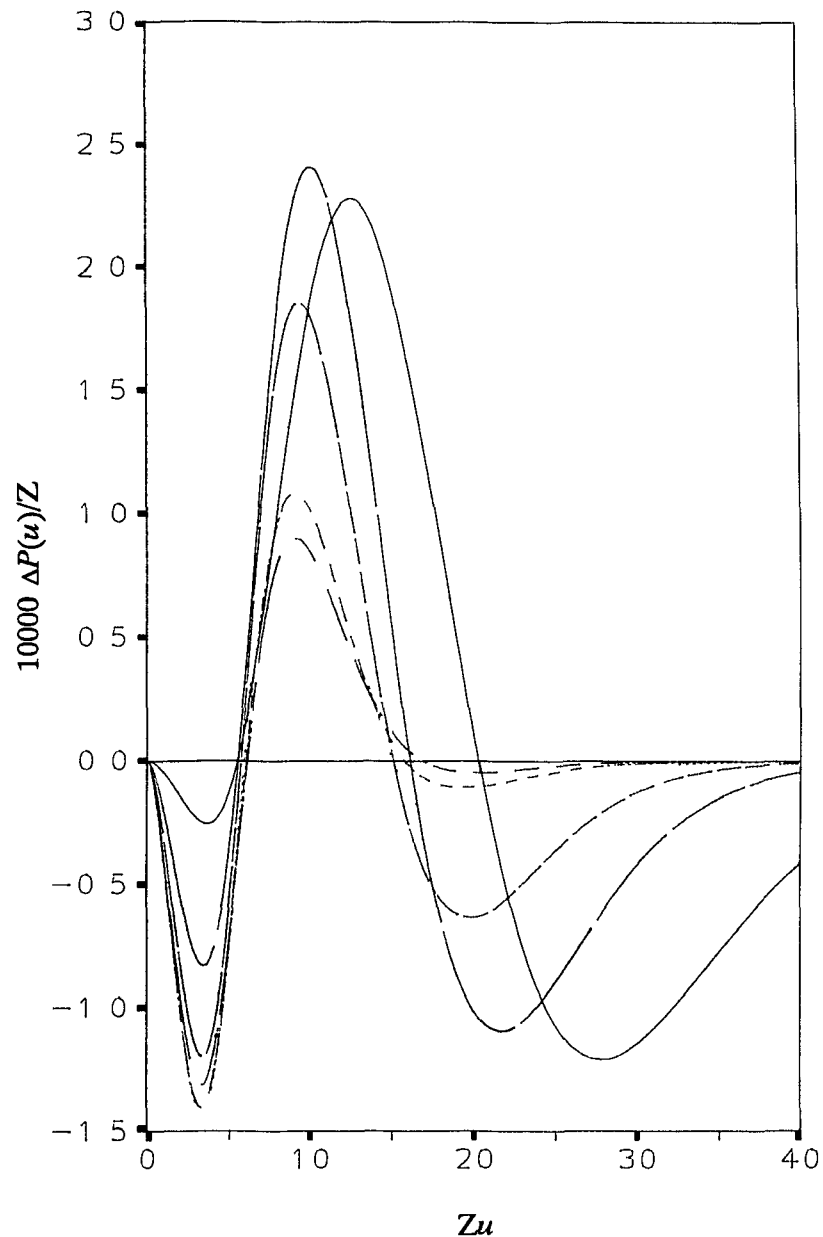


Figure 4.5.3: Z-scaled Coulomb holes for the  $3^1\text{D}$  state of He,  $\text{Li}^+$ ,  $\text{Be}^{2+}$ ,  $\text{C}^{4+}$ ,  $\text{O}^{6+}$  and  $\text{Ne}^{8+}$ . The solid line is for He, and the curves for the other ions can be identified by noting that the maximum of the hole decreases with increasing  $Z$ .

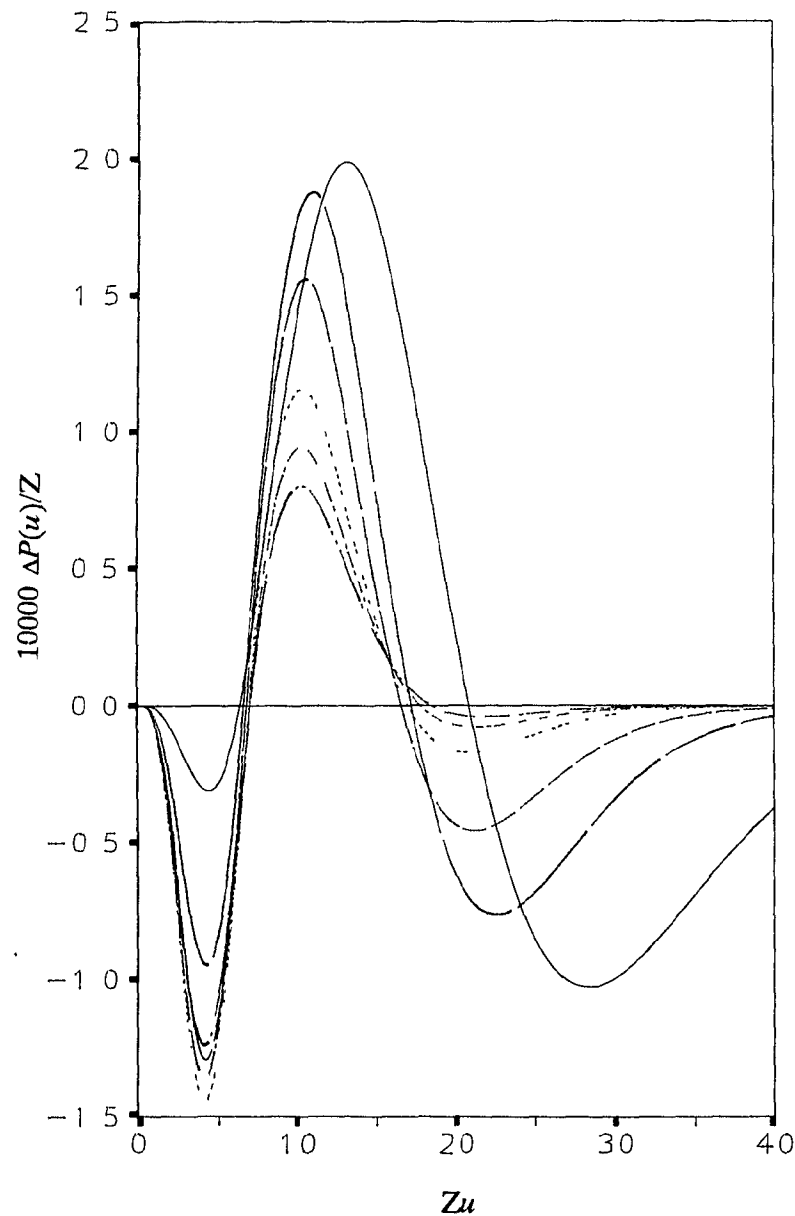


Figure 4.5.4: Z-scaled Coulomb holes for the  $3^3\text{D}$  state of He,  $\text{Li}^+$ ,  $\text{Be}^{2+}$ ,  $\text{C}^{4+}$ ,  $\text{O}^{6+}$  and  $\text{Ne}^{8+}$ . The solid line is for He, and the curves for the other ions can be identified by noting that the maximum of the hole decreases with increasing  $Z$ .

Table 4.5.3: Moments of the correlated radial intracule  $P(u)$  and the Coulomb hole  $\Delta P(u)$  for the  $3^1D$  (S) and  $3^3D$  (T) states of the heliumlike ions. A(-n) means  $A \times 10^{-n}$ .

Z	Correlated				Correlated - SCF			
	$\langle 1/u^2 \rangle$	$\langle 1/u \rangle$	$\langle u \rangle$	$\langle u^4 \rangle$	$\langle 1/u^2 \rangle$	$\langle 1/u \rangle$	$\langle u \rangle$	$\langle u^4 \rangle$
2	S 0.014966	0.111216	10.5133	25693	-1.13(-5)	1.48(-4)	-1.79(-2)	-1.63( 2)
	T 0.014973	0.111297	10.5076	25652	4.55(-6)	1.13(-4)	-1.49(-2)	-1.44( 2)
3	S 0.060195	0.222117	5.27216	1625.3	-3.96(-4)	1.59(-6)	-5.41(-3)	-7.54( 0)
	T 0.060038	0.222390	5.26609	1619.6	-1.71(-4)	-3.98(-5)	-3.36(-3)	-5.70( 0)
4	S 0.13616	0.332977	3.52105	323.46	-1.25(-3)	-2.79(-4)	-1.37(-3)	-8.02(-1)
	T 0.13520	0.333336	3.51627	322.13	-5.15(-4)	-2.27(-4)	-6.89(-4)	-6.63(-1)
5	S 0.24319	0.443897	2.64364	102.83	-2.39(-3)	-5.14(-4)	-3.12(-4)	-1.60(-1)
	T 0.24045	0.444215	2.64000	102.40	-9.53(-4)	-3.84(-4)	7.24(-5)	-1.24(-1)
6	S 0.38146	0.554882	2.11639	42.254	-3.73(-3)	-7.16(-4)	7.99(-5)	-4.12(-2)
	T 0.37578	0.555061	2.11358	42.079	-1.44(-3)	-5.07(-4)	2.91(-4)	-3.07(-2)
7	S 0.55105	0.665920	1.76450	20.424	-5.21(-3)	-8.85(-4)	2.27(-4)	-1.25(-2)
	T 0.54120	0.665887	1.76229	20.343	-1.97(-3)	-6.04(-4)	3.38(-4)	-9.02(-3)
8	S 0.75203	0.776999	1.51295	11.043	-6.79(-3)	-1.03(-3)	2.75(-4)	-4.08(-3)
	T 0.73671	0.776700	1.51118	11.001	-2.51(-3)	-6.81(-4)	3.32(-4)	-2.83(-3)
9	S 0.98444	0.888111	1.32417	6.4814	-8.44(-3)	-1.15(-3)	2.83(-4)	-1.32(-3)
	T 0.96230	0.887506	1.32273	6.4584	-3.07(-3)	-7.45(-4)	3.07(-4)	-8.78(-4)
10	S 1.2483	0.999247	1.17728	4.0504	-1.01(-2)	-1.25(-3)	2.72(-4)	-3.67(-4)
	T 1.2180	0.998305	1.17608	4.0368	-3.64(-3)	-7.97(-4)	2.78(-4)	-2.16(-4)

inner trough reaches a maximum at intermediate  $Z$ . Although the  $\langle 1/u^2 \rangle$  moments predict that the trough will be deepest for  $B^{5+}$ , figures 4.5.3 and 4.5.4 show that the minimum occurs at  $C^{4+}$ . The correct structure of the Coulomb hole for He  $3^3D$  is not obtainable directly from the moments since  $\langle 1/u^2 \rangle$  is actually larger for the correlated wavefunction; however, the initial minimum may be predicted on the basis of the electron-electron cusp condition [2.38].

The total and outer volumes of the  $Z$ -scaled Coulomb and one-electron density holes are given in table 4.5.4. A comparison of the total volumes clearly shows that correlation effects are more pronounced in the singlet. For the one-electron radial density holes, the ratio of  $V_{PO}$  to  $V_{DT}$  decreases slightly with increasing  $Z$ . However, for the Coulomb hole, the decrease of  $V_{PO}$  with increasing  $Z$  shows quantitatively the disappearance of the large- $u$  trough in figures 4.5.3 and 4.5.4. As  $Z$  increases, the ratio of total volumes,  $V_{PT}/V_{DT}$ , changes from 0.86 to 1.64 in the singlet and 0.87 to 2.71 in the triplet. For both spin states of He approximately 14% more charge is redistributed by the density hole than the Coulomb hole, but as  $Z$  increases the Coulomb hole dominates and the volume ratio becomes strongly spin dependent.

Statistical correlation coefficients for the correlated and SCF wavefunctions are given in tables 4.6.5 and 4.6.6. Since radial and angular correlation are more important for the singlet, the correlation coefficients are larger in magnitude. As  $Z$  increases, radial correlation decreases by roughly 7% for the core and 4% for the outer region. Angular correlation varies rapidly with  $Z$ ;  $\tau_{\bar{r}/r}$  varies by  $\approx 50\%$  and reaches a maximum for  $Li^+$ ,  $\tau_{\bar{r}/r}$  doubles from He to  $Li^+$  and reaches a maximum for  $B^{3+}$  with a total variation

**Table 4.5.4:** Total and outer volumes of the density and Coulomb holes.

Z	3 <sup>1</sup> D				3 <sup>3</sup> D			
	$10^4 V_{DT}$	$10^4 V_{DO}$	$10^4 V_{PT}$	$10^4 V_{PO}$	$10^4 V_{DT}$	$10^4 V_{DO}$	$10^4 V_{PT}$	$10^4 V_{PO}$
2	23.089	22.404	19.933	19.146	19.720	19.248	17.151	16.178
3	18.581	17.634	15.397	12.754	13.446	12.952	11.902	8.754
4	12.353	11.502	10.381	6.437	8.814	8.436	9.002	4.586
5	9.162	8.453	8.431	3.832	6.029	5.756	7.455	2.502
6	6.997	6.416	7.193	2.312	4.363	4.151	6.548	1.486
7	5.486	4.995	6.362	1.433	3.315	3.129	5.929	0.946
8	4.419	4.014	5.768	0.895	2.613	2.448	5.440	0.622
9	3.616	3.266	5.323	0.562	2.108	1.954	5.052	0.438
10	3.032	2.733	4.982	0.362	1.741	1.598	4.719	0.318

Table 4.5.5: Statistical correlation coefficients from SCF and correlated wavefunctions for the  $3^1D$  state of the heliumlike ions.

<b>Z</b>		$\tau_{1/r}$	$\tau_r$	$\tau_{\bar{r}/r}$	$\tau_{\bar{r}\bar{r}}$
<b>2</b>	Corr	-0.308241	-0.748477	-3.60(-3)	-3.07(-5)
	SCF	-0.308315	-0.749012	0	0
<b>3</b>	Corr	-0.299780	-0.737038	-4.21(-3)	-6.47(-5)
	SCF	-0.299853	-0.737441	0	0
<b>4</b>	Corr	-0.295545	-0.730957	-3.98(-3)	-7.78(-5)
	SCF	-0.295865	-0.732075	0	0
<b>5</b>	Corr	-0.292999	-0.727165	-3.62(-3)	-8.08(-5)
	SCF	-0.293030	-0.727351	0	0
<b>6</b>	Corr	-0.291298	-0.724567	-3.27(-3)	-7.94(-5)
	SCF	-0.291317	-0.724691	0	0
<b>7</b>	Corr	-0.290080	-0.722675	-2.97(-3)	-7.64(-5)
	SCF	-0.290091	-0.722756	0	0
<b>8</b>	Corr	-0.289165	-0.721235	-2.71(-3)	-7.27(-5)
	SCF	-0.289170	-0.721286	0	0
<b>9</b>	Corr	-0.288452	-0.720101	-2.49(-3)	-6.89(-5)
	SCF	-0.288452	-0.720131	0	0
<b>10</b>	Corr	-0.287880	-0.719185	-2.30(-3)	-6.52(-5)
	SCF	-0.287878	-0.719200	0	0

Table 4.5.6: Statistical correlation coefficients from SCF and correlated wavefunctions for the  $3^3D$  state of the heliumlike ions.

Z		$\tau_{1/r}$	$\tau_r$	$\tau_{\vec{r}/z}$	$\tau_{\vec{r}r}$
2	Corr	-0.308218	-0.748277	-3.55(-3)	-3.06(-5)
	SCF	-0.308273	-0.748650	0	0
3	Corr	-0.299711	-0.736596	-4.05(-3)	-6.38(-5)
	SCF	-0.299749	-0.736783	0	0
4	Corr	-0.295451	-0.730423	-3.75(-3)	-7.60(-5)
	SCF	-0.296479	-0.733312	0	0
5	Corr	-0.292895	-0.726610	-3.36(-3)	-7.81(-5)
	SCF	-0.292899	-0.726622	0	0
6	Corr	-0.291191	-0.724023	-3.00(-3)	-7.63(-5)
	SCF	-0.291188	-0.724004	0	0
7	Corr	-0.289975	-0.722153	-2.70(-3)	-7.29(-5)
	SCF	-0.289862	-0.721958	0	0
8	Corr	-0.289063	-0.720737	-2.45(-3)	-6.90(-5)
	SCF	-0.289053	-0.720692	0	0
9	Corr	-0.288353	-0.719629	-2.23(-3)	-6.52(-5)
	SCF	-0.288342	-0.719587	0	0
10	Corr	-0.287786	-0.718738	-2.05(-3)	-6.15(-5)
	SCF	-0.287774	-0.718684	0	0

of  $\approx 61\%$ . In contrast with the ground state where angular correlation increases in importance with  $Z$ , the ratios  $\tau_{\bar{r}/r} / \tau_{1/r}$  and  $\tau_{\bar{r}r} / \tau_r$  reach a maximum for  $\text{Li}^+$  and  $\text{B}^{3+}$ , respectively.

The correlation coefficients show clearly that the SCF wavefunctions for these open-shell states have some radial but no angular statistical correlation built into them. The structure of the Coulomb and density holes is due to the change in radial correlation and the inclusion of angular correlation by the correlated wavefunction. Angular correlation allows the electrons to stay on opposite sides of the nucleus; the result is a reduction in the screening of the outer electron and consequent contraction of the charge cloud. An increase in radial correlation is most likely to increase the interelectronic separation by a contraction of the core electron distribution. Similarly, a decrease in radial correlation would probably move the core electron away from the nucleus and closer to the outer electron. For the 3D states, radial correlation is overestimated by the SCF wavefunction for the singlets and low- $Z$  triplets, but underestimated for the high- $Z$  triplets. The small- $r$  maximum in the  $3^3\text{D}$  density hole is due to the core electron distribution moving inward upon an increase in radial correlation.

## CHAPTER 5: OSCILLATOR STRENGTHS

### 5.1 Overview

Dipole oscillator strengths (*DOS*) are fundamental quantities in spectroscopy but they are difficult to calculate by nonempirical quantum mechanical methods. Hence, very many calculations of these quantities have been made for two-electron atoms which are the simplest atomic species for which exact dipole oscillator strengths are not known. However, most such studies have concentrated on a few select transitions with the aim of demonstrating that the method being used was generally useful. Only a few studies of high accuracy dealing with many transitions and many ions of the helium isoelectronic series have been reported.

Schiff, Pekeris and Accad [5.1] used variationally determined wavefunctions to calculate dipole oscillator strengths for 36 S-P transitions in each of the ions from He through  $\text{Ne}^{8+}$ . Kono and Hattori [2.6] improved and extended their work on He, and then reported *DOS* for 24 P-D transitions [2.7] in each of the ions from  $\text{Li}^+$  through  $\text{N}^{5+}$ . A less accurate but much more extensive study was carried out by Sanders and Knight [5.2] who used Z-dependent, variational perturbation theory of low order to obtain dipole oscillator strengths for 136 S-P and 112 P-D transitions for each of the ions through  $Z=30$ .

In contrast to the *DOS*, very few studies of quadrupole oscillator strengths (*QOS*) have appeared in the literature [5.3][5.4] even though a few transitions have been

detected experimentally [5.5][5.6].

The 100 term wavefunctions described in chapter 2 have been used to calculate *DOS* and *QOS* for each of the ions from He to Ne<sup>8+</sup>. *DOS* and *QOS* have been calculated for 55 S→P and 40 P→D transitions, and 44 S→D transitions, respectively. The accuracies of 739 of the 855 *DOS* and all the *QOS* considered have been improved. Estimates of coefficients in the 1/Z expansions of the dipole oscillator strengths are also obtained.

## 5.2 Computational notes

In reduced tensor notation, the length and velocity formulations of the *DOS* are given respectively by:

$$DOS_l = \frac{2}{3} \frac{(E_1 - E_0)}{(2L+1)} \left\langle \gamma L \left\| \sum_i \vec{r}_i \right\| \gamma' L' \right\rangle^2 \quad (5.1)$$

and

$$DOS_v = \frac{2}{3(E_1 - E_0)(2L+1)} \left\langle \gamma L \left\| \sum_i \nabla_i \right\| \gamma' L' \right\rangle^2 \quad (5.2)$$

and, for the *QOS*,

$$QOS_l = \frac{(E_1 - E_0)^3}{30\alpha^2(2L+1)} \left\langle \gamma L \left\| \sum_i \vec{r}_i^2 \right\| \gamma' L' \right\rangle^2 \quad (5.3)$$

and

$$QOS_v = \frac{2(E_1 - E_0)}{15\alpha^2(2L+1)} \left| \gamma L \left\langle \sum_i \vec{r}_i \nabla_i \right| \gamma' L' \right|^2 \quad (5.4)$$

where  $\alpha$  is the fine structure constant,  $L$  and  $L'$  are the angular momentum quantum numbers of the initial and final states, respectively, and the  $\gamma$ 's denote the collection of all other quantum numbers.  $E_0$  and  $E_1$  are the initial and final state energies, respectively.

The formulae for the dipole and quadrupole oscillator strengths, in the length formulation, are given in appendix 6. In particular,  $DOS_l$  are given for the S→P and P→D transitions and  $QOS_l$  are given for the S→D, P→P, and D→D transitions. The  $DOS$  and  $QOS$  values were computed in quadruple precision to reduce roundoff errors arising from cancellation among contributing terms that in turn is a consequence of the near linear dependence of the basis functions.

Previous studies of the  $DOS$  [5.1] indicated that the velocity formulation was prone to numerical instability. However, in this study, the length and velocity forms proved to be equally susceptible to roundoff errors. Both length and velocity forms are equivalent if initial and final state wavefunctions are exact, but give different results if approximate wavefunctions are used. There is no consensus in the literature [5.1][2.6] [2.7] as to which approximate value is more reliable and under what circumstances. The average of the length and velocity results,  $DOS = (DOS_l + DOS_v)/2$ , was used in this study. The difference between the two values,  $\delta DOS = DOS_l - DOS_v$ , was used as an estimate of the accuracy of the mean. Thus the mean  $DOS$  values are rounded on the basis of  $\delta DOS$ . A regular entry indicates that  $\delta DOS$  was between 0.7 and 2.99 units in the last quoted

digit, whereas an underlined last digit indicates that  $\delta DOS$  was between 3 and 6.99 units in that digit. Since agreement between the two forms is not an infallible indicator of accuracy [5.1], the tabulated values are limited to six decimal digits whenever the length and velocity values agree to more than six digits.

Due to the limited number of *QOS* studies, the convention chosen above for the *DOS* has also been applied to the tabulation of *QOS* values.

### 5.3 Results and discussion

Tables 5.3.1, 5.3.2, 5.3.3, and 5.3.4 give *DOS* for the  $^1S \rightarrow ^1P$ ,  $^3S \rightarrow ^3P$ ,  $^1P \rightarrow ^1D$ , and  $^3P \rightarrow ^3D$  transitions, respectively.  $\delta DOS$  is generally found to be smaller for transitions involving lower lying states and for the more highly charged ions. However, in contrast to previous work [5.1],  $\delta DOS$  is not always smaller for the triplet than for the corresponding singlet transition. For instance,  $\delta DOS$  values for transitions originating from the  $6^1S$ ,  $4^1P$  and  $5^1P$  states are smaller than for the corresponding triplet transitions.

For each  $m^1S-n^1P$  and  $m^3S-n^3P$  transition, the dipole oscillator strengths are monotonic functions of the nuclear charge; they increase monotonically with  $Z$  when  $n > m$  and decrease monotonically otherwise. Moreover, the *DOS* are monotonic functions of  $Z$  for all  $m^3P-n^3D$  transitions except  $2^3P-4^3D$  for which a maximum occurs at  $Z=4$ . On the other hand, the dipole oscillator strengths for the  $m^1P-n^1D$  transitions are unimodal functions of  $Z$ ; the extremum is usually a maximum if  $n \geq m$ .

Dipole oscillator strengths for 503 of the 855 transitions considered have been calculated previously [5.1][2.6][2.7] using variationally determined Hylleraas-type

wavefunctions. An unequivocal comparison is not always possible because the previously tabulated values are sometimes the  $DOS_l$  values, sometimes the  $DOS_v$  values, and sometimes extrapolations based on both length and velocity values obtained from a series of wavefunctions. Nevertheless, detailed comparison of the  $DOS_l$  and  $DOS_v$  values with the older work [5.1][2.6][2.7] reveals several trends. Generally, when a discrepancy occurs, one of the  $DOS_l$  and  $DOS_v$  values (usually the latter) lies outside the error margins cited whereas the other agrees closely with the older value. For each ion, there are more discrepancies between these results and older work [5.1][2.6][2.7] for the triplet rather than the singlet transitions. In general, an observed discrepancy for a given transition tends to occur for several of the ions.

For He, the  $DOS_l$  and  $DOS_v$  values lie within the recommended error margins of the values of Kono and Hattori [2.6] for 72 of the 95 transitions considered. If energies and suggested error margins in the oscillator strengths are taken as criteria, then the results of tables 5.3.1-5.3.4 are 'more accurate' than the Kono and Hattori [2.6] values for 60 transitions, comparable for 22, and 'less accurate' for 13 transitions. For the S-P transitions of the cations with  $Z > 2$ , a similar comparison with the work of Schiff et al. [5.1] suggests that the values given in tables 5.3.1 and 5.3.2 are 'more accurate' for 255 transitions and 'less accurate' for 33 transitions. Most of the latter involve the  $3^1S$  and  $3^3S$  states. Similarly, the values in tables 5.3.3 and 5.3.4 are 'more accurate' than those of Kono and Hattori [2.7] for 72, comparable for 19, and less accurate for 29 P-D transitions for the cations from  $\text{Li}^+$  through  $\text{N}^{5+}$ . There are also 152 S-P and 200 P-D transitions considered for which no previous high accuracy values are available.

Table 5.3.1: Dipole oscillator strengths for the  $m^1S$  to  $n^1P$  transitions in the two-electron ions.

$m$	$n$	He	$\text{Li}^+$	$\text{Be}^{2+}$	$\text{B}^{3+}$	$\text{C}^{4+}$	$\text{N}^{5+}$	$\text{O}^{6+}$	$\text{F}^{7+}$	$\text{Ne}^{8+}$
1	2	0.27617	0.45662 <u>7</u>	0.551555	0.608915	0.647067	0.674198	0.694449	0.710131	0.722625
	3	0.07343	0.110637	0.126850	0.13537 <u>3</u>	0.140479	0.143817	0.146149	0.147857	0.149158
	4	0.02986 <u>1</u>	0.04366 <u>7</u>	0.049227	0.051970	0.053529	0.054505	0.055161	0.055626	0.055971
	5	0.015039	0.021697	0.024273	0.025501	0.026178	0.026591	0.026862	0.027050	0.027186
	6	0.008627	0.012358	0.013767	0.014426	0.014782	0.014996	0.015134	0.015228	0.015296
2	2	0.37648	0.21258	0.14856	0.11437	0.09305 <u>7</u>	0.07848	0.067860	0.059783	0.053430
	3	0.15135	0.25708 <u>5</u>	0.30589	0.333730	0.35169	0.36424 <u>2</u>	0.373502	0.380615	0.38625 <u>1</u>
	4	0.04915	0.0727	0.08213	0.08704	0.09008 <u>9</u>	0.0921 <u>2</u>	0.0936 <u>0</u>	0.0947 <u>2</u>	0.0956 <u>0</u>
	5	0.02234	0.03155	0.03497	0.03670 <u>7</u>	0.03774 <u>6</u>	0.038444	0.038939	0.039312	0.039600
	6	0.01213 <u>6</u>	0.01677	0.01841	0.019237	0.01972 <u>1</u>	0.020044	0.020272	0.02044 <u>3</u>	0.020575

Table 5.3.1: Continued.

<i>m</i>	<i>n</i>	He	$\text{Li}^+$	$\text{Be}^{2+}$	$\text{B}^{3+}$	$\text{C}^{4+}$	$\text{N}^{5+}$	$\text{O}^{6+}$	$\text{F}^{7+}$	$\text{Ne}^{8+}$
3	2	0.145460	0.094671	0.077372	0.068542	0.063160	0.059528	0.056911	0.054936	0.053391
	3	0.6263	0.3627	0.2562	0.1982	0.1617	0.1365	0.1181	0.1041	0.0931
	4	0.1439	0.26506	0.32317	0.3571	0.37924	0.39487	0.40648	0.41541	0.42253
	5	0.0505	0.07976	0.09203	0.0986	0.1029	0.10574	0.1078	0.10943	0.11067
	6	0.0241	0.0362	0.04095	0.04346	0.04500	0.04605	0.04681	0.04737	0.04781
4	2	0.025865	0.018748	0.015950	0.014428	0.013466	0.012800	0.012312	0.011939	0.011645
	3	0.30753	0.20532	0.17001	0.15202	0.14110	0.13377	0.12852	0.12456	0.12148
	4	0.8581	0.5013	0.3554	0.2755	0.2249	0.1900	0.16442	0.1450	0.1296
	5	0.14628	0.28424	0.35183	0.39162	0.41783	0.43638	0.45020	0.46088	0.46939
	6	0.0528	0.0872	0.101893	0.11012	0.11529	0.11886	0.12147	0.12345	0.125011

Table 5.3.1: Continued.

<i>m</i>	<i>n</i>	He	$\text{Li}^+$	$\text{Be}^{2+}$	$\text{B}^{3+}$	$\text{C}^{4+}$	$\text{N}^{5+}$	$\text{O}^{6+}$	$\text{F}^{7+}$	$\text{Ne}^{8+}$
5	2	0.00966	0.00721 <u>7</u>	0.006210	0.00565 <u>5</u>	0.005297	0.005047	0.004863	0.004721	0.004609
	3	0.05550	0.04132	0.03564	0.032575	0.030649	0.029328	0.028366	0.027636	0.02706 <u>2</u>
	4	0.4758 <u>0</u>	0.32295 <u>0</u>	0.2696 <u>2</u>	0.24239	0.22584	0.21474	0.20678	0.20080	0.19614
	5	1.0833	0.6358	0.4516	0.3503	0.2861 <u>7</u>	0.2418 <u>3</u>	0.2093 <u>7</u>	0.1845 <u>9</u>	0.1650 <u>4</u>
	6	0.15264 <u>6</u>	0.3080 <u>0</u>	0.38515	0.4309	0.46108	0.48252	0.4985	0.51089	0.5208
6	2	0.00477 <u>1</u>	0.003618	0.003132	0.002859	0.002683	0.002560	0.002468	0.002397	0.002341
	3	0.0210 <u>9</u>	0.01623	0.014157	0.013021	0.01229 <u>9</u>	0.01180 <u>1</u>	0.01143 <u>7</u>	0.01117	0.010941
	4	0.08620	0.0654 <u>4</u>	0.05698	0.05239	0.04951	0.04753	0.04609	0.04499	0.04413
	5	0.6467 <u>7</u>	0.4437 <u>1</u>	0.37245	0.33596	0.31379	0.29889	0.28820 <u>2</u>	0.28016 <u>2</u>	0.27389 <u>7</u>
	6	1.3053 <u>7</u>	0.7683	0.5464	0.4242	0.3466	0.2929 <u>5</u>	0.2536 <u>7</u>	0.2236 <u>6</u>	0.19999

Table 5.3.2: Dipole oscillator strengths for the  $m^3S$  to  $n^3P$  transitions in the two-electron ions.

$m$	$n$	He	$\text{Li}^+$	$\text{Be}^{2+}$	$\text{B}^{3+}$	$\text{C}^{4+}$	$\text{N}^{5+}$	$\text{O}^{6+}$	$\text{F}^{7+}$	$\text{Ne}^{8+}$
2	2	0.5391	0.307944	0.213139	0.162626	0.131381	0.110178	0.094856	0.083267	0.074199
	3	0.06447	0.18707	0.25258	0.29122	0.31648	0.33423	0.347366	0.357482	0.365507
	4	0.02576	0.05754	0.07152	0.07903	0.083665	0.086803	0.089063	0.090765	0.092095
	5	0.012493	0.02560	0.030955	0.033733	0.035409	0.036526	0.037320	0.037911	0.038370
	6	0.006981	0.013745	0.016411	0.017769	0.018578	0.019112	0.019489	0.019770	0.019985
3	2	0.20852	0.11709	0.08870	0.075437	0.067845	0.062951	0.059543	0.057035	0.055116
	3	0.8910	0.5130	0.3558	0.2718	0.2198	0.1844	0.1588	0.13943	0.1243
	4	0.05006	0.18683	0.26406	0.31027	0.34067	0.36211	0.37802	0.39030	0.40004
	5	0.02291	0.06142	0.07930	0.08909	0.09520	0.09937	0.10238	0.104662	0.106450
	6	0.011985	0.028719	0.035918	0.03972	0.042045	0.043607	0.044721	0.045563	0.046215

Table 5.3.2: Continued.

<i>m</i>	<i>n</i>	He	$\text{Li}^+$	$\text{Be}^{2+}$	$\text{B}^{3+}$	$\text{C}^{4+}$	$\text{N}^{5+}$	$\text{O}^{6+}$	$\text{F}^{7+}$	$\text{Ne}^{8+}$
4	2	0.03171 <u>5</u>	0.021472	0.017328	0.01522 <u>1</u>	0.01396 <u>2</u>	0.013131	0.012541	0.012104	0.011764
	3	0.4357 <u>1</u>	0.2550 <u>1</u>	0.19746	0.17016	0.15437	0.14413	0.13695 <u>8</u>	0.13166 <u>3</u>	0.12759 <u>7</u>
	4	1.215 <u>4</u>	0.703 <u>7</u>	0.4891	0.3739	0.3025	0.2539	0.2188	0.1921	0.1713
	5	0.04422	0.1961 <u>5</u>	0.2852 <u>0</u>	0.3390 <u>0</u>	0.3745 <u>4</u>	0.3996 <u>7</u>	0.4183 <u>5</u>	0.43278	0.44424
	6	0.02163	0.06588	0.08720	0.09899	0.10641	0.11148	0.11516	0.117950	0.12014
5	2	0.0113 <u>2</u>	0.008061	0.00662 <u>3</u>	0.005876	0.005423	0.005120	0.004903	0.004742	0.004617
	3	0.06759	0.04799	0.0396 <u>2</u>	0.0352 <u>9</u>	0.03267 <u>4</u>	0.030921	0.02967	0.02874	0.028010
	4	0.6683 <u>5</u>	0.4000 <u>5</u>	0.31328	0.2717 <u>8</u>	0.24769	0.23199	0.22098	0.212823	0.20655 <u>5</u>
	5	1.5308	0.8898	0.6191	0.4737	0.3834	0.3219	0.2774	0.2436	0.2172
	6	0.04151	0.2093 <u>0</u>	0.31034	0.3717 <u>7</u>	0.41249	0.44134	0.46280	0.47938	0.49257

Table 5.3.2: Continued.

<i>m</i>	<i>n</i>	He	$\text{Li}^+$	$\text{Be}^{2+}$	$\text{B}^{3+}$	$\text{C}^{4+}$	$\text{N}^{5+}$	$\text{O}^{6+}$	$\text{F}^{7+}$	$\text{Ne}^{8+}$
6	2	0.00549 <u>2</u>	0.003990	0.003308	0.002947	0.002727	0.002579	0.002475	0.002396	0.002335
	3	0.0246 <u>8</u>	0.01845	0.01552 <u>8</u>	0.01396 <u>3</u>	0.01299 <u>8</u>	0.01235 <u>2</u>	0.01188	0.01153 <u>3</u>	0.01126 <u>7</u>
	4	0.1039 <u>7</u>	0.07588	0.0635	0.056980	0.0530	0.0503 <u>1</u>	0.0484 <u>0</u>	0.0469 <u>8</u>	0.0458 <u>6</u>
	5	0.9033	0.5482 <u>8</u>	0.4323 <u>3</u>	0.3766 <u>2</u>	0.34417	0.32300	0.30812	0.29709	0.288601
	6	1.8419	1.0737	0.7477	0.5724	0.4633	0.3891	0.3353	0.2945	0.2626

**Table 5.3.3:** Dipole oscillator strengths for the  $m^1\text{P}$  to  $n^1\text{D}$  transitions in the two-electron ions.

$m$	$n$	He	$\text{Li}^+$	$\text{Be}^{2+}$	$\text{B}^{3+}$	$\text{C}^{4+}$	$\text{N}^{5+}$	$\text{O}^{6+}$	$\text{F}^{7+}$	$\text{Ne}^{8+}$
2	3	0.71017	0.71161	0.708792	0.70633	0.704492	0.703132	0.702101	0.701303	0.700672
	4	0.12027	0.119270	0.119178	0.119314	0.119497	0.119678	0.119844	0.119990	0.120119
	5	0.04328	0.04274	0.042746	0.042875	0.043008	0.043129	0.043235	0.043325	0.043405
	6	0.020952	0.020654	0.020675	0.020752	0.020833	0.020907	0.020969	0.021024	0.021071
3	3	0.0211	0.0243	0.0210	0.0178	0.01525	0.01327	0.01171	0.01046	0.00945
	4	0.64810	0.651706	0.646698	0.642046	0.638449	0.635702	0.633569	0.631878	0.630512
	5	0.14132	0.141406	0.141040	0.140730	0.140492	0.140313	0.140176	0.140071	0.13998
	6	0.05626	0.05623	0.056183	0.056161	0.05615	0.056140	0.056136	0.05615	0.056132
4	3	0.015305	0.01501	0.01550	0.01595	0.016299	0.016570	0.016780	0.016951	0.017087
	4	0.04004	0.0439	0.03708	0.03090	0.02616	0.02256	0.01977	0.01755	0.01577
	5	0.64766	0.6511	0.64429	0.63828	0.633710	0.630271	0.627627	0.62554	0.623869
	6	0.15282	0.15314	0.15240	0.15173	0.15123	0.15084	0.15055	0.15030	0.150119

Table 5.3.3: Continued.

<i>m</i>	<i>n</i>	He	$\text{Li}^+$	$\text{Be}^{2+}$	$\text{B}^{3+}$	$\text{C}^{4+}$	$\text{N}^{5+}$	$\text{O}^{6+}$	$\text{F}^{7+}$	$\text{Ne}^{8+}$
5	3	0.003114	0.003067	0.003163	0.003249	0.003316	0.003366	0.003405	0.003437	0.003462
	4	0.039300	0.03878	0.03999	0.041067	0.041883	0.042505	0.042985	0.043364	0.043670
	5	0.05731	0.06159	0.051415	0.04251	0.03577	0.03072	0.02683	0.02379	0.02132
	6	0.66983	0.67310	0.664842	0.65773	0.652406	0.648425	0.645381	0.642992	0.641080
6	3	0.001190	0.001173	0.001210	0.001243	0.001267	0.001286	0.001301	0.001312	0.001321
	4	0.00838	0.00829	0.008532	0.00872	0.008896	0.009012	0.009104	0.009175	0.009232
	5	0.06842	0.067711	0.069746	0.071516	0.07284	0.07385	0.074629	0.075238	0.075728
	6	0.07360	0.0783	0.0648	0.0535	0.04487	0.0384	0.0335	0.0296	0.02654

**Table 5.3.4:** Dipole oscillator strengths for the  $m^3P$  to  $n^3D$  transitions in the two-electron ions.

$m$	$n$	He	$\text{Li}^+$	$\text{Be}^{2+}$	$\text{B}^{3+}$	$\text{C}^{4+}$	$\text{N}^{5+}$	$\text{O}^{6+}$	$\text{F}^{7+}$	$\text{Ne}^{8+}$
2	3	0.61024	0.624659	0.639126	0.649263	0.656473	0.661802	0.665883	0.669098	0.671696
	4	0.122850	0.123214	0.123275	0.12320	0.12310	0.123000	0.122903	0.122824	0.122748
	5	0.0470	0.046795	0.046447	0.046160	0.04593	0.045749	0.045602	0.045482	0.045384
	6	0.023472	0.023277	0.023016	0.022808	0.022647	0.022524	0.022427	0.022347	0.022282
3	3	0.1122	0.0908	0.0712	0.05781	0.04850	0.04171	0.03655	0.03252	0.02929
	4	0.47760	0.50338	0.52727	0.54377	0.555417	0.563999	0.570554	0.575714	0.579876
	5	0.124531	0.12785	0.13060	0.13241	0.133631	0.134484	0.13512	0.13561	0.135988
	6	0.05298	0.05388	0.05455	0.05495	0.055196	0.055366	0.05548	0.05557	0.055645
4	3	0.036960	0.03279	0.02930	0.02705	0.025540	0.024462	0.023660	0.023040	0.022548
	4	0.200947	0.1606	0.12526	0.10152	0.08505	0.07306	0.06399	0.05690	0.05122
	5	0.43839	0.47054	0.49949	0.51940	0.53346	0.54381	0.55172	0.55794	0.56296
	6	0.123972	0.12922	0.1337	0.13665	0.1386	0.14006	0.14114	0.14198	0.14264

Table 5.3.4: Continued.

<i>m</i>	<i>n</i>	He	$\text{Li}^+$	$\text{Be}^{2+}$	$\text{B}^{3+}$	$\text{C}^{4+}$	$\text{N}^{5+}$	$\text{O}^{6+}$	$\text{F}^{7+}$	$\text{Ne}^{8+}$
5	3	0.006902	0.006202	0.005613	0.005229	0.004967	0.004779	0.004639	0.004529	0.004442
	4	0.08831	0.07873	0.07090	0.065873	0.062492	0.060085	0.058294	0.056911	0.055813
	5	0.28009	0.2227	0.17337	0.14040	0.11756	0.10096	0.08841	0.07860	0.07073
	6	0.42944	0.46648	0.49946	0.52213	0.538144	0.54994	0.55895	0.566044	0.57177
6	3	0.002586	0.002331	0.002114	0.001975	0.001878	0.001809	0.001757	0.001717	0.001685
	4	0.017043	0.01544	0.01411	0.01323	0.012648	0.012221	0.011902	0.011656	0.011458
	5	0.14698	0.13157	0.119085	0.111089	0.105705	0.101873	0.099018	0.096816	0.095066
	6	0.35432	0.2811	0.21865	0.17702	0.14819	0.12726	0.11142	0.09906	0.08914

Recent absolute measurements [5.7][5.8] for He yield experimental dipole oscillator strengths of 0.280(0.007), 0.0741(0.0007), 0.0303(0.0007), 0.0152(0.0003), 0.00892(0.0005), 0.00587(0.0003) for the  $1^1S \rightarrow n^1P$ ,  $n=2-7$  transitions, respectively. The experimental uncertainties are shown in parentheses. These values agree with the values in table 5.3.1, in particular, the theoretical values are always smaller but still within experimental error. The experimental *DOS* measurements are obtained by measuring the intensity of forward scattered electrons in a high impact electron scattering experiment. The scattering of electrons by atoms will be the subject of the next chapter.

The dipole transition moment  $DTM$  is given by

$$\langle \gamma LM_l | z_1 + z_2 | \gamma' L' M'_l \rangle \quad (5.5)$$

which is, apart from a constant, simply the integral appearing in equation (5.1). The  $1/Z$  expansion of the  $DTM$  is

$$DTM = M_0 + M_1/Z + M_2/Z^2 + \dots + \dots + . \quad (5.6)$$

where the first two coefficients in this expansion are known [5.2][5.9] and have been tabulated for dipole transition moments of many transitions.

The third coefficient  $M_2$  in equation (5.6) has been estimated from the calculated transition moments  $DTM$  in both the length and velocity forms. Both differencing and least squares fitting of  $M^2$  were used, with  $M_0$  and  $M_1$  constrained to their known values [5.2][5.9]. The estimated coefficients are listed in tables 5.3.5 and 5.3.6 for the S-P and P-D transitions, respectively. Most of these estimates should be more accurate than previous values [5.2] obtained by differencing calculated transition moments themselves;

the latter procedure is not as reliable because the moments often change sign over the range of nuclear charges considered.

Quadrupole oscillator strengths for S→D transitions from the lowest three states,  $1^1S$ ,  $2^1S$ , and  $2^3S$ , of the ions from He to  $\text{Ne}^{8+}$  are given in table 5.3.7. Godefroid and Verhaegen [5.3] considered the  $1^1S \rightarrow 3^1D$ ,  $2^1S \rightarrow 3^1D$ , and  $2^3S \rightarrow 3^3D$  quadrupole transitions of the ions from He to  $\text{Ne}^{8+}$  using Hartree-Fock (HF) and multiconfiguration Hartree-Fock (MCHF) wavefunctions. Their MCHF length and velocity *QOS* are within 0.5% of the values of table 5.3.5. However, the agreement between their length and velocity results is not indicative of the overall accuracy of their values. Their results also show the importance of electron correlation: the calculated HF and MCHF quadrupole oscillator strengths were found to disagree by as much as 21%.

Cohen *et al* [5.4] calculated QOS for S→D transitions in He and  $\text{Li}^+$  using simple frozen core wavefunctions. The tabulated values are always within 13% of the values of table 5.3.7. Although these values are generally less accurate than the HF [5.3] values, they do show that relatively simple wavefunctions will produce reasonable quadrupole oscillator strengths. Cohen *et al* [5.4] chose to tabulate all of their calculated *QOS* values to three figures since the length and velocity results agreed to within one unit in the third figure. However, the authors also note that, for a large number of transitions, the length and velocity results agreed to six figures. This clearly illustrates the perils of such comparisons: none of the length and velocity results calculated from 100 term integral transform wavefunctions agreed to six figures.

**Table 5.3.5:** Second order coefficients for the  $1/Z$  expansion of the transition moments for the  $mS$  to  $nP$  transitions.

$m$	$n$	Singlet	Triplet	$m$	$n$	Singlet	Triplet
1	2	-0.359		4	2	0.53	0.68
1	3	-0.209		4	3	4.14	5.0
1	4	-0.103		4	4	-12.9	-10.7
1	5	-0.0609		4	5	-0.81	-3.4
1	6	-0.044		4	6	-0.5	-0.94
<hr/>							
2	2	-3.13	-2.054	5	2	0.28	0.372
2	3	-0.15	-0.977	5	3	1.4	1.4
2	4	0.1	-0.25	5	4	8.3	10
2	5	0.18	-0.11	5	5	-20.42	-17.46
2	6	0.14	-0.062	5	6	-1	-5.3
<hr/>							
3	2	1.7	2.0	6	2	0.19	0.25
3	3	-7.167	-5.626	6	3	0.8	0.874
3	4	-0.4	-2.03	6	4	2	2.8
3	5	0.09	-0.530	6	5	12.6	14.3
3	6	0.3	-0.22	6	6	-30.5	-25.90

**Table 5.3.6:** Second order coefficients for the  $1/Z$  expansion of the transition moments for the  $mP$  to  $nD$  transitions.

<i>m</i>	<i>n</i>	Singlet	Triplet	<i>m</i>	<i>n</i>	Singlet	Triplet
2	3	2.4	1.86	5	3	0.04	0.48
2	4	0.720	0.74	5	4	1.2	3.42
2	5	0.36	0.45	5	5	-17	-18
2	6	0.23	0.31	5	6	10.7	3.8
<hr/>							
3	3	-2	-5.21	6	3	-0.08	0.28
3	4	4.95	2.3	6	4	-2.4	1.0
3	5	1.6	1.1	6	5	2.7	5.93
3	6	0.85	0.74	6	6	-26.3	-26.0
<hr/>							
4	3	0.1	1.52				
4	4	-10.3	-10.7				
4	5	7.37	3.0				
4	6	2.3	1				

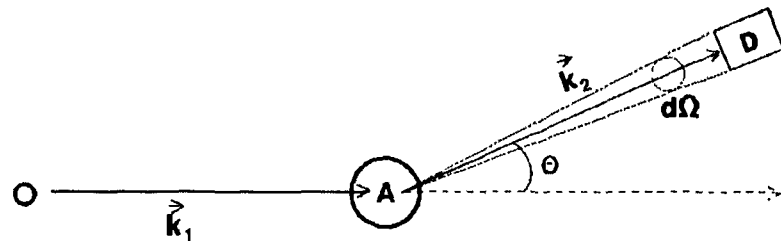
Table 5.3.7: Quadrupole oscillator strengths for S $\rightarrow$ D transitions from the three lowest states of the two-electron ions.

<i>Trans.</i>	He	Li <sup>+</sup>	Be <sup>2+</sup>	B <sup>3+</sup>	C <sup>4+</sup>	N <sup>5+</sup>	O <sup>6+</sup>	F <sup>7+</sup>	Ne <sup>8+</sup>
$1^1S \rightarrow 3^1D$	2.809(-7)	1.966(-6)	5.423(-6)	1.071(-5)	1.786(-5)	2.686(-5)	3.773(-5)	5.047(-5)	6.507(-5)
	4 <sup>1</sup> D	1.530(-7)	1.0355(-6)	2.811(-6)	5.500(-6)	9.11(-6)	1.364(-5)	1.910(-5)	2.548(-5)
	5 <sup>1</sup> D	8.596(-8)	5.731(-7)	1.545(-6)	3.010(-6)	4.972(-6)	7.43(-6)	1.039(-5)	1.780(-5)
	6 <sup>1</sup> D	5.204(-8)	3.443(-7)	9.25(-7)	1.797(-6)	2.965(-6)	4.427(-6)	6.18(-6)	8.24(-6)
$2^1S \rightarrow 3^1D$	1.9492(-7)	7.285(-6)	1.5881(-5)	2.7755(-5)	4.2912(-5)	6.136(-5)	8.309(-5)	1.0812(-4)	1.3644(-4)
	4 <sup>1</sup> D	2.703(-7)	7.07(-7)	1.3149(-6)	2.100(-6)	3.070(-6)	4.218(-6)	5.550(-6)	7.06(-6)
	5 <sup>1</sup> D	8.14179(-8)	1.712(-7)	2.828(-7)	4.216(-7)	5.861(-7)	7.80(-7)	1.00(-6)	1.247(-6)
	6 <sup>1</sup> D	3.494(-8)	6.32(-8)	9.527(-8)	1.338(-7)	1.7802(-7)	2.30(-7)	2.87(-7)	3.51(-7)
$2^3S \rightarrow 3^3D$	2.03120(-6)	7.9852(-6)	1.7385(-5)	3.0128(-5)	4.6187(-5)	6.5551(-5)	8.8215(-5)	1.14177(-4)	1.43435(-4)
	4 <sup>3</sup> D	4.6753(-7)	1.2967(-6)	2.2898(-6)	3.4482(-6)	4.7786(-6)	6.2847(-6)	7.969(-6)	9.833(-6)
	5 <sup>3</sup> D	1.812(-7)	4.246(-7)	6.69016(-7)	9.267(-7)	1.2038(-6)	1.5037(-6)	1.8278(-6)	2.1773(-6)
	6 <sup>3</sup> D	9.01(-8)	1.9185(-7)	2.8156(-7)	3.688(-7)	4.578(-7)	5.504(-7)	6.478(-7)	8.587(-7)

## CHAPTER 6: ELECTRON SCATTERING

### 6.1 Overview

The scattering of an electron by an atom may be represented graphically as



where the incident particle approaches, with momentum  $\vec{k}_1$ , along OA. The electron may transfer momentum to the atom A and be deflected during the collision. This deflection is represented by the angle  $\theta$ , the final electron momentum is  $\vec{k}_2$ , and the momentum transferred to atom A is  $\vec{K} = \vec{k}_1 - \vec{k}_2$ . When the target atom undergoes an electronic transition during the collision, the transition is termed 'inelastic'. Otherwise, elastic scattering has occurred. Conservation of energy and momentum limit the magnitude of the momentum transfer. When the incident particle is an electron, the

momentum transfer,  $K$ , is given by

$$K^2 = 4TM^2 \left[ 1 - \frac{\Delta E}{2MT} - \left( 1 - \frac{\Delta E}{MT} \right)^{1/2} \cos\theta \right] \quad (6.1)$$

where  $M \approx 1$  is the reduced mass of the colliding system,  $T$  is the kinetic energy of the incoming electron, and  $\Delta E$  is the excitation energy of atom A.

Experimentally, the number of particles scattered into the solid angle  $d\Omega$  about  $\theta$  per unit time is measured. The differential cross section,  $d\sigma/d\Omega$ , is the ratio of this quantity to the flux of incident particles. Also of interest is the total cross section,  $\sigma$ , the average of  $d\sigma/d\Omega$  over all angles  $\theta$ .

For sufficiently fast collisions, an impulse approximation can be applied. Thus the collision is regarded as producing a sudden transfer of energy and momentum to the electrons of atom A. With this approximation, the incident particle provides a sudden and small external perturbation to the atom and the differential cross section is calculated in the lowest order of the interaction between the particle and the atom. When this interaction is Coulombic [6.1][6.2], the first Born approximation for the differential cross section is:

$$\frac{d\sigma}{d\Omega} = \frac{4z^2 M^2 k_2 |FF(K)|^2}{k_1 K^4} \quad (6.2)$$

for inelastic scattering and

$$\frac{d\sigma}{d\Omega} = \frac{4z^2 M^2 k_2 |FF(K) - Z|^2}{k_1 K^4} \quad (6.3)$$

for elastic scattering. The form factor,  $FF(K)$ , depends only on the target atom and  $z$  is the charge on the scatterer. The additional term in the elastic cross section originates from the Coulombic term between the nucleus of atom A and the scatterer. This term vanishes for inelastic collisions due to the orthogonality of the target states.

The factor  $4z^2 M^2 k_2 / k_1 K^4$  in equations (6.2) and (6.3) may be evaluated from the observables concerning the incident particle only ( $k_1, k_2, \theta$ ). This factor is actually the Rutherford cross section for the scattering of a particle of charge  $z$  by a free and stationary electron which receives a momentum transfer  $K$ . From this perspective, the form factor may be regarded as the correction to the Rutherford cross section for moving electrons bound to a nucleus. Thus the differential cross section, within the impulse approximation, consists of two factors: one dealing with the incident particle, the other dealing with the target atom.

The form factor,  $FF(K)$ , is given by

$$FF(K) = \int \Psi_1^* \sum_{i=1}^n e^{i\vec{K}\cdot\vec{r}_i} \Psi_0 d\vec{r}_1 d\vec{r}_2 \dots d\vec{r}_n \quad (6.4)$$

where  $\Psi_1$  and  $\Psi_0$  are the final state and initial state wavefunctions of atom A, respectively. For inelastic scattering, theoretical studies generally concentrate on a slightly different quantity, the generalized oscillator strength  $GOS(K)$ , instead of  $FF(K)$ .

The  $GOS(K)$ , given by

$$GOS(K) = \frac{2\Delta E}{K^2} |FF(K)|^2, \quad (6.5)$$

is studied rather than  $FF(K)$  simply because, in the limit as  $K \rightarrow 0$ , the  $GOS(K)$  approaches the dipole oscillator strength,  $DOS$ , discussed in the previous chapter. Also, an analysis of the form factor is complicated by the fact that  $FF(K)$  may be positive, negative, purely real, or purely imaginary whereas the GOS is positive and real.

In the case of electron scattering, the Born approximation ignores the possibility of exchanging the incoming electron with an atomic electron. Furthermore, "polarization" corrections such as the distortion of the atomic charge cloud due to the presence of the incoming scatterer and the distortion of the plane wave due to the atom are also neglected. At sufficiently high energies these effects may be neglected and the first Born approximation is valid. However, at low impact energies, first Born cross sections may be grossly in error. Currently, the range of validity of Born cross sections is obtained by comparisons with experimentally determined cross sections or theoretical cross sections which include corrections for polarization and exchange.

Experimental measurements of cross sections are relative and require additional information to convert to absolute measurements. Often, absolute experimental cross sections are obtained by forcing a high impact energy experimental measurement to agree with a first Born calculation. Consequently the relevance of the first Born approximation extends also to intermediate and low impact energies.

Several reviews have been devoted to the first Born approximation [6.3-6.5] as well as more general reviews which consider lower impact energies as well [6.6-6.17].

## 6.2 Computational notes

The wavefunctions of chapter 2 have been used to calculate  $GOS(K)$  for the  $1^1S \rightarrow n^1S$ ,  $n^1P$ ,  $n^1D$ ,  $n=1-6$ , the  $2^1S \rightarrow n^1S$ ,  $n^1P$ ,  $n^1D$ ,  $n=2-6$ , and the  $2^3S \rightarrow n^3S$ ,  $n^3P$ ,  $n^3D$ ,  $n=2-6$  helium transitions. Experimentally, many differential cross sections have been measured for the He ground state. Far fewer experimental studies on the metastable states  $2^1S$  and  $2^3S$  have been performed [6.18-6.23]. All of the experiments on the metastable states, performed with low impact energies, are unsuitable for comparison with first Born calculations.

The  $1^1S \rightarrow 1^1S$  and  $1^1S \rightarrow 2^1P$  transitions for the  $Z=3, \dots, 10$  ions have also been calculated. The  $GOS(K)$  for these transitions are presented, in tabular form, in appendix 7. Only one experimental study [6.24] has been performed on these ions: the measurement of the cross section,  $\sigma$ , for the  $1^1S \rightarrow 2^3P$  transition of  $\text{Li}^+$  from a crossed beam experiment. Several theoretical calculations have been performed and recent compilations are available [6.25][6.26].

Formulae for the  $S \rightarrow S$ ,  $S \rightarrow P$ ,  $S \rightarrow D$ , and  $P \rightarrow D$  generalized oscillator strengths are presented in appendix 8. The latter also includes a discussion of the numerical instabilities which arise and the procedures used to circumvent them. Note that the formula for the  $S \rightarrow S$  transitions from integral transform wavefunctions has been given previously [6.27].

The following sections present comparisons with experimental measurements and theoretical calculations for the He transitions. Note that comparisons with theoretical

studies will be restricted to first Born calculations and that experimental comparisons are possible only for transitions originating from the ground state.

Small  $K$  expansion coefficients are useful for interpolation and extrapolation of tabular values of  $FF(K)$  or  $GOS(K)$  for  $K$  sufficiently small. For elastic scattering, the small  $K$  expansion of  $FF(K)$  is

$$FF(K) = 2 + a_1 K^2 + a_2 K^4 + \dots \quad (6.6)$$

where the first term is the number of target electrons. For inelastic scattering, the  $GOS(K)$  expansion coefficients are generally presented:

$$GOS(K) = b_0 + b_1 K^2 + b_2 K^4 + \dots \quad (6.7)$$

where,  $b_0=0$  for the optically forbidden S $\rightarrow$ S and S $\rightarrow$ D transitions and  $b_0=DOS$  for the optically allowed S $\rightarrow$ P transitions. Similarly, for large  $K$ , the  $GOS(K)$  and  $FF(K)$  may be expressed in power series of  $K$ . In general, the expansion of  $FF(K)$  for large  $K$  has the form

$$FF(K) = c_0 K^{-(L_1+L_2+4)} + c_1 K^{-(L_1+L_2+6)} + \dots \quad (6.8)$$

where  $L_1$  and  $L_2$  are the angular momentum quantum numbers of the initial and final states, respectively. The expression for the large  $K$  expansion of  $GOS(K)$  is easily obtained by substituting equation (6.8) into equation (6.5).

The first three small and large  $K$  expansion coefficients of  $FF(K)$ (elastic) or  $GOS(K)$ (inelastic) will be given for each of the 43 He transitions considered in this chapter. Appendix 8 discusses the calculation of these expansion coefficients.

### 6.3 Elastic scattering: The $1^1S$ , $2^1S$ , and $2^3S$ states of He

Tables 6.3.1, 6.3.2, and 6.3.3 give  $FF(K)$  for elastic scattering of the  $1^1S$ ,  $2^3S$ , and  $2^1S$  states, respectively. The form factors are given for a mesh of 63 values of  $K^2$ . As the table shows, as  $K$  increases,  $FF(K)$  decreases monotonically from the initial value of 2 at  $K=0$ .

The ground state elastic differential cross section obtained from the data of table 6.3.1 is compared with experimental measurements in figures 6.3.1 and 6.3.2 for incident electron energies of 100, and 400 and 700 eV, respectively. These figures also include the "recommended" values of Boesten and Tanaka [6.30]. These are obtained by fitting a rational function of the form

$$\frac{d\sigma}{d\Omega} = \frac{a_0 + a_1\theta + a_2\theta^2 + a_3\theta^3 + a_4\theta^4}{1 + b_1\theta + b_2\theta^2 + b_3\theta^3 + b_4\theta^4} \quad (6.9)$$

where  $\theta$  is in degrees, to experimental and theoretical data.

Figure 6.3.1 shows that, with the exception of the experimental values of McConkey [6.30] the theoretical cross sections are smaller than the experimental values at 100 eV. The first Born cross sections are reasonable for  $40^\circ \leq \theta \leq 90^\circ$  at 100 eV,  $\theta \geq 30^\circ$  at 400 eV, and  $\theta \geq 15^\circ$  for 700 eV. As the figures show, the convergence is slowest for small angles; the ratio of experimental to theoretical cross section at  $0^\circ$  is roughly 6 at 100 eV, 3 at 400 eV, and 2 at 700 eV.

The 100 eV data of Kurepa [6.32] and Crooks [6.33], and the 400 eV data of Jost [6.39] are consistently higher than the other experimental measurements. Note the following normalizations of relative measurements: The cross sections of Sethuraman

[6.34] have been normalized using the Bromberg [6.35] value for 500 eV incident electrons at  $60^{\circ}$ ; The data of McConkey [6.31] and Williams [6.36] have both been normalized to the  $20^{\circ}$  measurement of Vriens [6.37] which has, in turn, been normalized to the  $5^{\circ}$  measurements of Chamberlain [6.38]; The Jost [6.39] values have been normalized to the theoretical value of Fink [6.40] at  $90^{\circ}$ ; The Gupta [6.41] values have been normalized to the  $50^{\circ}$  measurement of Jansen [6.42]. Also, the Williams [6.36], Jost [6.39], and Crooks [6.33] measurements are quoted from table I of Kurepa [6.32].

The most accurate  $FF(K)$  published for elastic scattering in the ground state of He are those of Thakkar and Smith [6.27]. Their form factors are calculated from 66 term integral transform wavefunctions and are reported in terms of an interpolating function. The latter reproduces their calculated  $FF(K)$  to within  $10^{-8}$ . The form factors calculated from the interpolating function differ from the values in table 6.3.1 by less than 0.003%. Other first Born  $FF(K)$  calculations for elastic scattering of the He ground state include values obtained from Hartree-Fock [6.43][6.45], configuration interaction [6.46], and explicitly correlated wavefunctions [6.47][6.48]. There are no published first Born  $FF(K)$  for the elastic transitions from the  $2^1S$  and  $2^3S$  states.

The first three small and large  $K$  expansion coefficients of  $FF(K)$  for the  $1^1S$ ,  $2^1S$  and  $2^3S$  states are given in table 6.3.4 below. Using these coefficients, the  $FF(K)$  and  $GOS(K)$  can be calculated beyond the range of values given in tables 6.3.1-6.3.3.

Table 6.3.1: Elastic form factors FF(K) for squared momentum transfers,  $K^2$ , between 0.05 and 500 for the ground state of He.

$K^2$	FF(K)								
0.05	1.98027	0.70	1.75074	2.4	1.32140	5.0	0.93105	40	0.11122
0.10	1.96087	0.75	1.73494	2.6	1.28244	5.5	0.87751	50	0.08014
0.15	1.94178	0.80	1.71937	2.8	1.24534	6.0	0.82881	60	0.06056
0.20	1.92300	0.85	1.70403	3.0	1.20998	6.5	0.78436	70	0.04742
0.25	1.90453	0.90	1.68892	3.2	1.17624	7.0	0.74364	80	0.03815
0.30	1.88634	0.95	1.67403	3.4	1.14403	7.5	0.70623	90	0.03136
0.35	1.86845	1.00	1.65936	3.6	1.11324	8.0	0.67178	100	0.02625
0.40	1.85084	1.2	1.60275	3.8	1.08378	8.5	0.63995	200	0.00767
0.45	1.83350	1.4	1.54929	4.0	1.05559	9.0	0.61048	300	0.00360
0.50	1.81643	1.6	1.49873	4.2	1.02858	9.5	0.58313	400	0.00209
0.55	1.79963	1.8	1.45084	4.4	1.00268	10	0.55769	500	0.00136
0.60	1.78308	2.0	1.40544	4.6	0.97783	20	0.27420		
0.65	1.76679	2.2	1.36235	4.8	0.95397	30	0.16537		

**Table 6.3.2:** Elastic form factors FF(K) for squared momentum transfers,  $K^2$ , between 0.05 and 500 for the He  $2^3S$  state.

$K^2$	FF(K)								
0.05	1.82557	0.70	0.97683	2.4	0.73928	5.0	0.59015	40	0.08498
0.10	1.68011	0.75	0.95637	2.6	0.72650	5.5	0.56521	50	0.06115
0.15	1.55820	0.80	0.93826	2.8	0.71405	6.0	0.54152	60	0.04610
0.20	1.45554	0.85	0.92217	3.0	0.70185	6.5	0.51907	70	0.03600
0.25	1.36870	0.90	0.90780	3.2	0.68987	7.0	0.49782	80	0.02888
0.30	1.29491	0.95	0.89492	3.4	0.67807	7.5	0.47771	90	0.02368
0.35	1.23195	1.0	0.88332	3.6	0.66644	8.0	0.45870	100	0.01977
0.40	1.17801	1.2	0.84654	3.8	0.65499	8.5	0.44072	200	0.00570
0.45	1.13160	1.4	0.81995	4.0	0.64372	9.0	0.42372	300	0.00266
0.50	1.09152	1.6	0.79922	4.2	0.63262	9.5	0.40764	400	0.00154
0.55	1.05676	1.8	0.78190	4.4	0.62172	10	0.39241	500	0.00100
0.60	1.02550	2.0	0.76662	4.6	0.61100	20	0.20566		
0.65	1.00005	2.2	0.75257	4.8	0.60048	30	0.12598		

Table 6.3.3: Elastic form factors FF(K) for squared momentum transfers,  $K^2$ , between 0.05 and 500 for the He  $2^1S$  state.

$K^2$	FF(K)								
0.05	1.76323	0.70	0.90999	2.4	0.76903	5.0	0.60399	40	0.08372
0.10	1.57880	0.75	0.89830	2.6	0.75591	5.5	0.57644	50	0.06026
0.15	1.43424	0.80	0.88845	2.8	0.74264	6.0	0.55054	60	0.04545
0.20	1.32025	0.85	0.88006	3.0	0.72931	6.5	0.52621	70	0.03549
0.25	1.22989	0.90	0.87285	3.2	0.71600	7.0	0.50337	80	0.02849
0.30	1.15790	0.95	0.86659	3.4	0.70276	7.5	0.48194	90	0.02337
0.35	1.10026	1.0	0.86107	3.6	0.68966	8.0	0.46180	100	0.01952
0.40	1.05389	1.2	0.84387	3.8	0.67673	8.5	0.44289	200	0.00563
0.45	1.01641	1.4	0.83059	4.0	0.66400	9.0	0.42509	300	0.00263
0.50	0.98598	1.6	0.81855	4.2	0.65150	9.5	0.40834	400	0.00152
0.55	0.96115	1.8	0.80664	4.4	0.63923	10	0.39256	500	0.00099
0.60	0.94077	2.0	0.79445	4.6	0.62722	20	0.20326		
0.65	0.92395	2.2	0.78191	4.8	0.61547	30	0.12418		

Table 6.3.4: First three small and large K form factor expansion coefficients for the He  $1^1S$ ,  $2^1S$ , and  $2^3S$  states.

State	Small K			Large K		
	$K^0$	$K^2$	$K^4$	$K^{-4}$	$K^{-6}$	$K^{-8}$
$1^1S$	2	-0.39783( 0)	0.66226(-1)	0.36403( 3)	-0.12943( 5)	0.29683( 6)
$2^1S$	2	-0.53631( 1)	0.13763( 2)	0.26325( 3)	-0.84914( 4)	0.20130( 6)
$2^3S$	2	-0.38214( 1)	0.71400( 1)	0.26547( 3)	-0.84217( 4)	0.19989( 6)

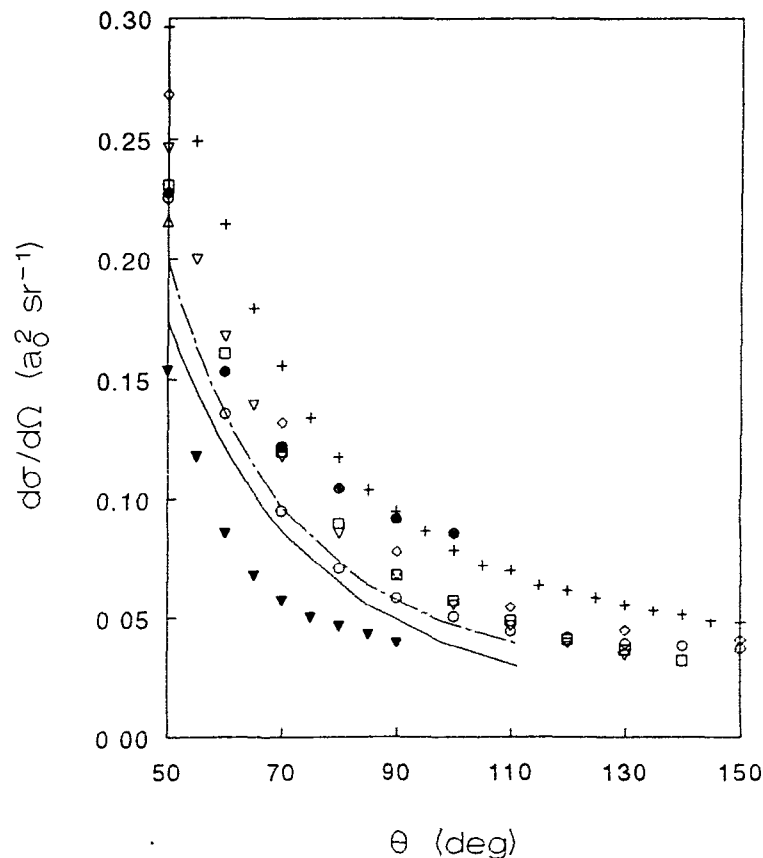
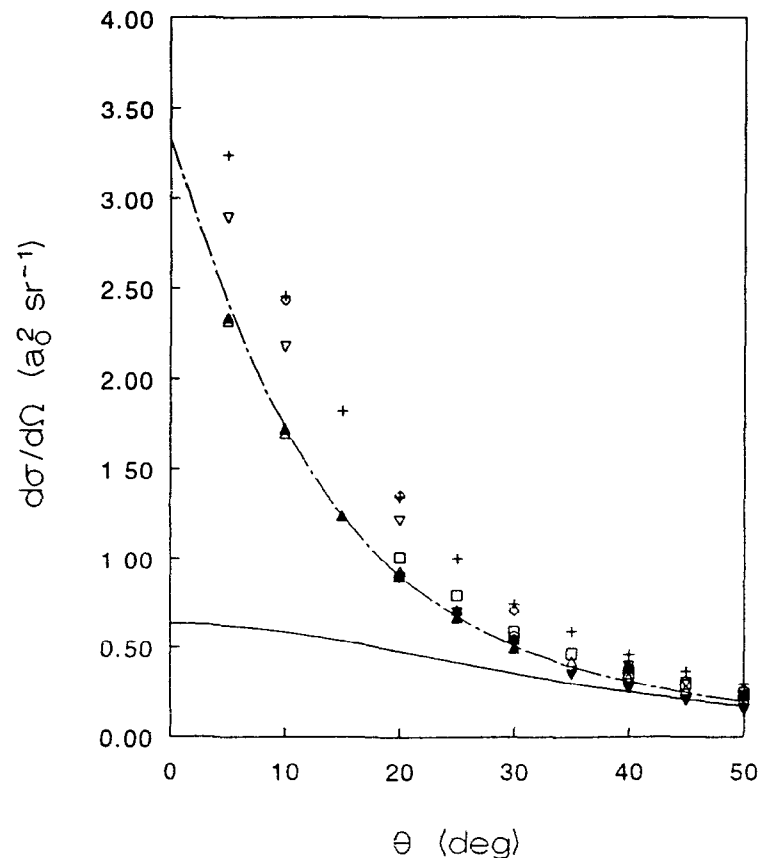


Figure 6.3.1: Differential cross sections for elastic scattering of 100 eV electrons incident on He ( $1^1S$ ). Legend: —, First Born; — · —, Boesten [6.30]; +, Kurepa [6.32];  $\Delta$ , Jansen [6.42];  $\circ$ , Sethuraman [6.34];  $\blacktriangle$ , Vriens [6.37];  $\bullet$ , Williams [6.36];  $\nabla$ , Jost [6.39];  $\diamond$ , Crooks [6.33];  $\square$ , Gupta [6.41];  $\blacktriangledown$ , McConkey [6.31]. [4]

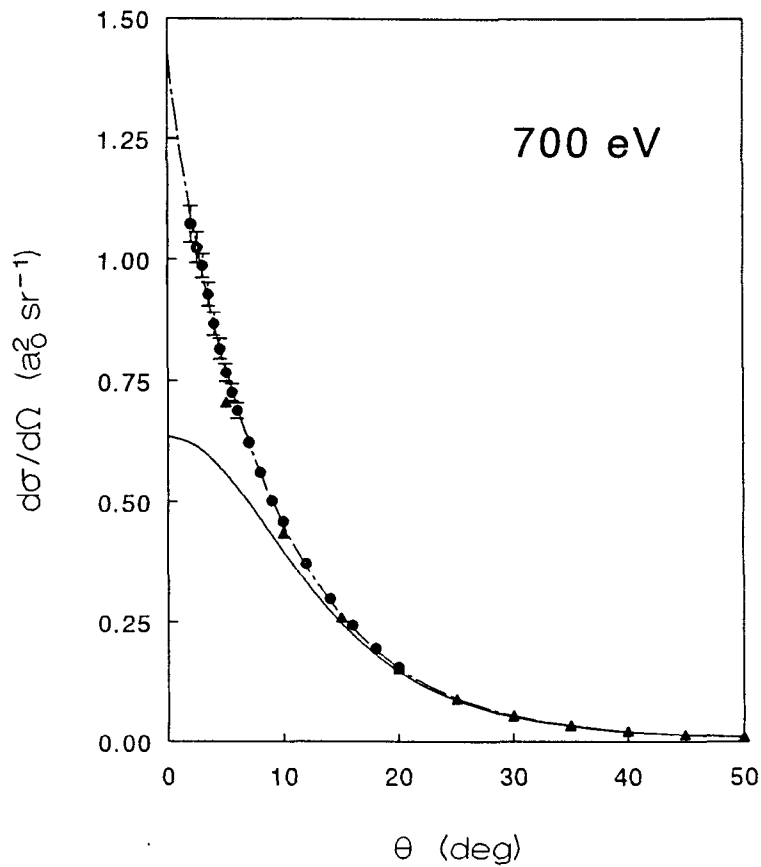
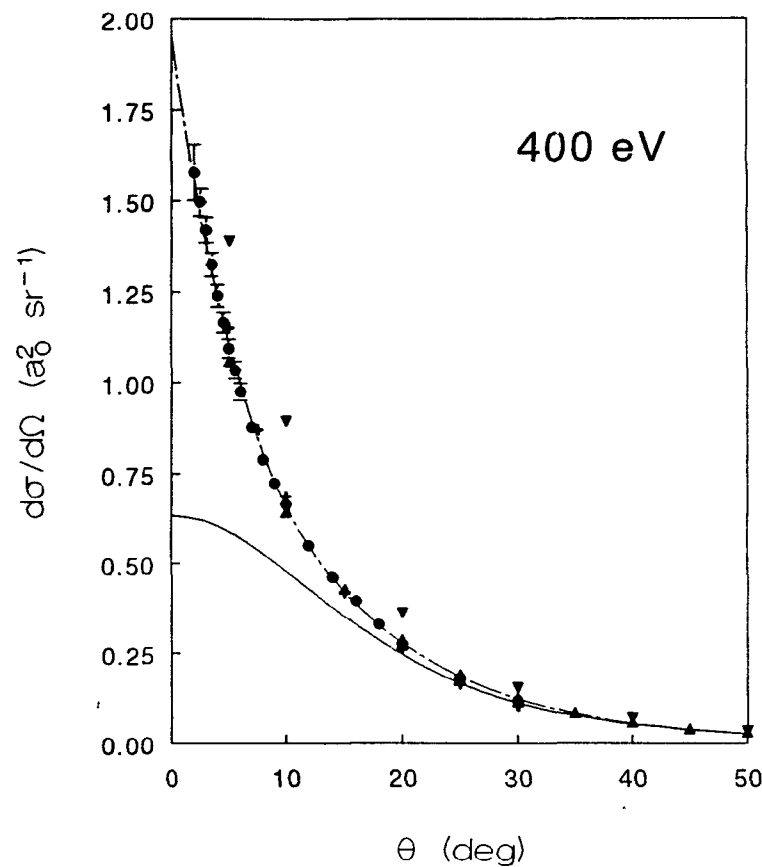


Figure 6.3.2: Differential cross sections for elastic scattering of 400 and 700 eV electrons incident on He ( $1^1S$ ). Legend:  
 —, First Born; — · —, Boesten [6.30]; +, Vriens [6.37];  $\blacktriangle$ , Jansen [6.42];  $\bullet$ , Bromberg [6.43];  
 $\blacktriangledown$ , Jost [6.39].

#### 6.4 Inelastic scattering: Transitions from the $1^1S$ , $2^1S$ , and $2^3S$ states of He

The generalized oscillator strengths for  $1^1S \rightarrow n^1S$ ,  $1^1S \rightarrow n^1P$ , and  $1^1S \rightarrow n^1D$  transitions are given in tables 6.4.1, 6.4.2 and 6.4.3, respectively. The  $S \rightarrow S$  GOS reach a maximum at  $K^2 \approx 1.0$ , the  $S \rightarrow P$  GOS decrease monotonically from the DOS value at  $K=0$ , and the  $S \rightarrow D$  GOS reach a maximum at  $K^2 \approx 0.5$ . At small and intermediate  $K$  values, the GOS ordering is generally  $S \rightarrow P > S \rightarrow S > S \rightarrow D$ .

The  $1^1S \rightarrow 2^1S$  differential cross sections are compared with experiment in figures 6.4.1 and 6.4.2 for incident electron energies of 100, and 400 and 700 eV, respectively. At 100 eV, the first Born differential cross section is qualitatively correct at small angles but falls markedly below the experimental values for large angle. The latter is a well known shortcoming of the first Born approximation; backward scattered electrons penetrate deeply into the charge cloud but, as noted previously, the attractive potential arising from the interaction of the incoming electron with the nucleus vanishes due to the orthogonality of the target states. For 400 eV with  $\theta \leq 35^\circ$ , and 700 eV with  $\theta \leq 17.5^\circ$  the first Born cross sections are quantitatively correct. However, these angular limits are determined solely by the available experimental data; the angular range will increase with impact energy.

The  $1^1S \rightarrow 3^1S$  differential cross sections are compared, in figure 6.4.3, with the recent 100 eV results of Trajmar [6.49]. As with the transition to the  $2^1S$  state, the Born values are too large, but qualitatively correct, at small angles. Unfortunately, these are the only experimental values available for this transition.

Figures 6.4.4 and 6.4.5 compare the experimental cross sections of Pochat [6.52] with the first Born cross sections for the  $1^1S \rightarrow 4^1S$  and  $1^1S \rightarrow 5^1S$  transitions, respectively. Both figures show 100 and 200 eV results for  $\theta \leq 20^\circ$ . The 100 eV Born cross sections are qualitatively incorrect over the angular range. The calculated 100 and 200 eV cross sections decrease less rapidly with  $\theta$  than the experimental values. However, the agreement between theory and experiment for 200 eV impact energy has improved markedly from the 100 eV results.

Figures 6.4.1-6.4.5 allow tentative remarks about the range of validity of the first Born approximation. At  $\theta \leq 40^\circ$  the calculated cross sections are larger than the experimental values. Exceptions occur at small angles for low incident energies. For the  $1^1S \rightarrow n^1S$ ,  $n=2-6$ , transitions, the first Born cross sections are quantitative for incident energies  $\geq 400$  eV and  $\theta \leq 40^\circ$ . Qualitative agreement between experiment and theory is estimated to occur for incident electron energies  $\geq 250$  eV. The angular limits are particularly tentative due to the limited data for  $\theta \geq 20^\circ$ .

The  $1^1S \rightarrow 2^1P$  differential cross sections are compared with experiment in figures 6.4.6 and 6.4.7 for incident electron energies of 100, and 400 and 700 eV, respectively. Even at 100 eV, the theoretical and experimental cross sections agree closely for  $\theta \leq 30^\circ$ . Note, in particular, the "recommended" value of Trajmar [6.53] at  $20^\circ$ . This value has been obtained from the analysis of experimental and theoretical cross sections for  $\theta = 20^\circ$ .

Figure 6.4.8 shows the  $1^1S \rightarrow 3^1P$  results of Cartwright [6.54] and Chutjian [6.55] for 100 eV incident electrons and  $5^\circ \leq \theta \leq 135^\circ$ . The first Born cross sections are accurate at this incident energy for  $\theta \leq 40^\circ$ .

Experimental results for the  $1^1S \rightarrow 4^1P$  and  $1^1S \rightarrow 5^1P$  transitions are scarce. Figures 6.4.9 and 6.4.10 compare the available data with the first Born values.

Figures 6.4.6-6.4.10 show that, in contrast to the  $S \rightarrow S$  transitions, the first Born  $S \rightarrow P$  cross sections are quantitative for incident energies as low as 100 eV and  $\theta \leq 40^\circ$ .

Unfortunately, there are no  $1^1S \rightarrow 3^1D$  differential cross sections reported in the literature. However, Pochat [6.52] has measured 100 and 200 eV differential cross sections for the  $1^1S \rightarrow 4^1D$  and  $1^1S \rightarrow 5^1D$  transitions for  $\theta \leq 20^\circ$ . These are shown in figures 6.4.11 and 6.4.12. At 100 eV the theoretical curves lie below the experimental values and the discrepancy is largest at smaller angles. At 200 eV the agreement between experiment and theory is much improved but still not quantitative. These results suggest that first Born results will be quantitative for incident energies  $\geq 300$  eV.

Generalized oscillator strengths for the  $1^1S \rightarrow n^1S$ ,  $n=1-7$ ,  $1^1S \rightarrow n^1P$ ,  $n=2-4$  and  $1^1S \rightarrow 3^1D$  have been calculated by Bell *et al* [6.48] for thirty  $K$  values. These calculations are performed with Hylleraas-type wavefunctions for the initial and final states. Their  $GOS(K)$  for  $1^1S \rightarrow n^1S$  transitions agree within 1% of the values in table 6.4.1 and the agreement is generally best for  $K=1$ . The  $1^1S \rightarrow 2^1P$ ,  $3^1P$ , and  $4^1P$  transitions agree with the  $GOS(K)$  of table 6.4.2 within 1% for  $K \leq 1$  but decrease too rapidly at large  $K$ . At  $K=10$ , their  $GOS(K)$  are too small by 13%, 41%, and 48% for the  $2^1P$ ,  $3^1P$ , and  $4^1P$  final states, respectively. The  $1^1S \rightarrow 3^1D$  are up to 6% smaller than the values of table 6.4.3 for  $K \leq 7$ . Bell *et al* [6.48] also considered  $GOS(K)$  for the  $1^1S \rightarrow 5^1P$ ,  $1^1S \rightarrow 6^1P$ ,  $1^1S \rightarrow 4^1D$ ,  $1^1S \rightarrow 5^1D$ , and  $1^1S \rightarrow 6^1D$  transitions. These calculations differ from those discussed above in that only ten  $K$  values were considered and the final state was

represented by a numerical Hartree-Fock wavefunction rather than a Hylleraas-type expansion. The  $GOS(K)$  are up to 10% and 15% smaller than the values of tables 6.4.2 and 6.4.3, respectively.

Explicitly correlated wavefunctions have also been used by Kim and Inokuti [6.57][6.58] to calculate  $GOS(K)$  for the  $1^1S \rightarrow 2^1S$ ,  $1^1S \rightarrow 3^1S$ ,  $1^1S \rightarrow 2^1P$ ,  $1^1S \rightarrow 3^1P$ ,  $1^1S \rightarrow 4^1P$ , and the  $1^1S \rightarrow 3^1D$  transition. The initial and final state wavefunction expansions contained over 50 terms and calculations were performed for over 60  $K$  values. Their  $1^1S \rightarrow 2^1S$  cross sections are larger by 2% at  $K^2=0.05$ , but the difference decreases rapidly as  $K$  increases and is less than 0.1% for  $K^2 \geq 1.4$ . For the  $1^1S \rightarrow 3^1S$  transition, the errors are largest for small  $K$  and large  $K$ , but the values agree within 5% and for  $0.5 < K^2 < 40$  the error is less than 1%. For the  $1^1S \rightarrow 2^1P$ ,  $1^1S \rightarrow 3^1P$ ,  $1^1S \rightarrow 4^1P$  transitions the values agree within 0.1%, 4%, and 5%, respectively, for  $K^2 \leq 10$ . For the  $1^1S \rightarrow 3^1D$  transition the values agree within 5% for  $K^2 < 10$ . For the 6 transitions considered by Kim and Inokuti [6.57][6.58], the cross sections always decrease more rapidly at large  $K$  than the values in tables 6.4.1, 6.4.2 and 6.4.3. These comparisons indicate that the  $GOS(K)$  are most sensitive to wavefunction quality at small and large  $K$ .

The up-to-60 term Hylleraas-type wavefunctions used by Kim and Inokuti [6.57][6.58] and Bell *et al* [6.48] for the final states lead to excitation energies which differ from the results of chapter 2 by as much as a millihartree. As a general rule, 50 term integral transform wavefunctions are energetically equivalent to 60 term Hylleraas-type wavefunctions. Therefore, the  $GOS(K)$  and  $FF(K)$  obtained from the 100 term integral transform wavefunctions of chapter 2 significantly improve upon the previously

published values. Finally, although the cross sections of Bell *et al* [6.48] and Kim and Inokuti [6.57][6.58] are the most accurate published values, others [6.54][6.59-6.66] have also calculated first Born cross sections for transitions from the ground state.

Generalized oscillator strengths for the  $2^3S \rightarrow n^3S$ ,  $n=3-6$ , the  $2^3S \rightarrow n^3P$ ,  $n=3-6$ , and the  $2^3S \rightarrow n^3D$ ,  $n=3-6$  transitions are given in tables 6.4.4, 6.4.5, and 6.4.6, respectively. The  $GOS(K)$  for the  $2^1S \rightarrow n^1S$ ,  $n=3-6$ , the  $2^1S \rightarrow n^1P$ ,  $n=3-6$ , and the  $2^1S \rightarrow n^1D$ ,  $n=3-6$  transitions are presented in tables 6.4.4, 6.4.5, and 6.4.6, respectively. The  $GOS(K)$  for these transitions from the metastable states are characterized by zeros in the  $GOS(K)$  for certain  $K$ . These zeros arise from the form factor changing signs at some  $K$  values.

The  $GOS(K)$  for  $S \rightarrow S$  transitions vanish at two intermediate  $K$  values: at  $K^2 \approx 1$  and 3.8 for  $2^3S \rightarrow 3^3S$ ; at  $K^2 \approx 1.2$  and 3.8 for  $2^3S \rightarrow 4^3S$ ; at  $K^2 \approx 1.2$  and 4 for  $2^3S \rightarrow 5^3S$ ; at  $K^2 \approx 1.4$  and 4 for  $2^3S \rightarrow 6^3S$ ; at  $K^2 \approx 0.8$  and 2 for  $2^1S \rightarrow 3^1S$ ; at  $K^2 \approx 0.85$  and 2.2 for  $2^1S \rightarrow 4^1S$ ; at  $K^2 \approx 0.9$  and 2.2 for  $2^1S \rightarrow 5^1S$ ; at  $K^2 \approx 0.95$  and 2.2 for  $2^1S \rightarrow 6^1S$ . Although both zeros shift to larger  $K$  as the  $n$  increases, this shift is relatively small.

The  $GOS(K)$  for  $S \rightarrow P$  transitions vanish at  $K^2 \approx 2.2$  and 1.4 for the  $2^3S \rightarrow 2^3P$  and  $2^1S \rightarrow 2^1P$  transitions, respectively. For the  $2^3S \rightarrow n^3P$ ,  $n=3-6$ , transitions the  $GOS$  vanishes at  $K^2 \approx 0.15$  and 2.6, and for the  $2^1S \rightarrow n^1P$ ,  $n=3-6$ , transitions the  $GOS$  vanishes at  $K^2 \approx 0.15$  and 1.6. The  $GOS(K)$  for the  $2^3S \rightarrow n^3D$  and the  $2^1S \rightarrow n^1D$ ,  $n=3-6$ , transitions vanish at  $K^2 \approx 3.2$  and at  $K^2 \approx 2$ , respectively. The location of the zeros seems to be largely independent of the final state wavefunctions. However, the latter certainly affect

the number of zeros. Also, relative to the singlet states, the zeros always occur at larger  $K$  for the triplets.

Kim and Inokuti [6.67] calculated  $GOS(K)$  for the  $2^1S \rightarrow 2^1P$ ,  $2^1S \rightarrow 3^1P$ ,  $2^1S \rightarrow 4^1P$ ,  $2^1S \rightarrow 3^1S$ , and  $2^1S \rightarrow 3^1D$  and the corresponding triplet transitions. They used Hylleraas-type wavefunctions with over 50 terms to calculate the  $GOS(K)$  for 31  $K$  values. With the exception of the vicinity of the zeros, their  $2^3S \rightarrow 3^3S$ ,  $2^3S \rightarrow 2^3P$ ,  $2^3S \rightarrow 3^3D$ ,  $2^1S \rightarrow 2^1P$ ,  $2^1S \rightarrow 3^1P$ , and  $2^1S \rightarrow 3^1D$  values are within 1% of the values in tables 6.4.4-6.4.9. For the  $2^3S \rightarrow 3^3P$ ,  $2^3S \rightarrow 4^3P$ , and  $2^1S \rightarrow 4^1P$  transitions, the errors at small  $K$  are as much as 50% due to the presence of a zero, but they decrease rapidly as  $K$  increases. Generally, the zeros in the  $GOS(K)$  calculated by Kim and Inokuti [6.67] occur at larger  $K$  than the values obtained from integral transform wavefunctions. For the  $2^1S \rightarrow 3^1S$  transition, this discrepancy is large enough to cause significant discrepancies. Although the Kim and Inokuti [6.67]  $GOS(K)$  are the most accurate published values, Khayralah [6.68] has also calculated  $GOS(K)$  for the  $2^3S \rightarrow 3^3S$  transition and Khurana [6.69] has calculated values for the  $2^1S \rightarrow 2^1P$ ,  $2^1S \rightarrow 3^1P$ ,  $2^3S \rightarrow 2^3P$ , and  $2^3S \rightarrow 3^3P$  transitions.

The small  $K$  expansion coefficients of the  $GOS(K)$  are given in tables 6.4.10, 6.4.11, and 6.4.12 for the  $S \rightarrow S$ ,  $S \rightarrow P$ , and  $S \rightarrow D$  transitions, respectively. Kim and Inokuti have also tabulated small  $K$  expansion coefficients for the  $1^1S \rightarrow 2^1S$ ,  $1^1S \rightarrow 3^1S$ ,  $1^1S \rightarrow 2^1P$ , and  $1^1S \rightarrow 3^1P$  transitions [6.57], the  $1^1S \rightarrow 3^1D$  and  $1^1S \rightarrow 4^1P$  transitions [6.58], and the ten transitions from the metastable states [6.67] discussed in the previous paragraph. For the transitions from the ground state, the agreement is within 2%, 5%, and 30%, for the first, second, and third coefficients, respectively. With the exception

of the  $2^1S \rightarrow 4^1P$  transition where the errors are 4%, 17% and 120%, the coefficients for the  $2^1S$  and  $2^3S$  transitions are within 3%, 4%, and 9% of the values in tables 6.4.11 and 6.4.12.

The large  $K$  expansion coefficients of the  $GOS(K)$  are given in tables 6.4.13, 6.4.14, and 6.4.15 for the  $S \rightarrow S$ ,  $S \rightarrow P$ , and  $S \rightarrow D$  transitions, respectively.

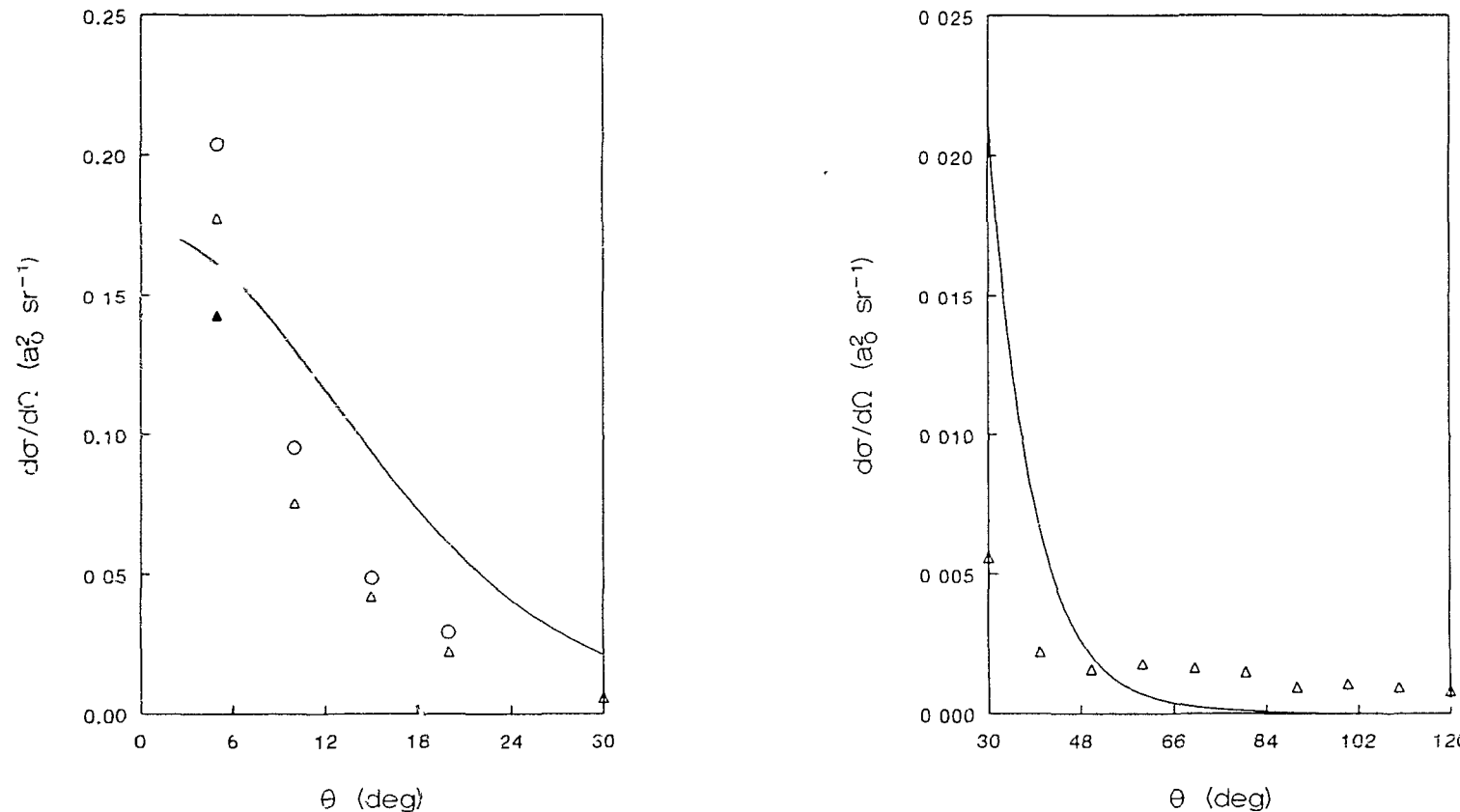


Figure 6.4.1: Differential cross sections for the  $1^1\text{S} \rightarrow 2^1\text{S}$  transition with 100 eV incident electrons. Legend: —, First Born;  $\blacktriangle$ , Chamberlain [6.38];  $\triangle$ , Trajmar [6.49];  $\circ$ , Vriens [6.50].

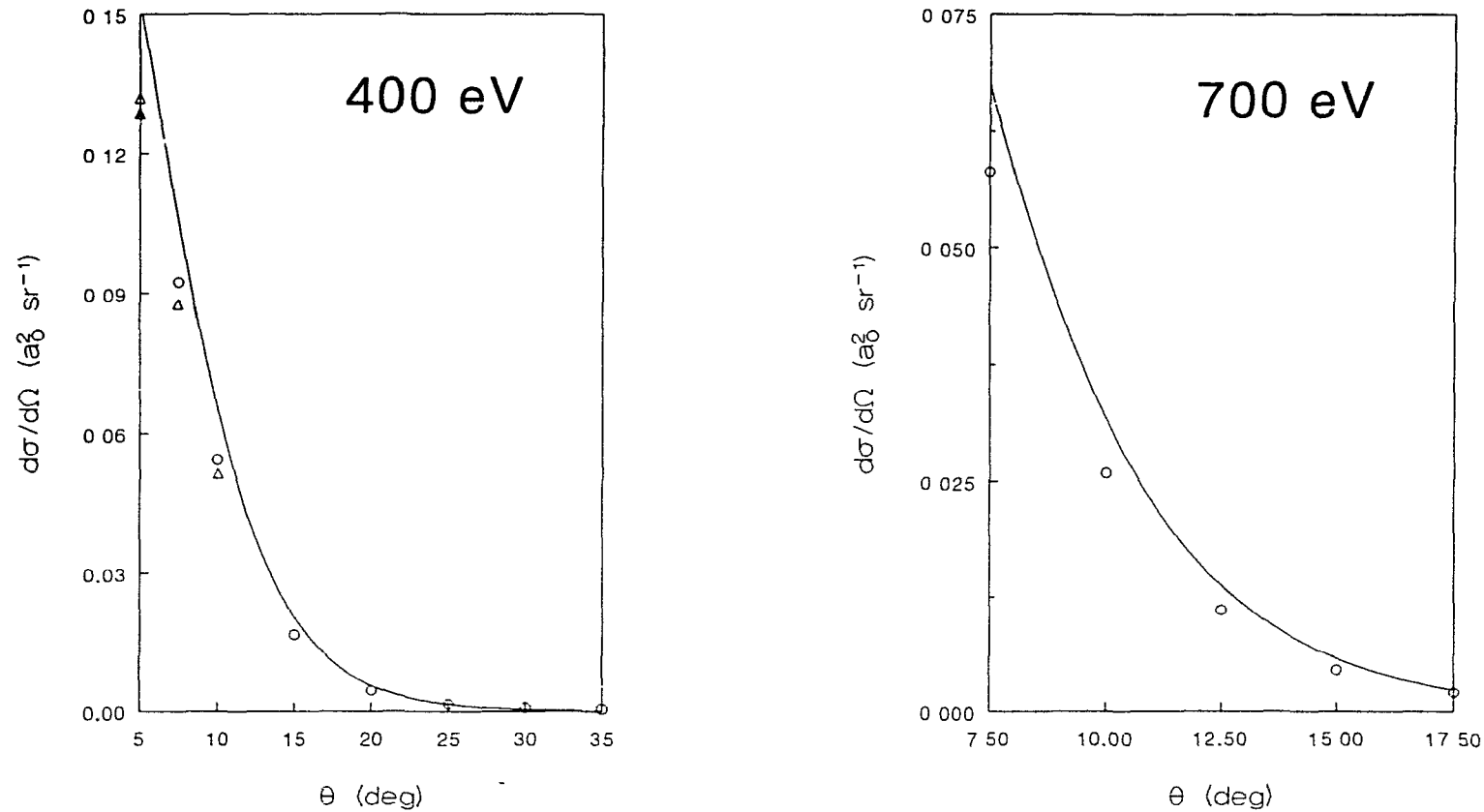


Figure 6.4.2: Differential cross sections for the  $1^1\text{S} \rightarrow 2^1\text{S}$  transition with 400 and 700 eV incident electrons. Legend: —, First Born;  $\blacktriangle$ , Chamberlain [6.38];  $\triangle$ , Vriens [6.50];  $\circ$ , Dillon [6.51].

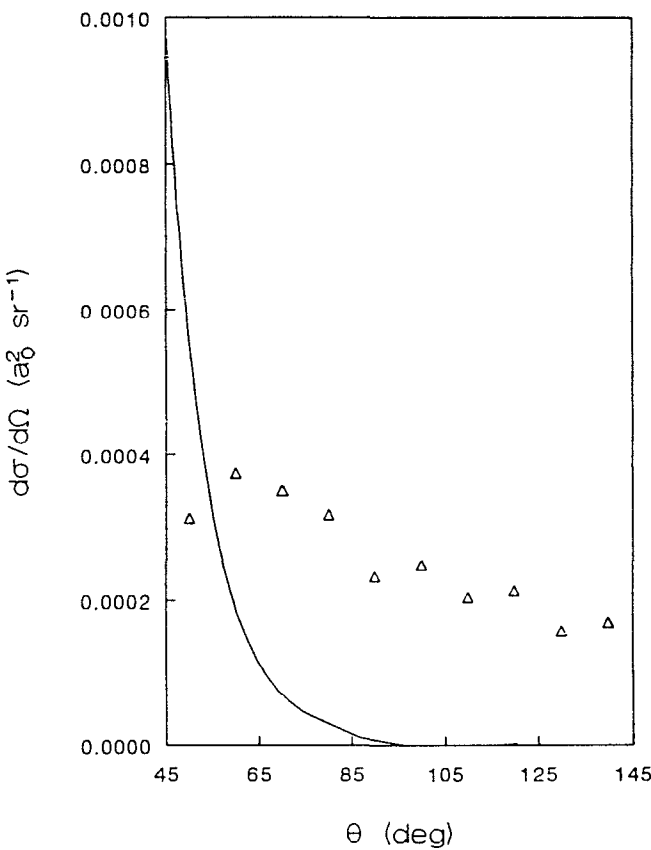
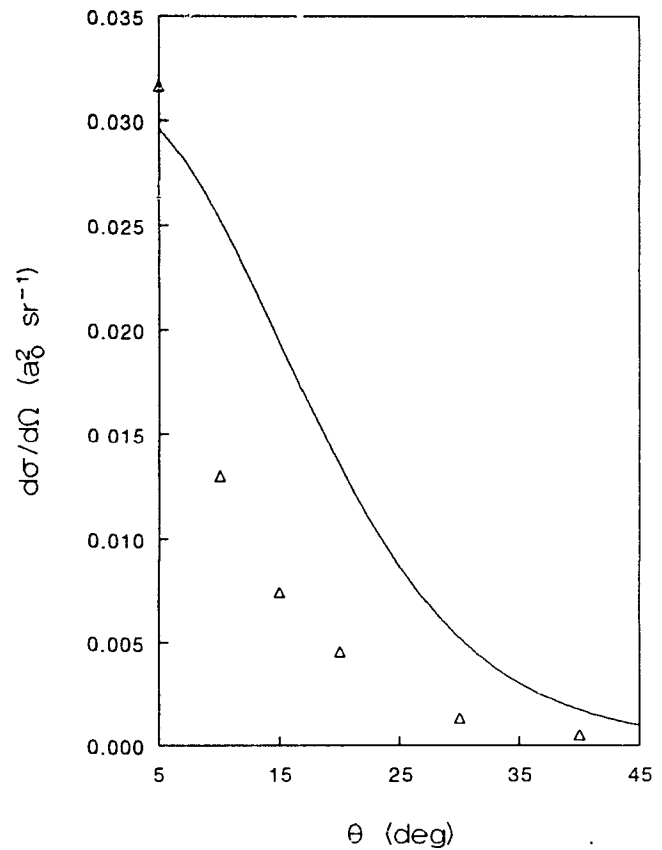


Figure 6.4.3: Differential cross sections for the  $1^1S \rightarrow 3^1S$  transition with 100 eV incident electrons. Legend: —, First Born;  $\Delta$ , Trajmar [6.49].

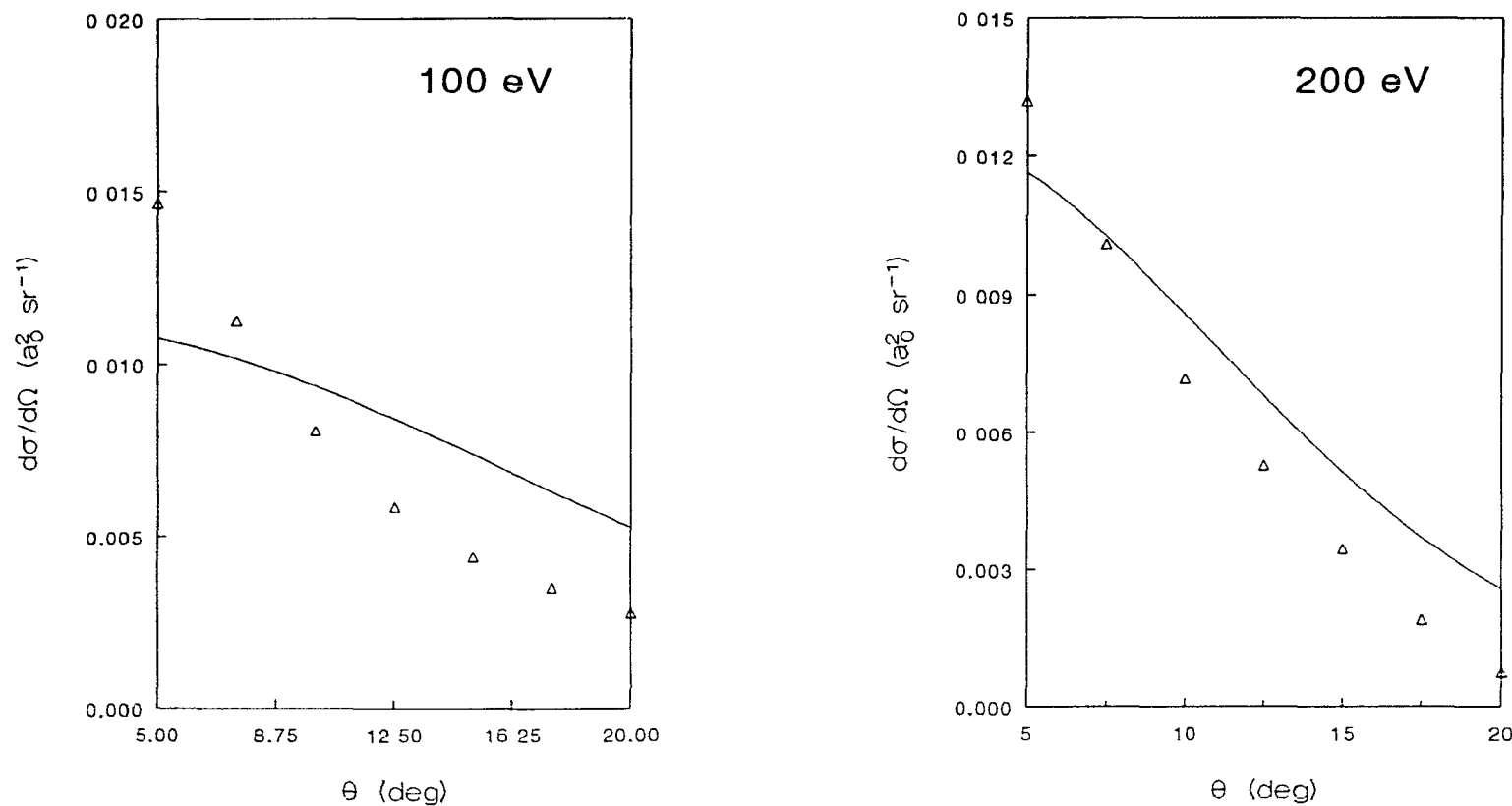


Figure 6.4.4: Differential cross sections for the  $1^1\text{S} \rightarrow 4^1\text{S}$  transition with 100 and 200 eV incident electrons. Legend: —, First Born:  $\Delta$ , Pochat [6.52].

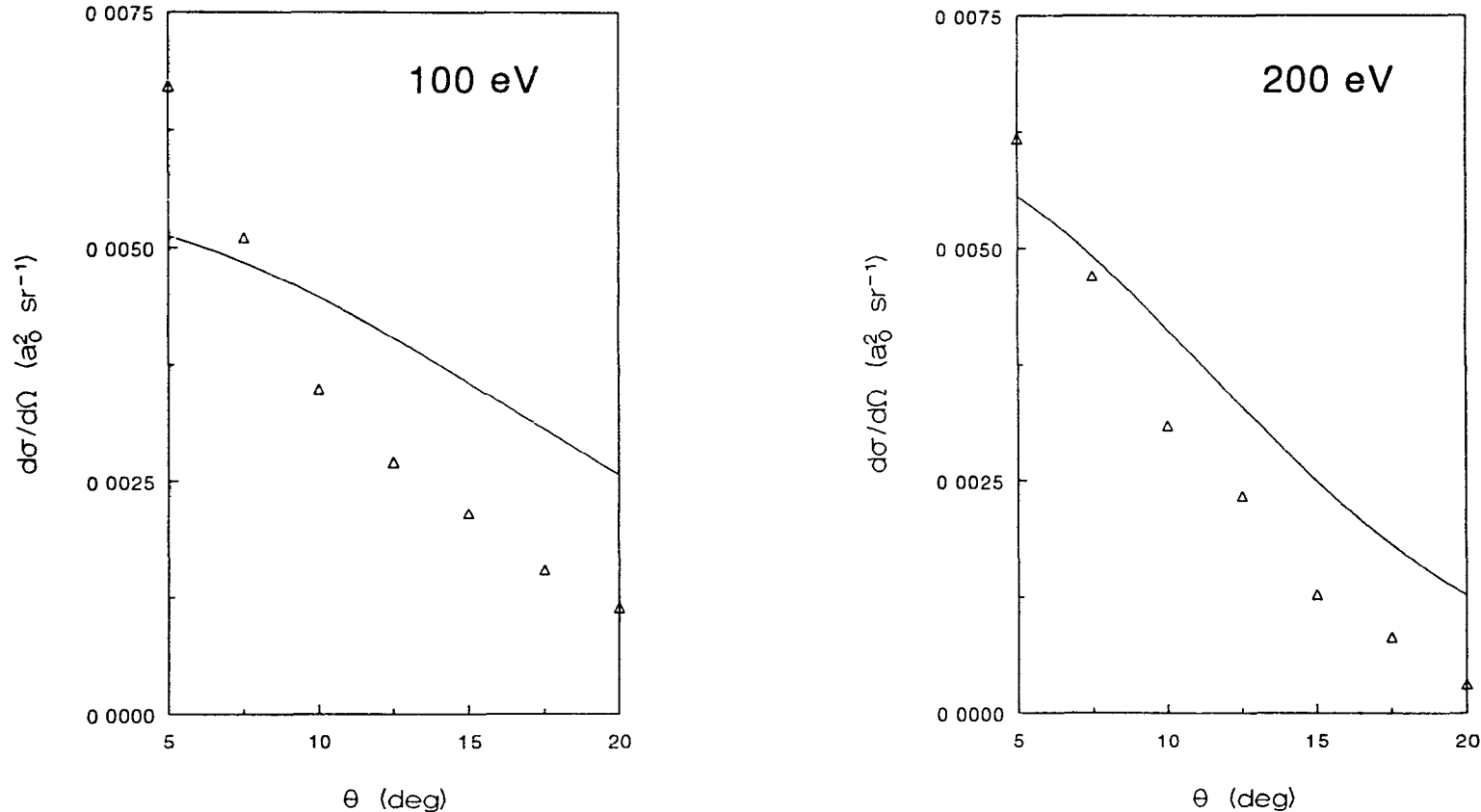


Figure 6.4.5: Differential cross sections for the  $1^1S \rightarrow 5^1S$  transition with 100 and 200 eV incident electrons. Legend: —, First Born;  $\Delta$ , Pochat [6.52].

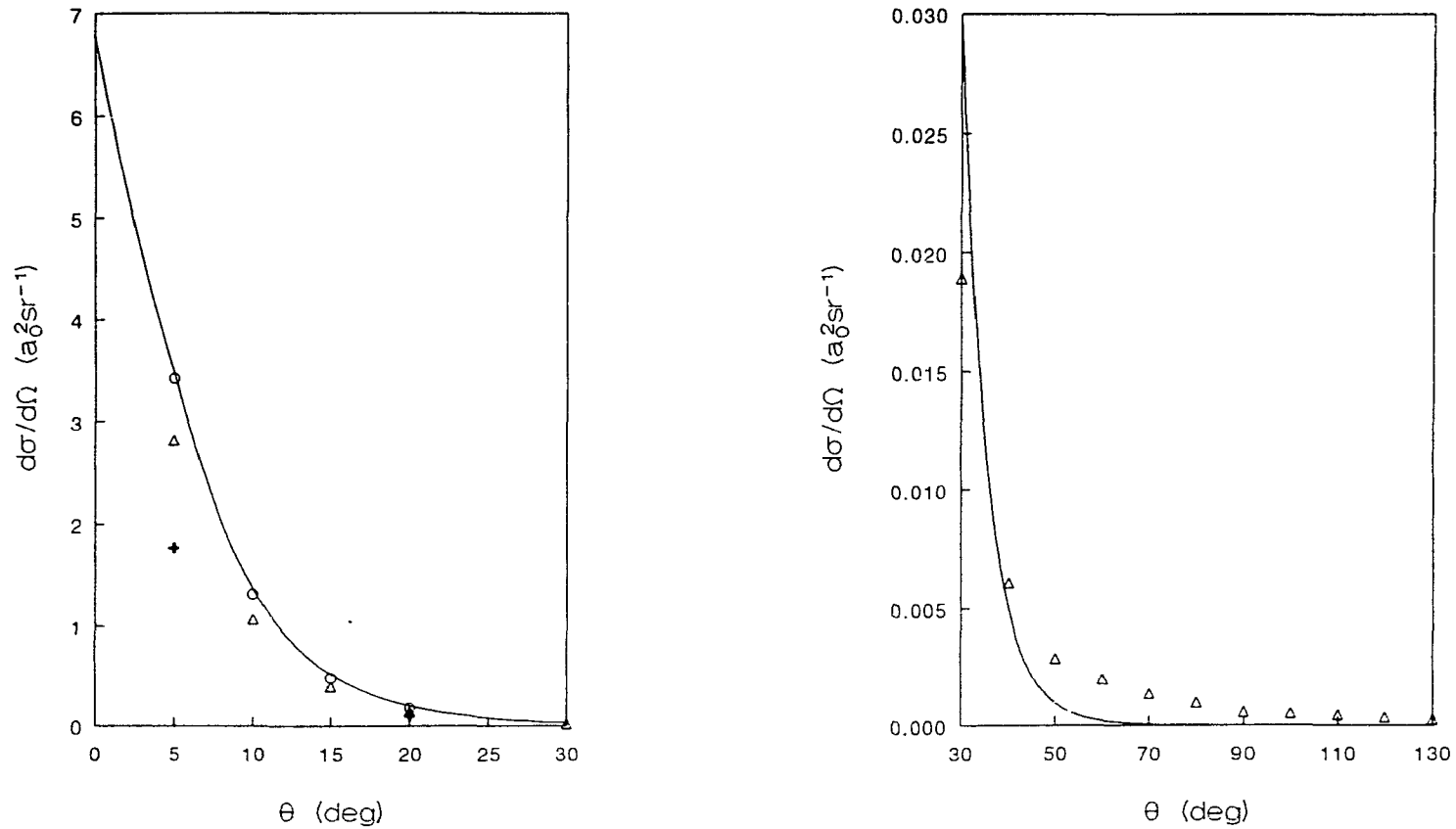


Figure 6.4.6: Differential cross sections for the  $1^1\text{S} \rightarrow 2^1\text{P}$  transition with 100 eV incident electrons. Legend: —, First Born; +, at  $5^\circ$  Chamberlain [6.38] and at  $20^\circ$  Trajmar [6.53]; ▲, Cartwright [6.54]; ○, Vriens [6.50].

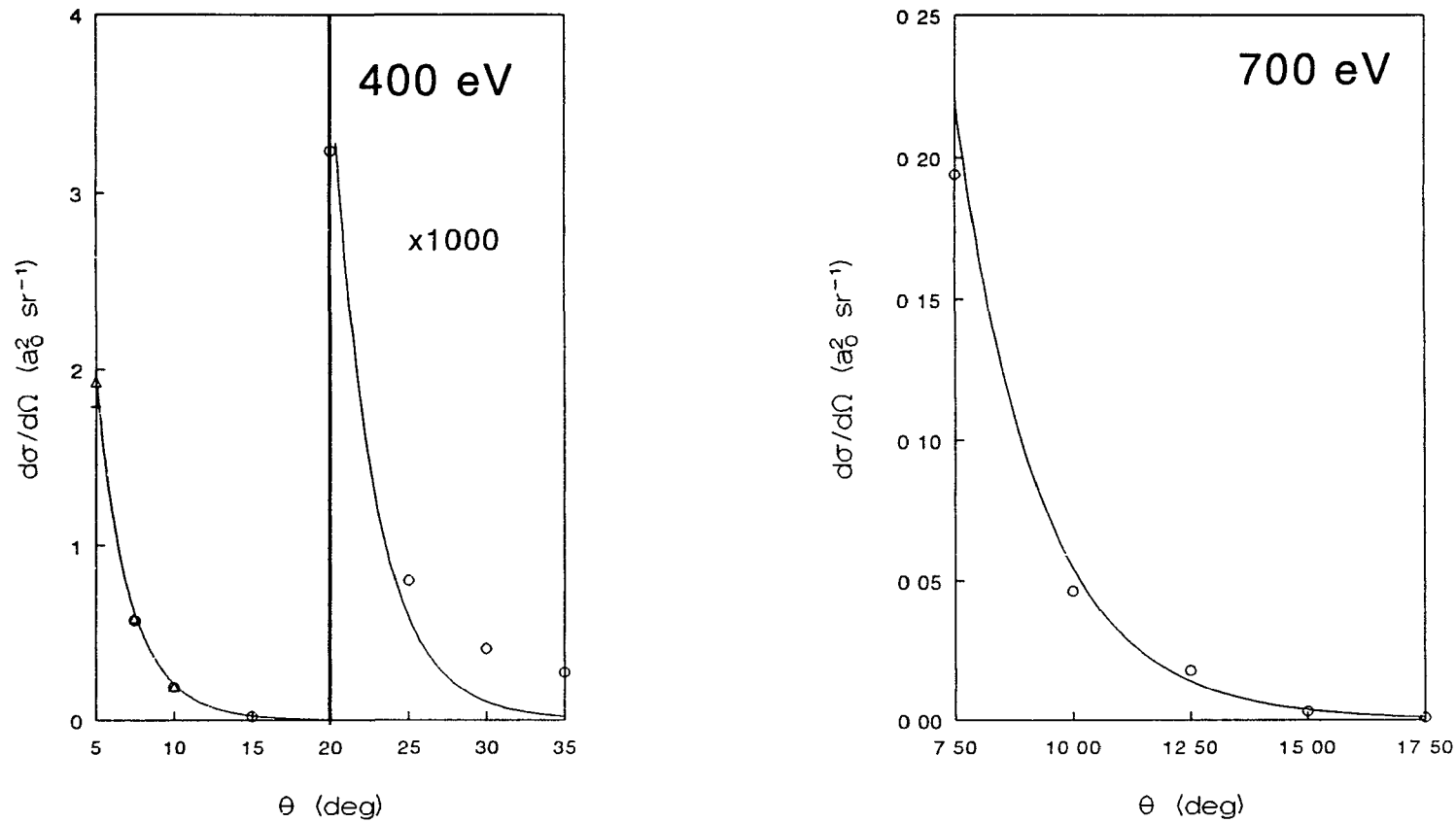


Figure 6.4.7: Differential cross sections for the  $1^1S \rightarrow 2^1P$  transition with 400 and 700 eV incident electrons. Legend: —, First Born; +, at  $5^\circ$  Chamberlain [6.38] and at  $20^\circ$  Trajmar [6.53];  $\Delta$ , Vriens [6.50];  $\circ$ , Dillon [6.51].

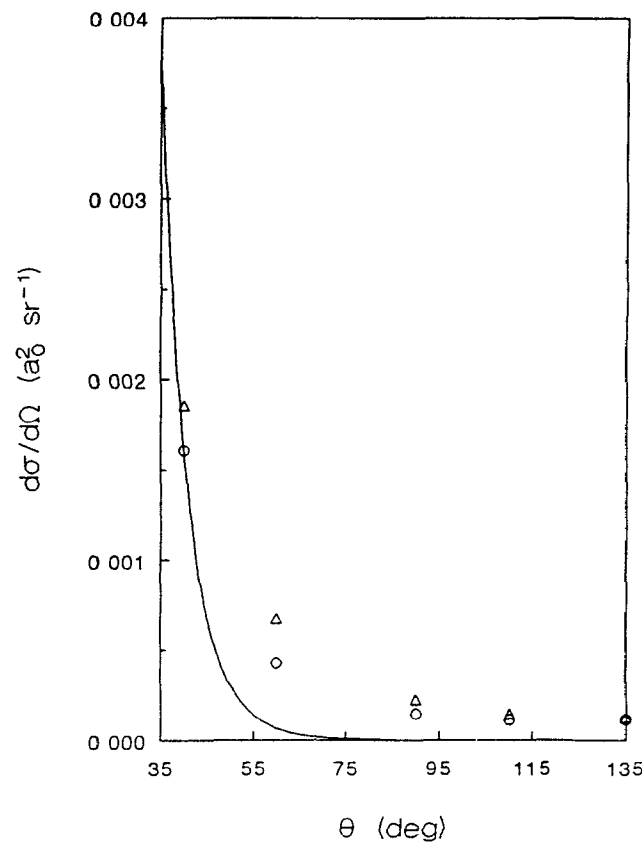
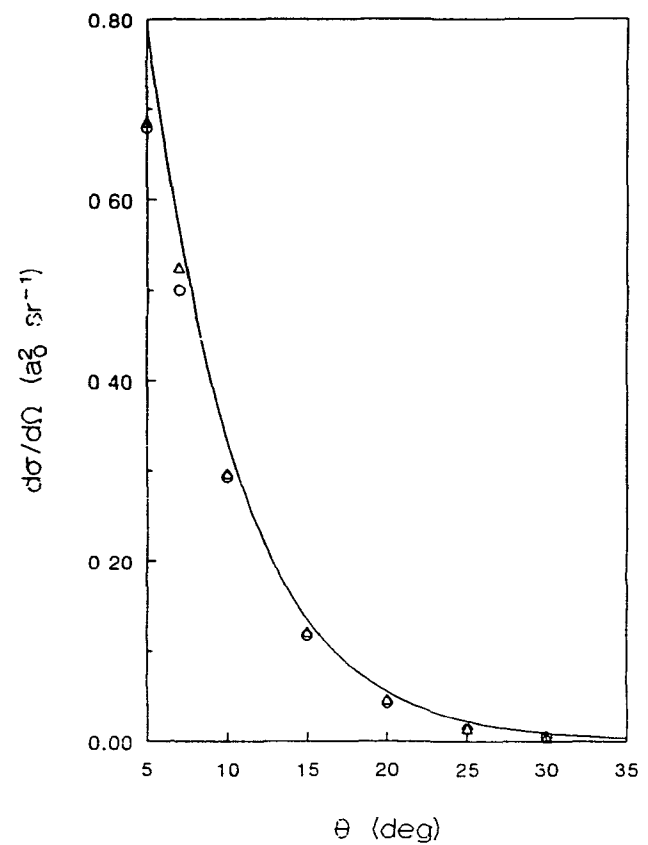


Figure 6.4.8: Differential cross sections for the  $1^1S \rightarrow 3^1P$  transition with 100 eV incident electrons. Legend: —, First Born;  $\Delta$ , Cartwright [6.54];  $\circ$ , Chutjian [6.55].

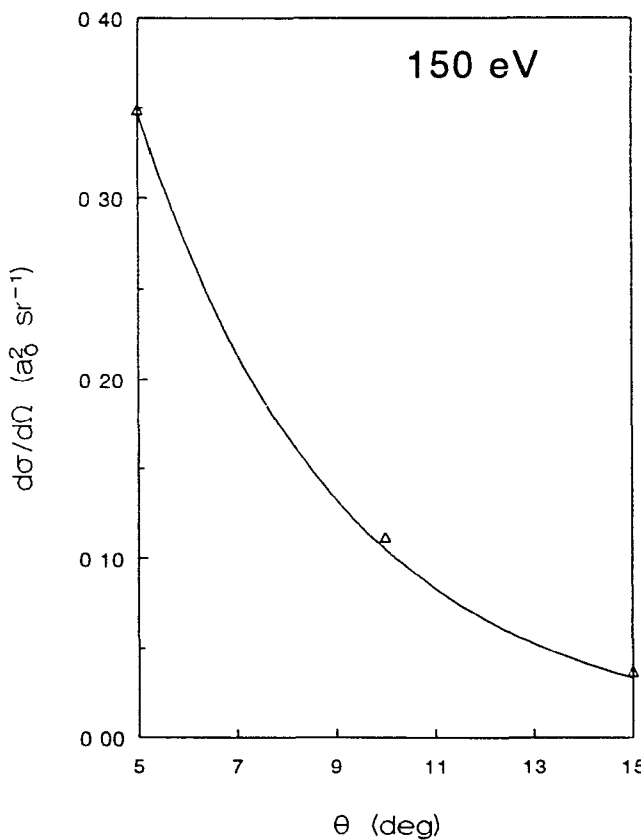
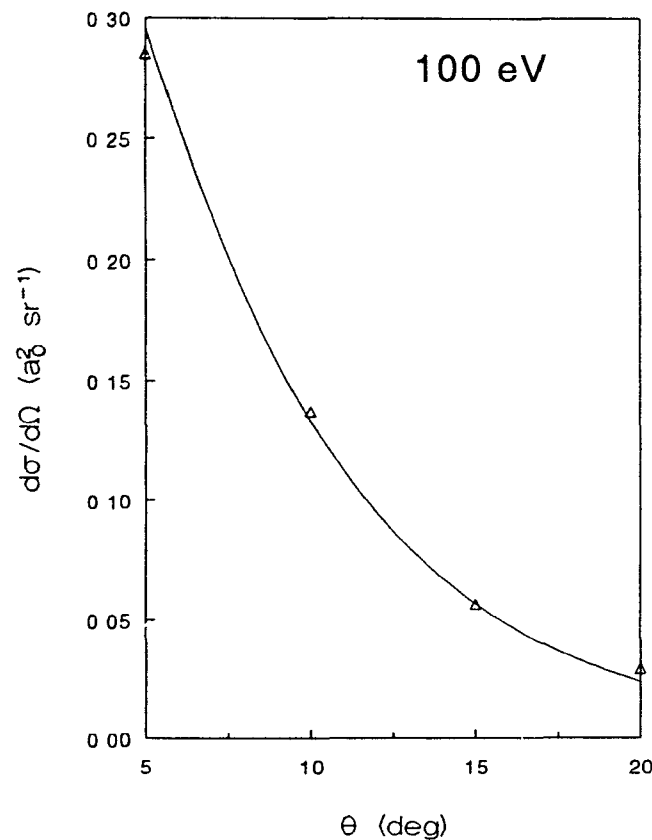


Figure 6.4.9: Differential cross sections for the  $1^1S \rightarrow 4^1P$  transition with 100 and 150 eV incident electrons. Legend: —, First Born;  $\Delta$ , Le Nadan [6.56].

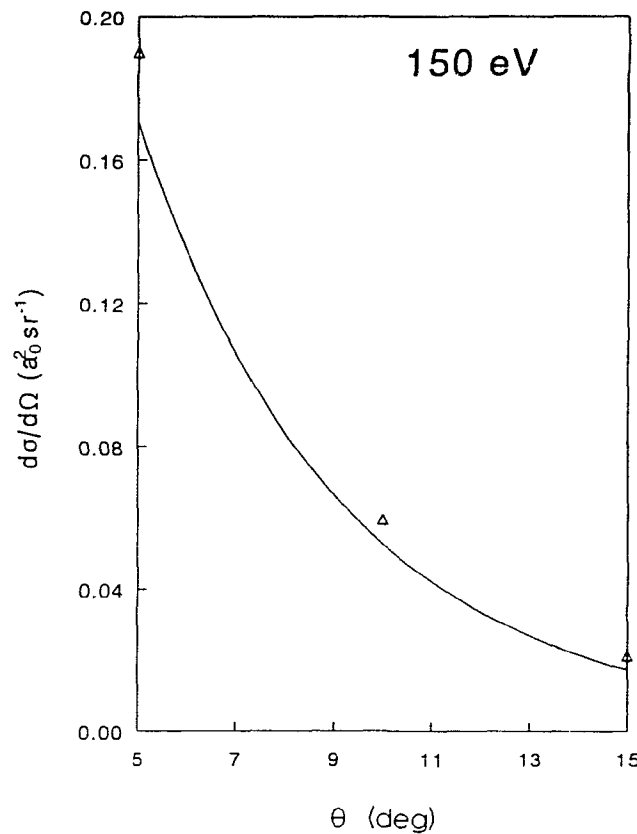
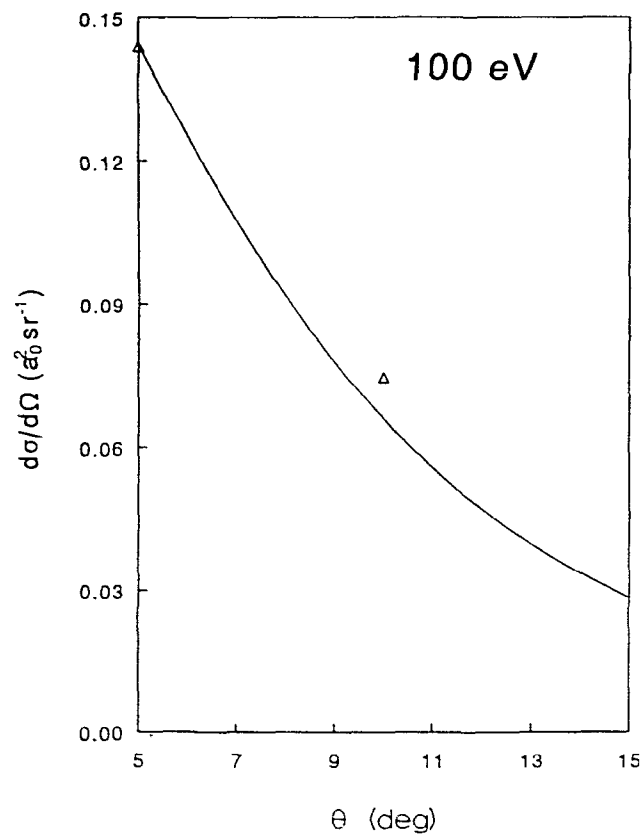


Figure 6.4.10: Differential cross sections for the  $1^1S \rightarrow 5^1P$  transition with 100 and 150 eV incident electrons. Legend: —, First Born;  $\Delta$ , Le Nadan [6.56].

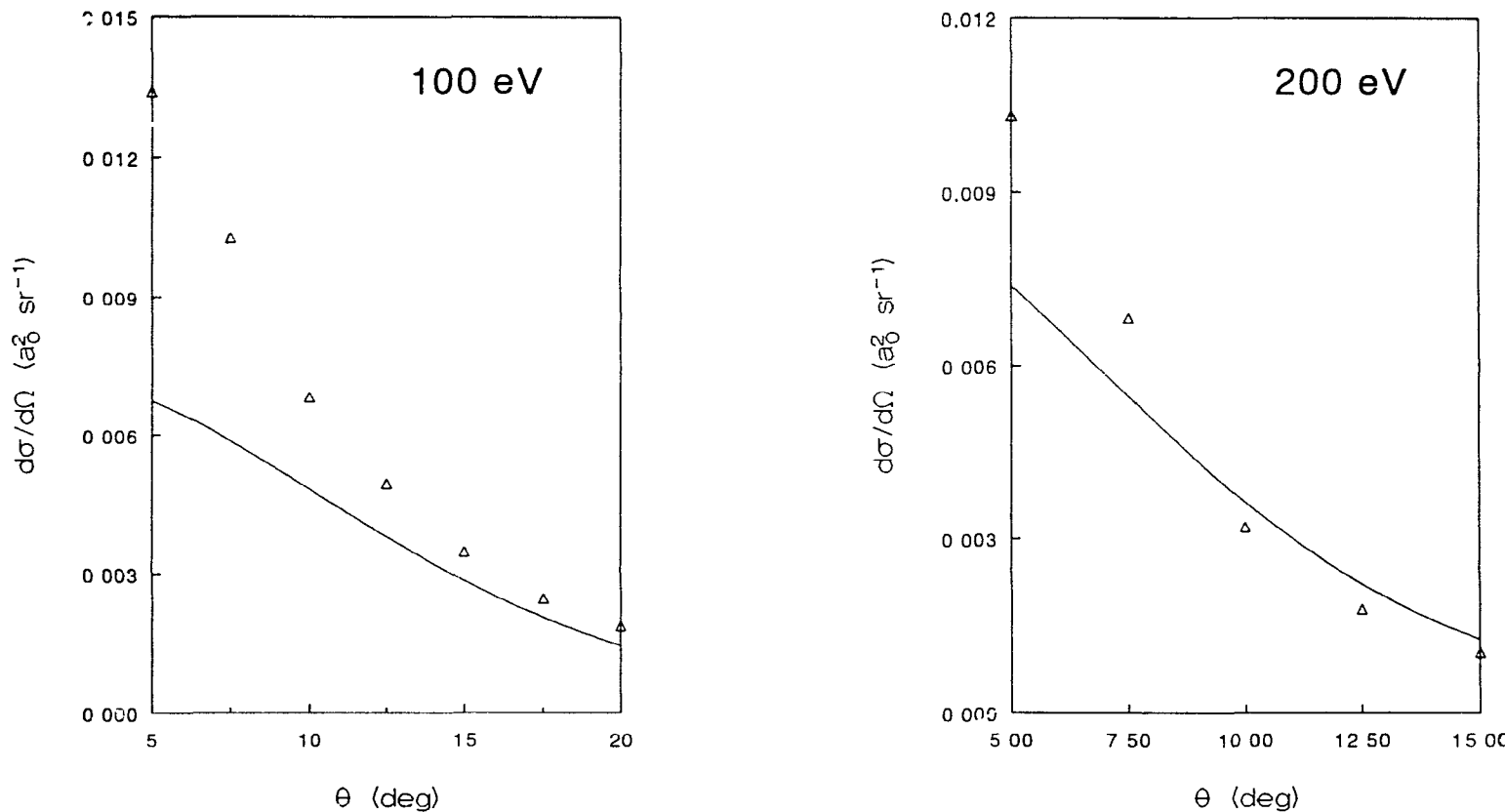


Figure 6.4.11: Differential cross sections for the  $1^1S \rightarrow 4^1D$  transition with 100 and 200 eV incident electrons. Legend: —, First Born;  $\Delta$ , Pochat [6.52].

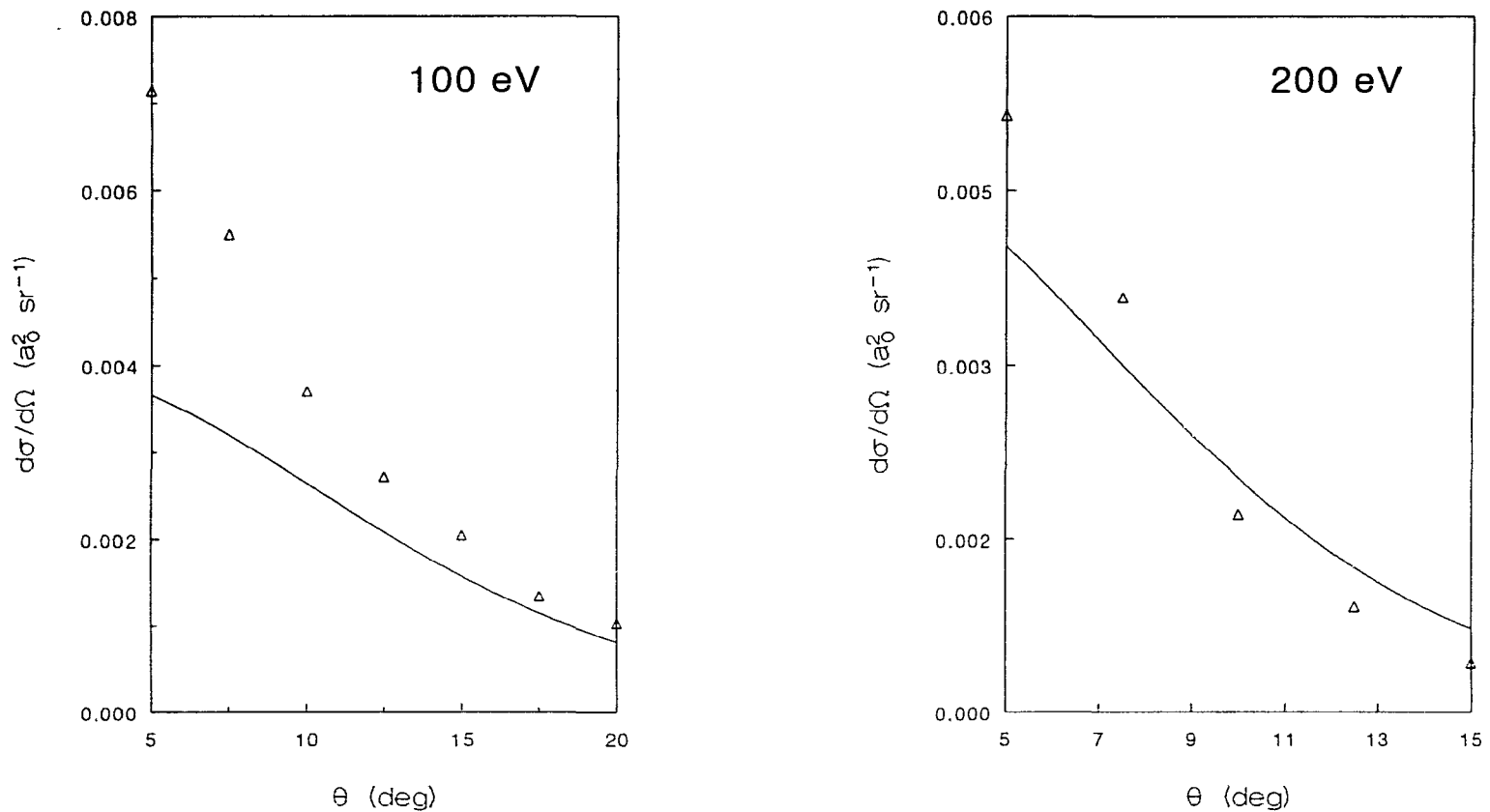


Figure 6.4.12: Differential cross sections for the  $1^1S \rightarrow 5^1D$  transition with 100 and 200 eV incident electrons. Legend: —, First Born;  $\Delta$ , Pochat [6.52].

Table 6.4.1: Generalized oscillator strengths,  $G_{\text{O.S.}}(K)$ , for the He  $1^1S \rightarrow n^1S$  transitions.

$K^2$	$2^1S$	$3^1S$	$4^1S$	$5^1S$	$6^1S$
0.05	3.89897(-3)	8.03902(-4)	2.99534(-4)	1.44441(-4)	8.07873(-5)
0.10	7.24932(-3)	1.52510(-3)	5.71442(-4)	2.76216(-4)	1.54652(-4)
0.15	1.01176(-2)	2.17033(-3)	8.17526(-4)	3.96047(-4)	2.21988(-4)
0.20	1.25633(-2)	2.74484(-3)	1.03916(-3)	5.04487(-4)	2.83073(-4)
0.25	1.46385(-2)	3.25381(-3)	1.23777(-3)	6.02132(-4)	3.38214(-4)
0.30	1.63888(-2)	3.70230(-3)	1.41483(-3)	6.89604(-4)	3.87733(-4)
0.35	1.78543(-2)	4.09519(-3)	1.57179(-3)	7.67535(-4)	4.31964(-4)
0.40	1.90701(-2)	4.43712(-3)	1.71010(-3)	8.36558(-4)	4.71243(-4)
0.45	2.00671(-2)	4.73250(-3)	1.83115(-3)	8.97295(-4)	5.05903(-4)
0.50	2.08724(-2)	4.98545(-3)	1.93628(-3)	9.50354(-4)	5.36271(-4)
0.55	2.15099(-2)	5.19983(-3)	2.02679(-3)	9.96318(-4)	5.62663(-4)
0.60	2.20006(-2)	5.37923(-3)	2.10388(-3)	1.03575(-3)	5.85385(-4)
0.65	2.23632(-2)	5.52697(-3)	2.16871(-3)	1.06918(-3)	6.04727(-4)
0.70	2.26138(-2)	5.64612(-3)	2.22236(-3)	1.09711(-3)	6.20967(-4)
0.75	2.27668(-2)	5.73952(-3)	2.26582(-3)	1.12002(-3)	6.34366(-4)
0.80	2.28351(-2)	5.80976(-3)	2.30005(-3)	1.13835(-3)	6.45170(-4)
0.85	2.28298(-2)	5.85923(-3)	2.32592(-3)	1.15252(-3)	6.53609(-4)
0.90	2.27608(-2)	5.89010(-3)	2.34422(-3)	1.16292(-3)	6.59899(-4)
0.95	2.26367(-2)	5.90438(-3)	2.35572(-3)	1.16989(-3)	6.64240(-4)
1.00	2.24654(-2)	5.90387(-3)	2.36109(-3)	1.17379(-3)	6.66819(-4)
1.2	2.14321(-2)	5.78491(-3)	2.33327(-3)	1.16434(-3)	6.62769(-4)
1.4	2.00627(-2)	5.53756(-3)	2.24963(-3)	1.12620(-3)	6.42150(-4)
1.6	1.85549(-2)	5.21876(-3)	2.13315(-3)	1.07081(-3)	6.11460(-4)
1.8	1.70258(-2)	4.86609(-3)	1.99948(-3)	1.00608(-3)	5.75219(-4)
2.0	1.55431(-2)	4.50385(-3)	1.85906(-3)	9.37338(-4)	5.36497(-4)
2.2	1.41434(-2)	4.14732(-3)	1.71866(-3)	8.68086(-4)	4.97331(-4)
2.4	1.28446(-2)	3.80566(-3)	1.58252(-3)	8.00566(-4)	4.59029(-4)
2.6	1.16531(-2)	3.48405(-3)	1.45317(-3)	7.36137(-4)	4.22394(-4)
2.8	1.05681(-2)	3.18497(-3)	1.33198(-3)	6.75558(-4)	3.87885(-4)
3.0	9.58513(-3)	2.90320(-3)	1.21954(-3)	6.19192(-4)	3.55724(-4)
3.2	8.69763(-3)	2.65646(-3)	1.11594(-3)	5.67132(-4)	3.25982(-4)
3.4	7.89799(-3)	2.42580(-3)	1.02096(-3)	5.19308(-4)	2.98630(-4)

Table 6.4.1: Continued.

K <sup>2</sup>	2 <sup>1</sup> S	3 <sup>1</sup> S	4 <sup>1</sup> S	5 <sup>1</sup> S	6 <sup>1</sup> S
3.6	7.17841(-3)	2.21590(-3)	9.34203(-4)	4.75541(-4)	2.73573(-4)
3.8	6.53126(-3)	2.02528(-3)	8.55141(-4)	4.35596(-4)	2.50686(-4)
4.0	5.94929(-3)	1.85238(-3)	7.83215(-4)	3.99207(-4)	2.29821(-4)
4.2	5.42580(-3)	1.69567(-3)	7.17848(-4)	3.66096(-4)	2.10823(-4)
4.4	4.95466(-3)	1.55366(-3)	6.58477(-4)	3.35990(-4)	1.93539(-4)
4.6	4.53031(-3)	1.42497(-3)	6.04563(-4)	3.08625(-4)	1.77821(-4)
4.8	4.14777(-3)	1.30832(-3)	5.55599(-4)	2.83751(-4)	1.63527(-4)
5.0	3.80256(-3)	1.20254(-3)	5.11118(-4)	2.61136(-4)	1.50525(-4)
5.5	3.07775(-3)	9.78776(-4)	4.16795(-4)	2.13127(-4)	1.22907(-4)
6.0	2.51129(-3)	8.02312(-4)	3.42177(-4)	1.75093(-4)	1.01012(-4)
6.5	2.06508(-3)	6.62285(-4)	2.82819(-4)	1.44804(-4)	8.35632(-5)
7.0	1.71078(-3)	5.50430(-4)	2.35306(-4)	1.20536(-4)	6.95765(-5)
7.5	1.42726(-3)	4.60467(-4)	1.97026(-4)	1.00969(-4)	5.82948(-5)
8.0	1.19865(-3)	3.87620(-4)	1.65985(-4)	8.50915(-5)	4.91371(-5)
8.5	1.01297(-3)	3.28239(-4)	1.40652(-4)	7.21264(-5)	4.16569(-5)
9.0	8.61111(-4)	2.79523(-4)	1.19846(-4)	6.14736(-5)	3.55092(-5)
9.5	7.36089(-4)	2.39308(-4)	1.02656(-4)	5.26683(-5)	3.04266(-5)
10	6.32515(-4)	2.05914(-4)	8.83700(-5)	4.53480(-5)	2.62004(-5)
20	6.48538(-5)	2.13282(-5)	9.18375(-6)	4.71916(-6)	2.72890(-6)
30	1.46922(-5)	4.83579(-6)	2.08284(-6)	1.07038(-6)	6.19020(-7)
40	4.85832(-6)	1.59773(-6)	6.87952(-7)	3.53558(-7)	2.04440(-7)
50	2.00102(-6)	6.57321(-7)	2.82909(-7)	1.45403(-7)	8.40586(-8)
60	9.51629(-7)	3.12260(-7)	1.34342(-7)	6.90463(-8)	3.99082(-8)
70	5.01125(-7)	1.64273(-7)	7.06503(-8)	3.63098(-8)	2.09833(-8)
80	2.84818(-7)	9.32862(-8)	4.01088(-8)	2.06117(-8)	1.19100(-8)
90	1.71799(-7)	5.62277(-8)	2.41695(-8)	1.24192(-8)	7.17556(-9)
100	1.08699(-7)	3.55530(-8)	1.52795(-8)	7.85016(-9)	4.53541(-9)
200	4.76189(-9)	1.55233(-9)	6.66528(-10)	3.41990(-10)	1.97620(-10)
300	7.08604(-10)	2.30713(-10)	9.90355(-11)	5.07707(-11)	2.93503(-11)
400	1.79027(-10)	5.82528(-11)	2.50027(-11)	1.28107(-11)	7.40837(-12)
500	6.09355(-11)	1.98202(-11)	8.50659(-12)	4.35695(-12)	2.52026(-12)

Table 6.4.2: Generalized oscillator strengths, GOS(K), for the He  $1^1S \rightarrow n^1P$  transitions.

K <sup>2</sup>	2 <sup>1</sup> P	3 <sup>1</sup> P	4 <sup>1</sup> P	5 <sup>1</sup> P	6 <sup>1</sup> P
0.05	2.54610(-1)	6.89783(-2)	2.82045(-2)	1.42379(-2)	8.17815(-3)
0.10	2.34999(-1)	6.47914(-2)	2.66300(-2)	1.34734(-2)	7.74825(-3)
0.15	2.17140(-1)	6.08557(-2)	2.51355(-2)	1.27447(-2)	7.33753(-3)
0.20	2.00856(-1)	5.71604(-2)	2.37196(-2)	1.20514(-2)	6.94595(-3)
0.25	1.85988(-1)	5.36941(-2)	2.23800(-2)	1.13931(-2)	6.57332(-3)
0.30	1.72396(-1)	5.04450(-2)	2.11143(-2)	1.07688(-2)	6.21928(-3)
0.35	1.59957(-1)	4.74012(-2)	1.99195(-2)	1.01775(-2)	5.88336(-3)
0.40	1.48558(-1)	4.45510(-2)	1.87928(-2)	9.61807(-3)	5.56501(-3)
0.45	1.38102(-1)	4.18828(-2)	1.77311(-2)	9.08931(-3)	5.26361(-3)
0.50	1.28499(-1)	3.93856(-2)	1.67311(-2)	8.58989(-3)	4.97849(-3)
0.55	1.19671(-1)	3.70487(-2)	1.57897(-2)	8.11847(-3)	4.70897(-3)
0.60	1.11547(-1)	3.48618(-2)	1.49038(-2)	7.67373(-3)	4.45435(-3)
0.65	1.04062(-1)	3.28153(-2)	1.40704(-2)	7.25431(-3)	4.21392(-3)
0.70	9.7600(-2)	3.09001(-2)	1.32866(-2)	6.85892(-3)	3.98698(-3)
0.75	9.07890(-2)	2.91074(-2)	1.25494(-2)	6.48628(-3)	3.77284(-3)
0.80	8.49025(-2)	2.74293(-2)	1.18562(-2)	6.13513(-3)	3.57083(-3)
0.85	7.94588(-2)	2.58579(-2)	1.12043(-2)	5.80429(-3)	3.38030(-3)
0.90	7.44201(-2)	2.43863(-2)	1.05914(-2)	5.49260(-3)	3.20062(-3)
0.95	6.97520(-2)	2.30076(-2)	1.00149(-2)	5.19897(-3)	3.03119(-3)
1.00	6.54236(-2)	2.17158(-2)	9.47279(-3)	4.92234(-3)	2.87142(-3)
1.2	5.09824(-2)	1.73051(-2)	7.60687(-3)	3.96669(-3)	2.31836(-3)
1.4	4.01386(-2)	1.38817(-2)	6.14171(-3)	3.21225(-3)	1.88046(-3)
1.6	3.19005(-2)	1.12086(-2)	4.98648(-3)	2.61470(-3)	1.53278(-3)
1.8	2.55743(-2)	9.10803(-3)	4.07123(-3)	2.13948(-3)	1.25569(-3)
2.0	2.06679(-2)	7.44680(-3)	3.34235(-3)	1.75979(-3)	1.03392(-3)
2.2	1.68277(-2)	6.12467(-3)	2.75878(-3)	1.45494(-3)	8.55584(-4)
2.4	1.37962(-2)	5.06586(-3)	2.28900(-3)	1.20895(-3)	7.11490(-4)
2.6	1.13841(-2)	4.21280(-3)	1.90881(-3)	1.00945(-3)	5.94493(-4)
2.8	9.45070(-3)	3.52149(-3)	1.59949(-3)	8.46833(-4)	4.99034(-4)
3.0	7.89017(-3)	2.95812(-3)	1.34654(-3)	7.13636(-4)	4.20773(-4)
3.2	6.62242(-3)	2.49653(-3)	1.13865(-3)	6.04009(-4)	3.56311(-4)
3.4	5.58624(-3)	2.11638(-3)	9.66967(-4)	5.13360(-4)	3.02971(-4)

Table 6.4.2: Continued.

K <sup>2</sup>	2 <sup>1</sup> P	3 <sup>1</sup> P	4 <sup>1</sup> P	5 <sup>1</sup> P	6 <sup>1</sup> P
3.6	4.73447(-3)	1.80175(-3)	8.24530(-4)	4.38067(-4)	2.58639(-4)
3.8	4.03049(-3)	1.54013(-3)	7.05826(-4)	3.75253(-4)	2.21634(-4)
4.0	3.44569(-3)	1.32159(-3)	6.06474(-4)	3.22631(-4)	1.90617(-4)
4.2	2.95753(-3)	1.13826(-3)	5.22976(-4)	2.78369(-4)	1.64516(-4)
4.4	2.54818(-3)	9.83814(-4)	4.52521(-4)	2.40993(-4)	1.42466(-4)
4.6	2.20342(-3)	8.53197(-4)	3.92846(-4)	2.09313(-4)	1.23770(-4)
4.8	1.91186(-3)	7.42311(-4)	3.42116(-4)	1.82364(-4)	1.07861(-4)
5.0	1.66432(-3)	6.47833(-4)	2.98838(-4)	1.59360(-4)	9.42757(-5)
5.5	1.19259(-3)	4.66835(-4)	2.15770(-4)	1.15168(-4)	6.81656(-5)
6.0	8.69634(-4)	3.42069(-4)	1.58370(-4)	8.45960(-5)	5.00919(-5)
6.5	6.44196(-4)	2.54468(-4)	1.17985(-4)	6.30663(-5)	3.73574(-5)
7.0	4.84048(-4)	1.91927(-4)	8.91024(-5)	4.76557(-5)	2.82384(-5)
7.5	3.68463(-4)	1.46590(-4)	6.81331(-5)	3.64595(-5)	2.16106(-5)
8.0	2.83826(-4)	1.13264(-4)	5.26981(-5)	2.82131(-5)	1.67275(-5)
8.5	2.21027(-4)	8.84507(-5)	4.11920(-5)	2.20625(-5)	1.30842(-5)
9.0	1.73862(-4)	6.97560(-5)	3.25139(-5)	1.74213(-5)	1.03343(-5)
9.5	1.38040(-4)	5.55166(-5)	2.58975(-5)	1.38811(-5)	8.23621(-6)
10	1.10550(-4)	4.45601(-5)	2.08019(-5)	1.11535(-5)	6.61933(-6)
20	4.31157(-6)	1.78497(-6)	8.40598(-7)	4.52500(-7)	2.69191(-7)
30	5.71851(-7)	2.39182(-7)	1.13030(-7)	6.09418(-8)	3.62062(-8)
40	1.34197(-7)	5.63115(-8)	2.66420(-8)	1.43685(-8)	8.51027(-9)
50	4.33801(-8)	1.82061(-8)	8.61402(-9)	4.64382(-9)	2.74134(-9)
60	1.71565(-8)	7.19231(-9)	3.40130(-9)	1.83238(-9)	1.07845(-9)
70	7.78894(-9)	3.26002(-9)	1.54057(-9)	8.29321(-10)	4.86859(-10)
80	3.90933(-9)	1.63342(-9)	7.71252(-10)	4.14878(-10)	2.43048(-10)
90	2.11800(-9)	8.83472(-10)	4.16791(-10)	2.24054(-10)	1.31033(-10)
100	1.21888(-9)	5.07628(-10)	2.39278(-10)	1.28552(-10)	7.50754(-11)
200	2.87684(-11)	1.18668(-11)	5.55728(-12)	2.97690(-12)	1.72828(-12)
300	2.95579(-12)	1.21439(-12)	5.66601(-13)	3.03288(-13)	1.75837(-13)
400	5.70978(-13)	2.34105(-13)	1.08974(-13)	5.83188(-14)	3.37963(-14)
500	1.57361(-13)	6.44393(-14)	2.99490(-14)	1.60268(-14)	9.28605(-15)

Table 6.4.3: Generalized oscillator strengths, GOS(K), for the He  $1^1S \rightarrow n^1D$  transitions.

K <sup>2</sup>	3 <sup>1</sup> D	4 <sup>1</sup> D	5 <sup>1</sup> D	6 <sup>1</sup> D
0.05	4.29032(-4)	2.22900(-4)	1.22518(-4)	7.33212(-5)
0.10	7.54666(-4)	3.95503(-4)	2.18207(-4)	1.30844(-4)
0.15	9.97842(-4)	5.27174(-4)	2.91875(-4)	1.75342(-4)
0.20	1.17532(-3)	6.25607(-4)	3.47514(-4)	2.09131(-4)
0.25	1.30056(-3)	6.97123(-4)	3.88436(-4)	2.34140(-4)
0.30	1.38435(-3)	7.46903(-4)	4.17381(-4)	2.51975(-4)
0.35	1.43540(-3)	7.79201(-4)	4.36618(-4)	2.63971(-4)
0.40	1.46069(-3)	7.97502(-4)	4.48021(-4)	2.71236(-4)
0.45	1.46586(-3)	8.04661(-4)	4.53139(-4)	2.74689(-4)
0.50	1.45544(-3)	8.03017(-4)	4.53248(-4)	2.75091(-4)
0.55	1.43307(-3)	7.94483(-4)	4.49400(-4)	2.73071(-4)
0.60	1.40170(-3)	7.80620(-4)	4.42462(-4)	2.69150(-4)
0.65	1.36368(-3)	7.62702(-4)	4.33143(-4)	2.63755(-4)
0.70	1.32089(-3)	7.41766(-4)	4.22027(-4)	2.57239(-4)
0.75	1.27484(-3)	7.18654(-4)	4.09590(-4)	2.49891(-4)
0.80	1.22672(-3)	6.94045(-4)	3.96218(-4)	2.41947(-4)
0.85	1.17748(-3)	6.68488(-4)	3.82228(-4)	2.33601(-4)
0.90	1.12787(-3)	6.42423(-4)	3.67873(-4)	2.25008(-4)
0.95	1.07847(-3)	6.16199(-4)	3.53357(-4)	2.16295(-4)
1.00	1.02973(-3)	5.90093(-4)	3.38845(-4)	2.07562(-4)
1.2	8.46980(-4)	4.90481(-4)	2.83003(-4)	1.73804(-4)
1.4	6.89945(-4)	4.03033(-4)	2.33478(-4)	1.43696(-4)
1.6	5.59863(-4)	3.29434(-4)	1.91484(-4)	1.18063(-4)
1.8	4.54090(-4)	2.68844(-4)	1.56711(-4)	9.67690(-5)
2.0	3.68871(-4)	2.19537(-4)	1.28280(-4)	7.93142(-5)
2.2	3.00478(-4)	1.79637(-4)	1.05184(-4)	6.51051(-5)
2.4	2.45630(-4)	1.47416(-4)	8.64730(-5)	5.35731(-5)
2.6	2.01589(-4)	1.21392(-4)	7.13186(-5)	4.4193(-5)
2.8	1.66139(-4)	1.00339(-4)	5.90300(-5)	3.66248(-5)
3.0	1.37512(-4)	8.32647(-5)	4.90432(-5)	3.04461(-5)
3.2	1.14310(-4)	6.93732(-5)	4.09039(-5)	2.54056(-5)
3.4	9.54305(-5)	5.80318(-5)	3.42484(-5)	2.12808(-5)
3.6	8.00043(-5)	4.87381(-5)	2.87871(-5)	1.78937(-5)

Table 6.4.3: Continued.

$K^2$	$3^1D$	$4^1D$	$5^1D$	$6^1D$
3.8	6.73474(-5)	4.10931(-5)	2.42892(-5)	1.51024(-5)
4.0	5.69194(-5)	3.47799(-5)	2.05709(-5)	1.27936(-5)
4.2	4.82922(-5)	2.95462(-5)	1.74855(-5)	1.08770(-5)
4.4	4.11260(-5)	2.51909(-5)	1.49157(-5)	9.27996(-6)
4.6	3.51498(-5)	2.15527(-5)	1.27674(-5)	7.94446(-6)
4.8	3.01467(-5)	1.85025(-5)	1.09650(-5)	6.82364(-6)
5.0	2.59425(-5)	1.59358(-5)	9.44745(-6)	5.87971(-6)
5.5	1.80703(-5)	1.11204(-5)	6.59776(-6)	4.10656(-6)
6.0	1.28205(-5)	7.90126(-6)	4.69057(-6)	2.91942(-6)
6.5	9.24954(-6)	5.70720(-6)	3.38960(-6)	2.10944(-6)
7.0	6.77599(-6)	4.18499(-6)	2.48637(-6)	1.54705(-6)
7.5	5.03382(-6)	3.11144(-6)	1.84903(-6)	1.15021(-6)
8.0	3.78784(-6)	2.34282(-6)	1.39252(-6)	8.65976(-7)
8.5	2.88407(-6)	1.78479(-6)	1.06098(-6)	6.59581(-7)
9.0	2.21994(-6)	1.37441(-6)	8.17102(-7)	5.07785(-7)
9.5	1.72601(-6)	1.06901(-6)	6.35568(-7)	3.94818(-7)
10	1.35454(-6)	8.39194(-7)	4.98947(-7)	3.09822(-7)
20	3.80236(-8)	2.35601(-8)	1.39909(-8)	8.60366(-9)
30	3.84252(-9)	2.37217(-9)	1.40735(-9)	8.57215(-10)
40	7.08574(-10)	4.35507(-10)	2.58230(-10)	1.56011(-10)
50	1.85301(-10)	1.13398(-10)	6.72061(-11)	4.03324(-11)
60	6.08715(-11)	3.71037(-11)	2.19790(-11)	1.31189(-11)
70	2.34778(-11)	1.42602(-11)	8.44299(-12)	5.01718(-12)
80	1.02010(-11)	6.17670(-12)	3.65512(-12)	2.16412(-12)
90	4.85942(-12)	2.93434(-12)	1.73553(-12)	1.02446(-12)
100	2.49088(-12)	1.50048(-12)	8.87029(-13)	5.22260(-13)
200	2.75371(-14)	1.63604(-14)	9.63709(-15)	5.60167(-15)
300	1.83398(-15)	1.08322(-15)	6.36888(-16)	3.68471(-16)
400	2.61746(-16)	1.54101(-16)	9.05076(-17)	5.22387(-17)
500	5.71760(-17)	3.35940(-17)	1.97170(-17)	1.13639(-17)

Table 6.4.4: Generalized oscillator strengths, GOS(K), for the He  $2^3S \rightarrow n^3S$  transitions.

$K^2$	$3^3S$	$4^3S$	$5^3S$	$6^3S$
0.05	1.16824(-2)	1.00914(-2)	3.83583(-3)	1.89327(-3)
0.10	1.34219(-2)	1.47891(-2)	6.09475(-3)	3.12129(-3)
0.15	1.17529(-2)	1.54279(-2)	6.78993(-3)	3.58924(-3)
0.20	9.27472(-3)	1.38887(-2)	6.44595(-3)	3.49888(-3)
0.25	6.94165(-3)	1.15179(-2)	5.58199(-3)	3.09752(-3)
0.30	5.03555(-3)	9.07171(-3)	4.55621(-3)	2.57547(-3)
0.35	3.57841(-3)	6.89845(-3)	3.56988(-3)	2.04975(-3)
0.40	2.50509(-3)	5.11358(-3)	2.71455(-3)	1.57968(-3)
0.45	1.73258(-3)	3.71629(-3)	2.01696(-3)	1.18753(-3)
0.50	1.18531(-3)	2.65697(-3)	1.47062(-3)	8.74889(-4)
0.55	8.02181(-4)	1.87221(-3)	1.05489(-3)	6.33492(-4)
0.60	5.36603(-4)	1.30108(-3)	7.45370(-4)	4.51535(-4)
0.65	3.54193(-4)	8.91473(-4)	5.18926(-4)	3.16983(-4)
0.70	2.30082(-4)	6.01527(-4)	3.55757(-4)	2.19086(-4)
0.75	1.46526(-4)	3.98846(-4)	2.39754(-4)	1.48891(-4)
0.80	9.09795(-5)	2.59005(-4)	1.58443(-4)	9.92681(-5)
0.85	5.46361(-5)	1.63914(-4)	1.02264(-4)	6.46985(-5)
0.90	3.13486(-5)	1.00357(-4)	6.40826(-5)	4.10033(-5)
0.95	1.68497(-5)	5.87847(-5)	3.86417(-5)	2.50689(-5)
1.0	8.19285(-6)	3.23576(-5)	2.21117(-5)	1.46052(-5)
1.2	8.64273(-8)	2.70861(-7)	4.91813(-7)	4.48922(-7)
1.4	2.79174(-6)	3.51163(-6)	1.43198(-6)	7.10461(-7)
1.6	4.62317(-6)	7.95280(-6)	3.91685(-6)	2.18814(-6)
1.8	4.77111(-6)	9.14228(-6)	4.75891(-6)	2.74380(-6)
2.0	4.03170(-6)	8.18352(-6)	4.37995(-6)	2.56433(-6)
2.2	3.03897(-6)	6.41006(-6)	3.49249(-6)	2.06451(-6)
2.4	2.11272(-6)	4.59326(-6)	2.53683(-6)	1.51039(-6)
2.6	1.36984(-6)	3.06207(-6)	1.71167(-6)	1.02546(-6)
2.8	8.25957(-7)	1.90183(-6)	1.07639(-6)	6.48923(-7)
3.0	4.55212(-7)	1.08744(-6)	6.24690(-7)	3.79375(-7)
3.2	2.20171(-7)	5.54976(-7)	3.25525(-7)	1.99683(-7)
3.4	8.48200(-8)	2.35401(-7)	1.43033(-7)	8.91981(-8)

Table 6.4.4: Continued.

$K^2$	$3^2S$	$4^3S$	$5^3S$	$6^3S$
3.5	1.91728(-8)	6.81089(-8)	4.48504(-8)	2.89921(-8)
3.8	6.77362(-11)	4.75806(-9)	4.75768(-9)	3.59757(-9)
4.0	1.04408(-8)	8.91837(-9)	2.78592(-9)	1.16585(-9)
4.2	3.81534(-8)	5.41982(-8)	2.43488(-8)	1.30039(-8)
4.4	7.48292(-8)	1.22082(-7)	5.91390(-8)	3.29457(-8)
4.6	1.14864(-7)	1.99972(-7)	1.00093(-7)	5.67502(-8)
4.8	1.54643(-7)	2.79583(-7)	1.42529(-7)	8.15948(-8)
5.0	1.91952(-7)	3.55702(-7)	1.83469(-7)	1.05676(-7)
5.5	2.67738(-7)	5.14046(-7)	2.69551(-7)	1.56586(-7)
6.0	3.16103(-7)	6.18388(-7)	3.27056(-7)	1.90825(-7)
6.5	3.40808(-7)	6.74376(-7)	3.58517(-7)	2.09732(-7)
7.0	3.47821(-7)	6.93481(-7)	3.69932(-7)	2.16782(-7)
7.5	3.42662(-7)	6.86822(-7)	3.67254(-7)	2.15468(-7)
8.0	3.29685(-7)	6.63367(-7)	3.55326(-7)	2.08650(-7)
8.5	3.12078(-7)	6.29762(-7)	3.37764(-7)	1.98465(-7)
9.0	2.92068(-7)	5.90696(-7)	3.17128(-7)	1.86430(-7)
9.5	2.71157(-7)	5.49360(-7)	2.95166(-7)	1.73585(-7)
10	2.50323(-7)	5.07854(-7)	2.73035(-7)	1.60618(-7)
20	4.49070(-8)	9.17001(-8)	4.94538(-8)	2.91290(-8)
30	1.13195(-8)	2.31166(-8)	1.24702(-8)	7.34444(-9)
40	3.79716(-9)	7.75247(-9)	4.18201(-9)	2.46275(-9)
50	1.54358(-9)	3.15066(-9)	1.69945(-9)	1.00071(-9)
60	7.18630(-10)	1.46651(-9)	7.90940(-10)	4.65718(-10)
70	3.69921(-10)	7.54774(-10)	4.07026(-10)	2.39658(-10)
80	2.05721(-10)	4.19690(-10)	2.26298(-10)	1.33244(-10)
90	1.21633(-10)	2.48117(-10)	1.33770(-10)	7.87635(-11)
100	7.55832(-11)	1.54167(-10)	8.31087(-11)	4.89346(-11)
200	2.98069(-12)	6.07752(-12)	3.27378(-12)	1.92793(-12)
300	4.24594(-13)	8.65656(-13)	4.66116(-13)	2.74534(-13)
400	1.04812(-13)	2.13682(-13)	1.15030(-13)	6.77570(-14)
500	3.51690(-14)	7.16992(-14)	3.85912(-14)	2.27331(-14)

Table 6.4.5: Generalized oscillator strengths, GOS(K), for the He  $2^3S \rightarrow n^3P$  transitions.

K <sup>2</sup>	$2^3P$	$3^3P$	$4^3P$	$5^3P$	$6^3P$
0.05	3.89386(-1)	5.99522(-3)	7.20860(-3)	4.53983(-3)	2.83586(-3)
0.10	2.84121(-1)	8.58286(-4)	6.00671(-4)	8.02400(-4)	6.41380(-4)
0.15	2.09243(-1)	8.48305(-3)	3.76626(-4)	5.67799(-6)	6.24753(-6)
0.20	1.55410(-1)	1.61523(-2)	2.43129(-3)	6.15525(-4)	2.17654(-4)
0.25	1.16326(-1)	2.08635(-2)	4.67453(-3)	1.61450(-3)	7.2834(-4)
0.30	8.76928(-2)	2.26998(-2)	6.31409(-3)	2.49846(-3)	1.23243(-3)
0.35	6.65388(-2)	2.24876(-2)	7.20454(-3)	3.09093(-3)	1.60228(-3)
0.40	5.07889(-2)	2.10393(-2)	7.45963(-3)	3.38205(-3)	1.81160(-3)
0.45	3.89782(-2)	1.89634(-2)	7.26109(-3)	3.42878(-3)	1.88069(-3)
0.50	3.00623(-2)	1.66626(-2)	6.77861(-3)	3.30328(-3)	1.84499(-3)
0.55	2.32900(-2)	1.43809(-2)	6.14442(-3)	3.07050(-3)	1.73980(-3)
0.60	1.81166(-2)	1.22523(-2)	5.45154(-3)	2.78093(-3)	1.59427(-3)
0.65	1.41437(-2)	1.03403(-2)	4.76035(-3)	2.47043(-3)	1.43012(-3)
0.70	1.10778(-2)	8.66531(-3)	4.10696(-3)	2.16260(-3)	1.26225(-3)
0.75	8.70112(-3)	7.22309(-3)	3.51053(-3)	1.87180(-3)	1.10024(-3)
0.80	6.85116(-3)	5.99645(-3)	2.97910(-3)	1.60580(-3)	9.49663(-4)
0.85	5.40572(-3)	4.96240(-3)	2.51370(-3)	1.36793(-3)	8.13326(-4)
0.90	4.27246(-3)	4.09637(-3)	2.11130(-3)	1.15871(-3)	6.92204(-4)
0.95	3.38120(-3)	3.37457(-3)	1.76669(-3)	9.76962(-4)	5.86106(-4)
1.00	2.67829(-3)	2.77516(-3)	1.47373(-3)	8.20565(-4)	4.94163(-4)
1.2	1.05507(-3)	1.25096(-3)	6.96762(-4)	3.96765(-4)	2.41932(-4)
1.4	4.06059(-4)	5.49766(-4)	3.18914(-4)	1.84954(-4)	1.13911(-4)
1.6	1.45787(-4)	2.32077(-4)	1.40392(-4)	8.28837(-5)	5.15390(-5)
1.8	4.47262(-5)	9.11116(-5)	5.81050(-5)	3.50337(-5)	2.20288(-5)
2.0	9.28869(-6)	3.11280(-5)	2.15485(-5)	1.33949(-5)	8.55682(-6)
2.2	3.21248(-7)	7.83363(-6)	6.41156(-6)	4.21702(-6)	2.77125(-6)
2.4	1.27767(-6)	7.10041(-7)	1.07001(-6)	8.25793(-7)	5.84396(-7)
2.6	5.23949(-6)	2.85975(-7)	8.70239(-10)	8.53165(-9)	1.46799(-8)
2.8	9.44231(-6)	2.25511(-6)	6.14045(-7)	2.38755(-7)	1.14016(-7)
3.0	1.29095(-5)	4.73064(-6)	1.72863(-6)	8.09556(-7)	4.39776(-7)
3.2	1.54137(-5)	6.95206(-6)	2.83717(-6)	1.41015(-6)	7.95086(-7)
3.4	1.70201(-5)	8.67233(-6)	3.74913(-6)	1.91854(-6)	1.10098(-6)

Table 6.4.5: Continued.

$K^2$	$2^3P$	$3^3P$	$4^3D$	$5^3P$	$6^3P$
3.6	1.78878(-5)	9.86771(-6)	4.41817(-6)	2.30007(-6)	1.33351(-6)
3.8	1.81873(-5)	1.06017(-5)	4.85899(-6)	2.55811(-6)	1.49299(-6)
4.0	1.80696(-5)	1.09628(-5)	5.10811(-6)	2.71042(-6)	1.58920(-6)
4.2	1.76579(-5)	1.10383(-5)	5.20606(-6)	2.77825(-6)	1.63446(-6)
4.4	1.70476(-5)	1.09036(-5)	5.18999(-6)	2.78165(-6)	1.64061(-6)
4.6	1.63112(-5)	1.06200(-5)	5.09109(-6)	2.73777(-6)	1.61790(-6)
4.8	1.55018(-5)	1.02356(-5)	4.93438(-6)	2.66049(-6)	1.57466(-6)
5.0	1.46581(-5)	9.78711(-6)	4.73928(-6)	2.56067(-6)	1.51744(-6)
5.5	1.25587(-5)	8.54727(-6)	4.17114(-6)	2.26203(-6)	1.34333(-6)
6.0	1.06335(-5)	7.31758(-6)	3.58777(-6)	1.95007(-6)	1.15956(-6)
6.5	8.95889(-6)	6.20395(-6)	3.05043(-6)	1.66036(-6)	9.88064(-7)
7.0	7.53963(-6)	5.23818(-6)	2.57996(-6)	1.40552(-6)	8.36806(-7)
7.5	6.35206(-6)	4.41901(-6)	2.17860(-6)	1.18750(-6)	7.07191(-7)
8.0	5.36410(-6)	3.73199(-6)	1.84077(-6)	1.00365(-6)	5.97790(-7)
8.5	4.54366(-6)	3.15881(-6)	1.55829(-6)	8.49740(-7)	5.06150(-7)
9.0	3.86195(-6)	2.68142(-6)	1.32269(-6)	7.21273(-7)	4.29632(-7)
9.5	3.29440(-6)	2.28362(-6)	1.12621(-6)	6.14087(-7)	3.65778(-7)
10	2.82058(-6)	1.95157(-6)	9.62144(-7)	5.24554(-7)	3.12436(-7)
20	2.35355(-7)	1.57681(-7)	7.71484(-8)	4.18595(-8)	2.49219(-8)
30	4.07404(-8)	2.69216(-8)	1.31284(-8)	7.09870(-9)	4.22832(-9)
40	1.04375(-8)	6.85339(-9)	3.33730(-9)	1.80040(-9)	1.07303(-9)
50	3.42525(-9)	2.24149(-9)	1.09075(-9)	5.87494(-10)	3.50325(-10)
60	1.33425(-9)	8.71452(-10)	4.23911(-10)	2.28057(-10)	1.36048(-10)
70	5.89482(-10)	3.84564(-10)	1.87034(-10)	1.00531(-10)	5.99916(-11)
80	2.86803(-10)	1.86967(-10)	9.09244(-11)	4.88379(-11)	2.91512(-11)
90	1.50590(-10)	9.81247(-11)	4.77180(-11)	2.56162(-11)	1.52931(-11)
100	8.41038(-11)	5.47867(-11)	2.66430(-11)	1.42960(-11)	8.53614(-12)
200	1.63349(-12)	1.06406(-12)	5.17745(-13)	2.77201(-13)	1.65592(-13)
300	1.53682(-13)	1.00174(-13)	4.87654(-14)	2.60888(-14)	1.55849(-14)
400	2.82901(-14)	1.84496(-14)	8.98423(-15)	4.80453(-15)	2.87000(-15)
500	7.56519(-15)	4.93554(-15)	2.40394(-15)	1.28526(-15)	7.67720(-16)

Table 6.4.6: Generalized oscillator strengths, GOS(K), for the He  $2^3S \rightarrow n^3D$  transitions.

$K^2$	$3^3D$	$4^3D$	$5^3D$	$6^3D$
0.05	1.01351(-1)	2.37380(-2)	9.04261(-3)	4.43918(-3)
0.10	1.18837(-1)	3.59929(-2)	1.51770(-2)	7.84120(-3)
0.15	1.07161(-1)	3.89445(-2)	1.77472(-2)	9.54642(-3)
0.20	8.78581(-2)	3.65484(-2)	1.76903(-2)	9.82517(-3)
0.25	6.89248(-2)	3.17981(-2)	1.61412(-2)	9.19767(-3)
0.30	5.28811(-2)	2.64614(-2)	1.39546(-2)	8.11863(-3)
0.35	4.01177(-2)	2.14247(-2)	1.16544(-2)	6.89674(-3)
0.40	3.02785(-2)	1.70502(-2)	9.51449(-3)	5.71027(-3)
0.45	2.28167(-2)	1.34230(-2)	7.65116(-3)	4.64630(-3)
0.50	1.72045(-2)	1.04982(-2)	6.09172(-3)	3.73616(-3)
0.55	1.29983(-2)	8.18023(-3)	4.81901(-3)	2.98058(-3)
0.60	9.84797(-3)	6.36286(-3)	3.79716(-3)	2.36556(-3)
0.65	7.48586(-3)	4.94730(-3)	2.98545(-3)	1.87147(-3)
0.70	5.71074(-3)	3.84881(-3)	2.34509(-3)	1.47801(-3)
0.75	4.37275(-3)	2.99787(-3)	1.84208(-3)	1.16646(-3)
0.80	3.36080(-3)	2.33896(-3)	1.44789(-3)	9.20650(-4)
0.85	2.59261(-3)	1.82847(-3)	1.13931(-3)	7.27095(-4)
0.90	2.00725(-3)	1.43247(-3)	8.97779(-4)	5.74821(-4)
0.95	1.55949(-3)	1.12478(-3)	7.08615(-4)	4.55028(-4)
1.00	1.21567(-3)	8.85207(-4)	5.60303(-4)	3.60735(-4)
1.2	4.62574(-4)	3.47266(-4)	2.23101(-4)	1.44842(-4)
1.4	1.82988(-4)	1.40550(-4)	9.12929(-5)	5.96398(-5)
1.6	7.42653(-5)	5.81524(-5)	3.81159(-5)	2.50314(-5)
1.8	3.04681(-5)	2.43040(-5)	1.60659(-5)	1.06041(-5)
2.0	1.24114(-5)	1.01049(-5)	6.74102(-6)	4.47385(-6)
2.2	4.89884(-6)	4.09277(-6)	2.76118(-6)	1.84499(-6)
2.4	1.80234(-6)	1.56319(-6)	1.07146(-6)	7.22724(-7)
2.6	5.73992(-7)	5.30680(-7)	3.73343(-7)	2.55664(-7)
2.8	1.31255(-7)	1.39771(-7)	1.03746(-7)	7.31962(-8)
3.0	8.93164(-9)	1.74757(-8)	1.55441(-8)	1.20163(-8)
3.2	7.46026(-9)	1.03821(-9)	1.01249(-10)	2.04208(-13)
3.4	4.30266(-8)	2.05265(-8)	1.02874(-8)	5.66845(-9)

Table 6.4.6: Continued.

$K^2$	$3^3D$	$4^3D$	$5^3D$	$6^3D$
3.6	8.23483(-8)	4.71531(-8)	2.64163(-8)	1.57541(-8)
3.8	1.13913(-7)	7.02100(-8)	4.09626(-8)	2.51037(-8)
4.0	1.35234(-7)	8.57081(-8)	5.16548(-8)	3.20956(-8)
4.2	1.47245(-7)	9.67397(-8)	5.83622(-8)	3.65653(-8)
4.4	1.51892(-7)	1.01441(-7)	6.17128(-8)	3.88781(-8)
4.6	1.51166(-7)	1.02137(-7)	6.25037(-8)	3.95299(-8)
4.8	1.46759(-7)	1.00013(-7)	6.14700(-8)	3.89875(-8)
5.0	1.39992(-7)	9.60227(-8)	5.92122(-8)	3.76368(-8)
5.5	1.18516(-7)	8.21572(-8)	5.09367(-8)	3.24894(-8)
6.0	9.65726(-8)	6.73434(-8)	4.18813(-8)	2.67625(-8)
6.5	7.73585(-8)	5.41269(-8)	3.37231(-8)	2.15681(-8)
7.0	6.15785(-8)	4.31657(-8)	2.69219(-8)	1.72226(-8)
7.5	4.89942(-8)	3.43750(-8)	2.14510(-8)	1.37204(-8)
8.0	3.90886(-8)	2.74325(-8)	1.71223(-8)	1.09464(-8)
8.5	3.13267(-8)	2.19818(-8)	1.37198(-8)	8.76508(-9)
9.0	2.52429(-8)	1.77051(-8)	1.10484(-8)	7.05234(-9)
9.5	2.04605(-8)	1.43417(-8)	8.94669(-9)	5.70522(-9)
10	1.66842(-8)	1.16859(-8)	7.28694(-9)	4.64185(-9)
20	7.46421(-10)	5.14535(-10)	3.17723(-10)	1.97764(-10)
30	9.28516(-11)	6.35121(-11)	3.90685(-11)	2.39268(-11)
40	1.88027(-11)	1.28156(-11)	7.88121(-12)	4.77519(-12)
50	5.11181(-12)	3.47805(-12)	2.14139(-12)	1.28787(-12)
60	1.69891(-12)	1.15495(-12)	7.12278(-13)	4.26097(-13)
70	6.53913(-13)	4.44376(-13)	2.74550(-13)	1.63591(-13)
80	2.81601(-13)	1.91345(-13)	1.18430(-13)	7.03532(-14)
90	1.32524(-13)	9.00527(-14)	5.58304(-14)	3.30878(-14)
100	6.70187(-14)	4.55470(-14)	2.82821(-14)	1.67299(-14)
200	6.62291(-16)	4.51132(-16)	2.82988(-16)	1.66101(-16)
300	4.15490(-17)	2.83499(-17)	1.78707(-17)	1.04684(-17)
400	5.72810(-18)	3.91277(-18)	2.47345(-18)	1.44776(-18)
500	1.22367(-18)	8.36510(-19)	5.29766(-19)	3.09965(-19)

Table 6.4.7: Generalized oscillator strengths, GOS(K), for the He  $2^1S \rightarrow n^1S$  transitions.

$K^2$	$3^1S$	$4^1S$	$5^1S$	$6^1S$
0.05	5.79249(-2)	1.36579(-2)	5.32225(-3)	2.65795(-3)
0.10	5.59071(-2)	1.77410(-2)	7.68852(-3)	4.03718(-3)
0.15	4.12177(-2)	1.60495(-2)	7.55715(-3)	4.12644(-3)
0.20	2.73820(-2)	1.23932(-2)	6.22811(-3)	3.52582(-3)
0.25	1.72076(-2)	8.75159(-3)	4.63382(-3)	2.69660(-3)
0.30	1.04244(-2)	5.82951(-3)	3.22270(-3)	1.91906(-3)
0.35	6.13275(-3)	3.71942(-3)	2.13346(-3)	1.29578(-3)
0.40	3.50848(-3)	2.28957(-3)	1.35720(-3)	8.38901(-4)
0.45	1.94632(-3)	1.36269(-3)	8.33006(-4)	5.23349(-4)
0.50	1.03973(-3)	7.82698(-4)	4.93285(-4)	3.14892(-4)
0.55	5.28251(-4)	4.31271(-4)	2.80756(-4)	1.82220(-4)
0.60	2.49800(-4)	2.25367(-4)	1.52289(-4)	1.00696(-4)
0.65	1.05630(-4)	1.09428(-4)	7.75213(-5)	5.24390(-5)
0.70	3.66581(-5)	4.75136(-5)	3.60068(-5)	2.51246(-5)
0.75	8.17453(-6)	1.69965(-5)	1.44294(-5)	1.05725(-5)
0.80	2.22231(-7)	3.97923(-6)	4.35874(-6)	3.51620(-6)
0.85	1.64504(-6)	1.45900(-7)	6.00428(-7)	6.59718(-7)
0.90	6.45468(-6)	6.71905(-7)	4.72148(-8)	1.06991(-11)
0.95	1.16382(-5)	2.87110(-6)	9.06702(-7)	3.61225(-7)
1.0	1.58504(-5)	5.33737(-6)	2.19558(-6)	1.08406(-6)
1.2	1.94726(-5)	9.80600(-6)	5.19105(-6)	3.01943(-6)
1.4	1.22484(-5)	7.18492(-6)	4.10409(-6)	2.49211(-6)
1.6	5.17341(-6)	3.46223(-6)	2.09439(-6)	1.31085(-6)
1.8	1.24562(-6)	1.05123(-6)	6.92902(-7)	4.52332(-7)
2.0	2.04029(-8)	8.87520(-8)	8.24893(-8)	6.21499(-8)
2.2	3.95120(-7)	8.50563(-8)	2.54522(-8)	9.92483(-9)
2.4	1.48409(-6)	5.62384(-7)	2.59641(-7)	1.40004(-7)
2.6	2.74319(-6)	1.20010(-6)	6.01006(-7)	3.40289(-7)
2.8	3.89100(-6)	1.81968(-6)	9.43653(-7)	5.45146(-7)
3.0	4.81034(-6)	2.33832(-6)	1.23644(-6)	7.22229(-7)
3.2	5.47476(-6)	2.72917(-6)	1.46112(-6)	8.59452(-7)
3.4	5.90239(-6)	2.99466(-6)	1.61701(-6)	9.55731(-7)

Table 6.4.7: Continued.

$K'$	$3^1S$	$4^1S$	$5^1S$	$6^1S$
3.6	6.12956(-6)	3.15040(-6)	1.71172(-6)	1.01523(-6)
3.8	6.19672(-6)	3.21637(-6)	1.75580(-6)	1.04411(-6)
4.0	6.14183(-6)	3.21240(-6)	1.76008(-6)	1.04877(-6)
4.2	5.99756(-6)	3.15611(-6)	1.73432(-6)	1.03506(-6)
4.4	5.79069(-6)	3.06230(-6)	1.68677(-6)	1.00797(-6)
4.6	5.54240(-6)	2.94284(-6)	1.62417(-6)	9.71553(-7)
4.8	5.26902(-6)	2.80705(-6)	1.55177(-6)	9.29029(-7)
5.0	4.98286(-6)	2.66203(-6)	1.47364(-6)	8.82868(-7)
5.5	4.26504(-6)	2.29054(-6)	1.27132(-6)	7.62645(-7)
6.0	3.60082(-6)	1.94074(-6)	1.07910(-6)	6.47899(-7)
6.5	3.02017(-6)	1.63187(-6)	9.08480(-7)	5.45798(-7)
7.0	2.52741(-6)	1.36809(-6)	7.62275(-7)	4.58173(-7)
7.5	2.11581(-6)	1.14680(-6)	6.39346(-7)	3.84423(-7)
8.0	1.77475(-6)	9.62882(-7)	5.37021(-7)	3.22988(-7)
8.5	1.49314(-6)	8.10676(-7)	4.52250(-7)	2.72063(-7)
9.0	1.26074(-6)	6.84861(-7)	3.82128(-7)	2.29919(-7)
9.5	1.06873(-6)	5.80781(-7)	3.24090(-7)	1.95025(-7)
10	9.09716(-7)	4.94503(-7)	2.75965(-7)	1.66081(-7)
20	7.73588(-8)	4.19956(-8)	2.34217(-8)	1.40925(-8)
30	1.60243(-8)	8.68098(-9)	4.83502(-9)	2.90820(-9)
40	5.11282(-9)	2.76573(-9)	1.53940(-9)	9.25604(-10)
50	2.07963(-9)	1.12378(-9)	6.25332(-10)	3.75855(-10)
60	9.86511(-10)	5.32689(-10)	2.96372(-10)	1.78075(-10)
70	5.20407(-10)	2.80856(-10)	1.56234(-10)	9.38470(-11)
80	2.96817(-10)	1.60124(-10)	8.90556(-11)	5.34827(-11)
90	1.79772(-10)	9.69529(-11)	5.39093(-11)	3.23700(-11)
100	1.14217(-10)	6.15839(-11)	3.42343(-11)	2.05534(-11)
200	5.14398(-12)	2.77050(-12)	1.53663(-12)	9.22192(-13)
300	7.74408(-13)	4.16897(-13)	2.30914(-13)	1.38590(-13)
400	1.96823(-13)	1.05929(-13)	5.86241(-14)	3.51893(-14)
500	6.72328(-14)	3.61778(-14)	2.00107(-14)	1.20129(-14)

Table 6.4.8 Generalized oscillator strengths, GOS(K), for the He  $2^1S \rightarrow n^1P$  transitions

K <sup>2</sup>	2 <sup>1</sup> P	3 <sup>1</sup> P	4 <sup>1</sup> P	5 <sup>1</sup> P	6 <sup>1</sup> P
0.05	2.47431(-1)	1 72241(-2)	1 48200(-2)	8.73627(-3)	5.31440(-3)
0.10	1.64680(-1)	1 07545(-4)	1.72059(-3)	1.76548(-3)	1.32093(-3)
0.15	1.10819(-1)	7 24441(-3)	1.89608(-4)	7 85994(-6)	4 93194(-5)
0.20	7.52992(-2)	1 46821(-2)	2 32760(-3)	5.73737(-4)	1.92931(-4)
0.25	5.15964(-2)	1 82026(-2)	4.57211(-3)	1.64334(-3)	7.53782(-4)
0.30	3.56114(-2)	1.84953(-2)	5.88578(-3)	2.46152(-3)	1 24890(-3)
0.35	2.47290(-2)	1 69337(-2)	6.26487(-3)	2.85930(-3)	1 52141(-3)
0.40	1.72582(-2)	1.45718(-2)	5.99676(-3)	2 90254(-3)	1 61021(-3)
0.45	1.20915(-2)	1 20475(-2)	5 37172(-3)	2 71407(-3)	1 54412(-3)
0.50	8.49522(-3)	9 69167(-3)	4 60230(-3)	2 40354(-3)	1 3939(-3)
0.55	5.97842(-3)	7.64474(-3)	3.82090(-3)	2.04898(-3)	1.20658(-3)
0.60	4.20906(-3)	5 94155(-3)	3 09929(-3)	1 69867(-3)	1 01284(-3)
0.65	2.96074(-3)	4 56408(-3)	2 46945(-3)	1 37865(-3)	8.30686(-4)
0.70	2.07776(-3)	3 47184(-3)	1 93965(-3)	1.10028(-3)	6.68955(-4)
0.75	1.45227(-3)	2 61819(-3)	1 50537(-3)	8.66056(-4)	5.30736(-4)
0.80	1.00903(-3)	1 95835(-3)	1 15609(-3)	6 73648(-4)	4.15770(-4)
0.85	6.95266(-4)	1.45286(-3)	8 79259(-4)	5 18419(-4)	3.22060(-4)
0.90	4.73718(-4)	1 06858(-3)	6 62413(-4)	3.94958(-4)	2 46872(-4)
0.95	3.17978(-4)	7 78481(-4)	4 94239(-4)	2 97909(-4)	1 87315(-4)
1.00	2.09242(-4)	5 60993(-4)	3 64966(-4)	2 22392(-4)	1 40653(-4)
1.2	2.64376(-5)	1 28890(-4)	9 47601(-5)	6 07411(-5)	3 94421(-5)
1.4	1.77554(-9)	1 64755(-5)	1 61504(-5)	1 14485(-5)	7 80555(-6)
1.6	7.48829(-6)	4.53793(-8)	3 45560(-7)	4.97660(-7)	4.39529(-7)
1.8	1.76759(-5)	7.13507(-6)	2 05911(-6)	7.93492(-7)	3 77610(-7)
2.0	2.41862(-5)	1.62732(-5)	6 71420(-6)	3.29393(-6)	1 84678(-6)
2.2	2.69741(-5)	2.23920(-5)	1 03240(-5)	5.38977(-6)	3.13640(-6)
2.4	2.71996(-5)	2.52600(-5)	1 22883(-5)	6.59996(-6)	3.90401(-6)
2.6	2.59276(-5)	2 57611(-5)	1 29271(-5)	7 05518(-6)	4 21133(-6)
2.8	2.39009(-5)	2 47979(-5)	1 26918(-5)	6 99696(-6)	4 20030(-6)
3.0	2.15823(-5)	2 30425(-5)	1 19509(-5)	6.63315(-6)	3 99705(-6)
3.2	1.92393(-5)	2 09371(-5)	1 09593(-5)	6 11150(-6)	3 69256(-6)
3.4	1.70154(-5)	1 87511(-5)	9.87909(-6)	5 52758(-6)	3.34623(-6)

Table 6.4.8: Continued.

$K^2$	$2^1P$	$3^1P$	$4^1P$	$5^1P$	$6^1P$
3.6	1.49784(-5)	1.66376(-5)	8.80605(-6)	4.93905(-6)	2.99426(-6)
3.8	1.31528(-5)	1.46757(-5)	7.79282(-6)	4.37832(-6)	2.65720(-6)
4.0	1.15385(-5)	1.28996(-5)	6.86489(-6)	3.86170(-6)	2.34559(-6)
4.2	1.01231(-5)	1.13171(-5)	6.03143(-6)	3.39572(-6)	2.06383(-6)
4.4	8.88855(-6)	9.92177(-6)	5.29222(-6)	2.98118(-6)	1.81273(-6)
4.6	7.81484(-6)	8.69956(-6)	4.64201(-6)	2.61576(-6)	1.59107(-6)
4.8	6.88231(-6)	7.63347(-6)	4.07313(-6)	2.29553(-6)	1.39661(-6)
5.0	6.07263(-6)	6.70581(-6)	3.57704(-6)	2.01594(-6)	1.22669(-6)
5.5	4.48221(-6)	4.88389(-6)	2.60068(-6)	1.46503(-6)	8.91519(-7)
6.0	3.35444(-6)	3.59889(-6)	1.91133(-6)	1.07575(-6)	6.54468(-7)
6.5	2.54528(-6)	2.68574(-6)	1.42178(-6)	7.99299(-7)	4.86059(-7)
7.0	1.95695(-6)	2.02985(-6)	1.07074(-6)	6.01173(-7)	3.65356(-7)
7.5	1.52336(-6)	1.55307(-6)	8.16167(-7)	4.57603(-7)	2.77909(-7)
8.0	1.19955(-6)	1.20219(-6)	6.29343(-7)	3.52345(-7)	2.13823(-7)
8.5	9.54668(-7)	9.40824(-7)	4.90608(-7)	2.74267(-7)	1.66313(-7)
9.0	7.67264(-7)	7.43854(-7)	3.86395(-7)	2.15688(-7)	1.30689(-7)
9.5	6.22249(-7)	5.93759(-7)	3.07249(-7)	1.71254(-7)	1.03687(-7)
10	5.08870(-7)	4.78180(-7)	2.46512(-7)	1.37199(-7)	8.30061(-8)
20	2.72989(-8)	2.09968(-8)	1.02554(-8)	5.58572(-9)	3.34822(-9)
30	4.18021(-9)	2.97087(-9)	1.41679(-9)	7.64829(-10)	4.55948(-10)
40	1.03299(-9)	7.12155(-10)	3.36258(-10)	1.80938(-10)	1.07357(-10)
50	3.37529(-10)	2.30372(-10)	1.08369(-10)	5.82560(-11)	3.44299(-11)
60	1.32588(-10)	9.03864(-11)	4.24795(-11)	2.28348(-11)	1.34530(-11)
70	5.93652(-11)	4.05773(-11)	1.90771(-11)	1.02584(-11)	6.02857(-12)
80	2.93161(-11)	2.01230(-11)	9.46923(-12)	5.09448(-12)	2.98795(-12)
90	1.56234(-11)	1.07750(-11)	5.07601(-12)	2.73242(-12)	1.60006(-12)
100	8.85020(-12)	6.13285(-12)	2.89244(-12)	1.55787(-12)	9.11112(-13)
200	1.88545(-13)	1.34934(-13)	6.41268(-14)	3.46841(-14)	2.01835(-14)
300	1.84979(-14)	1.34290(-14)	6.40102(-15)	3.47012(-15)	2.01731(-15)
400	3.48404(-15)	2.54871(-15)	1.21653(-15)	6.60447(-16)	3.83840(-16)
500	9.45103(-16)	6.94631(-16)	3.31807(-16)	1.80309(-16)	1.04786(-16)

Table 6.4.9: Generalized oscillator strengths, GOS(K), for the He  $2^1S \rightarrow n^1D$  transitions.

$K^2$	$3^1D$	$4^1D$	$5^1D$	$6^1D$
0.05	1.53833(-1)	2.70288(-2)	8.78849(-3)	3.93125(-3)
0.10	1.64042(-1)	4.32680(-2)	1.66919(-2)	8.16612(-3)
0.15	1.35351(-1)	4.64775(-2)	2.01915(-2)	1.05267(-2)
0.20	1.02050(-1)	4.21400(-2)	1.99587(-2)	1.09061(-2)
0.25	7.39299(-2)	3.49530(-2)	1.76659(-2)	1.00047(-2)
0.30	5.25588(-2)	2.75419(-2)	1.46364(-2)	8.52305(-3)
0.35	3.70509(-2)	2.10399(-2)	1.16326(-2)	6.92524(-3)
0.40	2.60432(-2)	1.57687(-2)	9.00016(-3)	5.45442(-3)
0.45	1.83097(-2)	1.16798(-2)	6.84186(-3)	4.20735(-3)
0.50	1.28979(-2)	8.58998(-3)	5.14136(-3)	3.20013(-3)
0.55	9.11210(-3)	6.29200(-3)	3.83458(-3)	2.41112(-3)
0.60	6.45920(-3)	4.59929(-3)	2.84631(-3)	1.80521(-3)
0.65	4.59473(-3)	3.35939(-3)	2.10657(-3)	1.34598(-3)
0.70	3.27969(-3)	2.45386(-3)	1.55648(-3)	1.00091(-3)
0.75	2.34856(-3)	1.79334(-3)	1.14904(-3)	7.43078(-4)
0.80	1.68666(-3)	1.31160(-3)	8.47941(-4)	5.51112(-4)
0.85	1.21432(-3)	9.60016(-4)	6.25679(-4)	4.08486(-4)
0.90	8.76020(-4)	7.03154(-4)	4.61662(-4)	3.02638(-4)
0.95	6.32899(-4)	5.15252(-4)	3.40606(-4)	2.24123(-4)
1.0	4.57650(-4)	3.77610(-4)	2.51219(-4)	1.65888(-4)
1.2	1.24376(-4)	1.07993(-4)	7.35590(-5)	4.92024(-5)
1.4	3.18570(-5)	2.93419(-5)	2.05047(-5)	1.39060(-5)
1.6	6.80693(-6)	6.90150(-6)	5.01297(-6)	3.46987(-6)
1.8	8.34026(-7)	1.09007(-6)	8.66038(-7)	6.27132(-7)
2.0	1.25222(-9)	2.07108(-8)	3.28529(-8)	3.10231(-8)
2.2	3.10912(-7)	1.30947(-7)	5.92665(-8)	3.04695(-8)
2.4	6.92841(-7)	4.04923(-7)	2.27329(-7)	1.35843(-7)
2.6	9.25852(-7)	5.98798(-7)	3.55526(-7)	2.20046(-7)
2.8	1.01416(-6)	6.88822(-7)	4.19572(-7)	2.63805(-7)
3.0	1.00506(-6)	7.02368(-7)	4.34071(-7)	2.75367(-7)
3.2	9.41018(-7)	6.69785(-7)	4.17766(-7)	2.66544(-7)
3.4	8.51280(-7)	6.13565(-7)	3.85111(-7)	2.46680(-7)

Table 6.4.9: Continued.

$K^2$	$3^1D$	$4^1D$	$5^1D$	$6^1D$
3.6	7.53710(-7)	5.48119(-7)	3.45578(-7)	2.21989(-7)
3.8	6.58308(-7)	4.81877(-7)	3.04819(-7)	1.96221(-7)
4.0	5.70110(-7)	4.19345(-7)	2.65923(-7)	1.71457(-7)
4.2	4.91213(-7)	3.62624(-7)	2.30392(-7)	1.48729(-7)
4.4	4.22058(-7)	3.12420(-7)	1.98785(-7)	1.28445(-7)
4.6	3.62219(-7)	2.68665(-7)	1.71139(-7)	1.10658(-7)
4.8	3.10857(-7)	2.30908(-7)	1.47216(-7)	9.52383(-8)
5.0	2.66989(-7)	1.98529(-7)	1.26657(-7)	8.19674(-8)
5.5	1.83781(-7)	1.36822(-7)	8.73767(-8)	5.65691(-8)
6.0	1.28205(-7)	9.54339(-8)	6.09664(-8)	3.94655(-8)
6.5	9.08137(-8)	6.75344(-8)	4.31395(-8)	2.79118(-8)
7.0	6.53446(-8)	4.85197(-8)	3.09814(-8)	2.00304(-8)
7.5	4.77436(-8)	3.53833(-8)	2.25801(-8)	1.45851(-8)
8.0	3.53956(-8)	2.61759(-8)	1.66922(-8)	1.07704(-8)
8.5	2.66030(-8)	1.96284(-8)	1.25065(-8)	8.06012(-9)
9.0	2.02516(-8)	1.49064(-8)	9.48930(-9)	6.10793(-9)
9.5	1.56007(-8)	1.14549(-8)	7.28530(-9)	4.68310(-9)
10	1.21509(-8)	8.89987(-9)	5.65488(-9)	3.63007(-9)
20	3.47753(-10)	2.44975(-10)	1.53629(-10)	9.56736(-11)
30	3.75671(-11)	2.59578(-11)	1.62743(-11)	9.85317(-12)
40	7.19572(-12)	4.92109(-12)	3.10094(-12)	1.83419(-12)
50	1.91476(-12)	1.30122(-12)	8.25301(-13)	4.79091(-13)
60	6.32660(-13)	4.28065(-13)	2.73284(-13)	1.56264(-13)
70	2.43910(-13)	1.64491(-13)	1.05656(-13)	5.96758(-14)
80	1.05585(-13)	7.10197(-14)	4.58697(-14)	2.56465(-14)
90	5.00288(-14)	3.35776(-14)	2.17943(-14)	1.20827(-14)
100	2.54879(-14)	1.70748(-14)	1.11318(-14)	6.12732(-15)
200	2.66903(-16)	1.76893(-16)	1.18413(-16)	6.27979(-17)
300	1.72300(-17)	1.13615(-17)	7.69766(-18)	4.02350(-18)
400	2.41304(-18)	1.58640(-18)	1.08225(-18)	5.61317(-19)
500	5.20541(-19)	3.41540(-19)	2.34044(-19)	1.20805(-19)

Table 6.4.10: First three small  $K$  expansion coefficients of the  $GOS(K)$  for the  $1^1S \rightarrow n^1S$ ,  $n^1P$ ,  $n^1D$ ,  $n=2-6$  He transitions.

Final	$K^0$	$K^2$	$K^4$	$K^6$
$2^1S$	0	0.84012(-1)	-0.12543( 0)	0.11097( 0)
$3^1S$	0	0.16890(-1)	-0.17198(-1)	0.62161(-2)
$4^1S$	0	0.62588(-2)	-0.56441(-2)	0.13753(-2)
$5^1S$	0	0.30114(-2)	-0.25691(-2)	0.47330(-3)
$6^1S$	0	0.16818(-2)	-0.13927(-2)	0.21278(-3)
$2^1P$	0.27617( 0)	-0.45227( 0)	0.43557( 0)	
$3^1P$	0.73426(-1)	-0.91606(-1)	0.53621(-1)	
$4^1P$	0.29860(-1)	-0.33921(-1)	0.16227(-1)	
$5^1P$	0.15038(-1)	-0.16357(-1)	0.70344(-2)	
$6^1P$	0.86270(-2)	-0.91644(-2)	0.37049(-2)	
$3^1D$	0	0.97924(-2)	-0.25833(-1)	0.38920(-1)
$4^1D$	0	0.50403(-2)	-0.12304(-1)	0.16615(-1)
$5^1D$	0	0.27595(-2)	-0.65080(-2)	0.84088(-2)
$6^1D$	0	0.16480(-2)	-0.38154(-2)	0.48137(-2)

Table 6.4.11: First three small  $K$  expansion coefficients of the  $GOS(K)$  for the  $2^1S \rightarrow n^1S$ ,  $n^1P$ ,  $n^1D$ ,  $n=2-6$  He transitions.

Final		$K^0$	$K^2$	$K^4$	$K^6$
$3^1S$	0		0.24572( 1)	-0.37608( 2)	0.30188( 3)
$4^1S$	0		0.36042( 0)	-0.10593( 1)	-0.23756( 2)
$5^1S$	0		0.12363( 0)	-0.42968(-1)	-0.81546( 1)
$6^1S$	0		0.58502(-1)	0.37812(-1)	-0.35982( 1)
$2^1P$	0.37644( 0)		-0.32104( 1)	0.14753( 2)	
$3^1P$	0.15135( 0)		-0.53019( 1)	0.77337( 2)	
$4^1P$	0.49145(-1)		-0.90153( 0)	0.29969(-1)	
$5^1P$	0.22336(-1)		-0.31160( 0)	0.51896(-1)	
$6^1P$	0.12134(-1)		-0.14651( 0)	-0.18161( 0)	
$3^1D$	0		0.59785( 1)	-0.81735( 2)	0.60698( 3)
$4^1D$	0		0.51448( 0)	0.31993( 1)	-0.68694( 2)
$5^1D$	0		0.12850( 0)	0.16617( 1)	-0.13672( 2)
$6^1D$	0		0.50164(-1)	0.82374( 0)	-0.38346( 1)

Table 6.4.12: First three small  $K$  expansion coefficients of the  $GOS(K)$  for the  $2^3S \rightarrow n^3S$ ,  $n^3P$ ,  $n^3D$ ,  $n=2-6$  He transitions.

final	$K^0$	$K^2$	$K^4$	$K^6$
$3^3S$	0	0.16576( 1)	-0.19337( 2)	0.11992( 3)
$4^3S$	0	0.24958( 0)	-0.67518( 0)	-0.89177( 1)
$5^3S$	0	0.86382(-1)	-0.74583(-1)	-0.27431( 1)
$6^3S$	0	0.40849(-1)	0.16829(-1)	-0.31891( 1)
$2^3P$	0.53909( 0)	-0.35654( 1)	0.12987( 2)	
$3^3P$	0.64462(-1)	-0.22703( 1)	0.31123( 2)	
$4^3P$	0.25769(-1)	-0.51731( 0)	0.28827( 1)	
$5^3P$	0.12493(-1)	-0.20018( 0)	0.71260( 0)	
$6^3P$	0.69791(-2)	-0.98315(-1)	0.88698(-1)	
$3^3D$	0	0.35560( 1)	-0.41045( 2)	0.25923( 3)
$4^3D$	0	0.56506( 0)	-0.10169( 1)	-0.23930( 2)
$5^3D$	0	0.18840( 0)	0.21481( 0)	-0.79555( 1)
$6^3D$	0	0.86576(-1)	0.26516( 0)	-0.86838( 1)

Table 6.4.13: First three large  $K$  expansion coefficients of the  $GOS(K)$  for the  $1^1S \rightarrow n^1S$ ,  $n^1P$ ,  $n^1D$ ,  $n=2-6$  He transitions.

Final	$K^{-10}$	$K^{-12}$	$K^{-14}$	$K^{-16}$	$K^{-18}$
$2^1S$	0.22211( 4)	-0.17161( 6)	0.65077( 7)		
$3^1S$	0.72142( 3)	-0.55262( 5)	0.20995( 7)		
$4^1S$	0.30960( 3)	-0.23737( 5)	0.92256( 6)		
$5^1S$	0.15828( 3)	-0.11956( 5)	0.43973( 6)		
$6^1S$	0.91710( 2)	-0.70347( 4)	0.28107( 6)		
$2^1P$	0	0.30177( 4)	-0.31209( 6)	0.16499( 8)	
$3^1P$	0	0.12299( 4)	-0.12452( 6)	0.66108( 7)	
$4^1P$	0	0.56710( 3)	-0.54716( 5)	0.25370( 7)	
$5^1P$	0	0.30367( 3)	-0.29525( 5)	0.14557( 7)	
$6^1P$	0	0.17598( 3)	-0.17197( 5)	0.88939( 6)	
$3^1D$	0	0	0.52724( 3)	-0.43847( 5)	0.11826( 7)
$4^1D$	0	0	0.30706( 3)	-0.24094( 5)	0.59785( 6)
$5^1D$	0	0	0.17967( 3)	-0.13810( 5)	0.36322( 6)
$6^1D$	0	0	0.10297( 3)	-0.76264( 4)	0.20337( 6)

Table 6.4.14: First three large  $K$  expansion coefficients of the  $GOS(K)$  for the  $2^1S \rightarrow n^1S$ ,  $n^1P$ ,  $n^1D$ ,  $n=2-6$  He transitions.

Final	$K^{-10}$	$K^{-12}$	$K^{-14}$	$K^{-16}$	$K^{-18}$
$3^1S$	0.24845( 1)	-0.20811( 3)	0.79351( 4)		
$4^1S$	0.13358( 1)	-0.11123( 3)	0.41805( 4)		
$5^1S$	0.73685( 0)	-0.60195( 2)	0.21075( 4)		
$6^1S$	0.44275( 0)	-0.36487( 2)	0.13638( 4)		
$2^1P$	0	0.16938( 2)	-0.11546( 4)	0.31582( 5)	
$3^1P$	0	0.12689( 2)	-0.98557( 3)	0.31066( 5)	
$4^1P$	0	0.60737( 1)	-0.47473( 3)	0.13169( 5)	
$5^1P$	0	0.33168( 1)	-0.26904( 3)	0.89012( 4)	
$6^1P$	0	0.19287( 1)	-0.15772( 3)	0.56549( 4)	
$3^1D$	0	0	0.45195( 1)	-0.21985( 3)	-0.80049( 4)
$4^1D$	0	0	0.29367( 1)	-0.12614( 3)	-0.69239( 4)
$5^1D$	0	0	0.20553( 1)	-0.11318( 3)	-0.14641( 4)
$6^1D$	0	0	0.10390( 1)	-0.45616( 2)	-0.16623( 4)

Table 6.4.15: First three large  $K$  expansion coefficients of the  $GOS(K)$  for the  $2^3S \rightarrow n^3S$ ,  $n^3P$ ,  $n^3D$ ,  $n=2-6$  He transitions.

Final	$K^{-10}$	$K^{-12}$	$K^{-14}$	$K^{-16}$	$K^{-18}$
$3^3S$	0.48354( 1)	-0.23097( 3)	0.58619( 4)		
$4^3S$	0.24645( 1)	-0.11782( 3)	0.30371( 4)		
$5^3S$	0.13255( 1)	-0.62758( 2)	0.15561( 4)		
$6^3S$	0.78108( 0)	-0.37158( 2)	0.94539( 3)		
$2^3P$	0	0.12764( 3)	-0.47427( 4)	0.12204( 4)	
$3^3P$	0	0.83450( 2)	-0.32118( 4)	0.18193( 5)	
$4^3P$	0	0.40693( 2)	-0.15953( 4)	0.13025( 5)	
$5^3P$	0	0.21735( 2)	-0.84118( 3)	0.64060( 4)	
$6^3P$	0	0.12979( 2)	-0.49942( 3)	0.32589( 4)	
$3^3D$	0	0	0.10211( 2)	-0.29946( 3)	-0.20248( 5)
$4^3D$	0	0	0.70085( 1)	-0.22282( 3)	-0.12045( 5)
$5^3D$	0	0	0.44764( 1)	-0.16369( 3)	-0.53252( 4)
$6^3D$	0	0	0.26174( 1)	-0.95963( 2)	-0.19924( 4)

## CHAPTER 7: CONCLUSIONS

The integral transform wavefunctions obtained and utilized in this research lead to the lowest variational energies for 180 of 261 states considered. Nonetheless, it is unfortunate that the comparison with previous work relies entirely on energies. The cusp ratios and the asymptotic density analysis provide a measure of the quality of an approximate wavefunction. However, if their use was more common, they could also enable wavefunction selection based on the requirements of the property under study. For instance  $\langle r^6 \rangle$  heavily weights the outer regions of the charge cloud and the asymptotic behaviour of the density should be the deciding factor in the selection of a wavefunction suitable for the calculation.

Although the perfectly screened hydrogenic density is conceptually appealing, its use requires care. In particular, as shown in chapter 3, its validity depends strongly on the angular momentum of the state of interest. Also, although the charge densities display pseudo-nodes, i.e. minima at which  $\rho(r) \approx 0$ , the one-electron Hund holes do not display a similarly sharp structure. Singlet-triplet Hund holes show that spin effects are much smaller in the D states; the S state holes are roughly twice as large as the P state holes and 400 times larger than the D state holes. The correlation coefficients confirm this observation since the  ${}^3D$  and  ${}^1D$  coefficients are close regardless of the coefficient under examination. However, the density holes for the  ${}^3D$  and  ${}^3D$  states show subtle

differences. In particular, radial correlation induces a redistribution of charge to very small  $r$  for the high- $Z$  triplets.

The dipole oscillator strengths presented in chapter 5 improve upon previous values for 739 of the 855 transitions considered. As well, all of the quadrupole oscillator strengths and generalized oscillator strengths improve upon previous theoretical calculations. The validity of the first Born approximation has been estimated as follows: at incident energies  $\geq 400$  eV for  $1^1S \rightarrow n^1S$  transitions,  $\geq 100$  eV for  $1^1S \rightarrow n^1P$  transitions, and  $\geq 300$  eV for  $1^1S \rightarrow n^1D$  transitions. These limits are tentative due to the limited experimental information; in particular, the lack of cross sections for large angles.

With few exceptions, the computations in this work were performed in quadruple precision. Although care was taken to provide alternate routines where numerical problems could arise, the near cancellation due to linear dependence of the basis functions required quadruple precision. These calculations were all performed on a multi-user VAX system, where the architecture is single precision, and were consequently very slow. Sufficiently so, in fact, that computation time was often the limiting factor. On some of the more recent generation of 'workstations', which have double precision architecture, the performance would be greatly enhanced.

Some work, not discussed in this document, is in various stages of completion: Generalized oscillator strengths have been calculated for the  $1^1S \rightarrow 2^1S$  and  $1^1S \rightarrow 3^1P$  transitions of the ions from  $Li^+$  to  $Ne^{8+}$ ; 200 term wavefunctions are being optimized for all the states of helium; quadrupole oscillator strengths are being calculated for the  $P \rightarrow P$  and  $D \rightarrow D$  transitions of the ions from He to  $Ne^{8+}$ ; partial densities and intracules are

being studied; and spin-forbidden optical transitions, such as  $1^1S \rightarrow 2^3S$ , are being studied. Although these projects are under way, there are many others worthwhile for study. The next few paragraphs discuss some of these.

Although the phrase 'variational energy optimization' is always interpreted as an upper bound minimization, lower bounds to the energy can also be calculated. Lower bounds remain largely ignored since they are very sensitive to the wavefunction quality and, consequently, are usually further from the true energy than the upper bounds. However, the integral transform wavefunctions of chapter 2 are sufficiently accurate to justify an attempt at lower bound optimization.

Hylleraas-type wavefunction expansions have been successfully applied to three electrons atoms. At least for the S states, integral transform expansions are mathematically feasible and could greatly reduce the expansion lengths required.

The application of the correlation coefficients discussed in chapter 4 to molecular systems immediately leads to a difficult problem: the coefficients are gauge-dependent. The study of these coefficients, or the selection of new coefficients, in molecular systems would be worthwhile. The goal would be to extract meaningful information about statistical electron correlation in molecules.

As noted in chapter 6, many theoretical studies of intermediate impact energy differential cross sections have appeared in the literature. At intermediate energies, electron exchange and polarization are very important and an accurate differential cross section requires the inclusion of these effects. Although there are many methods for calculating differential cross sections, most are probably not suitable for integral

transform expansions due to the mathematical requirements. However, the second Born approximation, or more precisely an approximation to the second Born cross section, with the addition of an exchange correction, shows promise. Also, distorted-wave methods are worth investigating further.

## Appendix 1

Table A1.1: Two iterations of Powell's algorithm for a 20 term wavefunction for the He  $1^1S$  state.

Calc. #	A <sub>1</sub>	A <sub>2</sub>	B <sub>1</sub>	B <sub>2</sub>	G <sub>1</sub>	G <sub>2</sub>	E
Search direction: $\vec{\xi}_1 = \hat{e}_1$							
1	0.30000	1.00000	1.50000	2.50000	-0.10000	0.30000	-2.902589760
2	0.31000	1.00000	1.50000	2.50000	-0.10000	0.30000	-2.902601304
3	0.32000	1.00000	1.50000	2.50000	-0.10000	0.30000	-2.902612637
4	0.42000	1.00000	1.50000	2.50000	-0.10000	0.30000	-2.902708937
5	0.52000	1.00000	1.50000	2.50000	-0.10000	0.30000	-2.902749595
6	0.54307	1.00000	1.50000	2.50000	-0.10000	0.30000	-2.902748587
Search direction: $\vec{\xi}_2 = \hat{e}_2$							
7	0.52000	1.01000	1.50000	2.50000	-0.10000	0.30000	-2.902791390
8	0.52000	1.02000	1.50000	2.50000	-0.10000	0.30000	-2.902830790
9	0.52000	1.12000	1.50000	2.50000	-0.10000	0.30000	-2.903126109
10	0.52000	1.22000	1.50000	2.50000	-0.10000	0.30000	-2.903308902
11	0.52000	1.32000	1.50000	2.50000	-0.10000	0.30000	-2.903429166
12	0.52000	1.42000	1.50000	2.50000	-0.10000	0.30000	-2.903510675
13	0.52000	1.52000	1.50000	2.50000	-0.10000	0.30000	-2.903566717
14	0.52000	1.62000	1.50000	2.50000	-0.10000	0.30000	-2.903605258
15	0.52000	1.72000	1.50000	2.50000	-0.10000	0.30000	-2.903631760
16	0.52000	1.82000	1.50000	2.50000	-0.10000	0.30000	-2.903651033
17	0.52000	1.92000	1.50000	2.50000	-0.10000	0.30000	-2.903667182
18	0.52000	2.02000	1.50000	2.50000	-0.10000	0.30000	-2.903683211
19	0.52000	2.12000	1.50000	2.50000	-0.10000	0.30000	-2.903700647
20	0.52000	2.22000	1.50000	2.50000	-0.10000	0.30000	-2.903700081
21	0.52000	2.16686	1.50000	2.50000	-0.10000	0.30000	-2.903706132

Table A1.1: Continued.

Calc. #	A <sub>1</sub>	A <sub>2</sub>	B <sub>1</sub>	B <sub>2</sub>	G <sub>1</sub>	G <sub>2</sub>	E
Search direction: $\vec{\xi}_3 = \hat{e}_3$							
22	0.52000	2.16686	1.51000	2.50000	-0.10000	0.30000	-2.903706001
23	0.52000	2.16686	1.49000	2.50000	-0.10000	0.30000	-2.903706167
24	0.52000	2.16686	1.49126	2.50000	-0.10000	0.30000	-2.903706170
25	0.52000	2.16686	1.49229	2.50000	-0.10000	0.30000	-2.903706171
Search direction: $\vec{\xi}_4 = \hat{e}_4$							
26	0.52000	2.16686	1.49229	2.51000	-0.10000	0.30000	-2.903706231
27	0.52000	2.16686	1.49229	2.52000	-0.10000	0.30000	-2.903706073
28	0.52000	2.16686	1.49229	2.50776	-0.10000	0.30000	-2.903706236
Search direction: $\vec{\xi}_5 = \hat{e}_5$							
29	0.52000	2.16686	1.49229	2.50776	-0.09000	0.30000	-2.903706331
30	0.52000	2.16686	1.49229	2.50776	-0.08000	0.30000	-2.903706381
31	0.52000	2.16686	1.49229	2.50776	-0.07409	0.30000	-2.903706387
Search direction: $\vec{\xi}_6 = \hat{e}_6$							
32	0.52000	2.16686	1.49229	2.50776	-0.07409	0.31000	-2.903707017
33	0.52000	2.16686	1.49229	2.50776	-0.07409	0.32000	-2.903707591
34	0.52000	2.16686	1.49229	2.50776	-0.07409	0.41955	-2.903711536
35	0.52000	2.16686	1.49229	2.50776	-0.07409	0.49182	-2.903713240
36	0.52000	2.16686	1.49229	2.50776	-0.07409	0.58188	-2.903714008
New search direction: $\vec{\xi} = \vec{p}_{36} - \vec{p}_1 = (0.22000, 1.16686, -0.00771, 0.00776, 0.02591, 0.28188)$							
37	0.74000	3.33372	1.48457	2.51552	-0.04819	0.86375	-2.903710430
38	0.62930	2.74659	1.48845	2.51162	-0.06122	0.72192	-2.903718978
39	0.61542	2.67295	1.48894	2.51113	-0.06286	0.70413	-2.903718013
40	0.65186	2.86621	1.48766	2.51241	-0.05857	0.75082	-2.903719928
41	0.65614	2.88894	1.48751	2.51257	-0.05806	0.75631	-2.903720018
42	0.66085	2.91390	1.48735	2.51273	-0.05751	0.76234	-2.903720087

End of iteration 1.  $\hat{e}_2$  replaced by  $\vec{\xi}$ .

Table A1.1: Continued.

Calc. #	A <sub>1</sub>	A <sub>2</sub>	B <sub>1</sub>	B <sub>2</sub>	G <sub>1</sub>	G <sub>2</sub>	E
Search direction: $\vec{\xi}_1 = \hat{e}_1$							
43	0.67085	2.91390	1.48735	2.51273	-0.05751	0.76234	-2.903720095
44	0.66595	2.91390	1.48735	2.51273	-0.05751	0.76234	-2.903720094
45	0.67011	2.91390	1.48735	2.51273	-0.05751	0.76234	-2.903720095
Search direction: $\vec{\xi}_3 = \hat{e}_3$							
46	0.67011	2.91390	1.49735	2.51273	-0.05751	0.76234	-2.903720161
47	0.67011	2.91390	1.49756	2.51273	-0.05751	0.76234	-2.903720162
48	0.67011	2.91390	1.59756	2.51273	-0.05751	0.76234	-2.903720558
49	0.67011	2.91390	1.63146	2.51273	-0.05751	0.76234	-2.903720586
Search direction: $\vec{\xi}_4 = \hat{e}_4$							
50	0.67011	2.91390	1.63146	2.52273	-0.05751	0.76234	-2.903720598
51	0.67011	2.91390	1.63146	2.51829	-0.05751	0.76234	-2.903720593
52	0.67011	2.91390	1.63146	2.59989	-0.05751	0.76234	-2.903720643
Search direction: $\vec{\xi}_5 = \hat{e}_5$							
53	0.67011	2.91390	1.63146	2.59989	-0.04751	0.76234	-2.903720438
54	0.67011	2.91390	1.63146	2.59989	-0.09583	0.76234	-2.903720876
55	0.67011	2.91390	1.63146	2.59989	-0.08684	0.76234	-2.903720889
56	0.67011	2.91390	1.63146	2.59989	-0.08848	0.76234	-2.903720889
Search direction: $\vec{\xi}_6 = \hat{e}_6$							
57	0.67011	2.91390	1.63146	2.59989	-0.08848	0.77234	-2.903720924
58	0.67011	2.91390	1.63146	2.59989	-0.08848	0.78633	-2.903720966
59	0.67011	2.91390	1.63146	2.59989	-0.08848	0.84808	-2.903721053
Search direction: $\vec{\xi} = \vec{p}_{36} - \vec{p}_1$							
60	0.67200	2.92390	1.63139	2.59995	-0.08825	0.85050	-2.903721096
61	0.67309	2.95623	1.63118	2.60017	-0.08754	0.85831	-2.903721125
62	0.67611	2.94568	1.63125	2.60010	-0.08777	0.85576	-2.903721134

Table A1.1: Continued.

Calc. #	A <sub>1</sub>	A <sub>2</sub>	B <sub>1</sub>	B <sub>2</sub>	G <sub>1</sub>	G <sub>2</sub>	E
New search direction: $\vec{\xi} = \vec{p}_{62} - \vec{p}_{42} = (0.01526, 0.03178, 0.14390, 0.08737, -0.03026, 0.09342)$							
63	0.69136	2.97746	1.77514	2.68746	-0.11803	0.94919	-2.903719205
64	0.68611	2.94568	1.63125	2.60010	-0.08777	0.85576	-2.903721127

## Appendix 2

Table A2.1:  $1^1S$  parallelotope parameters and virial scaling coefficients.

Z	A <sub>1</sub>	A <sub>2</sub>	B <sub>1</sub>	B <sub>2</sub>	G <sub>1</sub>	G <sub>2</sub>	1- $\eta$
1	0.19934	1.14712	1.16689	0.99562	-0.12963	0.76402	3.8500(-9)
2	0.96593	3.98584	1.55430	2.09751	-0.49093	3.21922	-1.1898(-12)
3	1.82480	6.02374	2.26622	3.99078	-0.89466	4.25997	-2.7107(-11)
4	4.31297	6.39227	3.17824	5.83218	-1.01280	4.89687	-1.1420(-11)
5	5.54175	7.38873	3.92261	6.40769	-0.67594	5.61929	3.9032(-12)
6	6.10057	10.79395	5.03773	9.13214	-1.65826	7.68071	-4.1820(-11)
7	6.23646	11.76333	4.41499	8.86489	-0.06975	12.19816	8.1263(-11)
8	7.17895	13.79924	5.01603	10.09200	-0.07061	13.00453	-1.5668(-10)
9	8.57186	13.51470	5.22259	11.45360	-0.31444	15.61981	-7.9888(-11)
10	10.28864	13.88795	6.81112	12.36805	-0.27054	14.62281	1.0365(-10)

Table A2.2:  $2^1S$  parallelotope parameters and virial scaling coefficients.

Z	A <sub>1</sub>	A <sub>2</sub>	B <sub>1</sub>	B <sub>2</sub>	G <sub>1</sub>	G <sub>2</sub>	1- $\eta$
2	1.96376	2.00667	0.33130	1.72457	-0.06832	1.04197	-5.4826(-8)
3	2.93424	3.10408	0.97045	2.73797	-0.34532	2.46189	5.2158(-12)
4	3.63915	4.40430	1.03381	4.19815	-0.32066	3.55295	-3.6027(-8)
5	4.85394	5.24628	1.88678	5.36123	-0.57080	4.22516	3.6747(-8)
6	5.61600	6.44486	1.76731	6.59565	-0.48991	5.32956	1.0288(-8)
7	6.81230	7.31818	2.82809	7.43349	-0.78618	5.70406	-1.4426(-8)
8	7.73857	8.45393	3.29451	8.70371	-0.92856	6.77833	-3.9168(-10)
9	8.44334	9.94549	3.73046	9.18196	-0.99990	7.38279	-4.9627(-9)
10	9.37189	11.09527	4.24446	10.26462	-1.10297	8.04448	1.0253(-9)

Table A2.3:  $2^3S$  parallelopotope parameters and virial scaling coefficients.

Z	A <sub>1</sub>	A <sub>2</sub>	B <sub>1</sub>	B <sub>2</sub>	G <sub>1</sub>	G <sub>2</sub>	1- $\eta$
2	0.30039	2.13995	1.89335	2.24210	-0.25917	0.46484	-1.3115(-12)
3	2.94086	3.08429	1.05269	2.69861	-0.11440	1.02880	-1.3402(-11)
4	3.84120	4.21134	1.34452	3.14411	-0.45471	2.41758	3.4216(-11)
5	4.90342	5.14948	2.06061	3.57139	-0.42377	3.03216	-4.0632(-12)
6	5.67967	6.61948	2.37624	4.89055	-0.75221	4.12759	-3.0487(-11)
7	6.52845	7.70498	2.89931	5.14131	-0.63528	5.22277	2.1367(-13)
8	7.89200	8.17088	3.59868	5.82052	-0.64432	4.55566	3.0497(-12)
9	8.83222	9.27231	4.01530	6.73528	-0.77707	5.50077	-1.1121(-12)
10	9.79361	10.24129	4.19810	7.22016	-0.62681	6.36664	3.8619(-12)

Table A2.4:  $3^1S$  parallelopotope parameters and virial scaling coefficients.

Z	A <sub>1</sub>	A <sub>2</sub>	B <sub>1</sub>	B <sub>2</sub>	G <sub>1</sub>	G <sub>2</sub>	1- $\eta$
2	2.03001	1.99704	0.17093	2.06519	-0.08117	0.26967	-6.4551(-11)
3	3.05773	2.98785	0.35426	2.59054	-0.50634	0.79140	1.7701(-9)
4	3.97195	4.04317	0.60177	2.25008	-0.69068	2.98507	-2.6647(-8)
5	4.96585	5.05971	1.16293	5.34085	-0.12813	0.99551	-6.2301(-11)
6	5.96157	6.06926	1.46623	6.71572	-0.12762	1.02810	5.0853(-9)
7	6.95702	7.07664	1.76581	7.82723	-0.14795	1.19574	5.3518(-9)
8	7.95290	8.07336	2.03413	8.74022	-0.25152	1.98647	-5.9575(-8)
9	8.96938	9.04776	2.34271	9.64991	-0.31196	2.49296	-8.0695(-9)
10	10.10211	9.83799	2.56193	4.96264	-0.98771	8.69210	-5.4213(-8)

Table A2.5:  $3^3S$  parallelopotope parameters and virial scaling coefficients.

Z	A <sub>1</sub>	A <sub>2</sub>	B <sub>1</sub>	B <sub>2</sub>	G <sub>1</sub>	G <sub>2</sub>	1- $\eta$
2	0.29215	0.70032	1.96216	1.99666	-0.09991	0.71887	6.0686(-10)
3	2.89321	3.20360	0.51453	2.96139	-0.03593	0.17619	5.9869(-11)
4	3.92491	4.13664	0.95524	3.51041	-0.03757	0.31794	2.0079(-10)
5	4.93112	5.11163	1.26450	3.57522	-0.13083	1.05521	2.3132(-10)
6	5.95470	6.06995	1.58469	4.24863	-0.15823	1.28139	6.4702(-11)
7	7.04393	6.92407	1.87942	4.55344	-0.21062	1.60514	-9.7710(-12)
8	7.90735	8.17693	1.93047	5.55819	-0.42968	1.96451	-2.0329(-12)
9	8.87629	9.20400	2.49774	6.11957	-0.29566	2.34051	3.8598(-11)
10	9.93751	10.09820	2.83625	4.92241	-0.44959	3.56711	1.4257(-11)

Table A2.6:  $4^1S$  parallelopotope parameters and virial scaling coefficients.

Z	A <sub>1</sub>	A <sub>2</sub>	B <sub>1</sub>	B <sub>2</sub>	G <sub>1</sub>	G <sub>2</sub>	1- $\eta$
2	2.00413	2.02494	0.12248	1.92112	-0.00911	0.03620	4.6622(-10)
3	2.98047	3.05342	0.26312	3.06064	-0.01883	0.09156	-3.0032(-10)
4	4.00315	4.00153	0.36874	4.10196	-0.06659	0.37476	8.3492(-7)
5	5.00753	5.01113	0.64912	5.04692	-0.09444	0.25244	1.1126(-7)
6	6.00936	6.01379	0.82537	6.06870	-0.11359	0.29548	1.7203(-7)
7	6.99918	7.00475	0.87690	6.92564	-0.10823	0.50800	-2.6370(-8)
8	7.99629	8.00288	1.05466	8.06618	-0.07554	0.56490	2.5489(-8)
9	9.02082	9.02808	1.39158	9.15736	-0.19702	0.36103	1.1421(-7)
10	10.01259	10.02014	1.52503	10.11529	-0.17166	0.48723	5.9146(-8)

Table A2.7:  $4^3S$  parallelopotope parameters and virial scaling coefficients.

Z	A <sub>1</sub>	A <sub>2</sub>	B <sub>1</sub>	B <sub>2</sub>	G <sub>1</sub>	G <sub>2</sub>	1- $\eta$
2	1.99485	2.00759	0.06564	1.60627	-0.03925	0.05093	1.4494(-10)
3	3.03562	2.99194	0.32498	2.14346	-0.02494	0.08775	4.6672(-10)
4	3.99727	4.03461	0.53717	2.92099	-0.03929	0.20551	2.0301(-9)
5	4.97717	5.05273	0.70916	3.78139	-0.06387	0.30792	-3.4741(-10)
6	6.00750	6.01665	0.99087	4.50560	-0.04428	0.21339	9.5667(-10)
7	7.07630	6.94396	1.08255	5.00753	-0.11700	0.42562	-3.5304(-10)
8	7.99647	8.01070	1.23228	6.79873	-0.06143	0.33650	-4.8382(-11)
9	9.03813	8.94643	1.79282	6.87656	-0.02609	0.25169	-4.7557(-10)
10	9.99522	10.01396	1.59016	8.63785	-0.07794	0.42784	1.0644(-10)

Table A2.8:  $5^1S$  parallelopotope parameters and virial scaling coefficients.

Z	A <sub>1</sub>	A <sub>2</sub>	B <sub>1</sub>	B <sub>2</sub>	G <sub>1</sub>	G <sub>2</sub>	1- $\eta$
2	1.99944	1.99987	0.04562	1.80808	-0.00363	0.03743	-3.9220(-7)
3	3.00098	3.00023	0.11567	2.53510	-0.04612	0.14701	4.2996(-8)
4	4.01778	3.99798	0.17837	3.73263	-0.03499	0.06810	5.9936(-10)
5	4.99395	5.01218	0.63094	4.54539	-0.00544	0.04361	3.4510(-9)
6	6.00077	6.00014	0.39528	6.75517	-0.00596	0.12873	-4.0713(-8)
7	7.04843	6.98464	0.15646	6.93028	-0.11254	0.08501	-1.9985(-9)
8	7.97581	8.04502	1.12316	6.22887	-0.01031	0.11366	-1.5847(-10)
9	8.99380	9.02619	0.83256	9.08089	-0.02270	0.10759	3.1694(-9)
10	9.97054	10.05468	1.45214	7.79607	-0.01248	0.13814	1.3243(-9)

Table A2.9:  $5^3S$  parallelotope parameters and virial scaling coefficients.

Z	A <sub>1</sub>	A <sub>2</sub>	B <sub>1</sub>	B <sub>2</sub>	G <sub>1</sub>	G <sub>2</sub>	1- $\eta$
2	1.99967	2.00065	0.15895	0.36396	-0.11027	0.61283	-1.8066(-7)
3	2.99531	2.98916	0.15476	1.89708	-0.00581	0.04180	-2.2897(-10)
4	3.99649	4.00535	0.24300	2.54105	-0.09340	0.14605	4.3179(-10)
5	5.01539	4.99748	0.52388	2.80658	-0.05159	0.19529	-3.7594(-11)
6	6.01717	5.99639	0.66121	3.42769	-0.06039	0.23069	-1.1189(-10)
7	7.00037	7.00679	0.82475	3.87420	-0.11686	0.34230	4.1503(-11)
8	8.00482	8.01746	1.00983	5.24018	-0.01598	0.09608	7.0914(-11)
9	9.00101	9.01916	1.11400	5.85569	-0.02475	0.13744	6.6608(-10)
10	10.00568	10.02610	1.24851	6.79318	-0.02035	0.11863	1.7827(-9)

Table A2.10:  $6^1S$  parallelotope parameters and virial scaling coefficients.

Z	A <sub>1</sub>	A <sub>2</sub>	B <sub>1</sub>	B <sub>2</sub>	G <sub>1</sub>	G <sub>2</sub>	1- $\eta$
2	2.00002	2.00001	0.02918	1.63453	-0.00142	0.01564	9.5742(-7)
3	3.00378	2.99859	0.04542	2.39523	-0.00665	0.00935	-1.6878(-9)
4	4.00661	4.00211	0.19195	3.19405	-0.00139	0.01706	1.5898(-8)
5	4.99385	5.00464	0.09050	3.82123	0.00301	0.04857	1.1704(-8)
6	6.00705	6.02179	0.40632	4.54419	-0.00541	0.01759	1.3986(-7)
7	6.99245	7.00705	0.18257	5.45067	0.00393	0.06616	2.7331(-10)
8	7.99196	8.00813	0.23256	6.24007	0.00426	0.07484	7.4351(-10)
9	9.00221	9.02300	0.67170	6.93907	-0.00791	0.02844	2.1114(-10)
10	10.02360	9.99324	0.73824	7.27330	-0.01531	0.06800	2.2099(-9)

Table A2.11:  $6^3S$  parallelotope parameters and virial scaling coefficients.

Z	A <sub>1</sub>	A <sub>2</sub>	B <sub>1</sub>	B <sub>2</sub>	G <sub>1</sub>	G <sub>2</sub>	1- $\eta$
2	2.00169	1.99752	0.05367	0.86410	-0.00254	0.01065	-1.8923(-10)
3	2.99955	3.00653	0.20437	1.42372	-0.00540	0.01619	-7.6009(-11)
4	3.99931	4.00767	0.31407	2.00057	-0.00717	0.02038	3.7936(-11)
5	4.99902	5.00860	0.42330	2.56843	-0.00883	0.02430	3.4898(-11)
6	6.00907	5.99784	0.34133	3.51469	-0.02218	0.04983	1.9776(-10)
7	6.99311	7.00823	0.55575	3.58470	-0.01833	0.05169	5.0695(-11)
8	7.99234	8.00981	0.59357	4.29592	-0.02090	0.06387	3.3128(-10)
9	8.99518	9.00009	0.76351	5.04335	-0.02287	0.05436	1.0825(-9)
10	9.99300	9.99868	0.83925	5.62308	-0.02685	0.06189	-1.0728(-9)

Table A2.12:  $2^1P$  parallelotope parameters and virial scaling coefficients.

Z	A <sub>1</sub>	A <sub>2</sub>	B <sub>1</sub>	B <sub>2</sub>	G <sub>1</sub>	G <sub>2</sub>	1- $\eta$
2	0.25777	1.98962	1.43474	3.23366	-0.26963	0.47087	1.5227(-9)
3	0.50659	3.92841	2.29509	4.49183	-0.52247	0.92463	-9.2622(-10)
4	0.58799	5.64958	3.35230	5.04765	-0.64130	1.30556	2.8177(-10)
5	0.30982	5.49872	3.94017	5.89686	-0.36997	2.83251	-4.7806(-10)
6	0.36599	6.87774	4.71684	7.06096	-0.44363	3.48931	-5.5425(-10)
7	0.87005	8.39162	6.79234	8.81484	-0.66727	3.02493	-1.7599(-10)
8	0.46219	9.73789	6.34841	9.34364	-0.57254	4.53643	-2.6272(-10)
9	3.22903	8.55559	7.45122	12.32272	-3.31621	5.82582	8.9994(-11)
10	3.64390	9.56211	8.25393	13.73479	-3.74313	6.58452	7.5190(-11)

Table A2.13:  $2^3P$  parallelotope parameters and virial scaling coefficients.

Z	A <sub>1</sub>	A <sub>2</sub>	B <sub>1</sub>	B <sub>2</sub>	G <sub>1</sub>	G <sub>2</sub>	1- $\eta$
2	0.04300	1.44017	1.48158	2.40004	-0.05100	0.64842	-4.5544(-10)
3	0.26626	2.52755	1.60601	4.11344	-0.26525	2.26785	-5.9548(-9)
4	0.66692	3.26615	2.51217	5.18704	-0.35918	3.13353	-5.0331(-10)
5	1.76196	5.02143	3.34587	5.00587	-0.53062	3.47134	-2.6968(-9)
6	1.76742	7.15723	4.05981	10.05632	-1.25957	2.26695	1.0983(-9)
7	2.15784	8.31946	4.68950	11.82716	-1.52907	2.73966	-1.1848(-9)
8	3.37550	8.51031	7.76414	12.48653	-0.44816	2.14241	-2.5297(-9)
9	3.88492	9.34394	8.81245	13.42272	-0.67195	3.26297	1.8405(-9)
10	4.34338	10.74742	9.75734	15.27077	-0.66554	3.21649	6.3185(-11)

Table A2.14:  $3^1P$  parallelotope parameters and virial scaling coefficients.

Z	A <sub>1</sub>	A <sub>2</sub>	B <sub>1</sub>	B <sub>2</sub>	G <sub>1</sub>	G <sub>2</sub>	1- $\eta$
2	0.10824	1.84180	1.93073	2.08138	-0.11803	0.11725	6.7438(-11)
3	0.31838	2.60155	2.91993	3.20340	-0.33708	0.58498	7.2573(-10)
4	0.50591	3.73410	3.87272	4.32153	-0.51676	0.88680	2.5988(-9)
5	0.45973	5.53826	4.87192	5.32348	-0.25860	0.52916	5.2321(-10)
6	0.33580	5.16061	5.50895	6.21471	-0.05923	1.94209	3.0636(-9)
7	0.43632	6.10950	6.40387	7.26118	-0.07085	2.23799	-2.7279(-9)
8	0.54114	7.04545	7.32880	8.29482	-0.07863	2.53548	3.1030(-10)
9	1.10219	7.55807	8.47285	9.98094	-1.17197	2.52711	-1.4281(-10)
10	1.32545	5.74989	8.32667	11.19417	-0.65485	5.25020	-2.4230(-12)

Table A2.15:  $3^3P$  parallelopotope parameters and virial scaling coefficients.

Z	A <sub>1</sub>	A <sub>2</sub>	B <sub>1</sub>	B <sub>2</sub>	G <sub>1</sub>	G <sub>2</sub>	1- $\eta$
2	0.04902	1.07898	1.79936	2.08549	-0.01395	0.69632	-4.7267(-8)
3	0.15763	3.41472	2.87226	3.26129	-0.17637	0.32680	-2.0078(-10)
4	0.80710	4.39309	3.99235	4.27107	-0.06785	0.30577	1.3901(-9)
5	1.07642	5.78709	4.98923	5.32821	-0.07781	0.35515	-4.3980(-11)
6	0.52946	7.64515	5.75023	6.52590	-0.31833	0.58856	1.0151(-11)
7	0.61866	9.32150	6.73087	7.57491	-0.35031	0.62608	3.9156(-11)
8	1.57635	11.11529	7.44213	8.15605	-0.35339	0.41864	9.7010(-11)
9	1.80955	12.57613	8.39106	9.17149	-0.38906	0.45672	2.8178(-11)
10	1.00223	13.60723	9.65236	10.77653	-0.47341	0.83045	-7.8791(-12)

Table A2.16:  $4^1P$  parallelopotope parameters and virial scaling coefficients.

Z	A <sub>1</sub>	A <sub>2</sub>	B <sub>1</sub>	B <sub>2</sub>	G <sub>1</sub>	G <sub>2</sub>	1- $\eta$
2	0.07032	1.71136	1.97188	2.00635	-0.05345	0.04373	-3.0838(-9)
3	0.03561	1.58388	2.90824	3.03577	-0.01836	0.62867	-5.1579(-9)
4	0.25431	3.86868	3.96184	4.04860	-0.26751	0.24660	6.8822(-9)
5	0.07576	3.31771	4.83878	5.08050	-0.06635	0.70060	2.4612(-8)
6	0.69458	6.38838	5.79994	6.02934	-0.16022	0.13502	5.4619(-10)
7	0.51983	6.41188	6.84239	7.21612	-0.30046	0.40388	-1.2847(-9)
8	0.74202	7.50983	7.79777	8.20914	-0.41733	0.37921	-8.7368(-11)
9	1.42549	4.13300	8.72194	9.64376	-1.46148	2.39063	1.6347(-9)
10	1.65059	4.42386	9.71327	10.65403	-1.68997	2.80049	1.2612(-9)

Table A2.17:  $4^3P$  parallelotope parameters and virial scaling coefficients.

Z	A <sub>1</sub>	A <sub>2</sub>	B <sub>1</sub>	B <sub>2</sub>	G <sub>1</sub>	G <sub>2</sub>	l- $\eta$
2	0.14386	0.44194	1.92709	2.02674	-0.02020	0.71861	7.6424(-10)
3	0.34698	2.33429	3.00026	3.04496	-0.02812	0.11442	5.1278(-11)
4	0.53878	3.18202	3.99731	4.08113	-0.03441	0.15779	1.3169(-11)
5	0.30336	4.95599	4.96128	5.06069	-0.27984	0.35944	-2.5550(-9)
6	0.92698	4.91919	5.98868	6.12508	-0.05434	0.23519	-5.7512(-12)
7	1.12210	5.77816	6.98494	7.14384	-0.06414	0.27075	1.3192(-10)
8	1.31801	6.62252	7.98118	8.16200	-0.07369	0.30617	-9.6993(-13)
9	1.75391	7.81924	8.73656	9.10830	-0.63535	0.07593	1.2539(-9)
10	1.71132	8.29639	9.97437	10.19631	-0.09228	0.37325	-6.7422(-13)

Table A2.18:  $5^1P$  parallelotope parameters and virial scaling coefficients.

Z	A <sub>1</sub>	A <sub>2</sub>	B <sub>1</sub>	B <sub>2</sub>	G <sub>1</sub>	G <sub>2</sub>	l- $\eta$
2	0.03481	1.24330	1.99885	2.00377	0.04106	-0.01585	1.2995(-9)
3	0.20128	2.55535	2.97857	3.00836	-0.03024	0.02666	4.6353(-9)
4	0.32309	3.60818	3.97442	4.01158	-0.03269	0.03210	-1.3880(-8)
5	0.44277	4.59285	4.94556	5.01430	-0.06123	0.03993	-2.4146(-10)
6	0.56581	5.59530	5.93377	6.01637	-0.07288	0.04551	3.8425(-10)
7	0.69053	6.57908	6.92316	7.01811	-0.08388	0.05087	1.9156(-10)
8	0.81654	7.54921	7.91324	8.01964	-0.09444	0.05606	2.2639(-11)
9	0.94375	8.50581	8.90382	9.02102	-0.10459	0.06110	-1.0638(-10)
10	1.07192	9.45214	9.89488	10.02231	-0.11449	0.06601	5.5247(-11)

Table A2.19:  $5^3P$  parallelotope parameters and virial scaling coefficients.

Z	A <sub>1</sub>	A <sub>2</sub>	B <sub>1</sub>	B <sub>2</sub>	G <sub>1</sub>	G <sub>2</sub>	1- $\eta$
2	0.01445	1.25392	2.00061	2.01277	-0.01730	0.00836	1.6863(-10)
3	0.22969	2.40892	2.99783	3.01241	-0.01286	0.03292	1.9601(-10)
4	0.31360	3.87540	3.96202	4.01396	-0.03089	0.02583	1.2606(-9)
5	0.43072	5.01181	4.95217	5.01603	-0.03709	0.02979	1.4069(-9)
6	0.54450	6.18368	5.94312	6.01750	-0.04386	0.03378	-7.6909(-10)
7	0.99411	6.33082	6.99633	7.00630	-0.14276	0.01108	1.1120(-9)
8	1.16360	7.26823	7.99605	8.00665	-0.15730	0.01179	1.8434(-9)
9	0.99879	7.29181	8.90846	9.00853	-0.24199	0.14340	3.6083(-10)
10	1.51277	7.86944	9.91550	10.04393	-0.02941	0.04389	-2.4455(-8)

Table A2.20:  $6^1P$  parallelotope parameters and virial scaling coefficients.

Z	A <sub>1</sub>	A <sub>2</sub>	B <sub>1</sub>	B <sub>2</sub>	G <sub>1</sub>	G <sub>2</sub>	1- $\eta$
2	0.09376	0.92289	2.00264	2.00053	-0.03525	0.00444	-6.4084(-8)
3	0.05091	2.23402	3.00377	2.99462	-0.01782	0.00615	2.6401(-9)
4	0.24393	2.92511	3.98228	4.00310	-0.01991	0.01622	-3.4279(-8)
5	0.33916	3.75835	4.97740	5.00403	-0.02449	0.02020	-1.9074(-9)
6	0.16262	5.31691	6.00325	6.02739	-0.02092	0.00049	-7.8166(-9)
7	0.52915	5.44326	6.96924	7.00487	-0.03270	0.02661	2.0619(-10)
8	0.62583	6.27073	7.96565	8.00514	-0.03650	0.02945	-3.3009(-10)
9	0.72387	7.08258	8.96268	9.00547	-0.04032	0.03211	6.2986(-9)
10	0.82178	7.90256	9.95925	10.00557	-0.04362	0.03462	-5.3798(-11)

Table A2.21:  $6^3P$  parallelotope parameters and virial scaling coefficients.

Z	A <sub>1</sub>	A <sub>2</sub>	B <sub>1</sub>	B <sub>2</sub>	G <sub>1</sub>	G <sub>2</sub>	1- $\eta$
2	0.00190	1.07885	2.00054	2.00944	-0.00358	0.00441	1.0599(-9)
3	0.02336	1.73956	2.99534	3.01157	-0.02587	0.01596	-2.3484(-12)
4	0.26278	2.88799	3.98513	4.00660	-0.00675	0.00979	1.1215(-8)
5	0.39170	4.27555	4.99997	5.00323	-0.02637	0.02696	3.1363(-8)
6	0.03971	4.94844	5.99490	6.02618	-0.01739	0.00883	6.1539(-10)
7	0.06410	5.83858	6.99401	7.02883	-0.01987	0.00957	-1.2360(-10)
8	0.29559	7.38069	7.99656	8.00365	-0.02520	0.00822	1.7072(-10)
9	0.81487	7.93098	8.99975	9.00412	-0.04443	0.04444	1.9785(-8)
10	0.08787	7.86995	10.00630	10.01434	-0.10522	0.00991	-4.8860(-10)

Table A2.22:  $3^1D$  parallelotope parameters and virial scaling coefficients

Z	A <sub>1</sub>	A <sub>2</sub>	B <sub>1</sub>	B <sub>2</sub>	G <sub>1</sub>	G <sub>2</sub>	1- $\eta$
2	0.22310	0.97605	1.96979	2.08047	-0.22371	0.41212	3.0222(-10)
3	0.37758	2.40966	2.73873	3.54848	-0.39375	0.70409	1.4895(-9)
4	0.57604	3.55469	3.49155	5.07302	-0.60448	1.07944	3.2164(-9)
5	0.81858	4.43283	4.36886	6.32747	-0.73183	1.30915	6.0210(-10)
6	0.68618	3.63629	5.36040	6.49246	-0.28103	2.48027	3.8936(-9)
7	1.36642	3.35561	6.42524	7.45711	-0.45497	3.78749	1.0760(-10)
8	1.66792	3.77928	7.42038	8.46456	-0.50706	4.19701	8.5215(-11)
9	1.52924	6.14518	8.45594	9.22833	-0.10733	3.79830	1.8701(-9)
10	1.04687	5.77142	6.77225	10.98828	-1.11475	5.10953	-4.5847(-9)

Table A2.23:  $3^3$ D parallelotope parameters and virial scaling coefficients.

Z	A <sub>1</sub>	A <sub>2</sub>	B <sub>1</sub>	B <sub>2</sub>	G <sub>1</sub>	G <sub>2</sub>	1- $\eta$
2	0.31490	0.86786	1.99471	2.18446	-0.05791	0.28892	5.9614(-9)
3	0.49963	1.67239	2.71361	3.60702	-0.50853	0.90762	2.9490(-10)
4	0.79191	2.25123	3.66810	4.70683	-0.80751	1.43785	1.5779(-10)
5	1.01115	3.27868	4.52585	6.00817	-1.03836	1.84699	-5.4992(-11)
6	1.65640	2.92414	5.47410	6.27577	-0.01643	2.56902	7.8619(-10)
7	1.93026	4.09582	6.94524	8.29332	-0.50693	2.46492	-7.9360(-11)
8	1.65286	3.58549	7.13190	8.14026	-0.45862	3.93762	1.0230(-11)
9	2.63888	4.47990	8.49467	9.26461	-0.02650	3.91204	2.7572(-10)
10	2.89035	6.35117	9.94054	11.54858	-0.65782	3.17247	2.7150(-9)

Table A2.24:  $4^1$ D parallelotope parameters and virial scaling coefficients.

Z	A <sub>1</sub>	A <sub>2</sub>	B <sub>1</sub>	B <sub>2</sub>	G <sub>1</sub>	G <sub>2</sub>	1- $\eta$
2	0.20545	0.51555	1.97415	1.99855	-0.08197	0.54242	-1.0740(-8)
3	0.29274	1.49036	2.97844	3.04103	-0.29808	0.53303	3.3333(-9)
4	0.35715	1.38228	3.83632	4.06286	-0.17684	1.45899	-3.7513(-10)
5	0.88879	2.95001	4.98976	5.02055	-0.03726	0.48580	2.1285(-8)
6	0.41014	2.73843	5.91223	6.02836	-0.26082	1.96822	2.3402(-9)
7	1.26022	2.86084	6.84699	7.00251	-0.35189	2.30790	-6.3761(-10)
8	0.80189	3.31685	7.81550	8.06489	-0.37232	3.00485	2.0202(-11)
9	0.93605	3.75621	8.79197	9.07219	-0.41823	3.38794	4.3712(-10)
10	1.07035	4.19453	9.75240	10.07809	-0.45471	3.68252	-5.7464(-10)

Table A2.25:  $4^3\text{D}$  parallelotope parameters and virial scaling coefficients.

Z	A <sub>1</sub>	A <sub>2</sub>	B <sub>1</sub>	B <sub>2</sub>	G <sub>1</sub>	G <sub>2</sub>	1- $\eta$
2	0.11511	0.89212	1.98928	2.01858	-0.10020	0.22848	-4.5683(-8)
3	0.11208	1.16923	3.00993	3.17277	-0.11677	0.62835	1.2514(-9)
4	0.69721	1.44396	4.03372	3.97999	-0.00156	1.14034	4.5067(-11)
5	0.86899	2.52212	4.99139	5.15912	-0.13145	0.61771	3.8258(-10)
6	0.87073	2.84787	5.92773	6.17935	-0.71065	1.28620	2.9342(-10)
7	1.32622	3.37600	6.98970	7.12961	-0.30691	1.42015	-6.4040(-10)
8	1.22606	4.15385	7.90857	8.24843	-0.86100	1.49352	-9.2847(-11)
9	1.14186	4.00626	8.71710	9.10307	-0.82821	2.32332	-5.0586(-11)
10	1.01313	5.37303	9.87533	10.05665	-0.05319	2.35571	-3.4488(-10)

Table A2.26:  $5^1\text{D}$  parallelotope parameters and virial scaling coefficients.

Z	A <sub>1</sub>	A <sub>2</sub>	B <sub>1</sub>	B <sub>2</sub>	G <sub>1</sub>	G <sub>2</sub>	1- $\eta$
2	0.14893	0.29346	2.00121	1.99503	-0.09107	0.57892	9.5079(-9)
3	0.23055	0.71707	2.99301	3.02205	-0.22549	0.74647	5.8837(-8)
4	0.31278	1.08509	4.02130	3.99755	-0.00947	0.89347	2.6285(-9)
5	0.47616	1.38289	4.98927	5.03237	-0.40697	1.35137	1.1966(-8)
6	0.61372	1.70560	5.98516	6.03662	-0.50107	1.61642	1.5218(-10)
7	0.74951	2.02949	6.98140	7.03957	-0.59457	1.88310	-7.1759(-12)
8	0.43109	3.45883	7.97850	8.01072	-0.01951	1.53925	3.7140(-8)
9	1.29365	1.92322	8.95834	9.01739	-0.11723	3.34469	4.5075(-9)
10	0.64061	4.20450	9.96902	10.01677	-0.02505	2.10102	1.3916(-8)

Table A2.27:  $5^3D$  parallelotope parameters and virial scaling coefficients.

Z	A <sub>1</sub>	A <sub>2</sub>	B <sub>1</sub>	B <sub>2</sub>	G <sub>1</sub>	G <sub>2</sub>	1- $\eta$
2	0.10700	0.61704	1.99939	2.00131	-0.10381	0.19490	-1.0542(-9)
3	0.15085	0.93544	2.99887	3.00088	-0.00922	0.52197	1.9802(-9)
4	0.19271	1.52914	3.98381	4.00816	-0.01533	0.47933	8.4452(-8)
5	0.53680	1.26787	4.99318	5.01356	-0.47511	1.48292	1.0996(-9)
6	0.43404	2.14653	5.96492	6.01855	-0.01345	1.10153	-1.0970(-8)
7	0.38214	3.07221	6.97549	7.01236	-0.03401	0.93573	7.4335(-9)
8	0.90624	5.84066	7.97849	8.00466	-0.40518	0.20346	-1.2996(-8)
9	0.74465	3.35694	8.95824	9.02310	-0.02641	1.61170	4.1594(-10)
10	1.16389	1.96497	9.98722	10.11214	-0.28270	2.96692	-1.6963(-12)

Table A2.28:  $6^1D$  parallelotope parameters and virial scaling coefficients.

Z	A <sub>1</sub>	A <sub>2</sub>	B <sub>1</sub>	B <sub>2</sub>	G <sub>1</sub>	G <sub>2</sub>	1- $\eta$
2	0.15665	0.28043	2.00067	1.99912	-0.09503	0.35157	-1.6217(-7)
3	0.23551	0.40722	2.99914	3.00124	-0.03177	0.77252	-4.1055(-8)
4	0.30348	1.18949	3.99720	3.99857	-0.06725	0.50643	4.0763(-7)
5	0.50054	1.29250	4.99289	5.01232	-0.13240	0.70411	1.5313(-9)
6	0.34342	1.60775	5.99349	6.00865	0.00294	0.92320	2.1028(-7)
7	0.59838	2.25079	6.99278	6.99631	-0.11157	0.94682	-1.5840(-9)
8	0.98207	2.30923	7.99747	7.99529	-0.32001	1.24060	-1.5544(-7)
9	0.81098	2.91490	8.99037	8.99512	-0.14587	1.23949	4.3081(-9)
10	1.24747	1.77274	9.99424	9.97815	-0.56941	3.11063	-1.9270(-8)

Table A2.29: 6<sup>3</sup>D parallelotope parameters and virial scaling coefficients.

Z	A <sub>1</sub>	A <sub>2</sub>	B <sub>1</sub>	B <sub>2</sub>	G <sub>1</sub>	G <sub>2</sub>	1- $\eta$
2	0.15607	0.27994	2.00045	1.99889	-0.09386	0.34611	-8.4563(-8)
3	0.17105	0.46172	3.00095	2.99481	-0.08168	0.68962	9.9847(-8)
4	0.12755	2.28564	4.01177	3.98192	0.03719	-0.00737	6.5384(-9)
5	0.30240	1.75358	5.00373	5.00799	-0.31105	0.50525	4.1838(-8)
6	0.48273	1.85141	5.99138	6.01299	-0.34248	0.67706	-1.1755(-9)
7	0.79198	1.70461	6.99872	6.99985	-0.24273	1.50441	-8.2917(-8)
8	1.02710	1.48404	7.99511	8.00463	0.01452	1.72267	-1.4026(-9)
9	0.80006	2.86920	8.98823	9.01652	-0.51405	1.01334	-1.0940(-8)
10	1.29508	2.10194	10.00455	9.99392	-0.41783	2.09751	9.9869(-9)

### Appendix 3

Table A3.1: Expectation values and quality checks for the  $1^1S$  state.

Z	$\langle r^3 \rangle$	$\langle r^4 \rangle$	$\langle u^3 \rangle$	$\langle u^4 \rangle$	$1-C_{ee}$	$1-C_{en}$	$\rho(0)$	$h(0)$	$\Delta E(nE_H)$	Ref.
1	1.520( 2)	1.29( 3)	1.806( 2)	1.59( 3)	5.56(-3)	4.97(-5)	3.29105(-1)	2.73931(-2)	[ 4.7]	[2.10]
2	3.936( 0)	7.95( 0)	5.308( 0)	1.30( 1)	-2.83(-4)	-4.20(-5)	3.62087( 0)	1.06345(-1)	[ 3.4]	[2.10]
3	8.826(-1)	1.06( 0)	1.189( 0)	1.77( 0)	7.77(-4)	-3.01(-5)	1.37041( 1)	5.33733(-1)	[ 3.1]	[2.34]
4	3.284(-1)	2.81(-1)	4.405(-1)	4.71(-1)	1.28(-3)	4.13(-6)	3.43963( 1)	1.52293( 0)	[ 4.4]	[2.34]
5	1.565(-1)	1.04(-1)	2.092(-1)	1.75(-1)	2.23(-3)	-1.67(-6)	6.95175( 1)	3.31253( 0)	[ 6.0]	[2.34]
6	8.646(-2)	4.71(-2)	1.153(-1)	7.89(-2)	8.83(-4)	-2.10(-6)	1.22887( 2)	6.14110( 0)	[ 5.4]	[2.34]
7	5.270(-2)	2.43(-2)	7.014(-2)	4.07(-2)	5.44(-5)	-7.05(-6)	1.98325( 2)	1.02474( 1)	[ 3.8]	[2.34]
8	3.446(-2)	1.38(-2)	4.579(-2)	2.31(-2)	4.73(-4)	-2.63(-6)	2.99651( 2)	1.58703( 1)	[ 3.8]	[2.34]
9	2.376(-2)	8.37(-3)	3.153(-2)	1.40(-2)	4.14(-4)	-2.87(-5)	4.30686( 2)	2.32484( 1)	[ 6.5]	[2.34]
10	1.706(-2)	5.38(-3)	2.263(-2)	9.01(-3)	2.16(-3)	-1.14(-5)	5.95246( 2)	3.26207( 1)	[ 7.8]	[2.34]

Table A3.2: Expectation values and quality checks for the  $2^1S$  state.

Z	$\langle r^3 \rangle$	$\langle r^4 \rangle$	$\langle u^3 \rangle$	$\langle u^4 \rangle$	$1-C_{ee}$	$1-C_{en}$	$\rho(0)$	$h(0)$	$\Delta E(nE_H)$	Ref.
2	2.161( 2)	1.65( 3)	2.240( 2)	1.74( 3)	1.18(-2)	6.47(-5)	2.61881( 0)	8.65438(-3)	[ 16.9]	[2.10]
3	3.344( 1)	1.36( 2)	3.529( 1)	1.47( 2)	9.01(-3)	5.41(-5)	9.03746( 0)	6.42866(-2)	[ 13.2]	[2.35]
4	1.069( 1)	2.95( 1)	1.138( 1)	3.24( 1)	9.83(-3)	4.54(-5)	2.17220( 1)	2.13981(-1)	[ 15.2]	[2.35]
5	4.684( 0)	9.80( 0)	5.017( 0)	1.09( 1)	7.29(-3)	7.05(-5)	4.28209( 1)	5.04914(-1)	[ 15.3]	[2.35]
6	2.455( 0)	4.13( 0)	2.639( 0)	4.61( 0)	8.44(-3)	3.33(-5)	7.44843( 1)	9.84309(-1)	[ 11.9]	[2.35]
7	1.443( 0)	2.03( 0)	1.555( 0)	2.28( 0)	8.67(-3)	5.17(-5)	1.18859( 2)	1.69931( 0)	[ 14.5]	[2.35]
8	9.188(-1)	1.11( 0)	9.923(-1)	1.25( 0)	8.53(-3)	4.60(-5)	1.78094( 2)	2.69703( 0)	[ 14.1]	[2.35]
9	6.207(-1)	6.59(-1)	6.714(-1)	7.44(-1)	9.22(-3)	6.04(-6)	2.54342( 2)	4.02473( 0)	[ 13.3]	[2.35]
10	4.388(-1)	4.15(-1)	4.752(-1)	4.69(-1)	8.96(-3)	2.78(-6)	3.49746( 2)	5.72944( 0)	[ 14.8]	[2.35]

Table A3.3: Expectation values and quality checks for the  $2^3S$  state.

Z	$\langle x^3 \rangle$	$\langle x^4 \rangle$	$\langle u^3 \rangle$	$\langle u^4 \rangle$	$1-C_{ee}$	$1-C_{en}$	$\rho(0)$	$h''(0)$	$\Delta E(nE_H)$	Ref.
2	1.304( 2)	8.57( 2)	1.367( 2)	9.16( 2)	1.16(-3)	-5.36(-7)	2.64071( 0)	1.49081(-3)	[ 0.06]	[2.10]
3	2.402( 1)	8.80( 1)	2.552( 1)	9.63( 1)	5.07(-3)	8.55(-7)	9.12759( 0)	2.42960(-2)	[-3.5, 1.1]	[2.5]
4	8.371( 0)	2.14( 1)	8.941( 0)	2.37( 1)	5.11(-3)	-4.67(-7)	2.19259( 1)	1.42358(-1)	[-9]	[2.5]
5	3.862( 0)	7.60( 0)	4.138( 0)	8.45( 0)	-1.31(-3)	1.59(-7)	4.31839( 1)	5.22933(-1)	[-1.1]	[2.5]
6	2.093( 0)	3.35( 0)	2.246( 0)	3.74( 0)	-7.57(-4)	-3.83(-7)	7.50504( 1)	1.46605( 0)	[-2.2]	[2.5]
7	1.260( 0)	1.70( 0)	1.354( 0)	1.90( 0)	-4.04(-3)	-3.94(-7)	1.19674( 2)	3.44346( 0)	[-1.3]	[2.5]
8	8.165(-1)	9.51(-1)	8.780(-1)	1.07( 0)	-2.86(-4)	5.49(-7)	1.79203( 2)	7.13877( 0)	[-1.5]	[2.5]
9	5.591(-1)	5.74(-1)	6.017(-1)	6.44(-1)	-1.67(-3)	3.81(-7)	2.55786( 2)	1.34851( 1)	[-1.5]	[2.5]
10	3.996(-1)	3.66(-1)	4.302(-1)	4.12(-1)	-3.32(-4)	3.45(-7)	3.51571( 2)	2.37067( 1)	[-1.6]	[2.5]

Table A3.4: Expectation values and quality checks for the  $2^1P$  state.

Z	$\langle x^3 \rangle$	$\langle x^4 \rangle$	$\langle u^3 \rangle$	$\langle u^4 \rangle$	$1-C_{ee}$	$1-C_{en}$	$\rho(0)$	$h(0)$	$\Delta E(nE_H)$	Ref.
2	2.185( 2)	1.76( 3)	2.259( 2)	1.84( 3)	1.31(-2)	-1.59(-5)	2.54880( 0)	7.36242(-4)	[ 6.3]	[2.11]
3	2.777( 1)	1.12( 2)	2.923( 1)	1.20( 2)	8.17(-3)	-2.65(-5)	8.61322( 0)	9.84257(-3)	[ 2.3, 2.8]	[2.5]
4	8.231( 0)	2.20( 1)	8.731( 0)	2.41( 1)	6.62(-3)	5.03(-5)	2.04220( 1)	4.12843(-2)	[ 4.9, 5.5]	[2.5]
5	3.465( 0)	6.92( 0)	3.690( 0)	7.65( 0)	2.11(-3)	5.70(-5)	3.98846( 1)	1.10373(-1)	[ 8.1, 8.8]	[2.5]
6	1.770( 0)	2.82( 0)	1.889( 0)	3.14( 0)	1.24(-3)	5.34(-5)	6.89107( 1)	2.32715(-1)	[ 8.0, 9.0]	[2.5]
7	1.022( 0)	1.35( 0)	1.093( 0)	1.51( 0)	5.26(-3)	4.41(-5)	1.09410( 2)	4.24018(-1)	[-13.3,-12.2]	[2.5]
8	6.429(-1)	7.29(-1)	6.876(-1)	8.17(-1)	7.96(-4)	4.74(-5)	1.63292( 2)	6.99848(-1)	[ 9.9, 11.1]	[2.5]
9	4.301(-1)	4.26(-1)	4.603(-1)	4.79(-1)	2.99(-3)	-6.99(-6)	2.32471( 2)	1.07609( 0)	[ 6.3, 7.7]	[2.5]
10	3.017(-1)	2.65(-1)	3.230(-1)	2.99(-1)	2.83(-3)	-7.07(-6)	3.18849( 2)	1.56832( 0)	[ 7.0, 8.5]	[2.5]

Table A3.5: Expectation values and quality checks for the  $2^3P$  state.

Z	$\langle r^3 \rangle$	$\langle r^4 \rangle$	$\langle u^3 \rangle$	$\langle u^4 \rangle$	$1-C_{ee}$	$1-C_{en}$	$\rho(0)$	$h''(0)$	$\Delta E(nE_H)$	Ref.
2	1.698( 2)	1.28( 3)	1.770( 2)	1.35( 3)	2.69(-2)	2.96(-5)	2.51770( 0)	4.12194(-3)	[ 9.2]	[2.11]
3	2.217( 1)	8.37( 1)	2.384( 1)	9.22( 1)	2.11(-2)	1.05(-6)	8.47012( 0)	8.91323(-2)	[ 2.8, 3.2]	[2.5]
4	6.848( 0)	1.74( 1)	7.485( 0)	1.96( 1)	2.18(-2)	1.20(-6)	2.00954( 1)	5.62313(-1)	[ 3.6, 4.2]	[2.5]
5	2.974( 0)	5.68( 0)	3.283( 0)	6.50( 0)	1.26(-2)	5.05(-5)	3.93042( 1)	2.13056( 0)	[ 5.2, 6.0]	[2.5]
6	1.555( 0)	2.38( 0)	1.727( 0)	2.75( 0)	2.81(-2)	5.93(-6)	6.80088( 1)	6.07397( 0)	[ 5.4, 5.5]	[2.5]
7	9.135(-1)	1.17( 0)	1.019( 0)	1.36( 0)	2.95(-2)	2.73(-6)	1.08117( 2)	1.44090( 1)	[ 5.4, 5.5]	[2.5]
8	5.820(-1)	6.40(-1)	6.517(-1)	7.48(-1)	1.90(-2)	-1.20(-5)	1.61540( 2)	3.00596( 1)	[ 5.3, 5.4]	[2.5]
9	3.935(-1)	3.80(-1)	4.417(-1)	4.45(-1)	2.54(-2)	2.22(-6)	2.30186( 2)	5.70502( 1)	[ 4.5, 4.6]	[2.5]
10	2.784(-1)	2.39(-1)	3.132(-1)	2.81(-1)	2.30(-2)	-5.12(-6)	3.15967( 2)	1.00629( 2)	[ 4.8, 4.9]	[2.5]

Table A3.6: Expectation values and quality checks for the  $3^1S$  state.

Z	$\langle r^3 \rangle$	$\langle r^4 \rangle$	$\langle u^3 \rangle$	$\langle u^4 \rangle$	$1-C_{ee}$	$1-C_{en}$	$\rho(0)$	$h(0)$	$\Delta E(nE_H)$	Ref.
2	2.593( 3)	4.23( 4)	2.612( 3)	4.27( 4)	2.90(-2)	4.65(-6)	2.56624( 0)	2.43861(-3)	[ 17.2]	[2.8]
3	3.717( 2)	3.16( 3)	3.759( 2)	3.22( 3)	3.71(-2)	5.77(-6)	8.71990( 0)	1.87987(-2)	[-746,-290]	[2.5]
4	1.156( 2)	6.65( 2)	1.171( 2)	6.79( 2)	1.80(-2)	1.17(-5)	2.07600( 1)	6.28128(-2)	[-3878,-3294]	[2.5]
5	4.995( 1)	2.17( 2)	5.071( 1)	2.22( 2)	2.26(-2)	1.26(-5)	4.06669( 1)	1.48165(-1)	[-3574,-3501]	[2.5]
6	2.596( 1)	9.07( 1)	2.638( 1)	9.30( 1)	2.18(-2)	9.04(-6)	7.04218( 1)	2.88311(-1)	[-3429,-3341]	[2.5]
7	1.517( 1)	4.43( 1)	1.543( 1)	4.55( 1)	2.21(-2)	7.53(-6)	1.12005( 2)	4.96805(-1)	[-3369,-3266]	[2.5]
8	9.623( 0)	2.41( 1)	9.791( 0)	2.48( 1)	2.21(-2)	8.43(-6)	1.67396( 2)	7.87141(-1)	[-3289,-3171]	[2.5]
9	6.482( 0)	1.43( 1)	6.598( 0)	1.46( 1)	1.80(-2)	2.34(-5)	2.38577( 2)	1.17279( 0)	[-3235,-3102]	[2.5]
10	4.571( 0)	8.95( 0)	4.655( 0)	9.20( 0)	1.55(-2)	-2.27(-6)	3.27532( 2)	1.66730( 0)	[-3220,-3073]	[2.5]

Table A3.7: Expectation values and quality checks for the  $3^3S$  state.

Z	$\langle r^3 \rangle$	$\langle r^4 \rangle$	$\langle u^3 \rangle$	$\langle u^4 \rangle$	$1-C_{ee}$	$1-C_{en}$	$\rho(0)$	$h''(0)$	$\Delta E(nE_H)$	Ref.
2	1.862( 3)	2.74( 4)	1.878( 3)	2.77( 4)	-1.37(-3)	1.38(-5)	2.57010( 0)	4.12437(-4)	[-0.67, 0.24]	[2.8]
3	2.990( 2)	2.37( 3)	3.029( 2)	2.42( 3)	8.28(-3)	1.26(-6)	8.73770( 0)	7.54296(-3)	[-7.8,-3.3]	[2.5]
4	9.846( 1)	5.38( 2)	9.994( 1)	5.51( 2)	1.02(-2)	2.02(-6)	2.08016( 1)	4.64318(-2)	[-15.5,-14.9]	[2.5]
5	4.403( 1)	1.84( 2)	4.475( 1)	1.88( 2)	5.22(-3)	3.06(-6)	4.07422( 1)	1.75297(-1)	[-13.5,-12.7]	[2.5]
6	2.339( 1)	7.91( 1)	2.379( 1)	8.11( 1)	4.18(-3)	1.06(-6)	7.05404( 1)	5.00096(-1)	[-12.7,-11.8]	[2.5]
7	1.389( 1)	3.94( 1)	1.413( 1)	4.05( 1)	3.86(-3)	3.15(-6)	1.12177( 2)	1.18898( 0)	[-11.6,-10.5]	[2.5]
8	8.910( 0)	2.18( 1)	9.072( 0)	2.24( 1)	1.93(-3)	-6.08(-7)	1.67632( 2)	2.48683( 0)	[-11.1,-9.9]	[2.5]
9	6.055( 0)	1.30( 1)	6.167( 0)	1.34( 1)	5.08(-4)	2.22(-6)	2.38885( 2)	4.72962( 0)	[-11.8,-10.5]	[2.5]
10	4.301( 0)	8.25( 0)	4.382( 0)	8.49( 0)	3.25(-4)	1.34(-6)	3.27919( 2)	8.35921( 0)	[-11.2,-9.7]	[2.5]

Table A3.8: Expectation values and quality checks for the  $3^1P$  state.

Z	$\langle r^3 \rangle$	$\langle r^4 \rangle$	$\langle u^3 \rangle$	$\langle u^4 \rangle$	$1-C_{ee}$	$1-C_{en}$	$\rho(0)$	$h(0)$	$\Delta E(nE_H)$	Ref.
2	2.905( 3)	4.97( 4)	2.923( 3)	5.02( 4)	2.19(-2)	2.69(-5)	2.54722( 0)	2.52656(-4)	[ 4.4, 5.3]	[2.8]
3	3.649( 2)	3.13( 3)	3.690( 2)	3.18( 3)	2.04(-2)	5.62(-6)	8.59894( 0)	3.34252(-3)	[-16.0,-11.6]	[2.5]
4	1.078( 2)	6.15( 2)	1.093( 2)	6.28( 2)	1.80(-2)	8.02(-6)	2.03820( 1)	1.38446(-2)	[-6.1,-0.3]	[2.5]
5	4.531( 1)	1.94( 2)	4.602( 1)	1.98( 2)	1.53(-2)	-4.33(-6)	3.98058( 1)	3.66325(-2)	[ 2.3, 9.6]	[2.5]
6	2.313( 1)	7.90( 1)	2.352( 1)	8.11( 1)	1.36(-2)	1.40(-5)	6.87793( 1)	7.66036(-2)	[ 6.0, 14.8]	[2.5]
7	1.336( 1)	3.80( 1)	1.360( 1)	3.90( 1)	1.36(-2)	1.22(-5)	1.09213( 2)	1.38663(-1)	[ 5.7, 16.0]	[2.5]
8	8.398( 0)	2.05( 1)	8.553( 0)	2.10( 1)	1.35(-2)	1.13(-5)	1.63017( 2)	2.27704(-1)	[ 3.1, 14.9]	[2.5]
9	5.618( 0)	1.20( 1)	5.725( 0)	1.23( 1)	1.94(-2)	-3.43(-6)	2.32103( 2)	3.48684(-1)	[ 12.1, 25.4]	[2.5]
10	3.941( 0)	7.46( 0)	4.018( 0)	7.69( 0)	1.13(-2)	-2.64(-5)	3.18380( 2)	5.06313(-1)	[ 14.3, 29.1]	[2.5]

Table A3.9: Expectation values and quality checks for the  $3^3P$  state.

Z	$\langle r^3 \rangle$	$\langle r^4 \rangle$	$\langle u^3 \rangle$	$\langle u^4 \rangle$	$1-C_{ee}$	$1-C_{en}$	$\rho(0)$	$h''(0)$	$\Delta E(nE_H)$	Ref.
2	2.464( 3)	4.01( 4)	2.482( 3)	4.06( 4)	2.01(-2)	2.90(-5)	2.53820( 0)	1.32288(-3)	[ 6.5, 7.4]	[2.8]
3	3.164( 2)	2.60( 3)	3.204( 2)	2.64( 3)	4.44(-2)	2.80(-5)	8.56118( 0)	2.79641(-2)	[ 5.4, 5.8]	[2.5]
4	9.609( 1)	5.29( 2)	9.757( 1)	5.41( 2)	4.98(-2)	3.34(-5)	2.03000( 1)	1.75887(-1)	[ 14.6, 15.2]	[2.5]
5	4.123( 1)	1.71( 2)	4.193( 1)	1.75( 2)	5.12(-2)	2.92(-5)	3.96649( 1)	6.66995(-1)	[ 20.1, 20.9]	[2.5]
6	2.136( 1)	7.12( 1)	2.175( 1)	7.31( 1)	4.97(-2)	2.67(-5)	6.85658( 1)	1.90336( 0)	[ 21.5, 22.4]	[2.5]
7	1.247( 1)	3.47( 1)	1.271( 1)	3.57( 1)	5.22(-2)	2.22(-5)	1.08913( 2)	4.52190( 0)	[ 24.3, 25.3]	[2.5]
8	7.903( 0)	1.89( 1)	8.059( 0)	1.95( 1)	5.68(-2)	2.08(-5)	1.62615( 2)	9.44808( 0)	[ 23.6, 24.8]	[2.5]
9	5.322( 0)	1.11( 1)	5.430( 0)	1.15( 1)	5.74(-2)	1.85(-5)	2.31583( 2)	1.79496( 1)	[ 24.1, 25.4]	[2.5]
10	3.753( 0)	7.00( 0)	3.831( 0)	7.22( 0)	5.32(-2)	1.62(-5)	3.17726( 2)	3.16905( 1)	[ 27.9, 29.4]	[2.5]

Table A3.10: Expectation values and quality checks for the  $3^1D$  state.

Z	$\langle r^3 \rangle$	$\langle r^4 \rangle$	$\langle u^3 \rangle$	$\langle u^4 \rangle$	$1-C_{ee}$	$1-C_{en}$	$\rho(0)$	$h(0)$	$\Delta E(nE_H)$	Ref.
2	1.694( 3)	2.54( 4)	1.710( 3)	2.57( 4)	6.02(-2)	4.03(-6)	2.54619( 0)	2.31535(-6)	[ 0.91]	[2.12]
3	2.123( 2)	1.59( 3)	2.157( 2)	1.63( 3)	4.18(-2)	4.49(-6)	8.59326( 0)	5.72886(-5)		
4	6.302( 1)	3.14( 2)	6.427( 1)	3.23( 2)	3.32(-2)	8.84(-6)	2.03699( 1)	3.10398(-4)		
5	2.662( 1)	9.96( 1)	2.721( 1)	1.03( 2)	3.48(-2)	1.05(-5)	3.97861( 1)	9.58492(-4)		
6	1.364( 1)	4.08( 1)	1.397( 1)	4.23( 1)	3.54(-2)	-2.50(-6)	6.87524( 1)	2.21695(-3)		
7	7.896( 0)	1.97( 1)	8.096( 0)	2.04( 1)	6.21(-3)	1.65(-6)	1.09178( 2)	4.30505(-3)		
8	4.974( 0)	1.06( 1)	5.105( 0)	1.10( 1)	5.58(-3)	1.97(-6)	1.62973( 2)	7.45844(-3)		
9	3.333( 0)	6.23( 0)	3.423( 0)	6.48( 0)	2.01(-2)	7.21(-6)	2.32047( 2)	1.19084(-2)		
10	2.341( 0)	3.89( 0)	2.406( 0)	4.05( 0)	2.89(-2)	-5.60(-6)	3.18313( 2)	1.78867(-2)		

Table A3.11: Expectation values and quality checks for the  $3^3D$  state.

Z	$\langle r^3 \rangle$	$\langle r^4 \rangle$	$\langle u^3 \rangle$	$\langle u^4 \rangle$	$1-C_{ee}$	$1-C_{en}$	$\rho(0)$	$h''(0)$	$\Delta E(nE_H)$	Ref.
2	1.692( 3)	2.53( 4)	1.708( 3)	2.57( 4)	1.01(-1)	2.76(-6)	2.54613( 0)	1.04326(-5)	[ 0.7]	[2.12]
3	2.117( 2)	1.58( 4)	2.151( 2)	1.62( 3)	4.44(-2)	-8.99(-7)	8.59245( 0)	5.00488(-4)		
4	6.281( 1)	3.13( 2)	6.406( 1)	3.22( 2)	4.09(-2)	1.62(-6)	2.03669( 1)	4.44245(-3)		
5	2.653( 1)	9.92( 1)	2.712( 1)	1.02( 2)	3.99(-2)	-4.49(-7)	3.97796( 1)	2.03312(-2)		
6	1.359( 1)	4.07( 1)	1.392( 1)	4.21( 1)	9.78(-3)	3.83(-7)	6.87400( 1)	6.52123(-2)		
7	7.871( 0)	1.96( 1)	8.070( 0)	2.03( 1)	1.84(-2)	-2.40(-6)	1.09158( 2)	1.68052(-1)		
8	4.959( 0)	1.06( 1)	5.089( 0)	1.10( 1)	2.03(-2)	-1.64(-7)	1.62944( 2)	3.72445(-1)		
9	3.324( 0)	6.21( 0)	3.413( 0)	6.46( 0)	3.29(-3)	-8.67(-7)	2.32008( 2)	7.39814(-1)		
10	2.335( 0)	3.88( 0)	2.399( 0)	4.04( 0)	2.68(-2)	-4.23(-6)	3.18259( 2)	1.35389( 0)		

Table A3.12: Expectation values and quality checks for the  $4^1S$  state.

Z	$\langle r^3 \rangle$	$\langle r^4 \rangle$	$\langle u^3 \rangle$	$\langle u^4 \rangle$	$1-C_{ee}$	$1-C_{en}$	$\rho(0)$	$h(0)$	$\Delta E(nE_H)$	Ref.
2	1.514( 4)	4.31( 5)	1.518( 4)	4.32( 5)	4.80(-2)	-7.15(-6)	2.55453( 0)	1.00260(-3)	[ 16.0, 17.0]	[2.8]
3	2.095( 3)	3.08( 4)	2.103( 3)	3.10( 4)	4.74(-2)	-1.28(-5)	8.64636( 0)	7.84242(-3)	[-583,-127]	[2.5]
4	6.433( 2)	6.38( 3)	6.461( 2)	6.42( 3)	2.87(-2)	1.04(-6)	2.05334( 1)	2.62734(-2)	[-8803,-8227]	[2.5]
5	2.763( 2)	2.07( 3)	2.777( 2)	2.08( 3)	3.41(-2)	5.69(-6)	4.01554( 1)	6.20042(-2)	[-8233,-7512]	[2.5]
6	1.431( 2)	8.59( 2)	1.438( 2)	8.66( 2)	3.51(-2)	3.44(-6)	6.94524( 1)	1.20650(-1)	[-8480,-7613]	[2.5]
7	8.341( 1)	4.18( 2)	8.388( 1)	4.22( 2)	3.44(-2)	1.86(-6)	1.10363( 2)	2.07849(-1)	[-8249,-7236]	[2.5]
8	5.281( 1)	2.27( 2)	5.311( 1)	2.29( 2)	3.42(-2)	2.68(-6)	1.64829( 2)	3.29248(-1)	[-8255,-7096]	[2.5]
9	3.552( 1)	1.34( 2)	3.573( 1)	1.35( 2)	3.83(-2)	1.50(-6)	2.34789( 2)	4.90540(-1)	[-7848,-6544]	[2.5]
10	2.503( 1)	8.40( 1)	2.518( 1)	8.48( 1)	3.66(-2)	-6.14(-7)	3.22183( 2)	6.97256(-1)	[-7932,-6482]	[2.5]

Table A3.13: Expectation values and quality checks for the  $4^3S$  state.

Z	$\langle r^3 \rangle$	$\langle r^4 \rangle$	$\langle u^3 \rangle$	$\langle u^4 \rangle$	$1-C_{ee}$	$1-C_{en}$	$\rho(0)$	$h''(0)$	$\Delta E(nE_H)$	Ref.
2	1.184( 4)	3.11( 5)	1.187( 4)	3.13( 5)	1.89(-2)	8.49(-6)	2.55569( 0)	1.65921(-4)	[-0.54, 0.37]	[2.8]
3	1.782( 3)	2.49( 4)	1.789( 3)	2.50( 4)	2.25(-2)	4.83(-7)	8.65215( 0)	3.17719(-3)	[-13.2, 32.3]	[2.5]
4	5.711( 2)	5.45( 3)	5.738( 2)	5.49( 3)	1.01(-2)	5.01(-6)	2.05473( 1)	1.99356(-2)	[-52.4,-46.6]	[2.5]
5	2.516( 2)	1.83( 3)	2.529( 2)	1.84( 3)	1.11(-2)	4.79(-6)	4.01810( 1)	7.61177(-2)	[-50.5,-43.3]	[2.5]
6	1.324( 2)	7.75( 2)	1.332( 2)	7.82( 2)	1.33(-2)	2.57(-6)	6.94929( 1)	2.18699(-1)	[-48.1,-39.4]	[2.5]
7	7.810( 1)	3.83( 2)	7.856( 1)	3.87( 2)	9.72(-3)	-9.70(-7)	1.10423( 2)	5.22440(-1)	[-43.5,-42.5]	[2.5]
8	4.988( 1)	2.11( 2)	5.018( 1)	2.13( 2)	8.70(-3)	1.94(-6)	1.64910( 2)	1.09659( 0)	[-41.6,-40.5]	[2.5]
9	3.377( 1)	1.25( 2)	3.398( 1)	1.26( 2)	2.68(-2)	-1.49(-6)	2.34895( 2)	2.09208( 0)	[-41.2,-39.8]	[2.5]
10	2.392( 1)	7.91( 1)	2.407( 1)	7.99( 1)	9.32(-3)	1.65(-6)	3.22316( 2)	3.70426( 0)	[-39.5,-38.1]	[2.5]

Table A3.14: Expectation values and quality checks for the  $4^1P$  state.

Z	$\langle r^3 \rangle$	$\langle r^4 \rangle$	$\langle u^3 \rangle$	$\langle u^4 \rangle$	$1-C_{ee}$	$1-C_{en}$	$\rho(0)$	$h(0)$	$\Delta E(nE_H)$	Ref.
2	1.711( 4)	5.09( 5)	1.714( 4)	5.11( 5)	2.87(-2)	-1.28(-6)	2.54682( 0)	1.11858(-4)	[ 3.2, 4.1]	[2.8]
3	2.145( 3)	3.19( 4)	2.152( 3)	3.21( 4)	3.98(-2)	1.56(-7)	8.59611( 0)	1.47505(-3)	[-237,-194]	[2.5]
4	6.336( 2)	6.29( 3)	6.364( 2)	6.33( 3)	2.36(-2)	2.83(-5)	2.03751( 1)	6.06940(-3)	[-255,-197]	[2.5]
5	2.666( 2)	1.98( 3)	2.679( 2)	2.00( 3)	4.30(-2)	-5.24(-6)	3.97945( 1)	1.60194(-2)	[-173,-101]	[2.5]
6	1.362( 2)	8.09( 2)	1.369( 2)	8.16( 2)	3.34(-2)	4.86(-6)	6.87623( 1)	3.33740(-2)	[-213,-126]	[2.5]
7	7.868( 1)	3.89( 2)	7.914( 1)	3.93( 2)	3.13(-2)	7.08(-6)	1.09190( 2)	6.02646(-2)	[-287,-186]	[2.5]
8	4.948( 1)	2.10( 2)	4.978( 1)	2.12( 2)	3.12(-2)	1.24(-5)	1.62985( 2)	9.87817(-2)	[-280,-164]	[2.5]
9	3.312( 1)	1.23( 2)	3.332( 1)	1.24( 2)	4.67(-2)	-1.50(-5)	2.32064( 2)	1.51110(-1)	[-134,-3]	[2.5]
10	2.324( 1)	7.66( 1)	2.339( 1)	7.74( 1)	4.40(-2)	-8.37(-6)	3.18328( 2)	2.19174(-1)	[-159,-14]	[2.5]

Table A3.15: Expectation values and quality checks for the  $4^3P$  state.

Z	$\langle r^3 \rangle$	$\langle r^4 \rangle$	$\langle u^3 \rangle$	$\langle u^4 \rangle$	$1-C_{ee}$	$1-C_{en}$	$\rho(0)$	$h''(0)$	$\Delta E(nE_H)$	Ref.
2	1.514( 4)	4.34( 5)	1.517( 4)	4.35( 5)	5.17(-3)	-2.33(-5)	2.54310( 0)	5.66568(-4)	[ 19.0, 20.0]	[2.8]
3	1.931( 3)	2.78( 4)	1.939( 3)	2.80( 4)	6.20(-2)	1.41(-5)	8.58091( 0)	1.19348(-2)	[ -64.7, -60.4]	[2.5]
4	5.827( 2)	5.63( 3)	5.854( 2)	5.67( 3)	5.82(-2)	9.49(-6)	2.03430( 1)	7.50842(-2)	[ -44.6, -38.8]	[2.5]
5	2.488( 2)	1.81( 3)	2.502( 2)	1.83( 3)	4.75(-2)	9.58(-6)	3.97391( 1)	2.84949(-1)	[ -34.3, -27.1]	[2.5]
6	1.285( 2)	7.50( 2)	1.292( 2)	7.56( 2)	6.03(-2)	6.68(-6)	6.86795( 1)	8.14570(-1)	[ -31.2, -22.5]	[2.5]
7	7.483( 1)	3.65( 2)	7.528( 1)	3.68( 2)	6.09(-2)	5.96(-6)	1.09074( 2)	1.93688( 0)	[ -31.6, -21.5]	[2.5]
8	4.735( 1)	1.98( 2)	4.765( 1)	2.00( 2)	6.15(-2)	5.33(-6)	1.62831( 2)	4.04974( 0)	[ -24.5, -12.9]	[2.5]
9	3.184( 1)	1.17( 2)	3.204( 1)	1.18( 2)	6.87(-2)	1.40(-5)	2.31861( 2)	7.70008( 0)	[ -20.9, -7.9]	[2.5]
10	2.243( 1)	7.31( 1)	2.258( 1)	7.38( 1)	6.23(-2)	4.47(-6)	3.18078( 2)	1.35994( 1)	[ -26.2, -11.7]	[2.5]

Table A3.16: Expectation values and quality checks for the  $4^1D$  state.

Z	$\langle r^3 \rangle$	$\langle r^4 \rangle$	$\langle u^3 \rangle$	$\langle u^4 \rangle$	$1-C_{ee}$	$1-C_{en}$	$\rho(0)$	$h(0)$	$\Delta E(nE_H)$	Ref.
2	1.306( 4)	3.61( 5)	1.309( 4)	3.63( 5)	5.99(-2)	1.09(-5)	2.54633( 0)	1.36470(-6)	[ 1.7]	[2.12]
3	1.635( 3)	2.26( 4)	1.642( 3)	2.28( 4)	8.41(-2)	7.64(-6)	8.59384( 0)	3.35037(-5)		
4	4.849( 2)	4.47( 3)	4.875( 2)	4.51( 3)	3.98(-2)	-6.15(-6)	2.03711( 1)	1.79035(-4)		
5	2.047( 2)	1.42( 3)	2.059( 2)	1.43( 3)	5.55(-2)	8.52(-6)	3.97876( 1)	5.50604(-4)		
6	1.048( 2)	5.80( 2)	1.055( 2)	5.86( 2)	4.11(-2)	6.12(-6)	6.87537( 1)	1.26805(-3)		
7	6.069( 1)	2.80( 2)	6.110( 1)	2.83( 2)	3.42(-2)	9.51(-6)	1.09179( 2)	2.45822(-3)		
8	3.822( 1)	1.51( 2)	3.849( 1)	1.53( 2)	3.84(-2)	4.57(-6)	1.62974( 2)	4.25133(-3)		
9	2.561( 1)	8.86( 1)	2.580( 1)	8.96( 1)	3.79(-2)	4.30(-6)	2.32048( 2)	6.77467(-3)		
10	1.799( 1)	5.53( 1)	1.812( 1)	5.60( 1)	3.76(-2)	3.30(-6)	3.18311( 2)	1.01590(-2)		

Table A3.17: Expectation values and quality checks for the  $4^3D$  state.

Z	$\langle r^3 \rangle$	$\langle r^4 \rangle$	$\langle u^3 \rangle$	$\langle u^4 \rangle$	$1-C_{ee}$	$1-C_{en}$	$\rho(0)$	$h''(0)$	$\Delta E(nE_H)$	Ref.
2	1.305(4)	3.61(5)	1.308(4)	3.62(5)	7.20(-2)	9.82(-6)	2.54630(0)	6.14574(-6)	[ 1.3]	[2.12]
3	1.631(3)	2.26(4)	1.638(3)	2.27(4)	8.29(-2)	-9.03(-7)	8.59343(0)	2.93917(-4)		
4	4.837(2)	4.46(3)	4.862(2)	4.49(3)	2.38(-2)	1.06(-5)	2.03693(1)	2.57688(-3)		
5	2.042(2)	1.41(3)	2.054(2)	1.42(3)	8.59(-2)	2.73(-6)	3.97841(1)	1.17889(-2)		
6	1.046(2)	5.79(2)	1.052(2)	5.84(2)	4.95(-2)	5.60(-6)	6.87472(1)	3.76617(-2)		
7	6.054(1)	2.79(2)	6.095(1)	2.82(2)	2.72(-2)	8.43(-6)	1.09169(2)	9.66915(-2)		
8	3.813(1)	1.51(2)	3.840(1)	1.52(2)	3.98(-2)	4.97(-6)	1.62959(2)	2.14046(-1)		
9	2.555(1)	8.84(1)	2.574(1)	8.93(1)	4.24(-2)	1.79(-6)	2.32027(2)	4.24598(-1)		
10	1.795(1)	5.52(1)	1.808(1)	5.58(1)	5.45(-2)	6.69(-6)	3.18282(2)	7.75811(-1)		

Table A3.18: Expectation values and quality checks for the  $5^1S$  state.

Z	$\langle r^3 \rangle$	$\langle r^4 \rangle$	$\langle u^3 \rangle$	$\langle u^4 \rangle$	$1-C_{ee}$	$1-C_{en}$	$\rho(0)$	$h(0)$	$\Delta E(nE_H)$	Ref.
2	5.936(4)	2.62(6)	5.941(4)	2.63(6)	4.14(-2)	9.19(-6)	2.55049(0)	5.04197(-4)	[ 20.2]	[2.8]
3	8.043(3)	1.82(5)	8.055(3)	1.83(5)	5.07(-2)	9.00(-6)	8.62064(0)	3.98344(-3)	[-814,-358]	[2.5]
4	2.452(3)	3.74(4)	2.456(3)	3.75(4)	6.84(-2)	-9.51(-6)	2.04540(1)	1.33970(-2)	[-13008,-12436]	[2.5]
5	1.049(3)	1.21(4)	1.052(3)	1.21(4)	7.50(-2)	-5.20(-6)	3.99754(1)	3.16240(-2)	[-13229,-12513]	[2.5]
6	5.421(2)	5.00(3)	5.433(2)	5.02(3)	4.95(-2)	2.32(-6)	6.91100(1)	6.14699(-2)	[-12940,-12080]	[2.5]
7	3.156(2)	2.43(3)	3.163(2)	2.44(3)	7.06(-2)	7.80(-7)	1.09783(2)	1.05985(-1)	[-12888,-11884]	[2.5]
8	1.996(2)	1.32(3)	2.001(2)	1.32(3)	8.27(-2)	-5.86(-6)	1.63921(2)	1.67930(-1)	[-12232,-11083]	[2.5]
9	1.341(2)	7.77(2)	1.345(2)	7.80(2)	6.82(-2)	1.71(-6)	2.33446(2)	2.50056(-1)	[-12112,-10819]	[2.5]
10	9.445(1)	4.87(2)	9.470(1)	4.88(2)	8.38(-2)	-5.18(-6)	3.20287(2)	3.55545(-1)	[-12796,-11359]	[2.5]

Table A3.19: Expectation values and quality checks for the  $5^3S$  state.

Z	$\langle x^3 \rangle$	$\langle x^4 \rangle$	$\langle u^3 \rangle$	$\langle u^4 \rangle$	$1-C_{ee}$	$1-C_{en}$	$\rho(0)$	$h''(0)$	$\Delta E(nE_H)$	Ref.
2	4.882( 4)	2.02( 6)	4.887( 4)	2.03( 6)	2.91(-2)	8.49(-6)	2.55099( 0)	8.21772(-5)	[ 0.86]	[2.8]
3	7.072( 3)	1.54( 5)	7.083( 3)	1.54( 5)	2.44(-2)	1.38(-6)	8.62317( 0)	1.61409(-3)	[-128, 328]	[2.5]
4	2.230( 3)	3.30( 4)	2.235( 3)	3.31( 4)	8.97(-3)	4.26(-6)	2.04600( 1)	1.02348(-2)	[-75.6,-75.1]	[2.5]
5	9.740( 2)	1.09( 4)	9.761( 2)	1.10( 4)	2.38(-2)	3.02(-6)	3.99866( 1)	3.93315(-2)	[-79.1,-78.3]	[2.5]
6	5.097( 2)	4.61( 3)	5.109( 2)	4.63( 3)	2.31(-2)	2.57(-6)	6.91282( 1)	1.13424(-1)	[-80.2,-79.3]	[2.5]
7	2.995( 2)	2.27( 3)	3.002( 2)	2.28( 3)	5.30(-3)	1.16(-6)	1.09810( 2)	2.71559(-1)	[-80.2,-79.2]	[2.5]
8	1.907( 2)	1.24( 3)	1.912( 2)	1.25( 3)	2.50(-2)	1.47(-6)	1.63957( 2)	5.71424(-1)	[-80.4,-79.2]	[2.5]
9	1.289( 2)	7.36( 2)	1.292( 2)	7.39( 2)	2.35(-2)	1.96(-6)	2.33494( 2)	1.09128( 0)	[-80.8,-79.5]	[2.5]
10	9.111( 1)	4.64( 2)	9.135( 1)	4.66( 2)	2.38(-2)	1.13(-6)	3.20347( 2)	1.93513( 0)	[-80.7,-79.3]	[2.5]

Table A3.20: Expectation values and quality checks for the  $5^1P$  state.

Z	$\langle x^3 \rangle$	$\langle x^4 \rangle$	$\langle u^3 \rangle$	$\langle u^4 \rangle$	$1-C_{ee}$	$1-C_{en}$	$\rho(0)$	$h(0)$	$\Delta E(nE_H)$	Ref.
2	6.658( 4)	3.06( 6)	6.664( 4)	3.07( 6)	4.05(-2)	-3.62(-7)	2.54665( 0)	5.86593(-5)	[ 4.8]	[2.8]
3	8.340( 3)	1.92( 5)	8.352( 3)	1.92( 5)	3.68(-2)	1.00(-5)	8.59518( 0)	7.69928(-4)	[-261,-219]	[2.5]
4	2.465( 3)	3.781( 4)	2.470( 3)	3.79( 4)	3.83(-2)	1.22(-5)	2.03734( 1)	3.16500(-3)	[-158,-101]	[2.5]
5	1.038( 3)	1.19( 4)	1.040( 3)	1.20( 4)	4.27(-2)	4.12(-6)	3.97912( 1)	8.32709(-3)	[-192,-120]	[2.5]
6	5.304( 2)	4.87( 3)	5.316( 2)	4.89( 3)	4.35(-2)	2.72(-6)	6.87582( 1)	1.73353(-2)	[-216,-130]	[2.5]
7	3.065( 2)	2.35( 3)	3.073( 2)	2.36( 3)	4.41(-2)	2.07(-6)	1.09184( 2)	3.12708(-2)	[-144,-134]	[2.5]
8	1.928( 2)	1.27( 3)	1.933( 2)	1.27( 3)	4.47(-2)	1.74(-6)	1.62979( 2)	5.12131(-2)	[-141,-129]	[2.5]
9	1.291( 2)	7.41( 2)	1.294( 2)	7.43( 2)	4.52(-2)	1.56(-6)	2.32053( 2)	7.82415(-2)	[-137,-124]	[2.5]
10	9.059( 1)	4.62( 2)	9.083( 1)	4.64( 2)	4.57(-2)	1.46(-6)	3.18316( 2)	1.13435(-1)	[-140,-126]	[2.5]

Table A3.21: Expectation values and quality checks for the  $5^3P$  state.

Z	$\langle r^3 \rangle$	$\langle r^4 \rangle$	$\langle u^3 \rangle$	$\langle u^4 \rangle$	$1-C_{ee}$	$1-C_{en}$	$\rho(0)$	$h''(0)$	$\Delta E(nE_H)$	Ref.
2	6.040( 4)	2.69( 6)	6.045( 4)	2.70( 6)	7.33(-2)	9.21(-6)	2.54475( 0)	2.93218(-4)	[ 10.5]	[2.8]
3	7.675( 3)	1.72( 5)	7.687( 3)	1.72( 5)	7.97(-2)	6.55(-6)	8.58764( 0)	6.13437(-3)	[-42.3,-38.0]	[2.5]
4	2.307( 3)	3.46( 4)	2.312( 3)	3.47( 4)	9.21(-2)	1.77(-6)	2.03575( 1)	3.86445(-2)	[-23.4,-17.7]	[2.5]
5	9.828( 2)	1.11( 4)	9.849( 2)	1.11( 4)	9.35(-2)	1.36(-6)	3.97641( 1)	1.46829(-1)	[-16.5,-9.4]	[2.5]
6	5.066( 2)	4.59( 3)	5.078( 2)	4.60( 3)	9.52(-2)	1.11(-6)	6.87174( 1)	4.19719(-1)	[-14.4,-5.8]	[2.5]
7	2.946( 2)	2.23( 3)	2.954( 2)	2.24( 3)	7.03(-2)	-2.47(-6)	1.09127( 2)	9.97715(-1)	[-9.8, 0.2]	[2.5]
8	1.863( 2)	1.21( 3)	1.867( 2)	1.21( 3)	7.05(-2)	-2.06(-6)	1.62904( 2)	2.08692( 0)	[-3.3, 8.2]	[2.5]
9	1.251( 2)	7.11( 2)	1.255( 2)	7.14( 2)	7.00(-2)	-2.81(-6)	2.31956( 2)	3.96820( 0)	[-3.8, 9.1]	[2.5]
10	8.810( 1)	4.45( 2)	8.834( 1)	4.47( 2)	1.02(-1)	5.65(-6)	3.18193( 2)	7.01724( 0)	[-2.6, 11.8]	[2.5]

Table A3.22: Expectation values and quality checks for the  $5^1D$  state.

Z	$\langle r^3 \rangle$	$\langle r^4 \rangle$	$\langle u^3 \rangle$	$\langle u^4 \rangle$	$1-C_{ee}$	$1-C_{en}$	$\rho(0)$	$h(0)$	$\Delta E(nE_H)$	Ref.
2	5.633( 4)	2.47( 6)	5.638( 4)	2.48( 6)	7.51(-2)	1.83(-5)	2.54637( 0)	7.99492(-7)	[ 6.5]	[2.12]
3	7.049( 3)	1.55( 5)	7.060( 3)	1.55( 5)	1.24(-1)	-9.34(-6)	8.59416( 0)	1.95412(-5)		
4	2.090( 3)	3.06( 4)	2.094( 3)	3.07( 4)	2.00(-2)	4.47(-6)	2.03713( 1)	1.02958(-4)		
5	8.821( 2)	9.69( 3)	8.842( 2)	9.72( 3)	2.67(-2)	8.45(-6)	3.97880( 1)	3.15962(-4)		
6	4.518( 2)	3.97( 3)	4.529( 2)	3.98( 3)	9.87(-2)	-7.88(-6)	6.87548( 1)	7.31706(-4)		
7	2.615( 2)	1.91( 3)	2.622( 2)	1.92( 3)	9.78(-2)	-5.92(-6)	1.09180( 2)	1.41653(-3)		
8	1.647( 2)	1.03( 3)	1.651( 2)	1.04( 3)	8.30(-2)	4.02(-6)	1.62974( 2)	2.44227(-3)		
9	1.103( 2)	6.06( 2)	1.106( 2)	6.08( 2)	1.60(-2)	2.69(-6)	2.32048( 2)	3.87656(-3)		
10	7.749( 1)	3.78( 2)	7.772( 1)	3.80( 2)	8.79(-2)	1.57(-6)	3.18311( 2)	5.82804(-3)		

Table A3.23: Expectation values and quality checks for the  $5^3D$  state.

Z	$\langle r^3 \rangle$	$\langle r^4 \rangle$	$\langle u^3 \rangle$	$\langle u^4 \rangle$	$1-C_{ee}$	$1-C_{en}$	$\rho(0)$	$h''(0)$	$\Delta E(nE_H)$	Ref.
2	5.628( 4)	2.47( 6)	5.633( 4)	2.47( 6)	8.94(-2)	1.01(-5)	2.54638( 0)	3.60412(-6)	[ 4.6]	[2.12]
3	7.036( 3)	1.54( 5)	7.047( 3)	1.55( 5)	8.42(-2)	1.44(-5)	8.59377( 0)	1.70272(-4)		
4	2.086( 3)	3.05( 4)	2.090( 3)	3.06( 4)	1.07(-1)	5.87(-7)	2.03705( 1)	1.50023(-3)		
5	8.802( 2)	9.66( 3)	8.822( 2)	9.69( 3)	5.05(-2)	7.20(-6)	3.97860( 1)	6.79011(-3)		
6	4.508( 2)	3.96( 3)	4.519( 2)	3.97( 3)	8.82(-2)	9.38(-6)	6.87503( 1)	2.17495(-2)		
7	2.610( 2)	1.91( 3)	2.616( 2)	1.92( 3)	1.00(-1)	3.30(-6)	1.09174( 2)	5.58172(-2)		
8	1.644( 2)	1.03( 3)	1.648( 2)	1.04( 3)	7.13(-2)	7.33(-6)	1.62965( 2)	1.23213(-1)		
9	1.101( 2)	6.04( 2)	1.104( 2)	6.07( 2)	9.01(-2)	5.92(-6)	2.32035( 2)	2.44524(-1)		
10	7.736( 1)	3.77( 2)	7.758( 1)	3.79( 2)	2.07(-2)	2.24(-6)	3.18295( 2)	4.45447(-1)		

Table A3.24: Expectation values and quality checks for the  $6^1S$  state.

Z	$\langle r^3 \rangle$	$\langle r^4 \rangle$	$\langle u^3 \rangle$	$\langle u^4 \rangle$	$1-C_{ee}$	$1-C_{en}$	$\rho(0)$	$h(0)$	$\Delta E(nE_H)$	Ref.
2	1.808( 5)	1.15( 7)	1.809( 5)	1.15( 7)	5.05(-2)	-4.81(-7)	2.54878( 0)	2.88601(-4)	[ 12.9, 13.8]	[2.8]
3	2.417( 4)	7.84( 5)	2.418( 4)	7.85( 5)	8.94(-2)	-2.05(-6)	8.60945( 0)	2.29870(-3)		
4	7.331( 3)	1.60( 5)	7.338( 3)	1.60( 5)	9.45(-2)	4.49(-6)	2.04189( 1)	7.73143(-3)		
5	3.130( 3)	5.14( 4)	3.134( 3)	5.15( 4)	9.43(-2)	1.00(-5)	3.98960( 1)	1.82501(-2)		
6	1.615( 3)	2.13( 4)	1.616( 3)	2.13( 4)	9.70(-2)	-6.89(-6)	6.89604( 1)	3.55162(-2)		
7	9.390( 2)	1.03( 4)	9.401( 2)	1.03( 4)	9.60(-2)	8.26(-6)	1.09528( 2)	6.11822(-2)		
8	5.935( 2)	5.60( 3)	5.942( 2)	5.61( 3)	9.67(-2)	7.52(-6)	1.63520( 2)	9.69123(-2)		
9	3.987( 2)	3.29( 3)	3.991( 2)	3.30( 3)	9.94(-2)	-2.63(-6)	2.32857( 2)	1.44370(-1)		
10	2.806( 2)	2.06( 3)	2.809( 2)	2.07( 3)	1.02(-1)	4.47(-6)	3.19450( 2)	2.05221(-1)		

Table A3.25: Expectation values and quality checks for the  $6^3S$  state.

Z	$\langle x^3 \rangle$	$\langle x^4 \rangle$	$\langle u^3 \rangle$	$\langle u^4 \rangle$	$1-C_{ee}$	$1-C_{en}$	$\rho(0)$	$h''(0)$	$\Delta E(nE_H)$	Ref.
2	1.538( 5)	9.26( 6)	1.538(5)	9.27( 6)	4.25(-2)	-3.53(-6)	2.54902( 0)	4.65562(-5)	[ 0.49, 0.58]	[2.8]
3	2.172( 4)	6.80( 5)	2.173( 4)	6.81( 5)	4.39(-2)	-1.68(-7)	8.61075( 0)	9.28145(-4)		
4	6.777( 3)	1.44( 5)	6.783( 3)	1.44( 5)	4.69(-2)	1.59(-7)	2.04222( 1)	5.92923(-3)		
5	2.942( 3)	4.73( 4)	2.945( 3)	4.74( 4)	4.92(-2)	4.40(-7)	3.99022( 1)	2.28534(-2)		
6	1.534( 3)	1.99( 4)	1.536( 3)	1.99( 4)	3.23(-2)	1.49(-7)	6.89694( 1)	6.60043(-2)		
7	8.991( 2)	9.74( 3)	9.002( 2)	9.76( 3)	3.76(-2)	2.58(-6)	1.09542( 2)	1.58384(-1)		
8	5.715( 2)	5.322( 3)	5.722( 2)	5.33( 3)	3.51(-2)	3.31(-6)	1.63539( 2)	3.33441(-1)		
9	3.856( 2)	3.149( 3)	3.861( 2)	3.16( 3)	3.74(-2)	1.88(-6)	2.32880( 2)	6.37420(-1)		
10	2.723( 2)	1.981( 3)	2.727( 2)	1.98( 3)	3.78(-2)	2.15(-6)	3.19483( 2)	1.13109( 0)		

Table A3.26: Expectation values and quality checks for the  $6^1P$  state.

Z	$\langle x^3 \rangle$	$\langle x^4 \rangle$	$\langle u^3 \rangle$	$\langle u^4 \rangle$	$1-C_{ee}$	$1-C_{en}$	$\rho(0)$	$h(0)$	$\Delta E(nE_H)$	Ref.
2	2.009( 5)	1.32( 7)	2.009( 5)	1.32( 7)	7.69(-2)	2.11(-7)	2.54659( 0)	3.46125(-5)	[ 9.0, 9.9]	[2.8]
3	2.515( 4)	8.29( 5)	2.517( 4)	8.29( 5)	5.22(-2)	1.34(-5)	8.59476( 0)	4.51152(-4)		
4	7.436( 3)	1.63( 5)	7.443( 3)	1.63( 5)	4.95(-2)	-1.12(-6)	2.03728( 1)	1.85051(-3)		
5	3.131( 3)	5.15( 4)	3.134( 3)	5.16( 4)	5.08(-2)	2.60(-7)	3.97901( 1)	4.86156(-3)		
6	1.601( 3)	2.11( 4)	1.603( 3)	2.11( 4)	5.17(-2)	2.92(-5)	6.87549( 1)	1.01121(-2)		
7	9.254( 2)	1.01( 4)	9.265( 2)	1.02( 4)	5.17(-2)	1.07(-6)	1.09182( 2)	1.82281(-2)		
8	5.823( 2)	5.47( 3)	5.830( 2)	5.48( 3)	5.21(-2)	1.08(-6)	1.62977( 2)	2.98376(-2)		
9	3.898( 2)	3.20( 3)	3.903( 2)	3.21( 3)	5.25(-2)	8.55(-7)	2.32051( 2)	4.55665(-2)		
10	2.736( 2)	2.00( 3)	2.740( 2)	2.00( 3)	5.28(-2)	8.74(-7)	3.18313( 2)	6.60414(-2)		

Table A3.27: Expectation values and quality checks for the  $6^3P$  state.

Z	$\langle r^3 \rangle$	$\langle r^4 \rangle$	$\langle u^3 \rangle$	$\langle u^4 \rangle$	$1-C_{ee}$	$1-C_{en}$	$\rho(0)$	$h''(0)$	$\Delta E(nE_H)$	Ref.
2	1.852( 5)	1.19( 7)	1.853( 5)	1.19( 7)	9.06(-2)	7.54(-6)	2.54549( 0)	1.70292(-4)	[ 12.7, 13.7]	[2.8]
3	2.347( 4)	7.56( 5)	2.349( 4)	7.57( 5)	8.58(-2)	-9.79(-6)	8.59062( 0)	3.55460(-3)		
4	7.039( 3)	1.52( 5)	7.046( 3)	1.52( 5)	9.74(-2)	4.93(-6)	2.03636( 1)	2.24027(-2)		
5	2.994( 3)	4.85( 4)	2.997( 3)	4.86( 4)	7.89(-2)	3.69(-7)	3.97747( 1)	8.50631(-2)		
6	1.541( 3)	2.00( 4)	1.543( 3)	2.00( 4)	1.07(-1)	-1.43(-6)	6.87336( 1)	2.43584(-1)		
7	8.957( 2)	9.71( 3)	8.967( 2)	9.73( 3)	1.08(-1)	-1.16(-6)	1.09150( 2)	5.79607(-1)		
8	5.658( 2)	5.26( 3)	5.665( 2)	5.27( 3)	8.97(-2)	2.45(-6)	1.62934( 2)	1.21183( 0)		
9	3.800( 2)	3.10( 3)	3.805( 2)	3.10( 3)	8.33(-2)	2.70(-7)	2.31995( 2)	2.30435( 0)		
10	2.674( 2)	1.93( 3)	2.677( 2)	1.94( 3)	1.00(-1)	1.33(-6)	3.18243( 2)	4.07473( 0)		

Table A3.28: Expectation values and quality checks for the  $6^1D$  state.

Z	$\langle r^3 \rangle$	$\langle r^4 \rangle$	$\langle u^3 \rangle$	$\langle u^4 \rangle$	$1-C_{ee}$	$1-C_{en}$	$\rho(0)$	$h(0)$	$\Delta E(nE_H)$	Ref.
2	1.790( 5)	1.14( 7)	1.790( 5)	1.14( 7)	1.16(-1)	-1.13(-5)	2.54647( 0)	5.03401(-7)	[ 14.9]	[2.12]
3	2.239( 4)	7.13( 5)	2.241( 4)	7.14( 5)	8.92(-2)	1.53(-5)	8.59410( 0)	1.19479(-5)		
4	6.638( 3)	1.41( 5)	6.644( 3)	1.41( 5)	1.30(-1)	1.53(-5)	2.03714( 1)	6.42835(-5)		
5	2.801( 3)	4.46( 4)	2.804( 3)	4.47( 4)	2.02(-1)	-9.90(-7)	3.97886( 1)	1.98111(-4)		
6	1.435( 3)	1.83( 4)	1.436( 3)	1.83( 4)	1.71(-1)	-9.67(-7)	6.87548( 1)	4.52348(-4)		
7	8.303( 2)	8.82( 3)	8.313( 2)	8.84( 3)	1.30(-1)	1.01(-5)	1.09179( 2)	8.70546(-4)		
8	5.229( 2)	4.76( 3)	5.236( 2)	4.77( 3)	7.10(-2)	4.13(-6)	1.62974( 2)	1.49632(-3)		
9	3.503( 2)	2.79( 3)	3.508( 2)	2.80( 3)	1.30(-1)	7.98(-6)	2.32047( 2)	2.38892(-3)		
10	2.460( 2)	1.74( 3)	2.464( 2)	1.75( 3)	4.03(-2)	4.22(-6)	3.18309( 2)	3.56093(-3)		

Table A3.29: Expectation values and quality checks for the  $6^3D$  state.

Z	$\langle r^3 \rangle$	$\langle r^4 \rangle$	$\langle u^3 \rangle$	$\langle u^4 \rangle$	$1-C_{ee}$	$1-C_{en}$	$\rho(0)$	$h''(0)$	$\Delta E(nE_H)$	Ref.
2	1.788( 5)	1.14( 7)	1.789( 5)	1.14( 7)	5.26(-2)	-1.00(-5)	2.54645( 0)	2.21569(-6)	[ 9.7]	[2.12]
3	2.235( 4)	7.12( 5)	2.237( 4)	7.13( 5)	1.72(-1)	2.36(-5)	8.59390( 0)	1.05854(-4)		
4	6.626( 3)	1.41( 5)	6.632( 3)	1.41( 5)	1.66(-1)	-5.47(-6)	2.03712( 1)	9.28780(-4)		
5	2.796( 3)	4.45( 4)	2.799( 3)	4.46( 4)	7.14(-2)	8.15(-6)	3.97870( 1)	4.18225(-3)		
6	1.432( 3)	1.82( 4)	1.434( 3)	1.83( 4)	1.66(-1)	4.29(-6)	6.87522( 1)	1.34215(-2)		
7	8.289( 2)	8.80( 3)	8.299( 2)	8.82( 3)	6.52(-2)	-3.73(-8)	1.09177( 2)	3.41943(-2)		
8	5.221( 2)	4.75( 3)	5.227( 2)	4.76( 3)	7.87(-2)	-6.25(-7)	1.62970( 2)	7.56315(-2)		
9	3.498( 2)	2.79( 3)	3.503( 2)	2.79( 3)	1.60(-1)	3.61(-6)	2.32040( 2)	1.50398(-1)		
10	2.457( 2)	1.74( 3)	2.460( 2)	1.74( 3)	1.44(-1)	-4.22(-6)	3.18302( 2)	2.74046(-1)		

## Appendix 4

### Formulae for the charge density and intracule function

Formulae for the charge density  $\rho(x)$  and intracule function  $h(u)$  for the S and P states have been previously published. Thus only the D states will be considered here. For the wavefunction products required in the derivation of the  $\rho(x)$  and  $h(u)$  formulae, the D state wavefunctions are expressed in the form:

$$\begin{aligned}\Psi = & \sum_k^N C_k (1 \pm \hat{P}_{12}) r_2^2 \exp(-\alpha_k r_1) \exp(-\beta_k r_2) \exp(-\gamma_k r_{12}) Y_2^0(\Omega_2) Y_0^0(\Omega_1) \\ & + \sum_{l=1}^M D_l (1 \pm \hat{P}_{12}) r_1 r_2 \exp(-\alpha_l r_1) \exp(-\beta_l r_2) \exp(-\gamma_l r_{12}) Y(1,2)\end{aligned}$$

and

$$\begin{aligned}\Psi = & \sum_m^N C_m (1 \pm \hat{P}_{12}) r_2^2 \exp(-\alpha_m r_1) \exp(-\beta_m r_2) \exp(-\gamma_m r_{12}) Y_2^0(\Omega_2) Y_0^0(\Omega_1) \\ & + \sum_{n=1}^M D_n (1 \pm \hat{P}_{12}) r_1 r_2 \exp(-\alpha_n r_1) \exp(-\beta_n r_2) \exp(-\gamma_n r_{12}) Y(1,2)\end{aligned}$$

where

$$Y(1,2) = 2Y_1^0(\Omega_1)Y_1^0(\Omega_2) + Y_1^1(\Omega_1)Y_1^{-1}(\Omega_2) + Y_1^{-1}(\Omega_1)Y_1^1(\Omega_2)$$

Thus, summations over k and m, l and n, and k and l, result from the products of sd-sd, pp-pp, and sd-pp type terms, respectively. The charge density and intracule function are expressed in terms of

$$\begin{aligned}
 T(a,b,c,x) &= \frac{1}{32\pi^2 x^2} \int e^{-ar_1 - br_2 - cr_{12}} \delta(r_1 - x) d\vec{r}_1 d\vec{r}_2 \\
 &= \frac{e^{-ax}}{(b^2 - c^2)^2} \left[ ce^{-bx} + be^{-cx} + \frac{4bc}{(b^2 - c^2)x} (e^{-bx} - e^{-cx}) \right]
 \end{aligned}$$

and its derivatives

$$T_{mn}(a,b,c,x) = \left( \frac{-\partial}{\partial b} \right)^m \left( \frac{-\partial}{\partial c} \right)^n T(a,b,c,x)$$

$T(a, b, c, x)$  and its derivatives become numerically unstable when  $|b - c|$  is small.

Alternative formulae are derived by extracting  $e^{-bx}$  from the expressions and expanding the resulting expressions in  $(b - c)x$ . These alternate expressions, used when  $|b - c| < 0.3$ , are infinite series but converge rapidly. Computationally, the series are summed until the last term added is less than  $10^{-30}$  times the total.

For convenience, the following notation has been introduced:

$$\begin{aligned}
 a_1^{km} &= \alpha_k + \alpha_m, & a_1^{ln} &= \alpha_l + \alpha_n, & a_1^{kl} &= \alpha_k + \alpha_l \\
 b_1^{km} &= \beta_k + \beta_m, & b_1^{ln} &= \beta_l + \beta_n, & b_1^{kl} &= \beta_k + \beta_l \\
 a_2^{km} &= \alpha_k + \beta_m, & a_2^{ln} &= \alpha_l + \beta_n, & a_2^{kl} &= \alpha_k + \beta_l \\
 b_2^{km} &= \beta_k + \alpha_m, & b_2^{ln} &= \beta_l + \alpha_n, & b_2^{kl} &= \beta_k + \alpha_l \\
 g^{km} &= \gamma_k + \gamma_m, & g^{ln} &= \gamma_l + \gamma_n, & g^{kl} &= \gamma_k + \gamma_l
 \end{aligned}$$

The permutation operators  $P_{km}$ ,  $P_{\alpha_1\beta_1}$ ,  $P_{\alpha_n\beta_n}$ , have also been introduced along with the Kronecker deltas  $\delta_{km}$ ,  $\delta_{ln}$ .

The charge density is given by

$$\rho(x) = \frac{1}{8\pi} \sum_{k,m,n \leq k}^N c_k c_m (2 - \delta_{km}) (1 + P_{km}) \left[ \begin{array}{l} +4x^4 T(a_1^{km}, b_1^{km}, g^{km}, x) + 4T_{40}(b_1^{km}, a_1^{km}, g^{km}, x) \\ \pm 3x^4 T(a_2^{km}, b_2^{km}, g^{km}, x) \pm 3T_{40}(a_2^{km}, b_2^{km}, g^{km}, x) \\ \pm 3T_{40}(a_2^{km}, g^{km}, b_2^{km}, x) \mp 6x^2 T_{20}(a_2^{km}, g^{km}, b_2^{km}, x) \\ \mp 6T_{22}(a_2^{km}, b_2^{km}, g^{km}, x) \pm 2x^2 T_{20}(a_2^{km}, b_2^{km}, g^{km}, x) \end{array} \right]$$

$$+ \frac{9}{20\pi} \sum_{l,n,n \leq l}^M d_l d_n (2 - \delta_{ln}) (1 \pm P_{\alpha_l \beta_l}) (1 \pm P_{\alpha_n \beta_n}) \left[ \begin{array}{l} +18x^2 T_{20}(a_1^{ln}, b_1^{ln}, g^{ln}, x) + x^4 T(a_1^{ln}, b_1^{ln}, g^{ln}, x) \\ + T_{40}(a_1^{ln}, b_1^{ln}, g^{ln}, x) + T_{40}(a_1^{ln}, g^{ln}, b_1^{ln}, x) \\ - 2x^2 T_{20}(a_1^{ln}, g^{ln}, b_1^{ln}, x) - 2T_{22}(a_1^{ln}, b_1^{ln}, g^{ln}, x) \end{array} \right]$$

$$+ \frac{6}{\sqrt{5}\pi} \sum_{k=1}^N \sum_{l=1}^M c_k d_l (1 \pm P_{\alpha_l \beta_l}) \left[ \begin{array}{l} +x^4 T(a_1^{kl}, b_1^{kl}, g^{kl}, x) + T_{40}(b_1^{kl}, a_1^{kl}, g^{kl}, x) \\ + x^2 T_{20}(a_1^{kl}, b_1^{kl}, g^{kl}, x) + x^2 T_{20}(b_1^{kl}, a_1^{kl}, g^{kl}, x) \\ - x^2 T_{20}(a_1^{kl}, g^{kl}, b_1^{kl}, x) - T_{22}(b_1^{kl}, a_1^{kl}, g^{kl}, x) \end{array} \right]$$

The intracule density is given by

$$\begin{aligned}
 h(u) = & \frac{1}{16\pi} \sum_{k,m,m \leq k}^N c_k c_m (2 - \delta_{km}) (1 + P_{km}) \left[ \begin{array}{l} +8T(g^{km}, a_1^{km}, b_1^{km}, u) \pm 3u^4 T(g^{km}, b_2^{km}, a_2^{km}, u) \\ \pm 6T_{40}(g^{km}, a_2^{km}, b_2^{km}, u) \mp 12u^2 T_{20}(g^{km}, a_2^{km}, b_2^{km}, u) \\ \pm 2T_{22}(g^{km}, b_2^{km}, a_2^{km}, u) \end{array} \right] \\
 & + \frac{9}{40\pi} \sum_{l,n,n \leq l}^M d_l d_n (2 - \delta_{ln}) (1 \pm P_{\alpha_l \beta_l}) (1 \pm P_{\alpha_n \beta_n}) \left[ \begin{array}{l} +14T_{22}(g^{ln}, a_1^{ln}, b_1^{ln}, u) + u^4 T(g^{ln}, a_1^{ln}, b_1^{ln}, u) \\ -2u^2 T_{20}(g^{ln}, a_1^{ln}, b_1^{ln}, u) + 2T_{40}(g^{ln}, a_1^{ln}, b_1^{ln}, u) \end{array} \right] \\
 & + \frac{6}{\sqrt{5}\pi} \sum_{k=1}^N \sum_{l=1}^M c_k d_l (1 \pm P_{\alpha_l \beta_l}) \left[ \begin{array}{l} +T_{40}(g^{kl}, a_1^{kl}, b_1^{kl}, u) + T_{22}(g^{kl}, b_1^{kl}, a_1^{kl}, u) \\ -u^2 T_{20}(g^{kl}, a_1^{kl}, b_1^{kl}, u) \end{array} \right]
 \end{aligned}$$

Formulae for the partial densities and intracules of the S, P and D states have also been derived. The partial charge density is given by

$$\rho(x,y) = \frac{1}{16\pi^2 x^2 y^2} \int \Psi^* [\delta(r_1 - x) \delta(r_2 - y) + \delta(r_2 - x) \delta(r_1 - y)] \Psi d\vec{r}_1 d\vec{r}_2$$

and the partial intracule is given by

$$h(x,u) = \frac{1}{16\pi^2 x^2 u^2} \int \Psi^* [\delta(r_1 - x) \delta(r_{12} - u) + \delta(r_2 - x) \delta(r_{12} - u)] \Psi d\vec{r}_1 d\vec{r}_2$$

$\rho(x, y)$  and  $h(x, u)$  are expressed in terms of the function

$$\begin{aligned} S(a, b, c, x, y) &= \frac{1}{256\pi^3 x^2 y^2} \int e^{(-ar_1 - br_2 - cr_{12})} \delta(r_1 - x) \delta(r_2 - y) d\vec{r}_1 d\vec{r}_2 \\ &= \frac{e^{-ax} e^{-by}}{32\pi c^2} [c|x-y| e^{-c|x-y|} - c(x+y) e^{-c(x+y)} + e^{-c|x-y|} - e^{-c(x+y)}] \end{aligned}$$

and its derivatives

$$S_n(a, b, c, x, y) = \left( \frac{-\partial}{\partial c} \right)^n S(a, b, c, x, y)$$

and the abbreviations previously introduced for  $\rho(x)$  and  $h(u)$ .

For the S states:

$$\rho(x, y) = \frac{2}{\pi} \sum_{k, m, m \leq k}^N c_k c_m (2 - \delta_{km}) (1 \pm P_{\alpha_k \beta_m}) (1 \pm P_{\alpha_m \beta_m}) [S(a_1^{km}, b_1^{km}, g^{km}, x, y)]$$

$$h(x, u) = \frac{2}{\pi} \sum_{k, m, m \leq k}^N c_k c_m (2 - \delta_{km}) (1 \pm P_{\alpha_k \beta_m}) (1 \pm P_{\alpha_m \beta_m}) [S(a_1^{km}, g^{km}, b_1^{km}, x, u)]$$

For the P states:

$$\rho(x, y) = \frac{1}{\pi} \sum_{k, m, m \leq k}^N c_k c_m (2 - \delta_{km}) (1 + P_{km}) \left[ \begin{array}{l} +x^2 S(a_1^{km}, b_1^{km}, g^{km}, x, y) + y^2 S(b_1^{km}, a_1^{km}, g^{km}, x, y) \\ \pm (x^2 + y^2) S(a_2^{km}, b_2^{km}, g^{km}, x, y) \mp S_2(a_2^{km}, b_2^{km}, g^{km}, x, y) \end{array} \right]$$

$$h(x, u) = \frac{1}{\pi} \sum_{k, m, m \leq k}^N c_k c_m (2 - \delta_{km}) (1 + P_{km}) \left[ \begin{array}{l} +x^2 S(a_1^{km}, g^{km}, b_1^{km}, x, u) + S_2(b_1^{km}, g^{km}, a_1^{km}, x, u) \\ \pm (x^2 - u^2) S(a_2^{km}, g^{km}, b_2^{km}, x, u) \pm S_2(a_2^{km}, g^{km}, b_2^{km}, x, u) \end{array} \right]$$

For the D states:

$$\begin{aligned}
 \rho(x,y) = & \frac{1}{4\pi} \sum_{k,m,n \leq k}^N c_k c_m (2 - \delta_{km}) (1 + P_{km}) \left[ \begin{array}{l} +4x^4 S(a_1^{km}, b_1^{km}, g^{km}, x, y) + 4y^4 S(b_1^{km}, a_1^{km}, g^{km}, x) \\ \pm(3x^4 + 2x^2y^2 + 3y^4) S(a_2^{km}, b_2^{km}, g^{km}, x, y) \\ \mp 6(x^2 + y^2) S_2(a_2^{km}, b_2^{km}, g^{km}, x, y) \\ \pm 3S_4(a_2^{km}, b_2^{km}, g^{km}, x, y) \end{array} \right] \\
 & + \frac{9}{10\pi} \sum_{l,n, n \leq l}^M d_l d_n (2 - \delta_{ln}) (1 \pm P_{\alpha_l \beta_l}) (1 \pm P_{\alpha_n \beta_n}) \left[ \begin{array}{l} +(x^4 + 14x^2y^2 + y^4) S(a_1^{ln}, b_1^{ln}, g^{ln}, x, y) \\ + 2(x^2 + y^2) S_2(a_1^{ln}, b_1^{ln}, g^{ln}, x, y) + S_4(a_1^{ln}, b_1^{ln}, g^{ln}, x, y) \end{array} \right] \\
 & + \frac{6}{\sqrt{5}\pi} \sum_{k=1}^N \sum_{l=1}^M c_k d_l (1 \pm P_{\alpha_l \beta_l}) \left[ \begin{array}{l} +(x^4 + x^2y^2) S(a_1^{kl}, b_1^{kl}, g^{kl}, x, y) \\ - x^2 S_2(a_1^{kl}, b_1^{kl}, g^{kl}, x, y) - y^2 S_2(b_1^{kl}, a_1^{kl}, g^{kl}, x, y) \\ +(x^4 + x^2y^2) S(b_1^{kl}, a_1^{kl}, g^{kl}, x, y) \end{array} \right]
 \end{aligned}$$

$$\begin{aligned}
h(x,u) = & \frac{1}{4\pi} \sum_{k,m,m \leq k}^N c_k c_m (2 - \delta_{km}) (1 + P_{km}) \left[ \begin{array}{l} +4x^4 S(a_1^{km}, g^{km}, b_1^{km}, x, u) + 4S(b_1^{km}, g^{km}, a_1^{km}, x, u) \\ \pm 3(x^2 - u^2)^2 S(a_2^{km}, g^{km}, b_2^{km}, x, u) \\ \pm 2(x^2 - 3u^2) S_2(a_2^{km}, g^{km}, b_2^{km}, x, u) \\ \pm 3S_4(a_2^{km}, g^{km}, b_2^{km}, x, u) \end{array} \right] \\
& + \frac{9}{10\pi} \sum_{l,n,n \leq l}^M d_l d_n (2 - \delta_{ln}) (1 \pm P_{\alpha_l \beta_l}) (1 \pm P_{\alpha_n \beta_n}) \left[ \begin{array}{l} +(x^2 - u^2)^2 S(a_1^{ln}, g^{ln}, b_1^{ln}, x, u) + S_4(a_1^{ln}, g^{ln}, b_1^{ln}, x, u) \\ + 2(7x^2 - u^2) S_2(a_1^{ln}, g^{ln}, b_1^{ln}, x, u) \end{array} \right] \\
& + \frac{6}{\sqrt{5}\pi} \sum_{k=1}^N \sum_{l=1}^M c_k d_l (1 \pm P_{\alpha_l \beta_l}) \left[ \begin{array}{l} +(x^4 - x^2 u^2) S(a_1^{kl}, g^{kl}, b_1^{kl}, x, u) \\ + x^2 S_2(a_1^{kl}, g^{kl}, b_1^{kl}, x, u) + u^4 S(b_1^{kl}, g^{kl}, a_1^{kl}, x, u) \\ +(x^2 - u^2) S_2(b_1^{kl}, a_1^{kl}, g^{kl}, x, u) \end{array} \right]
\end{aligned}$$

## Appendix 5

Table A5.1: Correlation coefficients for the ground state.

$Z$	$\tau_{1/r}$	$\tau_{r^2}$	$\tau_{\bar{r}r}$
1	-0.129604	-0.151046	-0.011845
2	-0.044761	-0.082825	-0.027383
3	-0.027661	-0.052911	-0.021461
4	-0.020052	-0.038812	-0.017156
5	-0.015734	-0.030641	-0.014203
6	-0.012948	-0.025310	-0.012091
7	-0.011002	-0.021560	-0.010517
8	-0.009565	-0.018778	-0.009300
9	-0.008460	-0.016632	-0.008334
10	-0.007584	-0.014926	-0.007548
$\infty$	0	0	0

Table A5.2:  $\tau_{1/r}$  for the excited states of helium-like ions.

Z	$n^1S$	$n^3S$	$n^1P$	$n^3P$	$n^1D$	$n^3D$
<hr/>						
<i>n</i> =2						
2	-0.254498	-0.272283	-0.276928	-0.268765		
3	-0.219837	-0.263993	-0.257760	-0.248523		
4	-0.199805	-0.260426	-0.247785	-0.239465		
5	-0.187028	-0.258427	-0.241650	-0.234353		
6	-0.178232	-0.257146	-0.237496	-0.231067		
7	-0.171827	-0.256254	-0.234498	-0.228780		
8	-0.166961	-0.255598	-0.232233	-0.227096		
9	-0.163142	-0.255094	-0.230460	-0.225804		
10	-0.160067	-0.254695	-0.229037	-0.224782		
$\infty$	-0.131716	-0.251262	-0.216000	-0.216000		
<i>n</i> =3						
2	-0.301421	-0.305927	-0.308133	-0.305916	-0.308241	-0.308218
3	-0.287619	-0.299571	-0.299330	-0.297190	-0.299780	-0.299711
4	-0.279901	-0.296485	-0.294770	-0.293006	-0.295545	-0.295451
5	-0.275090	-0.294644	-0.291991	-0.290529	-0.292999	-0.292895
6	-0.271822	-0.293419	-0.290126	-0.288887	-0.291298	-0.291191
7	-0.269466	-0.292543	-0.288787	-0.287716	-0.290080	-0.289975
8	-0.267690	-0.291887	-0.287781	-0.286840	-0.289165	-0.289063
9	-0.266302	-0.291376	-0.286996	-0.286158	-0.288452	-0.288353
10	-0.265188	-0.290967	-0.286367	-0.285613	-0.287880	-0.287786
$\infty$	-0.255098	-0.287275	-0.280702	-0.280702	-0.282686	-0.282686

Table A5.2: Continued.

$Z$	$n^1S$	$n^3S$	$n^1P$	$n^3P$	$n^1D$	$n^3D$
<hr/>						
$n=4$						
2	-0.316376	-0.318168	-0.319173	-0.318274	-0.319224	-0.319211
3	-0.309294	-0.314150	-0.314237	-0.313415	-0.314456	-0.314419
4	-0.305414	-0.312161	-0.311698	-0.311040	-0.312064	-0.312017
5	-0.303009	-0.310965	-0.310154	-0.309622	-0.310624	-0.310574
6	-0.301383	-0.310165	-0.309121	-0.308676	-0.309663	-0.309611
7	-0.300212	-0.309592	-0.308381	-0.308000	-0.308974	-0.308923
8	-0.299330	-0.309161	-0.307825	-0.307493	-0.308456	-0.308407
9	-0.298641	-0.308825	-0.307391	-0.307098	-0.308053	-0.308006
10	-0.298089	-0.308556	-0.307045	-0.306781	-0.307730	-0.307685
$\infty$	-0.293086	-0.306115	-0.303917	-0.303917	-0.304795	-0.304795
$n=5$						
2	-0.322873	-0.323762	-0.324288	-0.323839	-0.324318	-0.324309
3	-0.318632	-0.321067	-0.321151	-0.320749	-0.321268	-0.321250
4	-0.316336	-0.319725	-0.319543	-0.319227	-0.319741	-0.319714
5	-0.314922	-0.318916	-0.318569	-0.318316	-0.318822	-0.318793
6	-0.313967	-0.318375	-0.317918	-0.317707	-0.318205	-0.318178
7	-0.313280	-0.317987	-0.317451	-0.317272	-0.317765	-0.317738
8	-0.312761	-0.317695	-0.317101	-0.316945	-0.317435	-0.317409
9	-0.312358	-0.317468	-0.316828	-0.316691	-0.317177	-0.317152
10	-0.312034	-0.317285	-0.316610	-0.316487	-0.316971	-0.316947
$\infty$	-0.309099	-0.315630	-0.314639	-0.314639	-0.315098	-0.315098

Table A5.2: Continued.

Z	$n^1S$	$n^3S$	$n^1P$	$n^3P$	$n^1D$	$n^3D$
<hr/>						
<i>n=6</i>						
2	-0.326252	-0.326756	-0.327063	-0.326807	-0.327078	-0.327074
3	-0.323448	-0.324839	-0.324899	-0.324671	-0.324973	-0.324959
4	-0.321946	-0.323881	-0.323792	-0.323617	-0.323910	-0.323893
5	-0.321021	-0.323304	-0.323124	-0.322984	-0.323273	-0.323256
6	-0.320396	-0.322918	-0.322681	-0.322561	-0.322846	-0.322831
7	-0.319950	-0.322641	-0.322357	-0.322258	-0.322542	-0.322525
8	-0.319613	-0.322433	-0.322117	-0.322032	-0.322312	-0.322300
9	-0.319348	-0.322271	-0.321929	-0.321854	-0.322134	-0.322121
10	-0.319139	-0.322141	-0.321780	-0.321713	-0.321992	-0.321980
$\infty$	-0.317227	-0.320960	-0.320429	-0.320429	-0.320697	-0.320697

Table A5.3:  $\tau_r$  for the excited states of helium-like ions.

Z	$n^1S$	$n^3S$	$n^1P$	$n^3P$	$n^1D$	$n^3D$
<hr/>						
<i>n</i> =3						
2	-0.763224	-0.757724	-0.744018	-0.736240	-0.748477	-0.748277
3	-0.754771	-0.753137	-0.733951	-0.728790	-0.737038	-0.736596
4	-0.750263	-0.750241	-0.728458	-0.724960	-0.730957	-0.730423
5	-0.747573	-0.748339	-0.725101	-0.722547	-0.727165	-0.726610
6	-0.745799	-0.747008	-0.722856	-0.720880	-0.724567	-0.724023
7	-0.744543	-0.746028	-0.721254	-0.719659	-0.722675	-0.722153
8	-0.743609	-0.745278	-0.720055	-0.718726	-0.721235	-0.720737
9	-0.742887	-0.744685	-0.719124	-0.717990	-0.720101	-0.719629
10	-0.742312	-0.744205	-0.718381	-0.717394	-0.719185	-0.718738
$\infty$	-0.737245	-0.739678	-0.711765	-0.711765	-0.710526	-0.710526
<hr/>						
<i>n</i> =4						
2	-0.788462	-0.786393	-0.777263	-0.774165	-0.764227	-0.764101
3	0.784438	-0.783827	-0.772618	-0.770792	-0.759407	-0.759152
4	-0.782365	-0.782291	-0.770169	-0.769049	-0.756922	-0.756628
5	-0.781148	-0.781300	-0.768701	-0.767953	-0.755394	-0.755099
6	-0.780355	-0.780612	-0.767734	-0.767197	-0.754360	-0.754073
7	-0.779799	-0.780109	-0.767050	-0.766645	-0.753609	-0.753338
8	-0.779387	-0.779725	-0.766541	-0.766224	-0.753041	-0.752787
9	-0.779069	-0.779422	-0.766148	-0.765892	-0.752596	-0.752356
10	-0.778818	-0.779177	-0.765836	-0.765624	-0.752236	-0.752012
$\infty$	-0.776621	-0.776888	-0.763104	-0.763104	-0.748892	-0.748892

Table A5.3: Continued.

Z	$n^1S$	$n^3S$	$n^1P$	$n^3P$	$n^1D$	$n^3D$
<b><math>n=5</math></b>						
2	-0.799533	-0.798527	-0.792203	-0.790661	-0.780647	-0.780576
3	-0.797149	-0.796880	-0.789541	-0.788680	-0.777985	-0.777843
4	-0.795942	-0.795931	-0.788160	-0.787661	-0.776634	-0.776468
5	-0.795238	-0.795327	-0.787340	-0.787024	-0.775808	-0.775643
6	-0.794782	-0.794911	-0.786801	-0.786587	-0.775247	-0.775091
7	-0.794461	-0.794607	-0.786422	-0.786269	-0.774844	-0.774698
8	-0.794223	-0.794376	-0.786140	-0.786027	-0.774545	-0.774405
9	-0.794041	-0.794194	-0.785923	-0.785837	-0.774304	-0.774174
10	-0.793896	-0.794048	-0.785751	-0.785684	-0.774113	-0.773991
$\infty$	-0.792635	-0.792686	-0.784251	-0.784251	-0.772340	-0.772340
<b><math>n=6</math></b>						
2	-0.805371	-0.804810	-0.800212	-0.799332	-0.791132	-0.791086
3	-0.803792	-0.803654	-0.798484	-0.798008	-0.789446	-0.789350
4	-0.802999	-0.803005	-0.797596	-0.797330	-0.788579	-0.788488
5	-0.802536	-0.802597	-0.797071	-0.796909	-0.788065	-0.787965
6	-0.802235	-0.802316	-0.796728	-0.796622	-0.787715	-0.787623
7	-0.802025	-0.802113	-0.796485	-0.796413	-0.787458	-0.787376
8	-0.801869	-0.801958	-0.796305	-0.796254	-0.787265	-0.787192
9	-0.801748	-0.801837	-0.796166	-0.796130	-0.787119	-0.787048
10	-0.801653	-0.801739	-0.796056	-0.796029	-0.787004	-0.786930
$\infty$	-0.800821	-0.800835	-0.795099	-0.795099	-0.785903	-0.785903

Table A5.4:  $\tau_{L^2}$  for the excited states of helium-like ions.

Z	$n^1S$	$n^3S$	$n^1P$	$n^3P$	$n^1D$	$n^3D$
<hr/>						
<i>n</i> =2						
2	-0.414696	-0.387463	-0.357872	-0.334251		
3	-0.413544	-0.400278	-0.348497	-0.328169		
4	-0.410293	-0.404568	-0.341822	-0.325347		
5	-0.407673	-0.406619	-0.337228	-0.323538		
6	-0.405682	-0.407796	-0.333932	-0.322257		
7	-0.404140	-0.408551	-0.331466	-0.321301		
8	-0.402923	-0.409072	-0.329556	-0.320561		
9	-0.401942	-0.409452	-0.328036	-0.319971		
10	-0.401134	-0.409741	-0.326797	-0.319489		
$\infty$	-0.392985	-0.411777	-0.314767	-0.314767		
<i>n</i> =3						
2	-0.526806	-0.515273	-0.505791	-0.496725	-0.448157	-0.447957
3	-0.528697	-0.522489	-0.503811	-0.497148	-0.446015	-0.445596
4	-0.528956	-0.524958	-0.502375	-0.497513	-0.444721	-0.444224
5	-0.528994	-0.526147	-0.501443	-0.497691	-0.443847	-0.443343
6	-0.529002	-0.526831	-0.500809	-0.497780	-0.443215	-0.442729
7	-0.529004	-0.527269	-0.500355	-0.497825	-0.442741	-0.442279
8	-0.528998	-0.527572	-0.500016	-0.497848	-0.442371	-0.441934
9	-0.529003	-0.527793	-0.499753	-0.497858	-0.442074	-0.441663
10	-0.529000	-0.527960	-0.499543	-0.497863	-0.441830	-0.441443
$\infty$	-0.529001	-0.529123	-0.497712	-0.497712	-0.439362	-0.439362

Table A5.4: Continued.

Z	$n^1S$	$n^3S$	$n^1P$	$n^3P$	$n^1D$	$n^3D$
<b><math>n=4</math></b>						
2	-0.578180	-0.572566	-0.567444	-0.563196	-0.537507	-0.537396
3	-0.579445	-0.576442	-0.566738	-0.563753	-0.537021	-0.536797
4	-0.579755	-0.577833	-0.566251	-0.564112	-0.536740	-0.536474
5	-0.579895	-0.578528	-0.565931	-0.564315	-0.536538	-0.536274
6	-0.579986	-0.578939	-0.565730	-0.564434	-0.536397	-0.536140
7	-0.580050	-0.579208	-0.565586	-0.564513	-0.536285	-0.536045
8	-0.580098	-0.579398	-0.565481	-0.564568	-0.536199	-0.535972
9	-0.580135	-0.579539	-0.565400	-0.564608	-0.536128	-0.535916
10	-0.580166	-0.579647	-0.565340	-0.564639	-0.536070	-0.535872
$\infty$	-0.580451	-0.580456	-0.564836	-0.564836	-0.535462	-0.535462
<b><math>n=5</math></b>						
2	-0.604973	-0.601901	-0.598360	-0.596077	-0.580257	-0.580206
3	-0.605755	-0.604108	-0.598050	-0.596459	-0.580100	-0.579973
4	-0.605972	-0.604921	-0.597821	-0.596699	-0.580009	-0.579862
5	-0.606073	-0.605333	-0.597680	-0.596835	-0.579942	-0.579796
6	-0.606155	-0.605580	-0.597591	-0.596919	-0.579891	-0.579752
7	-0.606205	-0.605743	-0.597530	-0.596974	-0.579853	-0.579723
8	-0.606236	-0.605859	-0.597486	-0.597014	-0.579826	-0.579703
9	-0.606273	-0.605945	-0.597453	-0.597045	-0.579801	-0.579684
10	-0.606293	-0.606012	-0.597428	-0.597068	-0.579779	-0.579671
$\infty$	-0.606524	-0.606525	-0.597238	-0.597238	-0.579556	-0.579556

Table A5.4: Continued.

Z	$n^1S$	$n^3S$	$n^1P$	$n^3P$	$n^1D$	$n^3D$
<b><math>n=6</math></b>						
2	-0.620430	-0.618588	-0.615885	-0.614523	-0.603732	-0.603695
3	-0.620926	-0.619938	-0.615723	-0.614772	-0.603695	-0.603619
4	-0.621072	-0.620442	-0.615596	-0.614939	-0.603657	-0.603584
5	-0.621150	-0.620701	-0.615524	-0.615030	-0.603606	-0.603548
6	-0.621199	-0.620857	-0.615479	-0.615087	-0.603621	-0.603534
7	-0.621238	-0.620960	-0.615447	-0.615125	-0.603600	-0.603528
8	-0.621265	-0.621034	-0.615426	-0.615152	-0.603576	-0.603521
9	-0.621286	-0.621089	-0.615410	-0.615173	-0.603578	-0.603513
10	-0.621303	-0.621132	-0.615398	-0.615189	-0.603572	-0.603507
$\infty$	-0.621464	-0.621464	-0.615312	-0.615312	-0.603474	-0.603474

Table A5.5:  $\tau_{\bar{x}/x}$  for the excited states of helium-like ions.

Z	$n^1S$	$n^3S$	$n^1P$	$n^3P$	$n^1D$	$n^3D$
<hr/>						
$n=3$						
2	-4.3170(-3)	-4.2451(-3)	-1.1768(-3)	-1.0420(-2)	-3.5986(-3)	-3.5498(-3)
3	-4.5546(-3)	-3.7580(-3)	2.9488(-3)	-1.4617(-2)	-4.2088(-3)	-4.0459(-3)
4	-4.1461(-3)	-3.1583(-3)	6.0470(-3)	-1.6061(-2)	-3.9796(-3)	-3.7484(-3)
5	-3.6894(-3)	-2.6883(-3)	8.1546(-3)	-1.6700(-2)	-3.6190(-3)	-3.3582(-3)
6	-3.2877(-3)	-2.3296(-3)	9.6385(-3)	-1.7032(-2)	-3.2728(-3)	-3.0029(-3)
7	-2.9508(-3)	-2.0514(-3)	1.0729(-2)	-1.7223(-2)	-2.9693(-3)	-2.7007(-3)
8	-2.6702(-3)	-1.8308(-3)	1.1561(-2)	-1.7342(-2)	-2.7091(-3)	-2.4465(-3)
9	-2.4349(-3)	-1.6521(-3)	1.2215(-2)	-1.7419(-2)	-2.4869(-3)	-2.2335(-3)
10	-2.2359(-3)	-1.5046(-3)	1.2742(-2)	-1.7471(-2)	-2.2948(-3)	-2.0526(-3)
$\infty$	0	0	1.7578(-2)	-1.7578(-2)	0	0
$n=4$						
2	-1.7954(-3)	-1.6870(-3)	-4.6828(-4)	-4.2928(-3)	-1.5162(-3)	-1.4867(-3)
3	-1.9371(-3)	-1.5587(-3)	1.2157(-3)	-5.9242(-3)	-1.7771(-3)	-1.6849(-3)
4	-1.7756(-3)	-1.3346(-3)	2.4402(-3)	-6.4520(-3)	-1.6856(-3)	-1.5551(-3)
5	-1.5846(-3)	-1.1480(-3)	3.2570(-3)	-6.6696(-3)	-1.5344(-3)	-1.3900(-3)
6	-1.4144(-3)	-1.0016(-3)	3.8251(-3)	-6.7731(-3)	-1.3896(-3)	-1.2415(-3)
7	-1.2709(-3)	-8.8613(-4)	4.2393(-3)	-6.8266(-3)	-1.2623(-3)	-1.1151(-3)
8	-1.1509(-3)	-7.9357(-4)	4.5535(-3)	-6.8557(-3)	-1.1524(-3)	-1.0100(-3)
9	-1.0499(-3)	-7.1802(-4)	4.7997(-3)	-6.8717(-3)	-1.0583(-3)	-9.2086(-4)
10	-9.6448(-4)	-6.5533(-4)	4.9974(-3)	-6.8804(-3)	-9.7739(-4)	-8.4514(-4)
$\infty$	0	0	6.7948(-3)	-6.7948(-3)	0	0

Table A5.5: Continued.

Z	$n^1S$	$n^3S$	$n^1P$	$n^3P$	$n^1D$	$n^3D$
<hr/>						
$n=5$						
2	-9.0869(-4)	-8.3132(-4)	-2.3372(-4)	-2.1677(-3)	-7.7521(-4)	-7.5876(-4)
3	-9.9230(-4)	-7.8644(-4)	6.1516(-4)	-2.9721(-3)	-9.0942(-4)	-8.5626(-4)
4	-9.1312(-4)	-6.8028(-4)	1.2232(-3)	-3.2261(-3)	-7.9639(-4)	-7.9007(-4)
5	-8.1642(-4)	-5.8850(-4)	1.6252(-3)	-3.3274(-3)	-7.8612(-4)	-7.0565(-4)
6	-7.2967(-4)	-5.1533(-4)	1.9034(-3)	-3.3734(-3)	-7.1242(-4)	-6.2975(-4)
7	-6.5609(-4)	-4.5708(-4)	2.1055(-3)	-3.3956(-3)	-6.4711(-4)	-5.6488(-4)
8	-5.9437(-4)	-4.1012(-4)	2.2585(-3)	-3.4066(-3)	-5.9048(-4)	-5.1172(-4)
9	-5.4254(-4)	-3.7161(-4)	2.3782(-3)	-3.4117(-3)	-5.4242(-4)	-4.6674(-4)
10	-4.9848(-4)	-3.3955(-4)	2.4742(-3)	-3.4137(-3)	-5.0124(-4)	-4.2891(-4)
$\infty$	0	0	3.3452(-3)	-3.3452(-3)	0	0
<hr/>						
$n=6$						
2	-5.2103(-4)	-4.6860(-4)	-1.3345(-4)	-1.2434(-3)	-4.4856(-4)	-4.3866(-4)
3	-5.7365(-4)	-4.4995(-4)	3.5374(-4)	-1.6993(-3)	-5.2430(-4)	-4.9526(-4)
4	-5.2929(-4)	-3.9171(-4)	6.9977(-4)	-1.8418(-3)	-5.0108(-4)	-4.5517(-4)
5	-4.7382(-4)	-3.4009(-4)	9.2749(-4)	-1.8977(-3)	-4.5282(-4)	-4.0650(-4)
6	-4.2345(-4)	-2.9848(-4)	1.0846(-3)	-1.9224(-3)	-4.1206(-4)	-3.6291(-4)
7	-3.8111(-4)	-2.6519(-4)	1.1986(-3)	-1.9339(-3)	-3.7601(-4)	-3.2564(-4)
8	-3.4539(-4)	-2.3822(-4)	1.2848(-3)	-1.9393(-3)	-3.4181(-4)	-2.9457(-4)
9	-3.1533(-4)	-2.1604(-4)	1.3521(-3)	-1.9415(-3)	-3.1542(-4)	-2.6878(-4)
10	-2.8984(-4)	-1.9755(-4)	1.4061(-3)	-1.9419(-3)	-2.9047(-4)	-2.4666(-4)
$\infty$	0	0	1.8957(-3)	-1.8957(-3)	0	0

Table A5.6:  $\tau_{\bar{x}}$  for the excited states of helium-like ions.

Z	$n^1S$	$n^3S$	$n^1P$	$n^3P$	$n^1D$	$n^3D$
<hr/>						
$n=3$						
2	-3.3982(-4)	-4.2411(-4)	-2.2208(-4)	-5.0593(-4)	-4.8866(-4)	-4.8548(-4)
3	-4.7366(-4)	-4.9276(-4)	-1.6883(-4)	-8.9567(-4)	-7.6461(-4)	-7.4690(-4)
4	-4.8443(-4)	-4.6201(-4)	-3.3290(-5)	-1.0431(-3)	-8.1394(-4)	-7.8313(-4)
5	-4.5931(-4)	-4.1744(-4)	9.1534(-5)	-1.1002(-3)	-7.8967(-4)	-7.5084(-4)
6	-4.2642(-4)	-3.7563(-4)	1.9445(-4)	-1.1217(-3)	-7.4378(-4)	-7.0092(-4)
7	-3.9368(-4)	-3.3947(-4)	2.7798(-4)	-1.1279(-3)	-6.9421(-4)	-6.4928(-4)
8	-3.6339(-4)	-3.0878(-4)	3.4631(-4)	-1.1271(-3)	-6.4659(-4)	-6.0113(-4)
9	-3.3664(-4)	-2.8271(-4)	4.0286(-4)	-1.1232(-3)	-6.0296(-4)	-5.5793(-4)
10	-3.1326(-4)	-2.6044(-4)	4.5033(-4)	-1.1177(-3)	-5.6321(-4)	-5.1942(-4)
$\infty$	0	0	9.7256(-4)	-9.7256(-4)	0	0
$n=4$						
2	-5.9297(-5)	-7.0756(-5)	-4.2589(-5)	-7.7497(-5)	-6.9278(-5)	-6.8714(-5)
3	-8.5692(-5)	-8.9529(-5)	-4.6321(-5)	-1.3174(-4)	-1.0886(-4)	-1.0650(-4)
4	-8.8040(-5)	-8.7039(-5)	-3.3431(-5)	-1.4910(-4)	-1.1643(-4)	-1.1211(-4)
5	-8.4598(-5)	-8.0228(-5)	-1.9108(-5)	-1.5353(-4)	-1.1297(-4)	-1.0787(-4)
6	-7.8830(-5)	-7.3114(-5)	-6.6093(-6)	-1.5331(-4)	-1.0666(-4)	-1.0105(-4)
7	-7.2829(-5)	-6.6669(-5)	4.0354(-6)	-1.5140(-4)	-9.9627(-5)	-9.3751(-5)
8	-6.7384(-5)	-6.1015(-5)	1.2970(-5)	-1.4893(-4)	-9.2810(-5)	-8.6999(-5)
9	-6.2654(-5)	-5.6149(-5)	2.0494(-5)	-1.4635(-4)	-8.6562(-5)	-8.0758(-5)
10	-5.8247(-5)	-5.1921(-5)	2.6928(-5)	-1.4387(-4)	-8.0930(-5)	-7.5138(-5)
$\infty$	0	0	1.0257(-4)	-1.0257(-4)	0	0

Table A5.6: Continued.

Z	$n^1S$	$n^3S$	$n^1P$	$n^3P$	$n^1D$	$n^3D$
<hr/>						
$n=5$						
2	-1.4523(-5)	-1.7674(-5)	-1.1678(-5)	-1.8501(-5)	-1.6585(-5)	-1.6415(-5)
3	-2.1816(-5)	-2.3533(-5)	-1.4312(-5)	-3.1204(-5)	-2.6052(-5)	-2.5468(-5)
4	-2.3279(-5)	-2.3353(-5)	-1.2191(-5)	-3.4858(-5)	-2.6918(-5)	-2.7063(-5)
5	-2.1888(-5)	-2.1744(-5)	-9.4224(-6)	-3.5469(-5)	-2.6990(-5)	-2.6085(-5)
6	-2.0257(-5)	-1.9959(-5)	-6.7235(-6)	-3.5024(-5)	-2.5540(-5)	-2.4474(-5)
7	-1.9575(-5)	-1.8279(-5)	-4.3595(-6)	-3.4175(-5)	-2.3843(-5)	-2.2709(-5)
8	-1.7737(-5)	-1.6797(-5)	-2.3293(-6)	-3.3311(-5)	-2.2146(-5)	-2.1141(-5)
9	-1.6645(-5)	-1.5505(-5)	-5.8850(-7)	-3.2514(-5)	-2.0612(-5)	-1.9636(-5)
10	-1.5363(-5)	-1.4366(-5)	9.1065(-7)	-3.1653(-5)	-1.9366(-5)	-1.8252(-5)
$\infty$	0	0	1.9320(-4)	-1.9320(-4)	0	0
$n=6$						
2	-4.7547(-6)	-5.6970(-6)	-3.9594(-6)	-5.7233(-6)	-5.3088(-6)	-5.2718(-6)
3	-7.1758(-6)	-7.8159(-6)	-4.9819(-6)	-9.7788(-6)	-8.0897(-6)	-8.2144(-6)
4	-7.4907(-6)	-7.8691(-6)	-4.6741(-6)	-1.0702(-5)	-8.9775(-6)	-8.6116(-6)
5	-7.4132(-6)	-7.3942(-6)	-3.9219(-6)	-1.0799(-5)	-8.6108(-6)	-8.5086(-6)
6	-7.0264(-6)	-6.8144(-6)	-2.8093(-6)	-1.0592(-5)	-8.1631(-6)	-7.9292(-6)
7	-6.4232(-6)	-6.2718(-6)	-2.4375(-6)	-1.0301(-5)	-7.7624(-6)	-7.2135(-6)
8	-5.9555(-6)	-5.7719(-6)	-1.8203(-6)	-9.8152(-6)	-6.9937(-6)	-6.7335(-6)
9	-5.6215(-6)	-5.3263(-6)	-1.2868(-6)	-9.6888(-6)	-6.7679(-6)	-6.3706(-6)
10	-5.1413(-6)	-4.9452(-6)	-8.1932(-7)	-9.4786(-6)	-6.1930(-6)	-5.8285(-6)
$\infty$	0	0	5.0887(-6)	-5.0887(-6)	0	0

Table A5.7:  $\tau_{\bar{r}_x}$  for the excited states of helium-like ions.

Z	$n^1S$	$n^3S$	$n^1P$	$n^3P$	$n^1D$	$n^3D$
<hr/>						
$n=2$						
2	-4.9369(-4)	-7.5477(-4)	-2.9849(-4)	-8.3148(-4)		
3	-8.3909(-4)	-8.8226(-4)	-8.4616(-5)	-2.3256(-3)		
4	-9.4755(-4)	-8.2062(-4)	5.2329(-4)	-3.3801(-3)		
5	-9.5396(-4)	-7.3603(-4)	1.1713(-3)	-4.0899(-3)		
6	-9.2165(-4)	-6.5851(-4)	1.7565(-3)	-4.5881(-3)		
7	-8.7538(-4)	-5.9245(-4)	2.2616(-3)	-4.9539(-3)		
8	-8.2602(-4)	-5.3694(-4)	2.6930(-3)	-5.2327(-3)		
9	-7.7802(-4)	-4.9018(-4)	3.0617(-3)	-5.4519(-3)		
10	-7.3306(-4)	-4.5050(-4)	3.3788(-3)	-5.6284(-3)		
$\infty$	0	0	7.2433(-3)	-7.2433(-3)		
$n=3$						
2	-1.8599(-5)	-2.7528(-5)	-1.4335(-5)	-2.1054(-5)	-3.0695(-5)	-3.0601(-5)
3	-3.3150(-5)	-4.1113(-5)	-2.6411(-5)	-4.5486(-5)	-6.4676(-5)	-6.3801(-5)
4	-3.7664(-5)	-4.2711(-5)	-2.8778(-5)	-5.5130(-5)	-7.7848(-5)	-7.5970(-5)
5	-3.7761(-5)	-4.0820(-5)	-2.7334(-5)	-5.7980(-5)	-8.0803(-5)	-7.8124(-5)
6	-3.6408(-5)	-3.8059(-5)	-2.4656(-5)	-5.8078(-5)	-7.9401(-5)	-7.6275(-5)
7	-3.4501(-5)	-3.5250(-5)	-2.1703(-5)	-5.6980(-5)	-7.6361(-5)	-7.2880(-5)
8	-3.2389(-5)	-3.2650(-5)	-1.8826(-5)	-5.5452(-5)	-7.2691(-5)	-6.9047(-5)
9	-3.0446(-5)	-3.0305(-5)	-1.6175(-5)	-5.3814(-5)	-6.8920(-5)	-6.5193(-5)
10	-2.8715(-5)	-2.8221(-5)	-1.3738(-5)	-5.2200(-5)	-6.5214(-5)	-6.1541(-5)
$\infty$	0	0	2.3070(-5)	-2.3070(-5)	0	0

Table A5.7: Continued.

Z	$n^1S$	$n^3S$	$n^1P$	$n^3P$	$n^1D$	$n^3D$
<hr/>						
$n=4$						
2	-1.7830(-6)	-2.4747(-6)	-1.4576(-6)	-1.8579(-6)	-2.1661(-6)	-2.1561(-6)
3	-3.3346(-6)	-4.0562(-6)	-2.9732(-6)	-3.8750(-6)	-4.5291(-6)	-4.5183(-6)
4	-3.7582(-6)	-4.3836(-6)	-3.5119(-6)	-4.5999(-6)	-5.4609(-6)	-5.3870(-6)
5	-3.9002(-6)	-4.2800(-6)	-3.5632(-6)	-4.7525(-6)	-5.6374(-6)	-5.5707(-6)
6	-3.7837(-6)	-4.0451(-6)	-3.4536(-6)	-4.6497(-6)	-5.5561(-6)	-5.4618(-6)
7	-3.5761(-6)	-3.7821(-6)	-3.2665(-6)	-4.4731(-6)	-5.3391(-6)	-5.2309(-6)
8	-3.3744(-6)	-3.5245(-6)	-3.0601(-6)	-4.2704(-6)	-5.0657(-6)	-4.9651(-6)
9	-3.2104(-6)	-3.2898(-6)	-2.8406(-6)	-4.0723(-6)	-4.7975(-6)	-4.6897(-6)
10	-3.0097(-6)	-3.0755(-6)	-2.6439(-6)	-3.8736(-6)	-4.5422(-6)	-4.4221(-6)
$\infty$	0	0	6.3896(-7)	-6.3896(-7)	0	0
$n=5$						
2	-2.5106(-7)	-3.7989(-7)	-2.4562(-7)	-2.8122(-7)	-3.1581(-7)	-3.1201(-7)
3	-5.0435(-7)	-6.6311(-7)	-5.0905(-7)	-6.0575(-7)	-6.5505(-7)	-6.5304(-7)
4	-6.3092(-7)	-7.3354(-7)	-6.0654(-7)	-7.1979(-7)	-7.7739(-7)	-7.9205(-7)
5	-6.0577(-7)	-7.2150(-7)	-6.3264(-7)	-7.4101(-7)	-8.1641(-7)	-8.1865(-7)
6	-5.7693(-7)	-6.8743(-7)	-6.1784(-7)	-7.2434(-7)	-8.0241(-7)	-8.0590(-7)
7	-6.2341(-7)	-6.4604(-7)	-5.8984(-7)	-6.8850(-7)	-7.6922(-7)	-7.7176(-7)
8	-5.4649(-7)	-6.0475(-7)	-5.5768(-7)	-6.5465(-7)	-7.2961(-7)	-7.3801(-7)
9	-5.3316(-7)	-5.6700(-7)	-5.2523(-7)	-6.2551(-7)	-6.8541(-7)	-6.9548(-7)
10	-4.8848(-7)	-5.3094(-7)	-4.9420(-7)	-5.8652(-7)	-6.6016(-7)	-6.5063(-7)
$\infty$	0	0	4.5354(-8)	-4.5354(-8)	0	0

Table A5.7: Continued.

Z	$n^1S$	$n^3S$	$n^1P$	$n^3P$	$n^1D$	$n^3D$
<hr/>						
<i>n</i> =6						
2	-5.5436(-8)	-8.1713(-8)	-5.4305(-8)	-5.7308(-8)	-6.9037(-8)	-6.8877(-8)
3	-1.1065(-7)	-1.4685(-7)	-1.0677(-7)	-1.3453(-7)	-1.3025(-7)	-1.4175(-7)
4	-1.2827(-7)	-1.6561(-7)	-1.3599(-7)	-1.5135(-7)	-1.7073(-7)	-1.6868(-7)
5	-1.4337(-7)	-1.6553(-7)	-1.4300(-7)	-1.5543(-7)	-1.7656(-7)	-1.8595(-7)
6	-1.4483(-7)	-1.5876(-7)	-1.2271(-7)	-1.5200(-7)	-1.7323(-7)	-1.7786(-7)
7	-1.3247(-7)	-1.5006(-7)	-1.3545(-7)	-1.4619(-7)	-1.7283(-7)	-1.6016(-7)
8	-1.2533(-7)	-1.4067(-7)	-1.2879(-7)	-1.2792(-7)	-1.5366(-7)	-1.5523(-7)
9	-1.2368(-7)	-1.3112(-7)	-1.2203(-7)	-1.3201(-7)	-1.5777(-7)	-1.5397(-7)
10	-1.1020(-7)	-1.2324(-7)	-1.1523(-7)	-1.2981(-7)	-1.4052(-7)	-1.3720(-7)
$\infty$	0	0	5.5094(-9)	-5.5094(-9)	0	0

## Appendix 6

Formulae for the S→P and P→D dipole oscillator strengths and  
the S→D, P→P, D→D quadrupole oscillator strengths

Only the length formulation of the dipole(DOS) and quadrupole(QOS) oscillator strength formulae are presented in this appendix. For convenience, the linear and nonlinear parameters in the wavefunctions representing the initial and final states are subscripted with a 0 and a 1, respectively. Therefore, the initial S, P, and D state wavefunctions are written

$$\Psi = \sum_{k0}^{N0} C_{k0}(1 \pm \hat{P}_{12}) \exp(-\alpha_{k0} r_1) \exp(-\beta_{k0} r_2) \exp(-\gamma_{k0} r_{12}) Y_0^0(1) Y_0^0(2)$$

$$\Psi = \sum_{k0}^{N0} C_{k0}(1 \pm \hat{P}_{12}) r_1 \exp(-\alpha_{k0} r_1) \exp(-\beta_{k0} r_2) \exp(-\gamma_{k0} r_{12}) Y_1^0(1) Y_0^0(2)$$

and

$$\begin{aligned} \Psi = & \sum_{k0}^{N0} C_{k0}(1 \pm \hat{P}_{12}) r_1^2 \exp(-\alpha_{k0} r_1) \exp(-\beta_{k0} r_2) \exp(-\gamma_{k0} r_{12}) Y_2^0(\Omega_1) Y_0^0(\Omega_2) \\ & + \sum_{k0=N0+1}^{N0+M0} D_{k0}(1 \pm \hat{P}_{12}) r_1 r_2 \exp(-\alpha_{k0} r_1) \exp(-\beta_{k0} r_2) \exp(-\gamma_{k0} r_{12}) Y(1,2) \end{aligned}$$

where

$$Y(1,2) = 2Y_1^0(\Omega_1) Y_1^0(\Omega_2) + Y_1^1(\Omega_1) Y_1^{-1}(\Omega_2) + Y_1^{-1}(\Omega_1) Y_1^1(\Omega_2)$$

and the final S, P, and D states wavefunctions are written

$$\Psi = \sum_{kl}^{NI} C_{kl}(1 \pm \hat{P}_{12}) \exp(-\alpha_{kl} r_1) \exp(-\beta_{kl} r_2) \exp(-\gamma_{kl} r_{12}) Y_0^0(1) Y_0^0(2)$$

$$\Psi = \sum_{kl}^{NI} C_{kl}(1 \pm \hat{P}_{12}) r_1 \exp(-\alpha_{kl} r_1) \exp(-\beta_{kl} r_2) \exp(-\gamma_{kl} r_{12}) Y_1^0(1) Y_0^0(2)$$

and

$$\begin{aligned} \Psi &= \sum_{kl}^{NI} C_{kl}(1 \pm \hat{P}_{12}) r_1^2 \exp(-\alpha_{kl} r_1) \exp(-\beta_{kl} r_2) \exp(-\gamma_{kl} r_{12}) Y_2^0(\Omega_1) Y_0^0(\Omega_2) \\ &\quad + \sum_{kl=NI+1}^{NI+MI} D_{kl}(1 \pm \hat{P}_{12}) r_1 r_2 \exp(-\alpha_{kl} r_1) \exp(-\beta_{kl} r_2) \exp(-\gamma_{kl} r_{12}) Y(1,2) \end{aligned}$$

where

$$Y(1,2) = 2Y_1^0(\Omega_1)Y_1^0(\Omega_2) + Y_1^1(\Omega_1)Y_1^{-1}(\Omega_2) + Y_1^{-1}(\Omega_1)Y_1^1(\Omega_2)$$

In reduced tensor notation, the length formulation of the DOS and QOS are given respectively by:

$$DOS = \frac{2}{3} \frac{(E_1 - E_0)}{(2L+1)} \left| \left\langle \gamma L \left| \sum_i \vec{r}_i \right| \gamma' L' \right\rangle \right|^2$$

and

$$QOS = \frac{(E_1 - E_0)^3}{30\alpha^2(2L+1)} \left| \left\langle \gamma L \left| \sum_i \vec{r}_i^2 \right| \gamma' L' \right\rangle \right|^2$$

where  $\alpha$  is the fine structure constant,  $L$  and  $L'$  are the angular momentum quantum numbers of the initial and final states, respectively, and the  $\gamma$ 's denote the collection of all other quantum numbers.  $E_0$  and  $E_1$  are the initial and final state energies, respectively. Using the Wigner-Eckart theorem, these may be reexpressed as

$$DOS = \frac{\frac{2}{3} \frac{(E_1 - E_0)}{(2L+1)} \left| \left\langle \gamma LM_L \left| \sum_i r_i P_1(\cos\theta_i) \right| \gamma' L' M'_L \right\rangle \right|^2}{\begin{pmatrix} L' & 1 & L \\ -M'_L & 0 & M_L \end{pmatrix}^2}$$

$$QOS = \frac{\frac{(E_1 - E_0)^3}{30\alpha^2(2L+1)} \left| \left\langle \gamma LM_L \left| \sum_i r_i^2 P_2(\cos\theta_i) \right| \gamma' L' M'_L \right\rangle \right|^2}{\begin{pmatrix} L' & 2 & L \\ -M'_L & 0 & M_L \end{pmatrix}^2}$$

where

$$\begin{pmatrix} a & b & c \\ d & e & f \end{pmatrix}$$

is a Wigner  $3-j$  symbol. For the wavefunctions considered in this work  $M_L = M'_L = 0$ .

The formulae presented in this appendix are for the dipole (DTM) and quadrupole (QTM) transition moments given respectively by

$$DTM = \left\langle \gamma LM_L \left| \sum_i r_i P_1(\cos\theta_i) \right| \gamma' L' M'_L \right\rangle$$

and

$$QTM = \left\langle \gamma LM_L \left| \sum_i r_i^2 P_2(\cos\theta_i) \right| \gamma' L' M'_L \right\rangle$$

Clearly, the DOS and QOS are easily obtained from the DTM and QTM, respectively.

The expressions for the DTM and QTM are expanded in terms of the integral  $F(a, b, c, L, M, N)$  given by

$$F(a,b,c,L,M,\lambda) = \int e^{-ar_1} e^{-br_2} e^{-cr_{12}} r_1^L r_2^M Y_\lambda^0(\Omega_1) Y_\lambda^0(\Omega_2) d\vec{r}_1 d\vec{r}_2$$

where  $Y_\lambda^0$  is a spherical harmonic. The  $F(a,b,c,L,M,\lambda)$  are easily expressed, in closed form, such that  $|b-c|$  terms do not appear. Therefore these formulae are acceptable for all values of a, b, and c.

For S→P transitions the dipole transition moment is

$$DTM = \frac{i\sqrt{3}}{2\pi} \sum_{k0}^{N0} \sum_{kl}^{NI} C_{k0} C_{kl} (1 \pm \hat{P}_{\alpha_{k0}\beta_{k0}}) \begin{bmatrix} F(\alpha_{k0} + \alpha_{kl}, \beta_{k0} + \beta_{kl}, \gamma_{k0} + \gamma_{kl}, 1, 0, 0) \\ F(\beta_{k0} + \beta_{kl}, \alpha_{k0} + \alpha_{kl}, \gamma_{k0} + \gamma_{kl}, 0, 1, 1) \end{bmatrix}$$

For P→D transitions the dipole transition moment is

$$DTM = \frac{i\sqrt{3}}{2\pi\sqrt{5}} \sum_{k0}^{N0} \sum_{kl}^{NI} C_{k0} C_{kl} \begin{bmatrix} F(\alpha_{k0} + \alpha_{kl}, \beta_{k0} + \beta_{kl}, \gamma_{k0} + \gamma_{kl}, 3, 0, 0) \\ + F(\beta_{k0} + \beta_{kl}, \alpha_{k0} + \alpha_{kl}, \gamma_{k0} + \gamma_{kl}, 0, 3, 1) \\ \pm F(\alpha_{k0} + \beta_{kl}, \beta_{k0} + \alpha_{kl}, \gamma_{k0} + \gamma_{kl}, 1, 2, 2) \\ \pm F(\beta_{k0} + \alpha_{kl}, \alpha_{k0} + \beta_{kl}, \gamma_{k0} + \gamma_{kl}, 2, 1, 1) \end{bmatrix}$$

$$+ \frac{i\sqrt{3}}{10\pi} \sum_{k0}^{N0} \sum_{kl=Nl+1}^{NI+MI} C_{k0} D_{kl} (1 \pm \hat{P}_{\alpha_{k0}\beta_{kl}}) \begin{bmatrix} 6F(\alpha_{k0} + \alpha_{kl}, \beta_{k0} + \beta_{kl}, \gamma_{k0} + \gamma_{kl}, 2, 1, 1) \\ + 5F(\beta_{k0} + \beta_{kl}, \alpha_{k0} + \alpha_{kl}, \gamma_{k0} + \gamma_{kl}, 1, 2, 0) \\ + F(\beta_{k0} + \beta_{kl}, \alpha_{k0} + \alpha_{kl}, \gamma_{k0} + \gamma_{kl}, 1, 2, 2) \end{bmatrix}$$

For S→D transitions, the quadrupole transition moment is

$$QTM = \frac{1}{2\sqrt{5}\pi} \sum_{k0}^{N0} \sum_{kl}^{NI} C_{k0} C_{kl} (1 \pm \hat{P}_{\alpha_{k0}\beta_{k0}}) \begin{bmatrix} F(\alpha_{k0} + \alpha_{kl}, \beta_{k0} + \beta_{kl}, \gamma_{k0} + \gamma_{kl}, 4, 0, 0) \\ F(\beta_{k0} + \beta_{kl}, \alpha_{k0} + \alpha_{kl}, \gamma_{k0} + \gamma_{kl}, 2, 2, 2) \end{bmatrix}$$

$$+ \frac{1}{5\pi} \sum_{k0}^{N0} \sum_{kl=Nl+1}^{NI+MI} C_{k0} D_{kl} (1 \pm \hat{P}_{\alpha_{k0}\beta_{kl}}) (1 \pm \hat{P}_{\alpha_{k0}\beta_{k0}}) [F(\alpha_{k0} + \alpha_{kl}, \beta_{k0} + \beta_{kl}, \gamma_{k0} + \gamma_{kl}, 3, 1, 1)]$$

For P→P transitions, the quadrupole transition moment is

$$QTM = \frac{1}{3\pi} \sum_{k0}^{N0} \sum_{kl}^{N1} \begin{bmatrix} F(\alpha_{k0} + \alpha_{kl}, \beta_{k0} + \beta_{kl}, \gamma_{k0} + \gamma_{kl}, 4, 0, 0) \\ F(\beta_{k0} + \beta_{kl}, \alpha_{k0} + \alpha_{kl}, \gamma_{k0} + \gamma_{kl}, 2, 2, 2) \\ F(\alpha_{k0} + \beta_{kl}, \beta_{k0} + \alpha_{kl}, \gamma_{k0} + \gamma_{kl}, 3, 1, 1) \\ F(\beta_{k0} + \alpha_{kl}, \alpha_{k0} + \beta_{kl}, \gamma_{k0} + \gamma_{kl}, 3, 1, 1) \end{bmatrix}$$

For D→D transitions, the quadrupole transition moment is

$$\begin{aligned} QTM = & \frac{1}{7\pi} \sum_{k0}^{N0} \sum_{kl}^{N1} C_{k0} C_{kl} \begin{bmatrix} F(\alpha_{k0} + \alpha_{kl}, \beta_{k0} + \beta_{kl}, \gamma_{k0} + \gamma_{kl}, 6, 0, 0) \\ F(\beta_{k0} + \beta_{kl}, \alpha_{k0} + \alpha_{kl}, \gamma_{k0} + \gamma_{kl}, 2, 4, 2) \\ F(\alpha_{k0} + \beta_{kl}, \beta_{k0} + \alpha_{kl}, \gamma_{k0} + \gamma_{kl}, 4, 2, 2) \\ F(\beta_{k0} + \alpha_{kl}, \alpha_{k0} + \beta_{kl}, \gamma_{k0} + \gamma_{kl}, 4, 2, 2) \end{bmatrix} \\ & + \frac{6}{\sqrt{5}\pi} \sum_{k0}^{N0} \sum_{kl=NI+1}^{NI+MI} C_{k0} D_{kl} (1 \pm \hat{P}_{\alpha_{kl}\beta_{kl}}) \begin{bmatrix} \frac{1}{7} F(\alpha_{k0} + \alpha_{kl}, \beta_{k0} + \beta_{kl}, \gamma_{k0} + \gamma_{kl}, 5, 1, 1) \\ + \frac{1}{10} F(\beta_{k0} + \beta_{kl}, \alpha_{k0} + \alpha_{kl}, \gamma_{k0} + \gamma_{kl}, 3, 3, 1) \\ + \frac{3}{70} F(\beta_{k0} + \beta_{kl}, \alpha_{k0} + \alpha_{kl}, \gamma_{k0} + \gamma_{kl}, 3, 3, 3) \end{bmatrix} \\ & + \frac{6}{\sqrt{5}\pi} \sum_{k0=N0+1}^{N0+M0} \sum_{kl}^{N1} D_{k0} C_{kl} (1 \pm \hat{P}_{\alpha_{k0}\beta_{kl}}) \begin{bmatrix} \frac{1}{7} F(\alpha_{k0} + \alpha_{kl}, \beta_{k0} + \beta_{kl}, \gamma_{k0} + \gamma_{kl}, 5, 1, 1) \\ + \frac{1}{10} F(\beta_{k0} + \beta_{kl}, \alpha_{k0} + \alpha_{kl}, \gamma_{k0} + \gamma_{kl}, 3, 3, 1) \\ + \frac{3}{70} F(\beta_{k0} + \beta_{kl}, \alpha_{k0} + \alpha_{kl}, \gamma_{k0} + \gamma_{kl}, 3, 3, 3) \end{bmatrix} \\ & + \frac{3}{\pi} \sum_{k0=N0+1}^{N0+M0} \sum_{kl=NI+1}^{NI+MI} D_{k0} D_{kl} (1 \pm \hat{P}_{\alpha_{k0}\beta_{kl}}) (1 \pm \hat{P}_{\alpha_{kl}\beta_{k0}}) \begin{bmatrix} \frac{1}{5} F(\alpha_{k0} + \alpha_{kl}, \beta_{k0} + \beta_{kl}, \gamma_{k0} + \gamma_{kl}, 4, 2, 0) \\ + \frac{1}{7} F(\alpha_{k0} + \alpha_{kl}, \beta_{k0} + \beta_{kl}, \gamma_{k0} + \gamma_{kl}, 4, 2, 2) \end{bmatrix} \end{aligned}$$

## Appendix 7

Table A7.1: Ground state elastic form factors for various Z-scaled momentum transfers.

$(U/Z)^2$	Z=3	Z=4	Z=5	Z=6	Z=7	Z=8	Z=9	Z=10
0.0125	1.98638	1.98462	1.98530	1.98572	1.98601	1.98622	1.98638	1.98650
0.0250	1.97290	1.96943	1.97076	1.97159	1.97216	1.97258	1.97290	1.97315
0.0375	1.95956	1.95442	1.95639	1.95762	1.95847	1.95909	1.95956	1.95993
0.0500	1.94635	1.93958	1.94217	1.94380	1.94492	1.94573	1.94635	1.94684
0.0625	1.93328	1.92492	1.92812	1.93013	1.93151	1.93252	1.93328	1.93389
0.0750	1.92035	1.91044	1.91423	1.91661	1.91825	1.91944	1.92035	1.92106
0.0875	1.90755	1.89612	1.90049	1.90323	1.90512	1.90650	1.90755	1.90837
0.1000	1.89487	1.88197	1.88690	1.89000	1.89213	1.89369	1.89487	1.89580
0.1125	1.88233	1.86799	1.87346	1.87691	1.87928	1.88101	1.88233	1.88336
0.1250	1.86991	1.85417	1.86017	1.86396	1.86656	1.86846	1.86991	1.87105
0.1375	1.85761	1.84051	1.84703	1.85114	1.85397	1.85604	1.85761	1.85885
0.1500	1.84544	1.82700	1.83403	1.83846	1.84151	1.84374	1.84544	1.84678
0.1625	1.83339	1.81365	1.82117	1.82591	1.82918	1.83157	1.83339	1.83482
0.1750	1.82146	1.80045	1.80845	1.81350	1.81698	1.81952	1.82146	1.82298
0.1875	1.80964	1.78740	1.79586	1.80121	1.80490	1.80759	1.80964	1.81126
0.2000	1.79795	1.77450	1.78341	1.78905	1.79294	1.79578	1.79795	1.79965
0.2125	1.78637	1.76174	1.77110	1.77702	1.78110	1.78409	1.78637	1.78816
0.2250	1.77490	1.74913	1.75892	1.76511	1.76939	1.77251	1.77490	1.77678
0.2375	1.76354	1.73665	1.74686	1.75333	1.75779	1.76105	1.76354	1.76550
0.250	1.75229	1.72432	1.73493	1.74166	1.74630	1.74970	1.75229	1.75434
0.300	1.70839	1.67632	1.68846	1.69617	1.70150	1.70541	1.70839	1.71074
0.350	1.66614	1.63038	1.64390	1.65249	1.65844	1.66280	1.66614	1.66877
0.400	1.62546	1.58638	1.60112	1.61052	1.61703	1.62180	1.62546	1.62834
0.450	1.58628	1.54421	1.56005	1.57016	1.57718	1.58233	1.58628	1.58939
0.500	1.54852	1.50376	1.52058	1.53134	1.53881	1.54431	1.54852	1.55184
0.550	1.51211	1.46495	1.48264	1.49398	1.50186	1.50766	1.51211	1.51563
0.600	1.47699	1.42767	1.44614	1.45800	1.46625	1.47233	1.47699	1.48068
0.650	1.44310	1.39186	1.41101	1.42334	1.43192	1.43825	1.44310	1.44695
0.700	1.41039	1.35742	1.37719	1.38992	1.39881	1.40536	1.41039	1.41437
0.750	1.37879	1.32430	1.34461	1.35770	1.36685	1.37360	1.37879	1.38289
0.800	1.34825	1.29243	1.31320	1.32662	1.33600	1.34293	1.34825	1.35247

Table A7.1: Continued.

$(U/Z)^2$	Z=3	Z=4	Z=5	Z=6	Z=7	Z=8	Z=9	Z=10
0.850	1.31874	1.26173	1.28291	1.29661	1.30620	1.31329	1.31874	1.32306
0.900	1.29020	1.23215	1.25369	1.26764	1.27741	1.28464	1.29020	1.29460
0.950	1.26258	1.20365	1.22548	1.23965	1.24958	1.25693	1.26258	1.26707
1.000	1.23586	1.17615	1.19824	1.21259	1.22267	1.23012	1.23586	1.24042
1.050	1.21000	1.14963	1.17193	1.18644	1.19663	1.20418	1.21000	1.21461
1.100	1.18494	1.12402	1.14650	1.16114	1.17143	1.17906	1.18494	1.18961
1.150	1.16067	1.09929	1.12191	1.13666	1.14704	1.15474	1.16067	1.16539
1.200	1.13715	1.07539	1.09812	1.11296	1.12341	1.13117	1.13715	1.14190
1.250	1.11435	1.05230	1.07511	1.09002	1.10053	1.10833	1.11435	1.11913
1.375	1.06029	0.99783	1.02072	1.03573	1.04633	1.05421	1.06029	1.06513
1.500	1.01013	0.94761	0.97046	0.98549	0.99611	1.00402	1.01013	1.01500
1.625	0.96350	0.90122	0.92392	0.93889	0.94949	0.95739	0.96350	0.96837
1.750	0.92006	0.85826	0.88074	0.89558	0.90612	0.91398	0.92006	0.92491
1.875	0.87954	0.81840	0.84058	0.85527	0.86570	0.87350	0.87954	0.88435
2.000	0.84167	0.78134	0.80318	0.81767	0.82798	0.83569	0.84167	0.84644
2.125	0.80622	0.74682	0.76828	0.78255	0.79271	0.80032	0.80622	0.81094
2.250	0.77300	0.71460	0.73566	0.74969	0.75969	0.76718	0.77300	0.77765
2.375	0.74181	0.68449	0.70512	0.71889	0.72872	0.73609	0.74181	0.74639
2.500	0.71250	0.65629	0.67649	0.68999	0.69963	0.70687	0.71250	0.71700
5.00	0.36538	0.33032	0.34266	0.35106	0.35715	0.36176	0.36538	0.36829
7.50	0.22250	0.20008	0.20790	0.21327	0.21719	0.22016	0.22250	0.22439
10.0	0.14985	0.13456	0.13987	0.14353	0.14621	0.14824	0.14985	0.15114
12.5	0.10783	0.09684	0.10065	0.10329	0.10521	0.10668	0.10783	0.10877
15.0	0.08134	0.07309	0.07595	0.07792	0.07937	0.08047	0.08134	0.08204
17.5	0.06355	0.05715	0.05937	0.06090	0.06202	0.06288	0.06355	0.06410
20.0	0.05103	0.04592	0.04769	0.04892	0.04981	0.05049	0.05103	0.05147
22.5	0.04188	0.03771	0.03916	0.04016	0.04089	0.04144	0.04188	0.04224
25.0	0.03499	0.03153	0.03273	0.03356	0.03417	0.03463	0.03499	0.03529
50.0	0.01013	0.00916	0.00950	0.00973	0.00990	0.01003	0.01013	0.01021
75.0	0.00474	0.00430	0.00445	0.00456	0.00464	0.00469	0.00474	0.00478
100	0.00274	0.00248	0.00257	0.00263	0.00268	0.00271	0.00274	0.00276
125	0.00178	0.00162	0.00167	0.00171	0.00174	0.00176	0.00178	0.00179

Table A7.2: Generalized oscillator strengths for the  $1^1S \rightarrow 2^1P$  for various  $Z$ -scaled momentum transfers.

$(U/Z)^2$	$Z=3$	$Z=4$	$Z=5$	$Z=6$	$Z=7$	$Z=8$	$Z=9$	$Z=10$
0.0125	4.31146(-1)	5.25010(-1)	5.81962(-1)	6.19926(-1)	6.46963(-1)	6.67163(-1)	6.82816(-1)	6.95296(-1)
0.0250	4.07318(-1)	4.99948(-1)	5.56393(-1)	5.94107(-1)	6.21005(-1)	6.41122(-1)	6.56722(-1)	6.69166(-1)
0.0375	3.85018(-1)	4.76274(-1)	5.32128(-1)	5.69537(-1)	5.96256(-1)	6.16261(-1)	6.31785(-1)	6.44176(-1)
0.0500	3.64134(-1)	4.53902(-1)	5.09092(-1)	5.46146(-1)	5.72652(-1)	5.92519(-1)	6.07948(-1)	6.20270(-1)
0.0625	3.44566(-1)	4.32750(-1)	4.87214(-1)	5.23871(-1)	5.50134(-1)	5.69839(-1)	5.85155(-1)	5.97394(-1)
0.0750	3.26218(-1)	4.12743(-1)	4.66427(-1)	5.02651(-1)	5.28644(-1)	5.48167(-1)	5.63354(-1)	5.75497(-1)
0.0875	3.09004(-1)	3.93810(-1)	4.46671(-1)	4.82429(-1)	5.08128(-1)	5.27453(-1)	5.42496(-1)	5.54533(-1)
0.1000	2.92844(-1)	3.75885(-1)	4.27887(-1)	4.63152(-1)	4.88538(-1)	5.07647(-1)	5.22535(-1)	5.34455(-1)
0.1125	2.77665(-1)	3.58908(-1)	4.10020(-1)	4.44770(-1)	4.69824(-1)	4.88705(-1)	5.03428(-1)	5.15222(-1)
0.1250	2.63400(-1)	3.42821(-1)	3.93019(-1)	4.27235(-1)	4.51943(-1)	4.70584(-1)	4.85131(-1)	4.96792(-1)
0.1375	2.49986(-1)	3.27572(-1)	3.76838(-1)	4.10503(-1)	4.34852(-1)	4.53243(-1)	4.67607(-1)	4.79128(-1)
0.1500	2.37365(-1)	3.13110(-1)	3.61430(-1)	3.94532(-1)	4.18513(-1)	4.36645(-1)	4.50818(-1)	4.62193(-1)
0.1625	2.25483(-1)	2.99391(-1)	3.46754(-1)	3.79283(-1)	4.02886(-1)	4.20753(-1)	4.34729(-1)	4.45954(-1)
0.1750	2.14293(-1)	2.86369(-1)	3.32770(-1)	3.64718(-1)	3.87937(-1)	4.05532(-1)	4.19308(-1)	4.30377(-1)
0.1875	2.03747(-1)	2.74006(-1)	3.19442(-1)	3.50804(-1)	3.73633(-1)	3.90951(-1)	4.04521(-1)	4.15432(-1)
0.2000	1.93804(-1)	2.62262(-1)	3.06734(-1)	3.37506(-1)	3.59941(-1)	3.76979(-1)	3.90341(-1)	4.01090(-1)
0.2125	1.84424(-1)	2.51103(-1)	2.94613(-1)	3.24794(-1)	3.46832(-1)	3.63588(-1)	3.76737(-1)	3.87324(-1)
0.2250	1.75572(-1)	2.40496(-1)	2.83048(-1)	3.12638(-1)	3.34278(-1)	3.50749(-1)	3.63685(-1)	3.74106(-1)
0.2375	1.67213(-1)	2.30410(-1)	2.72012(-1)	3.01010(-1)	3.22252(-1)	3.38436(-1)	3.51158(-1)	3.61412(-1)
0.250	1.59317(-1)	2.20815(-1)	2.61475(-1)	2.89886(-1)	3.10729(-1)	3.26626(-1)	3.39132(-1)	3.49219(-1)
0.300	1.31802(-1)	1.86831(-1)	2.23835(-1)	2.49938(-1)	2.69203(-1)	2.83959(-1)	2.95603(-1)	3.05017(-1)

Table A7.2: Continued.

$(U/Z)^2$	Z=3	Z=4	Z=5	Z=6	Z=7	Z=8	Z=9	Z=10
0.350	1.09690(-1)	1.58809(-1)	1.92381(-1)	2.16279(-1)	2.34021(-1)	2.47665(-1)	2.58464(-1)	2.67215(-1)
0.400	9.17995(-2)	1.35583(-1)	1.65976(-1)	1.87802(-1)	2.04096(-1)	2.16677(-1)	2.26664(-1)	2.34774(-1)
0.450	7.72319(-2)	1.16234(-1)	1.43713(-1)	1.63613(-1)	1.78551(-1)	1.90127(-1)	1.99343(-1)	2.06842(-1)
0.500	6.52987(-2)	1.00040(-1)	1.24865(-1)	1.42989(-1)	1.56665(-1)	1.67302(-1)	1.75793(-1)	1.82717(-1)
0.550	5.54681(-2)	8.64245(-2)	1.08846(-1)	1.25342(-1)	1.37851(-1)	1.47616(-1)	1.55430(-1)	1.61816(-1)
0.600	4.73263(-2)	7.49282(-2)	9.51789(-2)	1.10189(-1)	1.21627(-1)	1.30585(-1)	1.37771(-1)	1.43655(-1)
0.650	4.05491(-2)	6.51817(-2)	8.34775(-2)	9.71351(-2)	1.07591(-1)	1.15806(-1)	1.22413(-1)	1.27832(-1)
0.700	3.48806(-2)	5.68867(-2)	7.34246(-2)	8.58544(-2)	9.54124(-2)	1.02946(-1)	1.09019(-1)	1.14008(-1)
0.750	3.01180(-2)	4.98008(-2)	6.47596(-2)	7.60761(-2)	8.48154(-2)	9.17246(-2)	9.73060(-2)	1.01900(-1)
0.800	2.60992(-2)	4.37264(-2)	5.72673(-2)	6.75757(-2)	7.55692(-2)	8.19071(-2)	8.70379(-2)	9.12683(-2)
0.850	2.26941(-2)	3.85015(-2)	5.07697(-2)	6.01656(-2)	6.74802(-2)	7.32961(-2)	7.80141(-2)	8.19103(-2)
0.900	1.97976(-2)	3.39927(-2)	4.51183(-2)	5.36885(-2)	6.03857(-2)	6.57249(-2)	7.00649(-2)	7.36546(-2)
0.950	1.73247(-2)	3.00899(-2)	4.01894(-2)	4.80124(-2)	5.41481(-2)	5.90524(-2)	6.30465(-2)	6.63550(-2)
1.000	1.52058(-2)	2.67015(-2)	3.58790(-2)	4.30259(-2)	4.86510(-2)	5.31585(-2)	5.68362(-2)	5.98870(-2)
1.050	1.33840(-2)	2.37514(-2)	3.20999(-2)	3.86347(-2)	4.37956(-2)	4.79409(-2)	5.13293(-2)	5.41440(-2)
1.100	1.18127(-2)	2.11758(-2)	2.87785(-2)	3.47589(-2)	3.94974(-2)	4.33124(-2)	4.64361(-2)	4.90344(-2)
1.150	1.04530(-2)	1.89212(-2)	2.58523(-2)	3.13304(-2)	3.56846(-2)	3.91979(-2)	4.20796(-2)	4.44796(-2)
1.200	9.27311(-3)	1.69427(-2)	2.32684(-2)	2.82910(-2)	3.22953(-2)	3.55333(-2)	3.81934(-2)	4.04116(-2)
1.250	8.24618(-3)	1.52022(-2)	2.09818(-2)	2.55911(-2)	2.92766(-2)	3.22631(-2)	3.47204(-2)	3.67720(-2)
1.375	6.21055(-3)	1.16923(-2)	1.63262(-2)	2.00602(-2)	2.30666(-2)	2.55147(-2)	2.75364(-2)	2.92292(-2)
1.500	4.73930(-3)	9.09504(-3)	1.28353(-2)	1.58780(-2)	1.83434(-2)	2.03600(-2)	2.20310(-2)	2.34339(-2)

Table A7.2: Continued.

$(U/Z)^2$	Z=3	Z=4	Z=5	Z=6	Z=7	Z=8	Z=9	Z=10
1.625	3.66022(-3)	7.14856(-3)	1.01873(-2)	1.26810(-2)	1.47133(-2)	1.63826(-2)	1.77702(-2)	1.89379(-2)
1.750	2.85807(-3)	5.67269(-3)	8.15707(-3)	1.02122(-2)	1.18961(-2)	1.32846(-2)	1.44422(-2)	1.54185(-2)
1.875	2.25439(-3)	4.54155(-3)	6.58495(-3)	8.28786(-3)	9.69010(-3)	1.08505(-2)	1.18205(-2)	1.26403(-2)
2.000	1.79490(-3)	3.66593(-3)	5.35633(-3)	6.77473(-3)	7.94808(-3)	8.92229(-3)	9.73865(-3)	1.04300(-2)
2.125	1.44146(-3)	2.98182(-3)	4.38790(-3)	5.57523(-3)	6.56164(-3)	7.38316(-3)	8.07317(-3)	8.65857(-3)
2.250	1.16695(-3)	2.44270(-3)	3.61842(-3)	4.61709(-3)	5.45007(-3)	6.14580(-3)	6.73141(-3)	7.22909(-3)
2.375	9.51810(-4)	2.01442(-3)	3.00243(-3)	3.84627(-3)	4.55272(-3)	5.14434(-3)	5.64334(-3)	6.06807(-3)
2.500	7.81767(-4)	1.67161(-3)	2.50585(-3)	3.22198(-3)	3.82360(-3)	4.32869(-3)	4.75550(-3)	5.11934(-3)
5.00	4.09532(-5)	9.81106(-5)	1.56714(-4)	2.09927(-4)	2.56383(-4)	2.96492(-4)	3.31113(-4)	3.61125(-4)
7.50	6.02517(-6)	1.49778(-5)	2.44265(-5)	3.31676(-5)	4.08997(-5)	4.76404(-5)	5.35023(-5)	5.86137(-5)
10.0	1.46010(-6)	3.67183(-6)	6.02889(-6)	8.22399(-6)	1.01752(-5)	1.18823(-5)	1.33712(-5)	1.46724(-5)
12.5	4.73458(-7)	1.19274(-6)	1.96102(-6)	2.67790(-6)	3.31609(-6)	3.87512(-6)	4.36319(-6)	4.79009(-6)
15.0	1.85664(-7)	4.66707(-7)	7.66649(-7)	1.04650(-6)	1.29565(-6)	1.51393(-6)	1.70453(-6)	1.87127(-6)
17.5	8.32253(-8)	2.08435(-7)	3.41784(-7)	4.66084(-7)	5.76679(-7)	6.73540(-7)	7.58100(-7)	8.32060(-7)
20.0	4.12016(-8)	1.02763(-7)	1.68157(-7)	2.29034(-7)	2.83151(-7)	3.30522(-7)	3.71861(-7)	4.08006(-7)
22.5	2.20252(-8)	5.47087(-8)	8.93342(-8)	1.21522(-7)	1.50108(-7)	1.75115(-7)	1.96928(-7)	2.15992(-7)
25.0	1.25175(-8)	3.09716(-8)	5.04714(-8)	6.85728(-8)	8.46322(-8)	9.86724(-8)	1.10913(-7)	1.21607(-7)
50.0	2.73555(-10)	6.60414(-10)	1.06212(-9)	1.43129(-9)	1.75642(-9)	2.03951(-9)	2.28542(-9)	2.49963(-9)
75.0	2.71958(-11)	6.49544(-11)	1.03850(-10)	1.39427(-10)	1.70651(-10)	1.97784(-10)	2.21313(-10)	2.41783(-10)
100	5.16161(-12)	1.22567(-11)	1.95338(-11)	2.61732(-11)	3.19888(-11)	3.70370(-11)	4.14111(-11)	4.52131(-11)
125	1.40710(-12)	3.32927(-12)	5.29547(-12)	7.08654(-12)	8.65351(-12)	1.00127(-11)	1.11899(-11)	1.22125(-11)

## Appendix 8

### Formulae for the S→S, S→P, S→D, and P→D generalized oscillator strengths

Within the first Born approximation, the GOS is easily expressed in terms of the form factor (FF):

$$\begin{aligned} GOS(K) &= \frac{2(E_1 - E_0)}{K^2} |FF(K)|^2 \\ &= \frac{2(E_1 - E_0)}{K^2} \left| \int \Psi_1^* \sum_{i=1}^n e^{i\vec{K} \cdot \vec{r}_i} \Psi_0 d\vec{r}_1 d\vec{r}_2 \dots d\vec{r}_n \right|^2 \end{aligned}$$

where the subscripts 0 and 1 refer to the initial and final target states, respectively, and the summation is over all n electrons in the target. K is the momentum transferred to the target from the collision and  $E_0$  and  $E_1$  are the energies of the initial and final states, respectively.

The expressions for the form factor are expanded in terms of the integral  $F(a,b,c,L,M,N,\lambda,K)$  given by

$$F(a,b,c,L,M,N,\lambda,K) = \int e^{-ar_1} e^{-br_2} e^{-cr_{12}} r_1^L r_2^M J_N(Kr_1) Y_\lambda^0(\Omega_1) Y_\lambda^0(\Omega_2) d\vec{r}_1 d\vec{r}_2$$

where  $J_N(Kr)$  is a spherical Bessel function of order N, and  $Y_\lambda^0$  is a spherical harmonic.

The evaluation of  $F(a,b,c,L,M,N,\lambda,K)$ , the derivation of alternate expressions when  $|b-c|$  is small, and the small-K and large-K expansions will be discussed at the end of this appendix.

For convenience, the linear and nonlinear parameters in the wavefunctions representing the initial and final states are subscripted with a 0 and a 1, respectively.

Therefore, the initial S and P state wavefunctions are written

$$\Psi = \sum_{k0}^{N0} C_{k0} (1 \pm \hat{P}_{12}) \exp(-\alpha_{k0} r_1) \exp(-\beta_{k0} r_2) \exp(-\gamma_{k0} r_{12}) Y_0^0(1) Y_0^0(2)$$

and

$$\Psi = \sum_{k0}^{N0} C_{k0} (1 \pm \hat{P}_{12}) r_1 \exp(-\alpha_{k0} r_1) \exp(-\beta_{k0} r_2) \exp(-\gamma_{k0} r_{12}) Y_1^0(1) Y_0^0(2)$$

and the final S, P, and D states wavefunctions are written

$$\Psi = \sum_{kl}^{NI} C_{kl} (1 \pm \hat{P}_{12}) \exp(-\alpha_{kl} r_1) \exp(-\beta_{kl} r_2) \exp(-\gamma_{kl} r_{12}) Y_0^0(1) Y_0^0(2)$$

$$\Psi = \sum_{kl}^{NI} C_{kl} (1 \pm \hat{P}_{12}) r_1 \exp(-\alpha_{kl} r_1) \exp(-\beta_{kl} r_2) \exp(-\gamma_{kl} r_{12}) Y_1^0(1) Y_0^0(2)$$

and

$$\begin{aligned} \Psi &= \sum_{kl}^{NI} C_{kl} (1 \pm \hat{P}_{12}) r_1^2 \exp(-\alpha_{kl} r_1) \exp(-\beta_{kl} r_2) \exp(-\gamma_{kl} r_{12}) Y_2^0(\Omega_1) Y_0^0(\Omega_2) \\ &+ \sum_{kl=NI+1}^{NI+MI} D_{kl} (1 \pm \hat{P}_{12}) r_1 r_2 \exp(-\alpha_{kl} r_1) \exp(-\beta_{kl} r_2) \exp(-\gamma_{kl} r_{12}) Y(1,2) \end{aligned}$$

where

$$Y(1,2) = 2Y_1^0(\Omega_1)Y_1^0(\Omega_2) + Y_1^1(\Omega_1)Y_1^{-1}(\Omega_2) + Y_1^{-1}(\Omega_1)Y_1^1(\Omega_2)$$

The form factor for S $\rightarrow$ S transitions is

$$FF(K) = \frac{1}{2\pi} \sum_{k0}^{N0} \sum_{kl}^{NI} C_{k0} C_{kl} (1 \pm \hat{P}_{\alpha_{k0} \beta_{k0}}) \begin{bmatrix} F(\alpha_{k0} + \alpha_{kl}, \beta_{k0} + \beta_{kl}, \gamma_{k0} + \gamma_{kl}, 0, 0, 0, 0, K) \\ F(\beta_{k0} + \beta_{kl}, \alpha_{k0} + \alpha_{kl}, \gamma_{k0} + \gamma_{kl}, 0, 0, 0, 0, K) \end{bmatrix}$$

For S→P transitions the form factor is

$$FF(K) = \frac{i\sqrt{3}}{2\pi} \sum_{k0}^{N0} \sum_{kl}^{Nl} C_{k0} C_{kl} (1 \pm \hat{P}_{\alpha_{k0} \beta_{k0}}) \begin{bmatrix} F(\alpha_{k0} + \alpha_{kl}, \beta_{k0} + \beta_{kl}, \gamma_{k0} + \gamma_{kl}, 1, 0, 1, 0, K) \\ F(\beta_{k0} + \beta_{kl}, \alpha_{k0} + \alpha_{kl}, \gamma_{k0} + \gamma_{kl}, 0, 1, 1, 1, K) \end{bmatrix}$$

For S→D transitions the form factor is

$$FF(K) = \frac{-\sqrt{5}}{2\pi} \sum_{k0}^{N0} \sum_{kl}^{Nl} C_{k0} C_{kl} (1 \pm \hat{P}_{\alpha_{k0} \beta_{k0}}) \begin{bmatrix} F(\alpha_{k0} + \alpha_{kl}, \beta_{k0} + \beta_{kl}, \gamma_{k0} + \gamma_{kl}, 2, 0, 2, 0, K) \\ F(\beta_{k0} + \beta_{kl}, \alpha_{k0} + \alpha_{kl}, \gamma_{k0} + \gamma_{kl}, 0, 2, 2, 2, K) \end{bmatrix}$$

$$\frac{-6}{2\pi} \sum_{k0}^{N0} \sum_{kl=Nl+1}^{Nl+Ml} C_{k0} D_{kl} (1 \pm \hat{P}_{\alpha_{k0} \beta_{k0}}) \begin{bmatrix} F(\alpha_{k0} + \alpha_{kl}, \beta_{k0} + \beta_{kl}, \gamma_{k0} + \gamma_{kl}, 1, 1, 2, 1, K) \\ F(\beta_{k0} + \beta_{kl}, \alpha_{k0} + \alpha_{kl}, \gamma_{k0} + \gamma_{kl}, 1, 1, 2, 1, K) \end{bmatrix}$$

For P→D transitions the form factor is

$$FF(K) = \frac{i\sqrt{3}}{4\pi\sqrt{5}} \sum_{k0}^{N0} \sum_{kl}^{Nl} C_{k0} C_{kl} \begin{bmatrix} 2F(\alpha_{k0} + \alpha_{kl}, \beta_{k0} + \beta_{kl}, \gamma_{k0} + \gamma_{kl}, 3, 0, 1, 0, K) \\ -3F(\alpha_{k0} + \alpha_{kl}, \beta_{k0} + \beta_{kl}, \gamma_{k0} + \gamma_{kl}, 3, 0, 3, 0, K) \\ +2F(\beta_{k0} + \beta_{kl}, \alpha_{k0} + \alpha_{kl}, \gamma_{k0} + \gamma_{kl}, 0, 3, 1, 1, K) \\ -3F(\beta_{k0} + \beta_{kl}, \alpha_{k0} + \alpha_{kl}, \gamma_{k0} + \gamma_{kl}, 0, 3, 3, 3, K) \\ \pm 2F(\alpha_{k0} + \beta_{kl}, \beta_{k0} + \alpha_{kl}, \gamma_{k0} + \gamma_{kl}, 1, 2, 1, 2, K) \\ \mp 3F(\alpha_{k0} + \beta_{kl}, \beta_{k0} + \alpha_{kl}, \gamma_{k0} + \gamma_{kl}, 1, 2, 3, 2, K) \\ \pm 2F(\beta_{k0} + \alpha_{kl}, \alpha_{k0} + \beta_{kl}, \gamma_{k0} + \gamma_{kl}, 2, 1, 1, 1, K) \\ \mp 3F(\beta_{k0} + \alpha_{kl}, \alpha_{k0} + \beta_{kl}, \gamma_{k0} + \gamma_{kl}, 2, 1, 3, 1, K) \end{bmatrix}$$

$$\frac{+i\sqrt{3}}{10\pi} \sum_{k0}^{N0} \sum_{kl=Nl+1}^{Nl+Ml} C_{k0} D_{kl} (1 \pm \hat{P}_{\alpha_{kl} \beta_{kl}}) \begin{bmatrix} 6F(\alpha_{k0} + \alpha_{kl}, \beta_{k0} + \beta_{kl}, \gamma_{k0} + \gamma_{kl}, 2, 1, 1, 1, K) \\ -9F(\alpha_{k0} + \alpha_{kl}, \beta_{k0} + \beta_{kl}, \gamma_{k0} + \gamma_{kl}, 2, 1, 3, 1, K) \\ +5F(\beta_{k0} + \beta_{kl}, \alpha_{k0} + \alpha_{kl}, \gamma_{k0} + \gamma_{kl}, 1, 2, 1, 0, K) \\ +F(\beta_{k0} + \beta_{kl}, \alpha_{k0} + \alpha_{kl}, \gamma_{k0} + \gamma_{kl}, 1, 2, 1, 2, K) \\ -9F(\beta_{k0} + \beta_{kl}, \alpha_{k0} + \alpha_{kl}, \gamma_{k0} + \gamma_{kl}, 1, 2, 3, 2, K) \end{bmatrix}$$

Each  $F(a,b,c,L,M,N,\lambda,K)$  integral is expanded into a sum of integrals of the form

$$J_{m,n}(K,a) = \int_0^\infty r^m j_n(Kr) e^{-ar} dr$$

and these are evaluated by applying the following three recursion relations

$$aJ_{m,n}(K,a) + KJ_{m,n+1}(K,a) = (m+n)J_{m-1,n}(K,a)$$

$$(K^2 + a^2)J_{m+1,n}(K,a) + (m+n)(m-n-1)J_{m-1,n}(K,a) = 2maJ_{m,n}(K,a)$$

and

$$J_{n+1,n}(K,a) = \frac{2nK}{K^2 + a^2} J_{n,n-1}(K,a)$$

successively to  $J_{0,0}$  and  $J_{1,0}$ . Both of these are readily evaluated:

$$J_{0,0}(K,a) = \int_0^\infty j_0(Kr) e^{-ar} dr = \int_0^\infty \frac{\sin(Kr)}{Kr} e^{-ar} dr = \frac{1}{K} \tan^{-1}\left(\frac{K}{a}\right)$$

and

$$J_{1,0}(K,a) = \int_0^\infty r j_0(Kr) e^{-ar} dr = \int_0^\infty \frac{\sin(Kr)}{K} e^{-ar} dr = \frac{1}{K^2 + a^2}$$

Clearly different transitions require different  $J_{m,n}$ : the S $\rightarrow$ S transitions require  $J_{1,0}$  and  $J_{2,0}$ ; the S $\rightarrow$ P transitions require  $J_{0,1}$ ,  $J_{1,1}$ ,  $J_{2,1}$ ,  $J_{3,1}$ ; the S $\rightarrow$ D transitions require  $J_{1,2}$ ,  $J_{0,2}$ ,  $J_{1,2}$ ,  $J_{2,2}$ ,  $J_{3,2}$ , and  $J_{4,2}$ ; the P $\rightarrow$ D transitions require  $J_{0,1}$ ,  $J_{1,1}$ ,  $J_{2,1}$ ,  $J_{3,1}$ ,  $J_{4,1}$ ,  $J_{5,1}$ ,  $J_{2,3}$ ,  $J_{1,3}$ ,  $J_{2,3}$ ,  $J_{3,3}$ ,  $J_{4,3}$ , and  $J_{5,3}$ .

Large and small K expansion of  $F(a,b,c,L,M,N,\lambda,K)$  are obtained by a Taylor expansion of the  $J_{mn}(K,a)$  about  $a/K$  and  $K/c$ , respectively. These expansions are substituted into the expression for  $F(a,b,c,L,M,N,\lambda,K)$ . The first few terms in the expansions of  $F(a,b,c,L,M,N,\lambda,K)$  cancel; for instance the lowest order terms in the small K expansions of  $J_{20}(K,a)$  and  $J_{10}(K,a)$  are of the order of  $K^0$  but the lowest order term in the small K expansion of  $F(a,b,c,0,0,0,0,K)$  is  $K^2$ . Each coefficient in the small and large K expansion will suffer from numerical instabilities when  $|b-c|$  is small. Alternate expressions were derived for the first three expansion coefficients. Although the program allows any number of expansion terms to be calculated, numerical instabilities may arise in terms beyond the third order.

$F(a,b,c,L,M,N,\lambda,K)$  becomes numerically unstable when  $|b-c|$  is small. The alleviation of this problem will be illustrated using  $F(a,b,c,0,3,1,1,K)$  as an example. Each  $F(a,b,c,L,M,N,\lambda,K)$  required individual consideration but the example illustrates the general procedure.

$$\begin{aligned}
F(a,b,c,0,3,1,1,K) &= \pi \int e^{-ar_1} e^{-br_2} e^{-cr_1} r_2^3 j_1(Kr_1) Y_1^0(\Omega_1) Y_1^0(\Omega_2) d\vec{r}_1 d\vec{r}_2 \\
&= \pi \int_0^\infty e^{-ar_1} j_1(Kr_1) \left[ \begin{array}{l} \frac{8cr_1^5 e^{-br_1}}{(b^2-c^2)^2} + \frac{128bc r_1^4 e^{-br_1}}{(b^2-c^2)^3} + \frac{32cr_1^3(31b^2+5c^2)e^{-br_1}}{(b^2-c^2)^4} \\ + \frac{192bc r_1^2 [(23b^2+9c^2)e^{-br_1} + (5b^2+3c^2)e^{-cr_1}]}{(b^2-c^2)^5} \\ + \frac{1536bc r_1 (7b^2+3c^2)(be^{-br_1}-ce^{-cr_1})}{(b^2-c^2)^6} \\ + \frac{1536bc (7b^2+3c^2)(e^{-br_1}-e^{-cr_1})}{(b^2-c^2)^6} \end{array} \right]
\end{aligned}$$

When  $|b-c|$  is sufficiently large, the above is written as

$$\begin{aligned}
F(a,b,c,0,3,1,1,K) &= \pi \left[ \begin{array}{l} \frac{8c J_{5,1}(K,a+b)}{(b^2-c^2)^2} + \frac{128bc J_{4,1}(K,a+b)}{(b^2-c^2)^3} + \frac{32c(31b^2+5c^2)J_{3,1}(K,a+b)}{(b^2-c^2)^4} \\ + \frac{192bc [(23b^2+9c^2)J_{2,1}(K,a+b) + (5b^2+3c^2)J_{2,1}(K,a+c)]}{(b^2-c^2)^5} \\ + \frac{1536bc (7b^2+3c^2)(bJ_{1,1}(K,a+b)-cJ_{1,1}(K,a+c))}{(b^2-c^2)^6} \\ + \frac{1536bc (7b^2+3c^2)(J_{0,1}(K,a+b)-J_{0,1}(K,a+c))}{(b^2-c^2)^6} \end{array} \right]
\end{aligned}$$

and evaluated using the expressions for  $J_{m,n}(K,a)$ . Otherwise,  $e^{-br_1}$  is extracted from the

term in brackets and the resulting exponentials are Taylor expanded.  $F(a,b,c,0,3,1,1,K)$

becomes

$$F(a,b,c,0,3,1,1,K) = \frac{8\pi}{(b+c)^6} \int_0^\infty e^{-(a+b)r_1} J_1(Kr_1) \times$$

$$\left[ \begin{aligned} & 20cr_1^3 + 20bcr_1^4 + \frac{cr_1^5(49b^2+6bc+5c^2)}{5} \\ & + 24bc \sum_{l=1}^\infty \frac{(b-c)^{l+4}r_1^{l+5}}{(l+5)!} [(b+c)(5b^2+3c^2)(l^2+9l+20) \\ & \quad - 8(7b^2+3c^2)(c(l+5)+(b-c))] \end{aligned} \right]$$

or, expressed in terms of  $J_{m,n}(K,a)$ ,

$$F(a,b,c,0,3,1,1,K) = \frac{8\pi}{(b+c)^6} \left[ \begin{aligned} & 20cJ_{3,1}(K,a+b) + 20bcJ_{4,1}(K,a+b) \\ & + cJ_{5,1}(K,a+b)(49b^2+6bc+5c^2) \\ & + 24bc \sum_{l=1}^\infty \frac{(b-c)^{l+4}J_{l+5,1}(K,a+b)}{(l+5)!} [(b+c)(5b^2+3c^2)(l^2+9l+20) \\ & \quad - 8(7b^2+3c^2)(c(l+5)+(b-c))] \end{aligned} \right]$$

For each  $J_{l+5,1}(K,a+b)$  may be evaluated by

$$J_{l+5,1}(K,a+b) = \frac{2(l+4)(a+b)J_{l+4,1}(K,a+b) - (l+5)(l+2)J_{l+3,1}(K,a+b)}{K^2 + (a+b)^2}$$

which is simply a substitution ( $n=1, m=l+4$ ) and rearrangement of one of the previous recursion relations. Although the infinite summation does converge, it is currently a product of increasingly small  $((b-c)^{l+4}/(l+5)!)$  and large  $(J_{l+5,1}(K,a+b))$  terms. Therefore, numerical instabilities arise. These are avoided by introducing the function

$$J'_{l+5,1}(K,a+b) = \frac{(b-c)^{l+4}J_{l+5,1}(K,a+b)}{(l+5)!}$$

Substituting this function in the expression for  $J_{l+5,1}(K,a+b)$  yields

$$J'_{i+5,1}(K, a+b) = \frac{(b-c)}{K^2 + (a+b)^2} \left[ \frac{2(i+4)(a+b)J'_{i+4,1}(K, a+b)}{(i+5)} - \frac{(i+2)(b-c)J'_{i+3,1}(K, a+b)}{(i+4)} \right]$$

and  $F(a, b, c, 0, 3, 1, 1, K)$  becomes

$$F(a, b, c, 0, 3, 1, 1, K) = \frac{8\pi}{(b+c)^6} \left[ \begin{array}{l} \frac{20cJ_{3,1}(K, a+b) + 20bcJ_{4,1}(K, a+b)}{5} \\ \quad + cJ_{5,1}(K, a+b)(49b^2 + 6bc + 5c^2) \\ + 24bc \sum_{i=1}^{\infty} J'_{i+5,1}(K, a+b) [(b+c)(5b^2 + 3c^2)(i^2 + 9i + 20) \\ \quad - 8(7b^2 + 3c^2)(c(i+5) + (b-c))] \end{array} \right]$$

## REFERENCES

### Chapter 1

- [1.1] Chemistry of the elements, N. N. Greenwood and A. Earnshaw, (Pergamon, Great Britain, 1984)
- [1.2] The chemical elements, K. J. Laidler and M. H. Ford-Smith, (Bogden and Quigley, New York, 1970)
- [1.3] Discovery of the elements, M. E. Weeks and H. M. Leicester, (Mark printing, Powan, 1968)
- [1.4] Oscillator strengths for S-P and P-D transitions in heliumlike ions, N. M. Cann and A. J. Thakkar, *Phys. Rev. A*, **46**, 5397(1992)
- [1.5] Charge and intracule densities in singly excited states of heliumlike ions, N. M. Cann, R. J. Boyd, and A. J. Thakkar, *J. Chem. Phys.*, **98**, 7132(1993)
- [1.6] Correlation effects on one-electron densities and two-electron intracules:  $3^3D$  and  $3^1D$  states of helium-like ions, N. M. Cann, R. J. Boyd, and A. J. Thakkar, *Int. J. Quantum Chem.*, in press
- [1.7] Statistical correlation coefficients in heliumlike ions, N. M. Cann, A. J. Thakkar, and R. J. Boyd, *Int. J. Quantum Chem.*, submitted

### Chapter 2

- [2.1] Separation of angles in the two-electron problem, G. Breit, *Phys. Rev.* **35**, 569 (1930)

- [2.2] Lamb shift in the Helium atom, C. Schwartz, *Phys. Rev.*, **123**, 1700 (1961)
- [2.3] Neue Berechnung der Energie des Heliums im Grundzustande, sowie des tiefsten Terms von Ortho-helium, E. A. Hylleraas, *Z. Phys.*, **54**, 347 (1929)
- [2.4] Two-electron S and P term values with smooth Z dependence, Y. Accad, C. L. Pekeris, B. Schiff, *Phys. Rev. A*, **11**, 1479(1975)
- [2.5] S and P states of the Helium Isoelectronic Sequence up to Z=10, Y. Accad, C. L. Pekeris, B. Schiff, *Phys. Rev. A*, **4**, 516(1971) and references therein
- [2.6] Accurate nonrelativistic oscillator strengths for P-D transitions in the helium isoelectronic sequence, A. Kono, S. Hattori, *Phys. Rev. A*, **30**, 2093(1984)
- [2.7] Accurate oscillator strengths for neutral helium, A. Kono, S. Hattori, *Phys. Rev. A*, **29**, 2981(1984)
- [2.8] Energy levels for S, P, and D states in He through precision variational calculations, A. Kono, S. Hattori, *Phys. Rev. A*, **34**, 1727(1986)
- [2.9] Variational calculations for excited states in He I: Improved estimation of the ionization energy from accurate energies for the n<sup>3</sup>S, n<sup>1</sup>D, n<sup>3</sup>D series, A. Kono, S. Hattori, *Phys. Rev. A*, **31**, 1199(1985)
- [2.10] High precision variational calculations for the 1s<sup>1</sup><sup>2</sup>S state of H<sup>-</sup> and the 1s<sup>2</sup><sup>1</sup>S, 1s2s <sup>1</sup>S and 1s2s <sup>3</sup>S states of helium, G. W. F. Drake, *Nucl. Instr. Meth. Phys. Res.*, **B31**, 7(1988)
- [2.11] High-precision eigenvalues for the 1s2p <sup>1</sup>P and <sup>3</sup>P states of helium, G. W. F. Drake, A. J. Makowski, *J. Opt. Soc. Am. B*, **5**, 2207(1988)

- [2.12] New Variational Techniques for the 1snd States of Helium, G. W. F. Drake, *Phys. Rev. Lett.*, **59**, 1549(1987)
- [2.13] Eigenvalues and retardation effects in the n=10 states of helium, G. W. F. Drake, *J. Phys. B*, **22**, L651(1989)
- [2.14] Variational eigenvalues for the Rydberg states of helium: Comparison with experiment and with asymptotic expansions, G. W. F. Drake, *Phys. Rev. Lett.*, **65**, 2769(1990)
- [2.15] Energies and relativistic corrections for the Rydberg states of helium: Variational results and asymptotic analysis, G. W. F. Drake and Z.-C. Yan, *Phys. Rev. A*, **46**, 2378(1992)
- [2.16] Ground State of the Helium Atom, T. Kinoshita, *Phys. Rev.*, **105**, 1490(1957)
- [2.17] Ground State of the Helium Atom. II., T. Kinoshita, *Phys. Rev.*, **115**, 366(1959)
- [2.18] Logarithmic Terms in the Wave Functions of the Ground State of Two-Electron Atoms, K. Frankowski and C. L. Pekeris, *Phys. Rev.*, **146**, 46(1966) and references therein
- [2.19] Logarithmic Terms in the Wave Functions of the 2<sup>1</sup>S and 2<sup>3</sup>S States of Two-Electron Atoms, K. Frankowski, *Phys. Rev.*, **160**, 1(1967)
- [2.20] Ground State of the Helium Atom, C. Schwartz, *Phys. Rev.*, **128**, 1146(1962)

- [2.21] Radius of convergence and analytic behaviour of the 1/Z expansion, J. D. Baker, D. E. Freund, R. N. Hill, J. D. Morgan III, *Phys. Rev. A*, **41**, 1247(1990)
- [2.22] The Atomic Three-body Problem. An Accurate Lower Bound Calculation Using Wave Functions with Logarithmic Terms, H. Kleindienst, R. Emrich, *Int. J. Quantum Chem.*, **37**, 257(1990)
- [2.23] Correlated Orbitals for Excited States of He and H<sup>-</sup>, H. O. Pritchard, A. Wallis, *J. Chem. Phys.*, **42**, 3548(1965)
- [2.24] The normal state of helium, J. C. Slater, *Phys. Rev.*, **32**, 349(1928)
- [2.25] The reduction of the multi-dimensional Schrodinger equation to a one-dimensional integral equation, C. M. Rosenthal, *Chem. Phys. Lett.*, **10**, 381(1971)
- [2.26] The dimensional and numerical equivalence of the space-filling-curve approach and multi-dimensional integration methods for integral-transform trial functions, R. L. Somorjai, J. D. Power, *Chem. Phys. Lett.*, **12**, 502(1972)
- [2.27] Correlated wavefunctions, energies, and one-electron radial densities for S states of the He atom, P. Winkler, R. N. Porter, *J. Chem. Phys.*, **61**, 2038(1974)
- [2.28] Compact and accurate integral-transform wave functions. I. The 1'S state of the helium-like ions from H<sup>-</sup> through Mg<sup>10+</sup>, A. J. Thakkar, V. H. Smith Jr., *Phys. Rev. A*, **15**, 1(1977)

- [2.29] Compact and accurate integral-transform wave functions. II. The  $2^1S$ ,  $2^3S$ ,  $2^1P$ , and  $2^3P$  states of the helium-like ions from He through Mg<sup>10+</sup>, A. J. Thakkar, V. H. Smith Jr., *Phys. Rev. A*, **15**, 16(1977)
- [2.30] An efficient method for finding the minimum of a function of several variables without calculating derivatives, M. J. D. Powell, *Comp. J.*, **7**, 155(1965)
- [2.31] A simple method of treating atomic integrals containing functions of  $r!$ , J. L. Calais, P. Löwdin, *J. Mol. Spectr.*, **8**, 203(1962)
- [2.32] Recursive Evaluation of Some Atomic Integrals, R. A. Sack, C. C. J. Roothaan, and W. Kolos, *J. Math. Phys.*, **8**, 1093(1967)
- [2.33] Scaling Problem, Virial Theorem, and Connected Relations in Quantum Mechanics, P. O. Löwdin, *J. Mol. Spectr.*, **3**, 46(1959)
- [2.34] Variational calculations on the helium isoelectronic sequence, D. E. Freund, B. D. Huxtable, J. D. Morgan III, *Phys. Rev. A*, **29**, 980(1984)
- [2.35] Logarithmic Terms in the Wave Functions of the  $2^1S$  and  $2^3S$  States of Two-Electron Atoms, K. Frankowski, *Phys. Rev.*, **160**, 1(1967)
- [2.36] On the Eigenfunctions of Many-Particle Systems in Quantum Mechanics, T. Kato, *Pure Appl. Math.*, **10**, 151(1957)
- [2.37] Cusp Conditions for Molecular Wavefunctions, R. T. Pack, W. Byers Brown, *J. Chem. Phys.*, **45**, 556(1966)
- [2.38] Charge Densities in Atoms, E. Steiner, *J. Chem. Phys.*, **39**, 2365(1963)

- [2.39] The electron-electron cusp condition for the spherical average of the intracule matrix, A. J. Thakkar, V. H. Smith Jr., *Chem. Phys. Lett.*, **42**, 476(1976)
- [2.40] The higher order electron-electron coalescence condition for the intracule function for states of maximum spin multiplicity, A. J. Thakkar, *J. Chem. Phys.*, **84**, 6830(1986)
- [2.41] Asymptotic behaviour of atomic and molecular wave functions, J. Katriel, E. R. Davidson, *Proc. Natl. Acad. Sci. USA*, **77**, 4403(1980)
- [2.42] Bounds on the decay of electron densities with screening, R. Ahlrichs, M. Hoffmann-Ostenhof, T. Hoffmann-Ostenhof, J. D. Morgan III, *Phys. Rev. A*, **23**, 2106(1981)
- [2.43] Two-Electron Atoms III A sixth-Order Perturbation Study of the  $1^1S$  Ground State, C.W. Scherr and R.E. Knight, *Rev. Mod. Phys.*, **35**, 436 (1963)
- [2.44] Some First-Order Perturbation Energy Values, F.C. Sanders and C.W. Scherr, *J. Chem. Phys.*, **42**, 4314 (1965)
- [2.45] Energies and Z-expansion coefficients for the D states in the helium sequence, P. Blanchard, G. W. F. Drake, *J. Phys. B*, **6**, 2495(1973)
- [2.46] Variational perturbation theory investigation on two-electron atomic systems. III Nonrelativistic results for the state  $1s2s\ ^3S$ , K. Aashamar, J. Midtdal and G. Lyslo, *J. Chem. Phys.*, **60**, 3403 (1974)
- [2.47] Variational perturbation theory investigation on two-electron atomic systems. IV Nonrelativistic results for the state  $1s3s\ ^3S$ , K. Aashamar, J. Midtdal and G. Lyslo, *J. Chem. Phys.*, **61**, 1345 (1974)

- [2.48] Variational Perturbation Theory Study of Some Excited States of Two-Electron Atoms, K. Aashamar, G. Lysig and J. Midtdal, *J. Chem. Phys.*, **52**, 3324 (1970)
- [2.49] Energy of the excited states of helium, A.N. Ivanova, U.I. Safronova and V.N. Kharitonova, *Opt. Spectrosc.*, **24**, 355 (1968) [ *Opt. Spektrosk.*, **24**, 660 (1968)].
- [2.50] S, P, and D states of two-electron ions via Z-dependent perturbation theory, F. C. Sanders, R. E. Knight, *Phys. Rev. A*, **27**, 1279(1983)
- [2.51] Nonrelativistic-energy Z-expansion coefficients for singly excited S and P states of two-electron ions, P. Blanchard, *Phys. Rev. A*, **13**, 1698(1976)

### Chapter 3

- [3.1] Atoms in molecules: a quantum theory, R. F. W. Bader, (Oxford, New York, 1990)
- [3.2] Density functional theory of atoms and molecules, R. G. Parr and W. Yang, (Oxford, New York, 1989)
- [3.3] Extracules, Intracules, Correlation Holes, Potentials, Coefficients and All That, A. J. Thakkar in Density matrices and density functionals, edited by R. M. Erdahl and V. H. Smith Jr., (Reidel, Dordrecht, Holland), 1987
- [3.4] Electron distributions and the chemical bond, edited by P. Coppens and M. B. Hall, (Plenum, New York, 1982)

- [3.5] High energy electron scattering, R. A. Bonham and M. Fink, (Van Nostrand, Reinhold, New York, 1974)
- [3.6] Some Recent Advances in Density Matrix Theory, R. McWeeny, *Rev. Mod. Phys.*, **32**, 335(1960)
- [3.7] Analysis of wave functions in terms of one- and two-electron density functions, R. J. Boyd, J. M. Ugalde in *Computational Chemistry: Struct., Inter. and React.*, edited by S. Fraga (Elsevier, Amsterdam, 1992)
- [3.8] Accurate charge densities and two-electron intracule functions for the heliumlike ions, A. J. Thakkar, V. H. Smith Jr., *J. Chem. Phys.*, **67**, 1191(1977)
- [3.9] Charge densities and two-electron intracules for the low-lying excited states of the helium-like ions, P. E. Regier, A. J. Thakkar, *J. Phys. B*, **17**, 3391(1984)
- [3.10] Atomic-charge convexity and the electron density at the nucleus, J. C. Angulo, J. S. Dehesa, and F. J. Galvez, *Phys. Rev. A*, **42**, 641(1990)
- [3.11] Erratum: Atomic-charge convexity and the electron density at the nucleus [Phys. Rev. A, 42, 641(1990)], J. C. Angulo, J. S. Dehesa, and F. J. Galvez, *Phys. Rev. A*, **43**, 4069(1991)
- [3.12] Atomic-charge log-convexity and radial expectation values, J. C. Angulo and J. S. Dehesa, *J. Phys. B*, **24**, L299(1991)
- [3.13] Atomic systems with a completely monotonic electron density, J. C. Angulo and J. S. Dehesa, *Phys. Rev. A*, **44**, 1516(1991)

- [3.14] New bounds for the atomic charge and momentum densities at the origin, J. C. Angulo, J. S. Dehesa, and F. J. Gálvez, *Z. Phys. D*, **18**, 127(1991)
- [3.15] Atomic charge density at the nucleus and inequalities among radial expectation values, F. J. Gálvez and I. Porras, *Phys. Rev. A*, **44**, 144(1991)
- [3.16] Spatial generalizations of Kato's cusp condition for atoms: Applications, I. Porras and F. J. Gálvez, *Phys. Rev. A*, **46**, 105(1992)
- [3.17] Locality of the Effect of the Pauli Principle in Atoms, J. Katriel, *Phys. Rev. A*, **5**, 1990(1972)
- [3.18] Theoretical Interpretation of Hund's Rule, J. Katriel, R. Pauncz, *Adv. Quantum Chem.*, **10**, 143(1977)
- [3.19] Hund's rule and Singlet-Triplet energy differences for Molecular Systems, K. V. Darvesh, R. J. Boyd, *J. Chem. Phys.*, **87**, 5329(1987)
- [3.20] Hund's rule and Singlet-triplet Differences for the lowest  $n\pi^*$  states of formaldehyde,  $\text{H}_2\text{CO}$ , K. V. Darvesh, R. J. Boyd, *J. Chem. Phys.*, **90**, 5638(1989)
- [3.21] Interpretation of Hund's Rule for First-Row Hydrides  $\text{AH}(\Lambda = \text{Li}, \text{B}, \text{N}, \text{F})$ , K. V. Darvesh, P. D. Fricker, R. J. Boyd, *J. Phys. Chem.*, **94**, 3480(1990)

#### Chapter 4

- [4.1] The Nature of Electron Correlation in Molecules, R. McWeeny, *Int. J. Quantum Chem.*, **1**, 351(1967)

- [4.2] On the Constitution of Metallic Sodium, E. Wigner and F. Seitz, *Phys. Rev.*, **43**, 804(1933)
- [4.3] On the Constitution of Metallic Sodium. II, E. Wigner and F. Seitz, *Phys. Rev.*, **46**, 509(1934)
- [4.4] Correlation coefficients for electronic wave functions, W. Kutzelnigg, G. Del Re, G. Berthier, *Phys. Rev.*, **172**, 49(1968)
- [4.5] Statistical electron correlation coefficients for the five lowest states of the heliumlike ions, A. J. Thakkar, V. H. Smith Jr, *Phys. Rev. A*, **23**, 473(1981)
- [4.6] Angular-correlation coefficients for first-row atoms, A. J. Thakkar, *Phys. Rev. A*, **25**, 1820(1982)
- [4.7] Statistical electron angular correlation coefficients for atoms within the Hohenberg-Kohn-Sham theory, R. K. Pathak, *Phys. Rev. A*, **31**, 2806(1985)
- [4.8] P. O. Lowdin, *Adv. Chem. Phys.*, **2**, 207(1959)
- [4.9] Electron Correlation in the Ground State of Helium, C. A. Coulson, A. H. Neilson, *Proc. Phys. Soc.*, **78**, 83!(1961)
- [4.10] Molecular X-ray- and electron-scattering intensities, A. J. Thakkar, A. N. Tripathi, V. H. Smith Jr., *Phys. Rev. A*, **29**, 1103(1984)
- [4.11] Coulomb hole in the ground state of two-electron atoms, R. F. Curl, Jr. and C. A. Coulson, *Proc. Phys. Soc.*, **85**, 647(1965)
- [4.12] The Radius of the Coulomb Hole, R. J. Boyd, *Can. J. Phys.*, **53**, 592(1975)

- [4.13] Fermi and Coulomb Correlations in the  $2^1S$  State of the Helium Isoelectronic Sequence, N. Moiseyev, J. Katriel, and R. J. Boyd, *Theor. Chim. Acta*, **45**, 61(1977)
- [4.14] The Coulomb Hole in the  $2^3S$  State of the Helium Isoelectronic Sequence, R. J. Boyd and J. Katriel, *Int. J. Quantum Chem.*, **8**, 255(1974)
- [4.15] Coulomb holes in the  $2^3P$  and  $2^1P$  states of helium-like ions, A. J. Thakkar, *J. Phys. B*, **20**, 3939(1987)
- [4.16] Coulomb holes and correlation coefficients for electronic shells: The Be-like ions, K. E. Banyard and M. M. Mashat, *J. Chem. Phys.*, **67**, 1405(1977)
- [4.17] Coulomb correlation in a doubly occupied K shell: the influence of outer electrons, K. E. Banyard, *J. Phys. B*, **23**, 777(1990)
- [4.18] C. C. J. Roothaan and P. S. Bagus, *Methods Comput. Phys.*, **2**, 47(1963)
- [4.19] R. M. Pitzer, *QCPE Bulletin*, **10**, 14(1990)
- [4.20] C. F. Fischer, *Comput. Phys. Comm.*, **4**, 107(1972)
- [4.21] The effect of electron correlation on one-electron properties in the  $2^3S$  and  $2^1S$  excited states of the helium atom, J. M. Ugalde, R. J. Boyd, *Chem. Phys. Lett.*, **114**, 197(1985)

## Chapter 5

- [5.1]  $f$  values for transitions between the low-lying S and P states of the helium isoelectronic sequence up to  $Z=10$ , B. Schiff, C. L. Pekeris, Y. Accad, *Phys. Rev. A*, **4**, 885(1971)

- [5.2] Oscillator strengths for S-P and P-D transitions for singly excited states of two-electron ions via Z-dependent perturbation theory, F. C. Sanders, R. E. Knight, *Phys. Rev. A*, **39**, 4387(1989)
- [5.3] MCHF calculations of electric dipole and quadrupole oscillator strengths along the helium isoelectronic sequence, M. Godefroid, G. Verhaegen, *J. Phys. B*, **13**, 3081(1980)
- [5.4] Length and velocity matrix elements in quadrupole transition calculations, M. Cohen, R. P. McEachran, D. Rosenthal, *J. Phys. B.*, **5**, 184(1972)
- [5.5] Motional-Stark-effect spectroscopy:  $7^1S$ - $9^1P$  energy separation and Zeeman tuning parameters for He, M. Rosenbluh, R. Panock, B. Lax, T. A. Miller, *Phys. Rev. A*, **18**, 1103(1978)
- [5.6] Laser magnetic resonance spectroscopy of normally forbidden transitions: Electrostatic fine structure of the  $n=9$ ,  $L=1-8$  He singlet states, R. Panock, M. Rosenbluh, B. Lax, T. A. Miller, *Phys. Rev. A*, **22**, 1050(1980)
- [5.7] Experimental determination of the absolute dipole oscillator strengths for the helium  $1^1S$ - $n^1P$  ( $n=2-7$ ) series, W. Chan, G. Cooper, K. Sze, C. E. Brion, *J. Phys. B*, **23**, L523(1990)
- [5.8] Absolute optical oscillator strengths for the electronic excitation of atoms at high resolution: Experimental methods and measurements for helium, W. F. Chan, G. Cooper, C. E. Brion, *Phys. Rev. A*, **44**, 186(1991)

- [5.9] Some transition moments via perturbation methods for the helium isoelectronic series, C. W. Scherr and F. C. Sanders, *Int. J. Quantum Chem.*, **2**, 29(1968)

## Chapter 6

- [6.1] The theory of atomic collisions, N. F. Mott and H. S. W. Massey, (Oxford, Clarendon, 3rd edition, 1965)
- [6.2] Introduction to the theory of atomic spectra, I. I. Sobel'man, (Oxford, Pergamon, 1972)
- [6.3] Inelastic collisions of fast charged particles with atoms and molecules - The Bethe theory revisited, M. Inokuti, *Rev. Mod. Phys.*, **43**, 297(1971)
- [6.4] Addenda: Inelastic collisions of fast charged particles with atoms and molecules - The Bethe theory revisited [Rev. Mod. Phys. 43, 297(1971)], M. Inokuti, Y. Itikawa, and J. E. Turner, *Rev. Mod. Phys.*, **50**, 23(1978)
- [6.5] The first Born approximation, K. L. Bell and A. E. Kingston, *Adv. Atom. Molec. Phys.*, **10**, 53(1974)
- [6.6] Applying large computers to problems in physics: electron collision cross sections in atomic physics, R. J. W. Henry, *Rep. Prog. Phys.*, **56**, 327(1993)
- [6.7] Comparisons of positron and electron scattering by gases, W. E. Kauppila and T. S. Stein, *Adv. Atom. Molec. Opt. Phys.*, **26**, 1(1989)
- [6.8] Electron impact excitation, R. J. W. Henry and A. E. Kingston, *Adv. Atom. Molec. Opt. Phys.*, **25**, 267(1988)

- [6.9] Distorted-wave methods in electron-impact excitation of atoms and ions, Y. Itikawa, *Phys. Rep.*, **143**, 69(1986)
- [6.10] Scattering of electrons by atoms, J. Callaway, *Adv. Phys.*, **29**, 771(1980)
- [6.11] Excitation of atoms by electron impact, D. W. O. Heddle, *Adv. Atom. Molec. Phys.*, **15**, 381(1978)
- [6.12] Electron scattering by atoms at intermediate energies II. Theoretical and experimental data for light atoms, B. H. Bransden and M. R. C. McDowell, *Phys. Rep.*, **46**, 249(1978)
- [6.13] Recent progress in atomic collisions theory, B. L. Moisewitsch, *Rep. Prog. Phys.*, **40**, 843(1977)
- [6.14] Electron scattering by atoms at intermediate energies I. Theoretical models, B. H. Bransden and M. R. C. McDowell, *Phys. Rep.*, **30**, 207(1977)
- [6.15] Electron scattering spectroscopy, J. B. Hasted, *Contemp. Phys.*, **14**, 357(1973)
- [6.16] The calculation of electron-atom excitation cross sections, M. R. H. Rudge, *Adv. Atom. Molec. Phys.*, **9**, 47(1973)
- [6.17] Electron scattering spectroscopy, J. B. Hasted, *Contemp. Phys.*, **14**, 357(1973)
- [6.18] Cross sections for electron excitation out of the metastable levels of helium into the higher singlet levels, R. B. Lockwood, F. A. Sharpton, L. W. Anderson, and C. C. Lin, *Phys. Lett A*, **166**, 357(1992)

- [6.19] Cross sections for electron-impact excitation out of metastable helium levels, D. L. A. Rall, F. A. Sharpton, M. B. Schulman, L. W. Anderson, J. E. Lawler, and C. C. Lin, *Phys. Rev. Lett.*, **62**, 2253(1989)
- [6.20] Inelastic differential electron scattering from metastable He( $2^3S$ ) atoms, R. Müller-Fiedler, P. Schlemmer, K. Jung, H. Hotop, and H. Ehrhardt, *J. Phys. B*, **17**, 259(1984)
- [6.21] Interaction of fast neutral helium atoms with an electron beam and with atoms of a gas target, V. A. Gostev, D. V. Elakhovskii, Y. V. Zaitsev, L. A. Luizova, and A. D. Khakhaev, *Opt. Spectrosc.*, **48**, 251(1980)
- [6.22] Excitation of metastable argon and helium atoms by electron impact, W. L. Borst, *Phys. Rev. A*, 1195(1974)
- [6.23] Resonances in the total cross sections for metastable excitation of noble gases by electron impact, F. M. J. Pichanick, J. Arol Simpson, *Phys. Rev.*, **168**, 64(1968)
- [6.24] Absolute emission cross section for electron-impact excitation of Li<sup>+</sup> to the ( $2^3P$ ) level, W. T. Rogers, J. O. Olsen, and G. H. Dunn, *Phys. Rev. A*, **18**, 1353(1978)
- [6.25] Recommended data for excitation rate coefficients of helium atoms and helium-like ions by electron impact, T. Kato and S. Nakazaki, *Atomic Data and Nuclear Data Tables*, **42**, 313(1989)

- [6.26] An evaluated compilation of theoretical data sources for electron-impact excitation of atomic ions, A. K. Pradhan and J. W. Gallagher, *Atomic Data and Nuclear Data Tables*, **52**, 227(1992)
- [6.27] Form factors and total scattering intensities for the helium-like ions from explicitly correlated wavefunctions, A. J. Thakkar and V. H. Smith, Jr., *J. Phys. B*, **11**, 3803(1978)
- [6.28] Absolute differential cross sections of elastically scattered electron I. He, N<sub>2</sub>, and CO at 500 eV, J. P. Bromberg, *J. Chem. Phys.*, **50**, 3906(1969)
- [6.29] Absolute differential cross sections of electrons elastically scattered by the rare gases. I. Small angle scattering between 200 and 700 eV, J. P. Bromberg, *J. Phys. Chem.*, **61**, 963(1974)
- [6.30] Rational function fits to the nonresonant elastic differential cross section(DCS) for e+He collisions, 0° -180°, 0.1 to 1000 eV, L. Boesten and H. Tanaka, *At. Data and Nucl. Data Tables*, **52**, 25(1992)
- [6.31] Differential elastic scattering of electrons by the rare gases I. Helium, J. W. McConkey and J. A. Preston, *J. Phys. B*, **8**, 63(1975)
- [6.32] Differential cross sections of 100, 150 and 200 eV electrons elastically scattered in helium, M. V. Kurepa and L. Vušković, *J. Phys. B*, **8**, 2067(1975)
- [6.33] G. B. Crooks and M. E. Rudd, *Bull. Am. Phys. Soc.*, **17**, 131(1972)

- [6.34] Angular differential cross sections for elastically scattered electrons in helium, S. K. Sethuraman, J. A. Rees, and J. R. Gibson, *J. Phys. B*, **7**, 1741(1974)
- [6.35] Absolute differential cross sections of elastically scattered electrons. I. He, N<sub>2</sub>, and CO at 500 eV, J. P. Bromberg, *J. Chem. Phys.*, **50**, 3906(1969)
- [6.36] K. G. Williams, *Proc. 6th Int. Conf. on Physics of Electronic and Atomic Collisions*, (Cambridge, Mass: MIT University Press) Abstracts p735
- [6.37] Tests of Born approximations; Differential and total cross sections for elastic scattering on 100- to 400-eV electrons by helium, L. Vriens, C. E. Kuyatt, and S. R. Mielczarek, *Phys. Rev.*, **170**, 163(1968)
- [6.38] Absolute measurement of differential cross sections for electron scattering in helium, G. E. Chamberlain, S. R. Mielczarek, and C. E. Kuyatt, *Phys. Rev. A*, **2**, 1905(1970)
- [6.39] K. Jost, M. Fink, and P. Herrmann, *Proc. 8th Int. Conf. on Physics of Electronic and Atomic Collisions*, (Beograd: Institute of Physics) Abstracts p277
- [6.40] Theoretical electron scattering amplitudes and spin polarizations, M. Fink and A. C. Yates, *Atomic Data*, **1**, 385(1970)
- [6.41] Absolute differential cross sections for 100 eV electrons elastically scattered by helium, neon, and argon, S. C. Gupta and J. A. Rees, *J. Phys. B*, **8**, 1267(1975)

- [6.42] Absolute differential cross sections for elastic scattering of electrons by helium, neon, argon and molecular nitrogen, R. H. J. Jansen, F. J. de Heer, H. J. Luyken, B. van Wingerden, and H. J. Blaauw, *J. Phys. B*, **9**, 185(1976)
- [6.43] Absolute differential cross sections of electrons elastically scattered by the rare gases. I. Small angle scattering between 200 and 700 eV, J. P. Bromberg, *J. Chem. Phys.*, **61**, 963(1974)
- [6.44] Elastic scattering of fast electrons by helium, F. W. Byron, Jr. and C. J. Joachain, *Phys. Rev. A*, **8**, 3266(1973)
- [6.45] Elastic scattering of electron and positrons by complex atoms at intermediate energies, F. W. Byron, Jr. and C. J. Joachain, *Phys. Rev. A*, **15**, 128(1977)
- [6.46] Coherent and incoherent X-ray scattering by bound electrons. I. Helium isoelectronic sequence, R. T. Brown, *Phys. Rev. A*, **1**, 1343(1970)
- [6.47] Atomic form factor and incoherent-scattering function of the helium atom, Y. K. Kim and M. Inokuti, *Phys. Rev.*, **165**, 39(1968)
- [6.48] Accurate first Born approximation cross sections for the excitation of helium by fast electrons, K. L. Bell, D. J. Kennedy, and A. E. Kingston, *J. Phys. B*, **2**, 26(1969)
- [6.49] Differential and integral cross sections for electron impact excitation of the  $n^3S$ ,  $n^1S$ , and  $n^3P$  ( $n=2,3$ ) levels in He, S. Trajmar, D. F. Register, D. C. Cartwright, and G. Csanak, *J. Phys. B*, 4889(1992)

- [6.50] Tests of Born approximations: Differential and total  $2^3S$ ,  $2^1P$ , and  $2^1S$  cross sections for excitation of He by 100- to 400-eV electrons, L. Vriens, J. A. Simpson, and S. R. Mielczarek, *Phys. Rev.*, **165**, 7(1968)
- [6.51] A collision cross section study of the  $1^1S \rightarrow 2^1P$  and  $1^1S \rightarrow 2^1S$  transitions in helium at kinetic energies from 200-700 eV. Failure of the Born approximation at large momentum changes, M. A. Dillon, and E. N. Lassettre, *J. Chem. Phys.*, **62**, 2373(1975)
- [6.52] Détermination des sections efficaces différentielles absolues pour les transitions  $1^1S \rightarrow 4^1S$ ,  $4^1D$ ,  $5^1S$  et  $5^1D$ , A. Pochat, D. Rozuel, et J. Peresse, *J. de Physique*, **34**, 701(1973)
- [6.53] Proposed standard inelastic differential electron scattering cross sections; Excitation of the  $2^1P$  level in He, S. Trajmar, J. M. Ratliff, G. Csanak, and D. C. Cartwright, *Z. Phys. D*, **22**, 457(1992)
- [6.54] Electron-impact excitation of the  $n^1P$  levels of helium: Theory and experiment, D. C. Cartwright, G. Csanak, S. Trajmar, and D. F. Register, *Phys. Rev. A*, **45**, 1602(1992)
- [6.55] Experimental-theoretical comparisons of  $1^1S \rightarrow 3^1P$  differential magnetic sublevel cross sections for electron-helium scattering of 80 and 100 eV, A Chutjian, *J. Phys. B*, **9**, 1749(1976)
- [6.56] A. Le Nadan, Thesis, Brest. 1970
- [6.57] Generalized oscillator strengths of the helium atoms. I, Y. K. Kim and M. Inokuti, *Phys. Rev.*, **175**, 176(1968)

- [6.58] Generalized oscillator strengths of the helium atoms. III. Transitions from the ground state to the  $3^1D$  and  $4^1P$  states, Y. K. Kim and M. Inokuti, *Phys. Rev.*, **184**, 38(1969)
- [6.59] Study of  $e^+$ -He scattering: a distorted-wave approximation, M. Kumar, R. Srivastava, and A. N. Tripathi, *J. Phys. B*, 4169(1985)
- [6.60] Collisions of fast electrons with helium III. Excitation of the  $(1s, nd) ^1D$  and  $(ns, mp) ^1P$  states, M. J. Woollings and M. R. C. McDowell, *J. Phys. B*, **6**, 450(1973)
- [6.61] Excitation of  $^1S$  ( $1s, 3s$ ) state of helium by electron impact in the Glauber approximation, A. C. Roy and N. C. Sil, *J. Phys. B*, 497(1979)
- [6.62] Effect of charge polarization on inelastic scattering: Differential and integral cross sections for excitation of the  $2^1S$  state of helium by electron impact, J. K. Rice, D. G. Truhlar, D. C. Cartwright, and S. Trajmar, *Phys. Rev. A*, **5**, 763(1972)
- [6.63] Distorted-wave calculation of the cross sections and correlation parameters for  $e^\pm$ -He( $1^1S$ ,  $2^1S \rightarrow 2^1P$ ,  $3^1S$ , and  $3^1P$ ) collisions, A. K. Katiyar and R. Srivastava, *Phys. Rev. A*, **38**, 2767(1988)
- [6.64] Positron collisions with helium at intermediate energies, S. L. Willis, J. Hata, M. R. C. McDowell, C. J. Joachain, and F. W. Byron Jr, *J. Phys. B*, **14**, 2687(1981)
- [6.65] A high energy approximation: III. Helium excitation by electrons, M. B. Hidalgo and S. Geltman, *J. Phys. B*, 617(1972)

- [6.66] Positron-impact excitation of helium at intermediate and high energies, S. Saxena, G. P. Gupta, and K. C. Mathur, *Phys. Rev. A*, **27**, 225(1983)
- [6.67] Generalized oscillator strengths of the helium atom. II. Transitions form the metastable states, Y. K. Kim and M. Inokuti, *Phys. Rev. A*, **181**, 205(1969)
- [6.68] Inelastic scattering of electrons by metastable helium: First Born and Glauber cross sections for  $2^3S \rightarrow 3^3S$  excitation, G. A. Khayrallah, S. T. Chen, and J. R. Rumble, Jr., *Phys. Rev. A*, **17**, 513(1978)
- [6.69] Excitation from the metastable states of helium by electrons, positrons and protons, I. Khurana, R. Srivastava, and A. N. Tripathi, *J. Phys. B*, **20**, 3515(1987)